Review of techniques in the large-N expansion for dilute magnetic alloys

N. E. Bickers

Institute for Theoretical Physics, Santa Barbara, California 93106

Magnetic ions embedded in a nonmagnetic host exhibit a number of unusual low-temperature properties known collectively as the Kondo effect. Conventional small-parameter expansions for the Kondo effect are plagued by infrared divergences, and the theory of dilute magnetic alloys has for many years centered on nonperturbative techniques. This paper reviews a novel perturbative approach to the magnetic alloy problem based on expansion in $1/N$, with N the ionic angular momentum degeneracy. This approach is analogous to perturbative expansions in statistical mechanics and field theory based on an integer-valued parameter (such as the number of spin components or the number of colors). The large-N expansion reproduces the essential features of the Kondo effect at $O(1)$ and appears to yield convergent (or asymptotic) expressions for ground-state properties. In contrast with previous nonperturbative approaches, the expansion provides information on dynamic, as well as static, properties. The evidence for convergence of the expansion is reviewed, and large-N calculations are compared with exact results for static properties. A number of independent, but essentially equivalent, approaches to the large-N expansion have been developed during the last five years. These techniques are reviewed pedagogically, and their relative strengths and weaknesses emphasized. A guide to notation in the recent literature is provided.

CONTENTS

I. OVERVIEW

A. Introductory remarks

In this paper we review a new approach, the large-degeneracy expansion, for investigating models of dilute magnetic alloys. Such alloys are produced by dissolving a small concentration of paramagnetic ions in a nonmagnetic metal; classic examples include *Cu*Fe and *La*Ce. [For an overview of experimental properties, see the review articles of Daybell (1973), Rizzuto (1974), and Tsvelick and Wiegmann (1983).] At high temperatures these systems display rather dull behavior: the impurities lead to Curie law paramagnetism and have an effect on transport properties comparable with that of nonmagnetic impurities. However, as the temperature is decreased below a characteristic scale (which is strongly material dependent), magnetic alloys exhibit striking effects. The magnetic susceptibility saturates, and the resistivity increases with decreasing temperature. The specific heat, thermoelectric power, and other properties display large anomalies, which have no analog in nonmagnetic alloys. Finally, at very low temperatures, properties become Fermi-liquid-like. The excess susceptibility becomes constant, and the excess specific heat linear in T. Despite this behavior, such systems remain unusual: on a per ion basis, the susceptibility and specific heat may be hundreds or thousands of times larger than the same properties in a nonmagnetic system. [The analogous behavior in concentrated alloys—the "heavy-electron metals"—is currently a subject of great interest; see, for example, Lee *et al.* (1986).]

Over the last twenty-five years, the problem of understanding this anomalous low-temperature behavior has been a recurring theme in condensed matter physics. A great number of sophisticated techniques have been employed to investigate this problem; many of these techniques were initially developed in other areas of many-particle physics. Examples include the numerical renormalization group (Wilson, 1974; Krishna-Murthy *et al.*, 1980a, 1980b), the Bethe-Yang ansatz (Andrei *et al.*, 1983; Tsvelick and Wiegmann, 1983), and quantum Monte Carlo (Hirsch and Fye, 1986; Gubernatis *et al.*, 1987).

We do not intend to review the previous literature on the magnetic impurity problem. A number of excellent review articles (which themselves comprise hundreds of pages) exist for most approaches to the problem. For reference we list a number of these articles at the end of this section in Table I. Instead, we wish to examine in some detail the techniques that have been developed in recent years based on the general concept of large-angular-momentum degeneracy.

Many interesting models in statistical mechanics and field theory contain integer-valued parameters N. In a spin system, N is the number of spin components (Abe, 1972; Ma, 1973); in quantum chromodynamics, the number of colors (Yaffe, 1982; Migdal, 1983); and in some condensed matter models, the number of electron species (Oppermann and Wegner, 1979; Ma and Fradkin, 1983). In each of these cases, expressions for the partition function (or S matrix) and correlation functions may (at least in principle) be generated by expanding perturbatively in $1/N$. Even in cases where N is rather small, such expansions may plausibly exhibit features that escape more conventional perturbation theories; such is the hope, for instance, in quantum chromodynamics. In all these systems, the partition function may be written in the form

$$Z=\int_{\sigma} e^{-NS(\sigma)}, \tag{1.1}$$

where $\int_{\sigma}$ indicates an integration over all degrees of freedom and $S(\sigma)$ is independent of N. (It is generally necessary to rescale some parameters of the system to obtain this simple form.) In these cases, the $1/N$ expansion resembles a semiclassical expansion in quantum mechanics, with $1/N$ taking the place of $\hbar$; in particular, in the limit $N\rightarrow\infty$, such systems may be described by a classical mechanics, based on Poisson bracket equations of motion and a phase space analogous to that in Newtonian mechanics. This interpretation of large-N limits has been reviewed extensively by Yaffe (1982).

The possibility of a large-N expansion for magnetic alloys was first put forward by Anderson (1981). In such alloys, the angular momentum degeneracy of the magnetic ion may, in principle, be large. For example, in the rare-earth ions Ce and Yb, magnetism arises from f electrons, and the degenerate configurations are f^1 and f^{13}. In both cases, if spin-orbit and crystalline electric field effects are ignored, the magnetic degeneracy is 14; even taking into account the relatively large spin-orbit effects in these ions, the ground-level degeneracies remain 6 and 8. In light of results from statistical mechanics and field theory, $1/N$ seems an attractive parameter for perturbation theory. Detailed investigations of the large-N expansion were initiated by Ramakrishnan (1981) and Ramakrishnan and Sur (1982) in Brillouin-Wigner studies of the Anderson model.

In the following pages we review progress in the development of a large-N expansion for magnetic alloys since 1981. We restrict attention to the dilute limit, i.e., to the properties of a single magnetic ion in a metallic host. This single-ion problem has been investigated rather thoroughly by a variety of techniques. In addition, a number of large-N studies have been carried out on concentrated alloy, or lattice, models. The lack of a viable nonperturbative approach for lattice models, which are

believed to describe the heavy-electron metals (Lee *et al.*, 1986) and concentrated valence fluctuators, has been a principal motivation in ongoing perturbative studies of the single ion and the lattice. Nevertheless, the applicability and convergence properties of the large-N expansion for concentrated alloys remain controversial, and a review of lattice studies may be premature at this time. We instead offer a list of references to recent large-N studies of the two-ion problem and the lattice at the end of this section (Table II).

While treatments regarding $1/N$ as an expansion parameter date only from 1981, the method has its roots in much earlier work. Many $O(1)$ results for ground-state properties were derived by other approaches before the existence of a systematic expansion parameter was realized. The variational large-N expansion is a descendant of previous variational treatments based on the assumption of a singlet ground state. Such methods reach back to the quasi-bound-state theory developed for the Kondo model by Yosida and collaborators in the late 1960s (Yosida and Yoshimori, 1973). Variational solutions for the Anderson model ground state were later studied extensively by Varma and Yafet (1976). Diagrammatic techniques in the large-N expansion also have a long history, dating from the work of Keiter and Kimball (1971). Later studies based on Brillouin-Wigner perturbation theory were carried out by Bringer and Lustfeld (1977) and by Grewe and Keiter (1981). Finally, the mean-field approximations introduced in zero-temperature functional integral treatments (see Sec. VI) have antecedents in the work of Takano and Ogawa (1966), Yoshimori and Sakurai (1970), and Chakravarty (1982).

The remainder of this paper is organized as follows: in Sec. I.B we introduce the models on which the large-N expansion is based—these are the finite-U and infinite-U Anderson models and the Coqblin-Schrieffer model. In Sec. I.C we discuss the parameter rescaling necessary for a large-N expansion. We summarize some of the main physical concepts that emerge from the expansion in Sec. I.D. In the following sections we review five distinct approaches to the large-N expansion. (Several approaches might conceivably be grouped together or subdivided.) The treatment is largely pedagogical, and we have attempted to include relatively complete mathematical details, even at the expense of some repetition. We illustrate how each approach may be used to calculate thermodynamic properties and correlation functions and review results obtained at zero and finite temperatures. We list below these approaches and the sections in which they are treated. The sections are relatively self-contained and may be read in any order.

(i) Diagrammatic expansions in $1/N$ from perturbation theory for strongly correlated systems (Zhang and Lee, 1983; Rasul and Hewson, 1984a, 1984b; Brandt, Keiter, and Liu, 1985), Sec. II.

(ii) Diagrammatic expansions in $1/N$ from perturbation theory with auxiliary bosons (Coleman, 1984; Bickers, 1986), Sec. III.

(iii) Systematic expansions and infinite-order summations in $1/N$ from variational theory at zero temperature (Gunnarsson and Schönhammer, 1983a, 1983b), Sec. IV.

(iv) Infinite-order summations in $1/N$ from integral equation solutions (Keiter and Kimball, 1971; Inagaki, 1979; Grewe, 1982; Keiter and Czycholl, 1983; Kuramoto, 1983; Coleman, 1984; Kuramoto and Kojima, 1984; Müller-Hartmann, 1984; Zhang and Lee, 1984; Bickers, Cox, and Wilkins, 1985, 1987; Maekawa *et al.*, 1985a, 1985b), Sec. V.

TABLE I. Theoretical review articles on the magnetic impurity problem.

1. Abrikosov, 1969. "Magnetic impurities in non-magnetic metals" (overview of early approaches).
2. Andrei, Furuya, and Lowenstein, 1983. "Solution of the Kondo problem" (Bethe ansatz solution of magnetic impurity models).
3. Fischer, 1970. "Magnetic impurities in metals: the s-d exchange model" (overview of early approaches).
4. Grüner and Zawadowski, 1974. "Magnetic impurities in non-magnetic metals" (overview of early approaches).
5. Grüner and Zawadowski, 1978 (renormalization group and scaling theory).
6. Keiter and Morandi, 1984. "Thermodynamic perturbation theory for systems with strong local correlations" (perturbation theory for the Kondo model, intermediate valence models, and other models with strong local correlations).
7. Kondo, 1969. "Theory of dilute magnetic alloy" (overview of early approaches).
8. Krishna-murthy, Wilkins, and Wilson, 1980a. "Renormalization group approach to the Anderson model of dilute magnetic alloys. I. Static properties for the symmetric case"; 1980b, "Renormalization group approach to the Anderson model of dilute magnetic alloys. II. Static properties for the asymmetric case" (renormalization group for the symmetric and asymmetric Anderson models).
9. Lawrence, Riseborough, and Parks, 1981. "Valence fluctuation phenomena" (overview of theory and experiment on mixed-valent alloys).
10. Newns and Read, 1987. "Mean field theory of intermediate valence—heavy fermion systems" (overview of mean field results in the large-N expansion for dilute and concentrated alloys).
11. Nozières, 1975 (renormalization group and Fermi-liquid theory).
12. Suhl, 1973. Ed., *Magnetism: Magnetic Properties of Metallic Alloys* (collection of review articles on early approaches).
13. Tsvelick and Wiegmann, 1983. "Exact results in the theory of magnetic alloys" (Bethe ansatz solutions of magnetic impurity models).
14. Varma, 1976. "Mixed-valence compounds" (overview of theory and experiment for mixed-valent alloys).
15. Wilson, 1975. "The renormalization group: critical phenomena and the Kondo problem" (renormalization group for the Kondo model).

TABLE II. Large-N treatments of the two-impurity and lattice problems.

1. Auerbach and Levin, 1986a. "Kondo bosons and the Kondo lattice: microscopic basis for the heavy Fermi liquid" (mean-field theory and fluctuations).
2. Auerbach and Levin, 1986b. "Experimental evidence for predicted universal behavior in low-temperature properties of Kondo lattices" (mean-field theory and fluctuations).
3. Brandt, Keiter, and Liu, 1985. "Large-N limit of mixed valence: diagrammatic expansion and rigorous results" [free energy and f Green's function to $O(1/N)$ for the two-impurity problem].
4. Coleman, 1983. "$1/N$ expansion for the Kondo lattice" (large-N formalism for the Coqblin-Schrieffer lattice).
5. Coleman, 1985a. "Large N as a classical limit of mixed valence" (mean-field theory for the lattice).
6. Coleman, 1985b. "Heavy fermions and broken symmetry in the generalized Anderson model" (mean-field theory for the lattice and two-impurity problems).
7. Coleman, 1987. "Mixed valence as an almost broken symmetry" (mean-field theory and fluctuations for the lattice and two-impurity problems).
8. Grewe, 1984. "One-particle excitation spectrum of the Kondo lattice" (proposed extension of NCA results to the lattice).
9. Lavagna, Millis, and Lee, 1987. "d-wave superconductivity in the large-degeneracy limit of the Anderson lattice" (quasiparticle superconductivity).
10. T. K. Lee, 1985. "The effective interactions in the Kondo lattice" (conduction-electron interactions in the Anderson lattice).
11. Millis and Lee, 1987. "Large-orbital-degeneracy expansion for the lattice Anderson model" (mean-field theory and fluctuations).
12. Rasul, Read, and Hewson, 1983. "Ground state properties of the Anderson lattice in the large-N limit" [equivalence of single-impurity and lattice thermodynamics at $O(1)$].
13. Rasul and Hewson, 1984c. "Ground state properties of the two-impurity Anderson model in a $1/N$ expansion" [ground-state energy to $O(1/N)$].
14. Read, Newns, and Doniach, 1984. "Stability of the Kondo lattice in the large-N limit" (mean-field theory for the lattice).

(v) Functional integral saddle-point methods and loop expansions in $1/N$ for the Coqblin-Schrieffer and infinite-U Anderson models and generalizations of these models (Read and Newns, 1983a; Coleman, 1985a, 1985b, 1987; Read, 1985; Houghton, Read, and Won, 1987), Sec. VI.

Throughout we attempt to maintain a consistent notation for quantities that appear in more than one context. To aid in comparison with the literature we present a translation table (Table XI) of notation at the end.

B. Model Hamiltonians for the large-N expansion

Treatments of dilute magnetic alloys center on two models, identified with the names of Anderson (1961), Kondo (1964), and Coqblin and Schrieffer (1969). Of the two, the more fundamental is the Anderson model. This model describes the interaction of delocalized conduction electrons with a highly localized magnetic impurity orbital. Impurity electrons are strongly correlated by the presence of an on-site Coulomb repulsion U, and mix weakly with conduction states through a hybridization matrix V. In the simplest case, the impurity orbital has only spin degeneracy, and the Hamiltonian may be written

$$\begin{aligned} &H_A = H_{\text{band}} + H_{\text{imp}} + H_{\text{mix}}, \quad H_{\text{band}} = \sum_{k\sigma} \varepsilon_{k\sigma} n_{k\sigma} , \\ &H_{\text{imp}} = \sum_{\sigma} \varepsilon_{d\sigma} n_\sigma + U n_\uparrow n_\downarrow , \\ &H_{\text{mix}} = \sum_{k\sigma} V_k (c^\dagger_{k\sigma} d_\sigma + \text{H.c.}) . \end{aligned} \tag{1.2}$$

Here $\varepsilon_{k\sigma}$ ($\varepsilon_{d\sigma}$) denotes the energy of the conduction (impurity) state with creation operator $c^\dagger_{k\sigma}$ ($d^\dagger_\sigma$) and number operator $n_{k\sigma}$ (n_σ). In the absence of a magnetic field, the level energies may be written ε_k and ε_d. Note that the hybridization is in general energy dependent. A measure of the hybridization strength is the impurity level width Γ, which follows from a golden rule calculation (ignoring the on-site repulsion). This is just

$$\Gamma \equiv \pi N(\varepsilon_d) V_k^2 , \tag{1.3a}$$

with $N(\varepsilon)$ the conduction density of states. For a flat band and constant hybridization,

$$\Gamma = \pi N(0) V^2 . \tag{1.3b}$$

This model is often used to describe transition metal alloys, in which the magnetic ions have quenched orbital degrees of freedom.

The model may be generalized to treat impurities with orbital degeneracy and arbitrarily complex multiplet structure. New forms for the on-site Coulomb interaction and the hybridization term are then required. For rare-earth ions, such as Ce and Yb, spin-orbit coupling is strong and, to good approximation, the total angular momentum about the impurity is conserved by the interactions (Coqblin and Schrieffer, 1969). In general, an exchange integral J, as well as the direct integral U, should be introduced to describe the Coulomb interaction. If this complication is ignored, the simplest Anderson Hamiltonian for rare-earth systems is

$$H_A = H_{\text{band}} + H_f + H_{\text{mix}}, \quad H_{\text{band}} = \sum_{km} \varepsilon_{km} n_{km} ,$$

$$H_f = \sum_m \varepsilon_{fm} n_m + U \sum_{m>m'} n_m n_{m'} , \tag{1.4a}$$

$$H_{\text{mix}} = \sum_{km} V_k (c_{km}^\dagger f_m + \text{H.c.}) .$$

In this case, the parameters have the same interpretation as before; now, however, $c_{km}^\dagger$ and $f_m^\dagger$ create spherical-wave states of fixed total and orbital angular momentum (j and l). The magnetic quantum number m varies between $-j$ and j: the impurity degeneracy is

$$N = 2j+1 . \tag{1.4b}$$

For $N=6$, this Hamiltonian describes the ground multiplet (f^1, $j=\frac{5}{2}$, $l=3$) of Ce; after a particle-hole transformation, the Hamiltonian may be used to describe Yb (f^{13}, $j=\frac{7}{2}$, $l=3$). The Hamiltonian above may be made more realistic by including additional spin-orbit multiplets or by breaking the ground-state degeneracy with crystalline electric fields (Hirst, 1978). Anderson models for thulium and uranium impurities have been treated within large-N approximations by Read *et al.* (1986) (Tm) and by Nunes *et al.* (1986) (U). For most of our purposes, however, the simple rare-earth Hamiltonian with an N-fold multiplet is adequate.

This Hamiltonian may be further simplified in the physically relevant limit of large U: in Ce systems, U is typically of order 5 eV. In such cases it is an excellent approximation to assume $U \to \infty$. In this case, the only possible impurity configurations are empty and singly occupied. We denote the $N+1$ possible configurations $|0\rangle$ and $|m\rangle$. The infinite-U Anderson Hamiltonian may then be written

$$H_A = H_{\text{band}} + H_f + H_{\text{mix}} ,$$

with H_{band} as before, and

$$H_f = \sum_m \varepsilon_{fm} |m\rangle\langle m| ,$$

$$H_{\text{mix}} = \sum_{km} V_k (c_{km}^\dagger |0\rangle\langle m| + \text{H.c.}) . \tag{1.5}$$

This Hamiltonian has been the starting point for most $1/N$ investigations. [In the following section we discuss the parameter rescaling required for generating a $1/N$ expansion. This is perhaps not obvious, since N does not appear explicitly in Eq. (1.5).]

An alternate Hamiltonian for magnetic alloys is the s-d, or Kondo, Hamiltonian (Kondo, 1964). This Hamiltonian may be derived (Schrieffer and Wolff, 1966) as an effective limiting form of the Anderson Hamiltonian in Eq. (1.2) for $-\varepsilon_f$ and U much larger than Γ. The Kondo Hamiltonian describes the interaction of conduction electrons with a local impurity spin through an antiferromagnetic contact coupling:

$$H_K = H_{\text{band}} + H_{\text{int}}, \quad H_{\text{band}} = \sum_{k\sigma} \varepsilon_{k\sigma} n_{k\sigma} ,$$

$$H_{\text{int}} = -J \sum_{kk'\alpha\alpha'} \mathbf{S}\cdot c_{k'\alpha'}^\dagger \boldsymbol{\sigma} c_{k\alpha}, \quad J<0 . \tag{1.6}$$

Here $\boldsymbol{\sigma}$ is a vector of Pauli matrices, and $\mathbf{S}$ a local spin-$\frac{1}{2}$ operator. The interaction may conveniently be rewritten in terms of local projection operators:

$$H_{\text{int}} = -J \sum_{kk'\alpha\alpha'} c_{k'\alpha'}^\dagger |\alpha\rangle\langle\alpha'| c_{k\alpha} + \tfrac{1}{2} J \sum_{kk'\alpha} c_{k'\alpha}^\dagger c_{k\alpha} . \tag{1.7}$$

The last term is just a correction to the one-body conduction-electron potential.

The generalization of this Hamiltonian for rare-earth alloys is the SU(N) Kondo, or Coqblin-Schrieffer, model (Coqblin and Schrieffer, 1969):

$$H_{\text{CS}} = H_{\text{band}} + H_{\text{int}}, \quad H_{\text{band}} = \sum_{km} \varepsilon_{km} n_{km} ,$$

$$H_{\text{int}} = -J \sum_{kk'mm'} c_{k'm'}^\dagger |m\rangle\langle m'| c_{km}, \quad J<0 . \tag{1.8}$$

Here, $|m\rangle\langle m'|$ is a projection operator that acts within the impurity Hilbert space $\{|m\rangle : m=-j,\ldots,j\}$. The relation of the interaction term in this model to that in the spin-$\frac{1}{2}$ Kondo model is clear. This Hamiltonian may be derived as a limiting form of the Anderson Hamiltonians in Eqs. (1.4) and (1.5) (Coqblin and Schrieffer, 1969). The Coqblin-Schrieffer model describes the interaction of conduction electrons with an N-fold degenerate impurity whose magnetic configuration fluctuates. This model has also served as a basis for numerous large-N studies (see Sec. II.E).

C. Parameter rescaling for the large-N expansion

In this section we describe in a simple way how $1/N$ may be regarded as an expansion parameter for the infinite-U Anderson and Coqblin-Schrieffer models. It is necessary to define the behavior of parameters in the large-N limit so that physical quantities do not diverge for $N \to \infty$. This preliminary step is necessary in all versions of the large-N expansion for magnetic alloys and for more general systems in statistical mechanics and field theory (Yaffe, 1982).

The parameter N does not explicitly appear in the An-

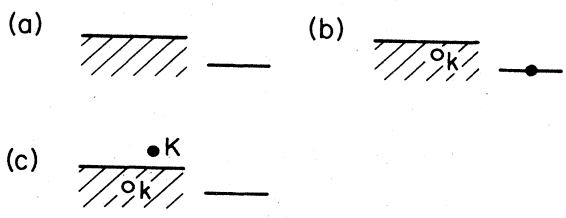

FIG. 1. Pictorial representation of many-particle states in Rayleigh-Schrödinger perturbation theory. The shaded rectangle represents the Fermi sea of conduction electrons, and the adjacent line the localized f level. (a) $|\Omega\rangle$, the filled Fermi sea and an empty f level. (b) $|\varepsilon_f \varepsilon_k m\rangle$, a state with one f electron and one conduction hole, both in magnetic channel m. (c) $|E_K \varepsilon_k m\rangle$, a state with one conduction electron (energy E_K) and one conduction hole (energy ε_k), both in magnetic channel m.

derson and Coqblin-Schrieffer Hamiltonians. Nevertheless, it arises in perturbation theory wherever there appear sums over magnetic quantum numbers in intermediate states. As an example, consider the many-particle state $|\Omega\rangle$, in which the f level is empty and the Fermi sea of conduction electrons fully occupied [see Fig. 1(a)]. For convenience, let this state define the zero of energy. In Rayleigh-Schrödinger perturbation theory, the lowest-order stabilization of this state by hybridization is (ignoring level broadening)

$$\begin{aligned}\Delta E_0 &= \mathrm{Re}\sum_N \frac{\langle\Omega|H_{\mathrm{mix}}|N\rangle\langle N|H_{\mathrm{mix}}|\Omega\rangle}{-E_N} \\ &= \mathrm{Re}\sum_{km} |V_k|^2 \frac{\langle\Omega|[\,|0\rangle\langle m|c_{km}^\dagger]\,|\varepsilon_k m\rangle\langle\varepsilon_k m|[\,|m\rangle\langle 0|c_{km}]\,|\Omega\rangle}{-(\varepsilon_f-\varepsilon_k)} \\ &= \mathrm{Re}\sum_k \frac{N|V_k|^2}{\varepsilon_k-\varepsilon_f} = -\frac{N\Gamma}{\pi}\ln\left[\frac{D}{|\varepsilon_f|}\right], \end{aligned} \tag{1.9}$$

assuming in the last step a flat band of half-width $D \gg |\varepsilon_f|$ and constant hybridization. The stabilization energy of $|\Omega\rangle$ is proportional to $N\Gamma$.

In contrast, consider the stabilization of the isoelectronic state

$$|\varepsilon_f\varepsilon_k m\rangle = f_m^\dagger c_{km}|\Omega\rangle\ . \tag{1.10}$$

In this state, one band electron in magnetic channel m has been moved onto the f orbital. The stabilization energy is

$$\begin{aligned}\Delta E_m &= \mathrm{Re}\sum_N \frac{\langle\varepsilon_f\varepsilon_k m|H_{\mathrm{mix}}|N\rangle\langle N|H_{\mathrm{mix}}|\varepsilon_f\varepsilon_k m\rangle}{\varepsilon_f-\varepsilon_k-E_N} \\ &= \mathrm{Re}\sum_K \frac{\langle\varepsilon_k m|[\,|m\rangle\langle 0|c_{Km}]\,|E_K\varepsilon_k m\rangle\langle E_K\varepsilon_k m|[\,|0\rangle\langle m|c_{Km}^\dagger]\,|\varepsilon_k m\rangle}{\varepsilon_f-\varepsilon_k-(E_K-\varepsilon_k)} \\ &= \mathrm{Re}\sum_K \frac{|V_K|^2}{\varepsilon_f-E_K} = -\frac{\Gamma}{\pi}\ln\left[\frac{D}{|\varepsilon_f|}\right], \end{aligned} \tag{1.11}$$

where

$$|E_K\varepsilon_k m\rangle = c_{Km}^\dagger c_{km}|\Omega\rangle\ . \tag{1.12}$$

This stabilization energy is proportional to Γ, but contains no factor of N.

Hence states with an empty impurity orbital are generally lowered in energy by amounts N times larger than comparable states with an occupied orbital. As pointed out by Ramakrishnan (Ramakrishnan, 1981; Ramakrishnan and Sur, 1982), this may be interpreted as a phase-space effect: there are simply more possibilities for hybridization of an empty impurity state.

The factors of N that arise in perturbation theory must be "scaled away" if the infinite-U Anderson model is to have a well-behaved large-N limit. This may be accomplished by fiat by setting

$$N|V_k|^2 = O(1),\quad N\to\infty\ . \tag{1.13}$$

Then $|V_k|^2 = N|V_k|^2/N = O(1/N)$, and the formal basis for expansions in $1/N$ becomes clear: in leading order, the only terms that contribute are those in which a factor of N accompanies each V^2 hybridization process. In the next order, terms enter with one "missing" factor of N, and so on.

Similar arguments from Rayleigh-Schrödinger perturbation theory establish that terms proportional to NJ enter expansions for the Coqblin-Schrieffer model. [This could also be established by appealing to the canonical transformation that links this model with the infinite-U Anderson model (Schrieffer and Wolff, 1966).] Hence it is required that

$$NJ = O(1),\quad N\to\infty \tag{1.14}$$

for perturbation theory in $1/N$ to be well behaved.

What is the physical meaning of the formal parametrizations in Eqs. (1.13) and (1.14)? The possibility that some perturbative processes are intrinsically "more important" than others of equal order in V^2 should be clear from Eqs. (1.9)—(1.11). However, we regard the parameter rescaling as largely a necessary technical device, which allows the investigation of magnetic impurity models from a new viewpoint. The success of various approximations must be established by comparison with other approaches (such as the numerical renormalization group and Bethe ansatz) and with experiment. In fact, the convergence properties of the $1/N$ expansion at finite temperature remain to be fully established. Nevertheless, in the course of this review, we argue that the ground-state properties of magnetic alloys are captured successfully by low-order expansions in $1/N$, and, further, that infinite-order resummations in $1/N$ provide one of the most complete descriptions of finite-temperature properties now available.

D. Some basic physics of the large-N expansion

Before describing detailed implementations of the large-N expansion, we outline briefly some of the concepts that underly the method's success. The question that must be confronted by any approach to the magnetic alloy problem is the following: what is the qualitative nature of the ground state formed when a magnetic ion is immersed in a sea of delocalized conduction electrons? One might naively argue that the ground state should be degenerate. The N magnetic configurations of the ion are equivalent, and, at least in the weak-coupling limit, each free-ion ground state should map perturbatively onto a ground state of the interacting system. This reasoning is, of course, false. The local coupling in the Coqblin-Schrieffer and Anderson models cannot be treated by perturbation theory, and the ground states of the noninteracting and interacting systems have different symmetries for arbitrarily weak coupling. As shown first by experiment, then by increasingly sophisticated theoretical methods, the ground state of the Coqblin-Schrieffer and infinite-U Anderson models is a total angular momentum singlet. Alternative perturbation theories must incorporate this fact at lowest order to have a chance of success.

The large-N expansion succeeds for just this reason. The $O(1)$ approximation amounts to solving for the lowest-energy singlet of the ion-conduction electron system, assuming the existence of no more than one hole in the conduction band. The basis states included in the $O(1)$ calculation for the infinite-U Anderson model are those shown in Figs. 1(a) and 1(b). The variational ansatz for the ground state is

$$|\phi_0\rangle = |\Omega\rangle + \frac{1}{\sqrt{N}} \sum_k^{\text{occ}} \alpha_k f_m^\dagger c_{km} |\Omega\rangle \ , \tag{1.15}$$

with $|\Omega\rangle$ the noninteracting Fermi sea. Since at most one hole is included, the determination of the ground state is a one-body calculation at this order. Higher-order approximations take into account the addition of electron-hole pairs to the variational state $|\phi_0\rangle$.

The resulting ground-state singlet is *not* a bound state in the usual sense, i.e., it is not separated by a gap from excited states. Approximate excited states may be found by (a) replacing $|\Omega\rangle$ with a noninteracting excited state $|\text{exc}\rangle$, which differs only by the presence of a few electron-hole pairs in the conduction band, then (b) repeating the ground-state calculation, taking into account states that differ from $|\text{exc}\rangle$ by the possible addition of one conduction hole and f electron. As emphasized by de Châtel (1982), the low-lying states of the interacting system may in this way be placed in one-to-one correspondence with the low-lying states of the noninteracting Fermi sea. Hence the interacting system behaves as a Fermi liquid within this simple approximation. From renormalization-group and Bethe ansatz studies, it is known that this Fermi-liquid behavior survives when the alloy models are solved exactly. The large-N expansion allows systematic corrections to the simple $O(1)$ picture of Eq. (1.15).

The energy scale for the ground state (the "Kondo scale") is exponentially small in the expansion parameters

$$\begin{aligned} g &= N(0)|J| \quad \text{(Coqblin-Schrieffer)} \ , \\ g &= \frac{N(0)V^2}{|\varepsilon_f|} = \frac{\Gamma}{\pi|\varepsilon_f|} \quad \text{(Anderson)} \ . \end{aligned} \tag{1.16}$$

In the simple one-hole, or $O(1)$, approximation mentioned above, the ground-state energy gain from conduction-electron mixing is

$$T_{\text{CS}}, T_A = De^{-1/Ng} \ , \tag{1.17}$$

with D the half-width of the conduction band. (For the Anderson model, this simple expression is valid in the Kondo limit $-\varepsilon_f \gg N\Gamma$.) Note that the Kondo scale is analytic in the parameter $1/N$, but nonanalytic in the coupling constant g.

The exponentially small Kondo scale, rather than the initial bandwidth D, is the characteristic energy for variations in the density of low-lying excited states. For this reason, the $T \to 0$ magnetic susceptibility and specific heat per impurity ion are greatly enhanced over the values for the noninteracting system. As shown in subsequent sections, the $O(1)$ values for the Anderson model are

$$\begin{aligned} \chi &= \frac{\mu_j^2}{3}\frac{n_f^{(1)}}{T_A}, \quad \gamma = \frac{\pi^2 k_B^2}{3}\frac{n_f^{(1)}}{T_A} \ , \\ \mu_j^2 &= j(j+1)(g\mu_B)^2 \ , \end{aligned} \tag{1.18}$$

with $n_f^{(1)}$ the lowest-order approximation for the fractional f-level occupancy, or valence. When the nonessential factors $\mu_j^2/3$ and $\pi^2 k_B^2/3$ are removed, the ratio of the susceptibility and specific-heat coefficient (the so-called Sommerfeld ratio) is just unity at this order. Fermi-liquid-like corrections emerge at higher order and may be treated systematically.

The Fermi-liquid properties of the Coqblin-Schrieffer and Anderson models for $T \to 0$ have long suggested a simple phenomenological interpretation (Schotte and Schotte, 1975; Newns and Hewson, 1980; Wilkins, 1982). Similar properties are exhibited by the nonmagnetic resonant level model

$$\begin{aligned} H_{RL} &= H_{\text{band}} + H_{\text{imp}} + H_{\text{mix}} \ , \\ H_{\text{band}} &= \sum_{km} \varepsilon_k n_{km}, \quad H_{\text{imp}} = \tilde{\varepsilon}_f \sum_m n_m \ , \\ H_{\text{mix}} &= \tilde{V} \sum_{km} (c_{km}^\dagger f_m + \text{H.c.}) \ , \end{aligned} \tag{1.19}$$

for suitably chosen values of the resonance position $\tilde{\varepsilon}_f$ and width $\tilde{\Gamma} = \pi N(0)\tilde{V}^2$. The resonant level model is conceptually simple to treat, since it involves only a one-body mixing term without strong local correlations. The low-temperature properties of the magnetic alloy models may be described by an *effective* resonant level model, with resonance position and width each of order the Kondo scale T_{CS} or T_A. [A complete study of resonant level phenomenology, or "local Fermi-liquid theory," for the magnetic alloy problem has been carried out by Newns

and Hewson (1980).] A principal motivation for studying the large-N expansion in the Fermi-liquid regime has been the desire to provide a microscopic basis for this simple phenomenology.

The $O(1)$ approximation for the Coqblin-Schrieffer and Anderson models is a one-body theory, in which noninteracting states of the Fermi sea are modified by the addition of a single hole and an f electron. For this reason, Fermi-liquid results may be rigorously described at this order by a resonant level model of the form described above (see Sec. VI). Effective resonance parameters may be deduced by asking what happens when an f electron is added to the $O(1)$ ground state. As shown in the following sections, the one-electron excitation spectrum has a quasiparticle contribution at energy $\omega-\mu=T_A$, with μ the Fermi energy. Hence the effective resonance position $\tilde{\varepsilon}_f$ is T_A. The weight of the f quasiparticle is just the probability $1-n_f^{(1)}$ for finding the f level empty in the ground state, i.e., the overlap between the ground state and the noninteracting Fermi sea (with the f level empty). In the Kondo regime, the quasiparticle weight becomes exponentially small as the f valence approaches unity. The effective resonance width $\tilde{\Gamma}$ is reduced from the bare f-level width Γ by the ground-state overlap factor $1-n_f^{(1)}$.

This simple picture for the Fermi-liquid physics breaks down when electron-hole pairs are included at higher orders in the large-N expansion. It is well known that when a Fermi sea is subjected to a localized nonmagnetic perturbation, the overlap between the initial ground state and the perturbed ground state vanishes (Anderson, 1967; Yamada and Yosida, 1982). The localized perturbation produces a cascade of low-energy electron-hole pairs, which overwhelm the contribution of the initial ground state. A similar infrared overlap catastrophe occurs when electron-hole pairs are included in the ground state for the magnetic alloy problem: all low-lying states of the unperturbed system appear with nearly equal weight in the interacting ground state. The appearance of pair cascades prevents a naive extension of the effective resonant level model to higher order. The Fermi excitations probed by the magnetic susceptibility and specific heat are not simply hybridized one-electron excitations in the basis of noninteracting states. Rather, within this basis, they are one-electron excitations dressed by an infinite number of electron-hole pairs. At higher orders in $1/N$, the effective resonant level model describes these local "quasiparticles," which are related in no simple way to the "bare" f electrons.

A particular version of the large-N expansion provides a rigorous means to generate, order by order, the quasiparticle resonant level model describing the Fermi-liquid regime. A functional integral saddle-point technique, combined with an all-orders rearrangement of perturbation theory (see Sec. VI.C), may be used to generate an effective Fermi Hamiltonian, together with Bose-type interactions between the underlying quasiparticles. Numerous extensions of this elegant technique have been proposed for lattice models describing the heavy-electron metals (see Table II). Such approximations amount to superposing the single-ion singlets described above while ignoring interion interactions. While this approximation is phenomenologically quite successful, its validity remains unclear at this time. We do not discuss treatments of the lattice problem in the present review, but refer the reader to the sources cited.

The simple picture for Fermi-liquid physics which emerges from the large-N saddle-point expansion does not extend to higher temperatures. In particular, a detailed numerical treatment is required to describe the crossover between the Fermi-liquid regime and the high-temperature limit, where magnetic impurities show free-ion-like behavior with perturbative corrections. At finite temperature, other versions of the large-N expansion (such as the diagrammatic resummations described in Sec. V) furnish quantitative information on magnetic alloy properties. These methods are largely complementary to those which succeed in the Fermi-liquid limit. Taken together, the various approaches provide quantitative results and additional physical insight for the full range of temperatures.

II. DIAGRAMMATIC LARGE-N EXPANSIONS FOR THE INFINITE-U ANDERSON MODEL

In this section we discuss diagrammatic $1/N$ expansions for the partition function and Green's functions of the infinite-U Anderson and Coqblin-Schrieffer models. The complicating feature of perturbation theory for these models is the presence of strong local correlations, which prevent an expansion based on free fermions. Methods for treating this complication date from the work of Keiter and Kimball (1971). Keiter and Kimball considered the finite-U Anderson model; in this case, standard finite-temperature perturbation theory may be applied formally. However, since U is typically much larger than the hybridization width Γ, it is a better approximation to include the Coulomb term in an "unperturbed" Hamiltonian. In this case, the Feynman diagrammatic approach is ruled out and more specialized methods are required. The same methods apply more generally to models with spin and projection operators. Since such methods may be unfamiliar, we begin by deriving general expressions for the partition function in strongly correlated electronic systems (Sec. II.A). We follow the approach of Keiter and Morandi (1984). In Sec. II.B we discuss the technical structure of finite-temperature perturbation theory for the infinite-U Anderson model and derive expressions for the partition function at $O(1)$ and $O(1/N)$ in the large-N expansion. Expressions for zero-temperature thermodynamic properties are derived within the same approximation in Sec. II.C. We discuss in this section the physical source of Fermi-liquid corrections in the Sommerfeld ratio χ/γ [the first corrections to Fermi-gas behavior appear at $O(1/N)$]. In Sec. II.D, expressions for the f-electron spectral density, which may be probed directly by photoemission and inverse photo-

emission experiments, are derived at $O(1)$ and $O(1/N)$. In this section we also discuss the effects of the ground-state overlap catastrophe, which first appear at $O(1/N)$. In Sec. II.E the large-N expansion for the Coqblin-Schrieffer model is developed, and the Schrieffer-Wolff transformation (1966) connecting this model and the Anderson model is described in diagrammatic terms. Finally, in Sec. II.F we briefly review the evidence for convergence of the large-N expansion from comparison with ground-state Bethe ansatz results.

A. Perturbation theory for systems with strong local correlations

Conventional perturbation theories in condensed matter physics rely on the ability to expand the partition function about a noninteracting ground state with free Fermi and Bose excitations. In order to model systems with strong localized interactions (including magnetic alloys), it is frequently necessary to introduce quantum spin and projection operators. In such cases, a Feynman propagator expansion is impossible. An alternate perturbation theory based on contour integral representations for the partition function and correlation functions has been devised to treat such systems. We briefly describe this approach below.

Quite generally, the partition function of a many-particle Hamiltonian may be written

$$Z=\mathrm{Tr}e^{-\beta H}=\int_\Gamma \frac{dz}{2\pi i}e^{-\beta z}\mathrm{Tr}(z-H)^{-1}\,, \tag{2.1}$$

where Γ is a contour in the complex plane, oriented counterclockwise, and surrounding all singularities of the *resolvent* $(z-H)^{-1}$. The resolvent may be expanded as

$$(z-H)^{-1}=(z-H_0)^{-1}\sum_{n=0}^{\infty}[V(z-H_0)^{-1}]^n\,, \tag{2.2a}$$

by decomposing the Hamiltonian into an "unperturbed" part and a perturbation:

$$H=H_0+V\,. \tag{2.2b}$$

Thus

$$Z=\int_\Gamma \frac{dz}{2\pi i}e^{-\beta z}\mathrm{Tr}\left[(z-H_0)^{-1}\sum_{n=0}^{\infty}[V(z-H_0)^{-1}]^n\right]. \tag{2.3}$$

The trace may be explicitly evaluated by inserting a complete set of states between consecutive factors of $V(z-H_0)^{-1}$. Alternatively, this expression may first be simplified by introducing a *self-energy operator* $\hat{\Sigma}(z)$ diagonal in the basis of H_0 eigenstates $|N\rangle$:

$$\begin{aligned}\Sigma_N(z)&\equiv\langle N|\hat{\Sigma}(z)|N\rangle\\&=\langle N|V[1-(z-H_0)^{-1}Q_NV]^{-1}|N\rangle\,,\\ Q_N&\equiv 1-P_N,\quad P_N\equiv|N\rangle\langle N|\,.\end{aligned} \tag{2.4}$$

This quantity is formally quite similar to proper self-energies in Feynman perturbation theory. Σ_N includes all contributions to the matrix element

$$\langle N|V[1-(z-H_0)^{-1}V]^{-1}|N\rangle$$

except those which contain $|N\rangle$ as an intermediate state. The partition function may be rewritten

$$Z=\int_\Gamma \frac{dz}{2\pi i}e^{-\beta z}\mathrm{Tr}\left[(z-H_0)^{-1}\sum_{n=0}^{\infty}[\hat{\Sigma}(z)(z-H_0)^{-1}]^n\right]=\int_\Gamma \frac{dz}{2\pi i}e^{-\beta z}\mathrm{Tr}\frac{1}{z-H_0-\hat{\Sigma}(z)}\,. \tag{2.5}$$

(There is no ambiguity in writing the operators in this way, since $[H_0,\hat{\Sigma}]=0$.) Alternatively, the $n=0$ term in Eq. (2.3) may be separated out to give

$$Z-Z_0=\int_\Gamma \frac{dz}{2\pi i}e^{-\beta z}\mathrm{Tr}\left[(z-H_0)^{-2}\sum_{n=1}^{\infty}V[(z-H_0)^{-1}V]^{n-1}\right], \tag{2.6a}$$

where the unperturbed partition function is just

$$Z_0=\mathrm{Tr}e^{-\beta H_0}\,. \tag{2.6b}$$

Since the trace is cyclically invariant, this expression may be further simplified:

$$Z-Z_0=\int_\Gamma \frac{dz}{2\pi i}e^{-\beta z}\frac{d}{dz}\mathrm{Tr}\sum_{n=1}^{\infty}\frac{-1}{n}[(z-H_0)^{-1}V]^n=-\beta\int_\Gamma \frac{dz}{2\pi i}e^{-\beta z}\mathrm{Tr}\sum_{n=1}^{\infty}\frac{1}{n}[(z-H_0)^{-1}V]^n\,. \tag{2.7}$$

The factor $1/n$ leads to awkward summations. This factor may be eliminated by introducing a coupling-constant integration, i.e., by writing

$$Z-Z_0=-\beta\int_0^1\frac{dg}{g}\int_\Gamma \frac{dz}{2\pi i}e^{-\beta z}\mathrm{Tr}\sum_{n=1}^{\infty}[(z-H_0)^{-1}gV]^n\,. \tag{2.8}$$

This expression may also be simplified by introducing a self-energy operator. In this case, let

$$\Sigma_N(z,g)=\langle N\,|\,\hat{\Sigma}(z,g)\,|\,N\rangle = \langle N\,|\,gV[1-(z-H_0)^{-1}Q_N gV]^{-1}\,|\,N\rangle\ , \tag{2.9}$$

with Q_N as in Eq. (2.4). Then it follows that

$$Z-Z_0=\int_0^1\frac{dg}{g}\int_\Gamma\frac{dz}{2\pi i}e^{-\beta z}\mathrm{Tr}\frac{\hat{\Sigma}(z,g)}{z-H_0-\hat{\Sigma}(z,g)}\ . \tag{2.10}$$

B. Perturbation theory for the infinite-U Anderson model

We discuss below the application of the general techniques from Sec. II.A to the infinite-U Anderson model

$$H=H_{\rm band}+H_f+H_{\rm mix}\ ,$$
$$H_{\rm band}=\sum_{km}\varepsilon_k n_{km},\quad H_f=\varepsilon_f\sum_m|\,m\,\rangle\langle\,m\,|\ , \tag{2.11a}$$
$$H_{\rm mix}=V\sum_{km}(c_{km}^\dagger\,|\,0\,\rangle\langle\,m\,|+|\,m\,\rangle\langle\,0\,|\,c_{km})\ .$$

(The zero of energy is set by the unperturbed Fermi sea and empty f level.) In this case the presence of projection operators prevents a conventional Feynman expansion.

We consider first the representation of Eq. (2.3). A complete set of eigenstates of the noninteracting Hamiltonian

$$H_0=H_{\rm band}+H_f \tag{2.11b}$$

must be introduced. It is convenient to trace separately over band and local states by letting

$$\mathrm{Tr}=\mathrm{Tr}_f\mathrm{Tr}_{\rm band}\ . \tag{2.12}$$

To further allow the separation of band and local degrees of freedom, the integration variable z in Eq. (2.3) may be shifted parallel to the real axis in each element of the trace by

$$z\rightarrow z+E_N^{\rm band}\ ,$$

where

$$H_{\rm band}\,|\,N\,\rangle=E_N^{\rm band}\,|\,N\,\rangle\ . \tag{2.13}$$

This shift amounts to subtracting out the energy of electron-hole pairs in excited states of the Fermi sea: local and band degrees of freedom may then be separated completely in the absence of hybridization. Applying these changes and dividing by $Z_{\rm band}$ gives

$$Z/Z_{\rm band}=\int_\Gamma\frac{dz}{2\pi i}e^{-\beta z}\mathrm{Tr}_f\left[\sum_{N_{\rm band}}\frac{e^{-\beta E_N^{\rm band}}}{Z_{\rm band}}\left\langle N_{\rm band}\left|\frac{1}{z-(H-E_N^{\rm band})}\right|N_{\rm band}\right\rangle\right]$$
$$=\int_\Gamma\frac{dz}{2\pi i}e^{-\beta z}\mathrm{Tr}_f\left[\sum_{N_{\rm band}}\frac{e^{-\beta E_N^{\rm band}}}{Z_{\rm band}}\left\langle N_{\rm band}\left|[z-(H_0-E_N^{\rm band})]^{-1}\sum_{n=0}^{\infty}\{V[z-(H_0-E_N^{\rm band})]^{-1}\}^n\right|N_{\rm band}\right\rangle\right]\ . \tag{2.14}$$

Note that the only band energies which remain in the denominators

$$[z-(H_0-E_N^{\rm band})]^{-1}$$

are intermediate-state electron-hole energies, measured relative to the initial state $|\,N_{\rm band}\,\rangle$.

The thermal average over band degrees of freedom may be carried out using Wick's theorem to contract the electron creation and destruction operators that appear in repeated factors of V. A simple set of diagrammatic rules to evaluate Eq. (2.14) is summarized in Table III and illustrated in step-by-step fashion in Fig. 2.

The same separation of band and local degrees of freedom may be applied in the representation for Z in Eq. (2.5). The self-energy operator, which acts within the full Hilbert space of band and local states, may be replaced by an f self-energy, which acts only within the space of local states. This is possible since, in thermal averages of the form

$$\sum_{N_{\rm band}}\frac{e^{-\beta E_N^{\rm band}}}{Z_{\rm band}}\langle N_{\rm band}\,|\,c_1^\dagger c_2 c_3\cdots\,|\,N_{\rm band}\,\rangle\langle N_{\rm band}\,|\,c_4 c_5^\dagger c_6\cdots\,|\,N_{\rm band}\,\rangle\cdots\ ,$$

Wick's theorem may be applied independently in successive matrix elements. Thus

$$\mathrm{Tr}_f\sum_{N_{\rm band}}\frac{e^{-\beta E_N^{\rm band}}}{Z_{\rm band}}\left\langle N_{\rm band}\left|[z-(H_0-E_N^{\rm band})]^{-1}\sum_{n=0}^{\infty}[\hat{\Sigma}(z+E_N^{\rm band})[z-(H_0-E_N^{\rm band})]^{-1}]^n\right|N_{\rm band}\right\rangle$$
$$=\mathrm{Tr}_f(z-H_f)^{-1}\sum_{n=0}^{\infty}[\hat{\Sigma}_f(z)(z-H_f)^{-1}]^n\ ,$$

where

TABLE III. Diagrammatic rules for evaluating the infinite-U Anderson partition function. We list below rules for evaluating the partition function Z_f using the expression in Eq. (2.14).

To compute a general contribution to Z_f of $O(V^{2n})$, $n \geq 1$:
(a) Set down $2n$ vertices in a vertical line. Draw wavy (dashed) lines entering the bottom vertex and leaving the top to indicate an initially empty (occupied) f level. Alternate wave and dashed lines between the vertices from bottom to top. (A total of $2n+1$ lines now appear.)
(b) Always working to the right of the vertical line, connect the vertices with full lines (representing conduction electrons) in all possible ways that maintain the direction of the dashed lines at each vertex.
(c) Assign quantum numbers km (m) to full lines (dashed lines), conserving angular momentum at each vertex.
(d) Assign to ascending conduction lines a factor $\langle c_{km} c_{km}^{\dagger} \rangle = 1 - f_{km}$ and to descending conduction lines a factor $\langle c_{km}^{\dagger} c_{km} \rangle = f_{km}$, with f the Fermi function. Draw a perpendicular to each local configuration line, and assign to it an energy denominator $(z - E_\alpha)^{-1}$, where E_α is found by adding the energies of ascending lines intersected by the perpendicular and subtracting the energies of descending lines intersected.
(e) Multiply the product of energy denominators and Fermi factors by $V^{2n}(-)^c$, where c is the number of conduction line crossings. Sum on all internal variables. Compute the contour integral

$$Z = \int_\Gamma \frac{dz}{2\pi i} e^{-\beta z} R(z) ,$$

where R is the result of the preceding operations and Γ encircles all singularities of R in a counterclockwise fashion.

$$\langle N_f \mid \hat{\Sigma}_f(z) \mid N_f \rangle \equiv \sum_{N_{\rm band}} \frac{e^{-\beta E_N^{\rm band}}}{Z_{\rm band}} \langle N_f N_{\rm band} \mid \hat{\Sigma}(z + E_N^{\rm band}) \mid N_f N_{\rm band} \rangle . \tag{2.15}$$

It follows that

$$Z / Z_{\rm band} = \int_\Gamma \frac{dz}{2\pi i} e^{-\beta z} {\rm Tr}_f \frac{1}{z - H_f - \hat{\Sigma}_f(z)} . \tag{2.16}$$

The complex function

$$G_0(z) \equiv \left\langle 0 \left| \frac{1}{z - H_f - \hat{\Sigma}_f(z)} \right| 0 \right\rangle = \left\langle 0 \left| \left[\sum_{N_{\rm band}} \frac{e^{-\beta E_N^{\rm band}}}{Z_{\rm band}} \left\langle N_{\rm band} \left| \frac{1}{z - (H - E_N^{\rm band})} \right| N_{\rm band} \right\rangle \right] \right| 0 \right\rangle \tag{2.17a}$$

is commonly called the empty-state *propagator*. Analogous propagators $G_m(z)$ may be defined for the occupied states. These quantities are the analog of Feynman propagators within the contour integral formalism. The associated densities,

$$\rho_{0,m}(\varepsilon) = -\frac{1}{\pi} {\rm Im} G_{0,m}(\varepsilon + i0^+) , \tag{2.17b}$$

have a simple physical interpretation at zero temperature. In this limit, the only band state contributing to the thermal average in Eq. (2.17) is the zero-energy Fermi sea $\mid \Omega \rangle$. Inserting the exact representation

$$(z - H)^{-1} = \sum_\Phi \frac{\mid \Phi \rangle \langle \Phi \mid}{z - E_\Phi} , \tag{2.17c}$$

with Φ the eigenstates of the full Anderson Hamiltonian, gives

$$\begin{aligned} \rho_0(\varepsilon) &= \sum_\Phi \mid \langle 0; \Omega \mid \Phi \rangle \mid^2 \delta(\varepsilon - E_\Phi) , \\ \rho_m(\varepsilon) &= \sum_\Phi \mid \langle m; \Omega \mid \Phi \rangle \mid^2 \delta(\varepsilon - E_\Phi) . \end{aligned} \tag{2.18}$$

The zero-temperature densities measure the overlap of the noninteracting "ground states" $\mid 0; \Omega \rangle$ and $\mid m; \Omega \rangle$ with interacting states of energy ε. As mentioned in Sec. I.D, one expects these overlaps to exhibit an infrared singularity for $\varepsilon \to E_G$, the ground-state energy of H.

Related densities $\bar{\rho}_0$ and $\bar{\rho}_m$ may be defined to measure the overlap of the exact ground state with noninteracting excited states:

$$\bar{\rho}_{0,m}(\varepsilon) \equiv (Z / Z_{\rm band})^{-1} e^{-\beta\varepsilon} \rho_{0,m}(\varepsilon) . \tag{2.19a}$$

It is easy to show that at zero temperature

$$\bar{\rho}_0(E_G - \varepsilon) = \sum_{N_{\rm band}} \mid \langle 0; N_{\rm band} \mid \Phi_0 \rangle \mid^2 \delta(\varepsilon - E_N^{\rm band}) , \tag{2.19b}$$

with $\mid \Phi_0 \rangle$ the interacting ground state. An analogous expression holds for the occupied states $\mid m; N_{\rm band} \rangle$. In this case, the overlap functions are expected to exhibit infrared singularities in the limit $\varepsilon \to 0$. We shall return to a more detailed discussion of the zero-temperature overlap functions and the infrared catastrophe in Sec. V.B.

For low-order perturbation theory in $1/N$ it is con-

venient to replace Eq. (2.16) with the analog of Eq. (2.10). The resulting representation for the partition function is

$$Z/Z_{\rm band}=1+Ne^{-\beta\varepsilon_f} -\beta\int_0^1\frac{dg}{g}\int_\Gamma\frac{dz}{2\pi i}e^{-\beta z}\mathrm{Tr}_f\frac{\hat\Sigma_f(z,g)}{z-H_f-\hat\Sigma_f(z,g)}\ , \tag{2.20a}$$

with

$$\hat\Sigma_f(z,g)=\hat\Sigma_f(z)\,|_{V\to gV}\ . \tag{2.20b}$$

Diagrammatic rules for evaluating the components of $\hat\Sigma_f$ may be obtained from those in Table III by (a) truncating the lines that leave the highest vertex and (b) dropping all diagrams that may be disconnected by cutting a single local configuration line. For convenience we summarize these rules separately in Table IV.

The work required in a large-N calculation based on Eq. (2.20) may be cut in half by the following observation: every empty-state contribution to $Z/Z_{\rm band}$ corresponds to an occupied-state contribution found by cyclically permuting vertices. (An example of two diagrams related by such a vertex permutation is shown in Fig. 3.) A further permutation yields an additional empty-state contribution. It is easy to show that diagrams related by a vertex permutation contribute equally to the partition function. Hence it suffices to calculate only empty-state contributions and multiply by a factor of 2. The partition function may then be rewritten

$$Z/Z_{\rm band}=1+Ne^{-\beta\varepsilon_f} -\beta\int_0^1\frac{dg}{g}\int\frac{dz}{\pi i}e^{-\beta z}\frac{\Sigma_0(z,g)}{z-\Sigma_0(z,g)}\ . \tag{2.21}$$

This expression has been used by Brandt, Keiter, and Liu (1985) to generate a $1/N$ expansion for the finite-temperature Anderson partition function. The ground-state energy, zero-temperature magnetic susceptibility, and f valence were previously derived at $O(1/N)$ by Rasul and Hewson (1984a) using a slightly different technique. The derivation of Brandt, Keiter, and Liu is sketched below.

The contribution to Σ_0 at $O(1)$ is shown in Fig. 4:

$$\Sigma_0^{(1)}(z,g)=g^2NV^2\sum_k\frac{f_k}{z+\varepsilon_k-\varepsilon_f}\ . \tag{2.22}$$

Contributions to Σ_0 of $O(1/N)$ are those shown in Fig. 5:

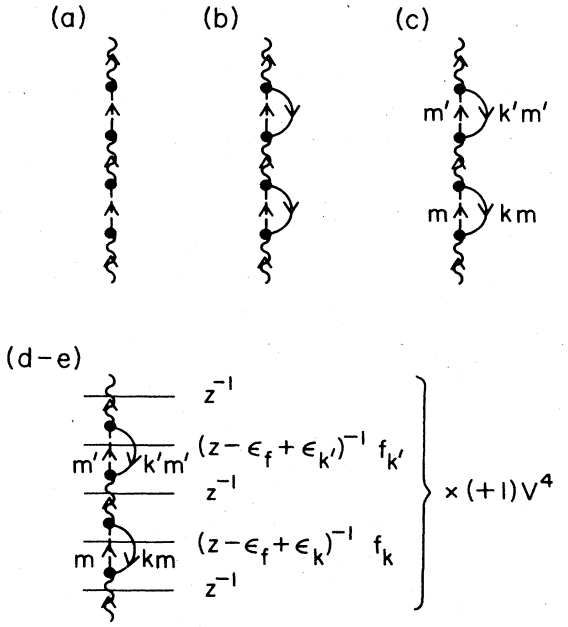

FIG. 2. Illustration of diagrammatic perturbation theory for the Anderson partition function [Eq. (2.14)]. The diagram constructed is an empty-state contribution of $O(V^4)$. (a) Vertices and f-electron lines. Four vertices (solid dots) appear, since the diagram is $O(V^4)$. Wavy lines represent the empty f level and dashed lines an occupied f level. (b) Addition of conduction electrons. Solid lines, representing conduction electrons, are added to the right of the diagram. Dashed and solid lines form continuous loops or paths through the diagram. (c) Assignment of quantum numbers. Occupied f lines receive a magnetic quantum number, and conduction lines a magnetic quantum number and momentum. Angular momentum is conserved at each vertex. (d) and (e) Assignment of Fermi functions, energy denominators, factors of V, and an overall sign. Since the perpendicular between the two lowest vertices intersects an ascending f line and a descending conduction line, the associated energy denominator is $(z+\varepsilon_k-\varepsilon_f)^{-1}$; other energy denominators are obtained in the same way. The diagram receives a factor of $(+1)V^4$, since no conduction line crossings appear and there are four vertices. There are in addition two angular momentum sums and two momentum sums. Thus the diagram contributes to $Z/Z_{\rm band}$

$$(NV^2)^2\int_\Gamma\frac{dz}{2\pi i}e^{-\beta z}\frac{1}{z}\left[\frac{1}{z}\sum_k\frac{f_k}{z+\varepsilon_k-\varepsilon_f}\right]^2,$$

a quantity of $O(1)$ in the large-N expansion.

$$\Sigma_0^{(1/N)}(z,g)=\frac{g^4}{N}(NV^2)^2\sum_{kk'}\frac{f_k(1-f_{k'})}{(z+\varepsilon_k-\varepsilon_f)^2}\frac{1}{z+\varepsilon_k-\varepsilon_{k'}-\Sigma_0^{(1)}(z+\varepsilon_k-\varepsilon_{k'},g)}\ . \tag{2.23}$$

Substituting Eq. (2.22) in (2.21) gives at leading order

$$Z^{(1)}/Z_{\rm band}=1+Ne^{-\beta\varepsilon_f}-\beta\int_0^1\frac{dg}{g}\int_\Gamma\frac{dz}{\pi i}e^{-\beta z}\frac{\Sigma_0^{(1)}(z,g)}{z-\Sigma_0^{(1)}(z,g)}=1+Ne^{-\beta\varepsilon_f}+\beta\int_\Gamma\frac{dz}{2\pi i}e^{-\beta z}\ln\left[\frac{z-\Sigma_0^{(1)}(z)}{z}\right], \tag{2.24a}$$

after performing the integration over g. Integration by parts gives finally

TABLE IV. Diagrammatic rules for evaluating configurational self-energies in the infinite-U Anderson model. We list below rules for evaluating the empty- and occupied-state self-energies defined in Eq. (2.20).

To compute a general contribution to the empty-state (occupied-state) self-energy at $O(V^{2n})$, $n \geq 1$:
(a) Set down $2n$ vertices in a vertical line. Beginning at the bottom with a dashed (wavy) line, connect the vertices with alternate dashed and wavy lines (all ascending). (A total of $2n-1$ lines now appear.)
(b) Always working to the right of the vertical line, connect the vertices with full lines in all possible ways that maintain the direction of the dashed lines at each vertex. Disregard diagrams that may be disconnected by cutting a single local configuration line—they do not contribute to the irreducible self-energy.
(c) Assign quantum numbers km (m) to full lines (dashed lines), conserving angular momentum at each vertex.
(d) Assign to ascending conduction lines a factor $1-f_{km}$ and to descending conduction lines a factor f_{km}, with f the Fermi function. Draw a perpendicular to each local configuration line, and assign to it an energy denominator $(z-E_\alpha)^{-1}$, where E_α is found by adding the energies of ascending lines intersected by the perpendicular and subtracting the energies of descending lines intersected.
(e) Multiply the product of energy denominators and Fermi factors by $(gV)^{2n}(-)^c$, where c is the number of conduction line crossings. Sum on all internal variables.

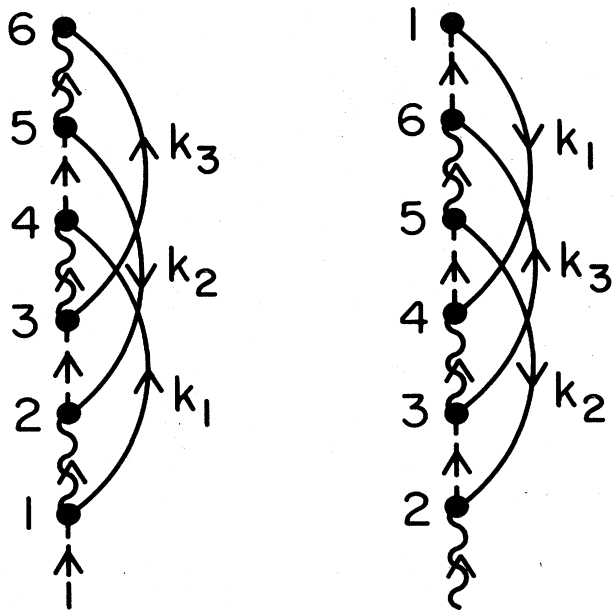

FIG. 3. A two-member family of coupling-constant diagrams [Eq. (2.20)]. The second diagram may be obtained from the first by detaching vertex 1 from the empty-state line above it, then swinging this vertex (together with its attached conduction and occupied-state lines) to the top of the diagram. After performing the coupling-constant integration, one obtains from these diagrams

$$(-1)V^6-\frac{\beta}{6}\int_\Gamma \frac{dz}{2\pi i}e^{-\beta z}\frac{1}{z-\varepsilon_f}\sum_{k_i}(1-f_{k_1})f_{k_2}(1-f_{k_3})\frac{1}{z-\varepsilon_{k_1}}\frac{1}{z-\varepsilon_{k_1}+\varepsilon_{k_2}-\varepsilon_f}\frac{1}{z-\varepsilon_{k_1}+\varepsilon_{k_2}-\varepsilon_{k_3}}\frac{1}{z+\varepsilon_{k_2}-\varepsilon_{k_3}-\varepsilon_f}\frac{1}{z-\varepsilon_{k_3}}$$

$$=(-1)V^6-\frac{\beta}{6}\int_\Gamma \frac{dz}{2\pi i}e^{-\beta z}\frac{1}{z}\sum_{k_i}f_{k_2}(1-f_{k_3})f_{k_1}\frac{1}{z+\varepsilon_{k_2}-\varepsilon_f}\frac{1}{z+\varepsilon_{k_2}-\varepsilon_{k_3}}$$

$$\times\frac{1}{z+\varepsilon_{k_2}-\varepsilon_{k_3}+\varepsilon_{k_1}-\varepsilon_f}\frac{1}{z-\varepsilon_{k_3}+\varepsilon_{k_1}}\frac{1}{z+\varepsilon_{k_1}-\varepsilon_f}.$$

The equality of the two expressions follows by letting $z\to z+\varepsilon_{k_1}$ in the first integral.

$$Z^{(1)}/Z_{\text{band}} = Ne^{-\beta\varepsilon_f} + \int_\Gamma \frac{dz}{2\pi i} e^{-\beta z} \frac{1-\partial\Sigma_0^{(1)}(z)/\partial z}{z-\Sigma_0^{(1)}(z)} . \tag{2.24b}$$

As noted by Brandt, Keiter, and Liu (1985), the first term is actually $O(N)$, rather than $O(1)$. This term formally dominates the expansion at finite temperature for $N\to\infty$. However, in the zero-temperature limit, this term is exponentially small and may be safely neglected.

The $O(1/N)$ contribution to Z/Z_{band} follows by similar manipulations. (The coupling-constant integration may be carried out exactly in each order of the expansion by suitable use of partial fraction techniques.) The resulting expression is

$$\begin{aligned} Z^{(1/N)}/Z_{\text{band}} &= -\beta \int_0^1 \frac{dg}{g} \int_\Gamma \frac{dz}{\pi i} e^{-\beta z} \left[\frac{\Sigma_0^{(1)}\Sigma_0^{(1/N)}}{(z-\Sigma_0^{(1)})^2} + \frac{\Sigma_0^{(1/N)}}{z-\Sigma_0^{(1)}} \right] \\ &= -\beta \int_\Gamma \frac{dz}{4\pi i} e^{-\beta z} \frac{1}{N} (NV^2)^2 \sum_{kk'} f_k(1-f_{k'}) \frac{1}{(z+\varepsilon_k-\varepsilon_f)^2} \frac{1}{[z-\Sigma_0^{(1)}(z)][z+\varepsilon_k-\varepsilon_{k'}-\Sigma_0^{(1)}(z+\varepsilon_k-\varepsilon_{k'})]} . \end{aligned} \tag{2.25}$$

The appearance of the factor $f_k(1-f_{k'})$ indicates the inclusion of one electron-hole pair beyond the $O(1)$ ground state. In the following section Eqs. (2.24) and (2.25) are used to derive the ground-state energy and zero-temperature thermodynamics at $O(1)$ and $O(1/N)$. The corrections to the partition function and thermodynamic properties of $O(1/N^2)$ have been computed by Bickers (1987).

C. Thermodynamic properties at zero temperature

Equations (2.24) and (2.25) may be used to derive the f valence (fractional occupancy of the f level), charge susceptibility, magnetic susceptibility, and specific heat to $O(1/N)$ in the Fermi-liquid regime. In this limit, the calculation may be simplified by noting that the contour integrals reduce to a pole contribution and branch-cut integrals. The contribution from branch cuts is exponentially small for $T\to 0$. We sketch the derivation below, assuming for simplicity a flat density of states, with sharp cutoffs at $\pm D$. [See Rasul and Hewson (1984a, 1984b); Brandt, Keiter, and Liu (1985).]

The dominant low-temperature contribution to $Z^{(1)}$ [Eq. (2.24b)] arises from a pole at $E_0(T)$, the most negative solution of the equation

$$\omega - \mathrm{Re}\Sigma_0^{(1)}(\omega) = 0 . \tag{2.26a}$$

For a flat density of states, $E_0(0)$ satisfies the equation

$$\omega = \frac{N\Gamma}{\pi} \ln \left| \frac{\varepsilon_f-\omega}{D} \right| . \tag{2.26b}$$

For convenience we frequently write this zero-temperature solution simply as E_0, and introduce the additional notation

$$T_A \equiv \varepsilon_f - E_0 . \tag{2.27a}$$

In the limit $|\varepsilon_f| \gg N\Gamma$, T_A is an exponentially small scale:

$$T_A \simeq D \exp\left[\frac{\pi\varepsilon_f}{N\Gamma} \right] . \tag{2.27b}$$

The solution to Eq. (2.26b) is plotted graphically in Fig. 6. Note that $E_0 < \varepsilon_f$. Thus

$$Z^{(1)}/Z_{\text{band}} \to Ne^{-\beta\varepsilon_f} + e^{-\beta E_0} \to e^{-\beta E_0} . \tag{2.28}$$

This identification holds to exponentially small terms, and E_0 is the Anderson ground-state energy to terms of $O(1)$. The zero-temperature valence, susceptibilities, and specific heat follow by differentiating $E_0(T)|_{T=0}$. The valence and susceptibilities are defined by the relations

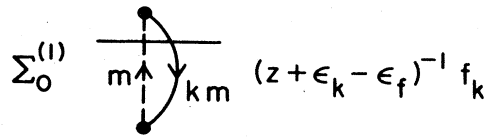

FIG. 4. Empty-state self-energy at $O(1)$, $\Sigma_0^{(1)}(z,g)$.

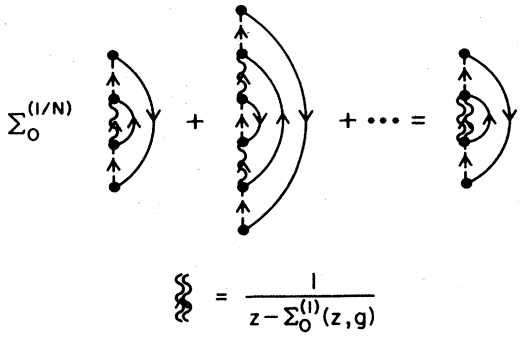

FIG. 5. Empty-state self-energy at $O(1/N)$, $\Sigma_0^{(1/N)}(z,g)$. The dressed $O(1)$ "propagator," $1/(z-\Sigma_0^{(1)})$, is denoted by a double wavy line.

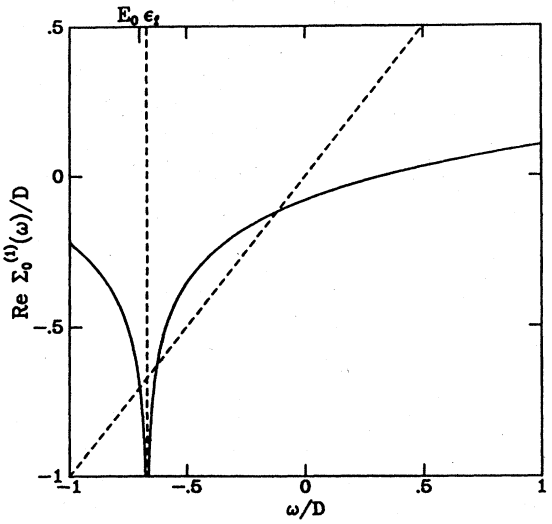

FIG. 6. Graphical solution of Eq. (2.26b) to find the ground-state energy at $O(1)$. For $\epsilon_f \ll 0$, there are in general three solutions. The lowest solution is the ground-state energy $E_0 \equiv \epsilon_f - T_A$; with exponential accuracy, $T_A = D\exp(\pi\epsilon_f/N\Gamma)$.

$$n_f^{(1)} = \frac{\partial E_0}{\partial \epsilon_f}, \quad \chi_c^{(1)} = \frac{\partial^2 E_0}{\partial \epsilon_f^2}, \quad \chi^{(1)} = -\left.\frac{\partial^2 E_0}{\partial H^2}\right|_{H\to 0} . \tag{2.29}$$

Since the free-energy $F = -T\ln Z$, the specific-heat coefficient may be found from

$$\left.\frac{\partial}{\partial T} T\ln(Z^{(1)}/Z_{\text{band}})\right|_{T\to 0} = -\left.\frac{\partial E_0(T)}{\partial T}\right|_{T\to 0} \sim \gamma^{(1)} T . \tag{2.30}$$

The valence is computed first. Differentiating Eq. (2.26) for $\omega = E_0$ gives

$$-\frac{\partial E_0}{\partial H} = -\frac{\Gamma}{\pi}\frac{\partial}{\partial H}\sum_m \int_{-D}^{D} d\varepsilon \frac{f(\varepsilon - mg\mu_B H)}{E_0 - \epsilon_f + \varepsilon}$$
$$= \frac{\Gamma}{\pi}\frac{\partial E_0}{\partial H}\sum_m \left[\int_{-D}^{D} d\varepsilon \frac{f(\varepsilon - mg\mu_B H)}{(E_0 - \epsilon_f + \varepsilon)^2} + mg\mu_B \int_{-D}^{D} d\varepsilon \frac{\partial f(\varepsilon - mg\mu_B H)}{\partial \varepsilon}\frac{1}{E_0 - \epsilon_f + \varepsilon}\right] . \tag{2.36a}$$

The right-hand side may be expanded to linear order in H as

$$\frac{N\Gamma}{\pi T_A}\left[\frac{\partial E_0}{\partial H} + \frac{1}{T_A}(g\mu_B)^2 H \frac{1}{N}\sum_m m^2\right] = \mu\left[\frac{\partial E_0}{\partial H} + \frac{\mu_j^2 H}{3T_A}\right], \tag{2.36b}$$

with

$$\mu_j^2 \equiv j(j+1)(g\mu_B)^2 . \tag{2.37}$$

Solving for $\partial E_0/\partial H$ in Eq. (2.36a), then differentiating with respect to H gives

$$\frac{\partial E_0}{\partial \epsilon_f} = \frac{N\Gamma}{\pi}\frac{\partial}{\partial \epsilon_f}\int_{-D}^{0} d\varepsilon \frac{1}{E_0 - \epsilon_f + \varepsilon}$$
$$= \left[1 - \frac{\partial E_0}{\partial \epsilon_f}\right]\frac{N\Gamma}{\pi}\int_{-D}^{0}\frac{d\varepsilon}{(E_0 - \epsilon_f + \varepsilon)^2}$$
$$= \frac{N\Gamma}{\pi T_A}\left[1 - \frac{\partial E_0}{\partial \epsilon_f}\right] . \tag{2.31}$$

Thus the $O(1)$ valence is just

$$n_f^{(1)} = \frac{\partial E_0}{\partial \epsilon_f} = \frac{\mu}{1+\mu} , \tag{2.32}$$

with

$$\mu = \frac{N\Gamma}{\pi T_A} . \tag{2.33}$$

The charge susceptibility results from differentiating Eq. (2.31) with respect to ϵ_f once more:

$$-\frac{\partial^2 E_0}{\partial \epsilon_f^2} = \frac{\partial^2 E_0}{\partial \epsilon_f^2}\frac{N\Gamma}{\pi}\int_{-D}^{0}\frac{d\varepsilon}{(E_0 - \epsilon_f + \varepsilon)^2} + \left[1 - \frac{\partial E_0}{\partial \epsilon_f}\right]^2 \frac{N\Gamma}{\pi}\int_{-D}^{0}\frac{2d\varepsilon}{(E_0 - \epsilon_f + \varepsilon)^3} , \tag{2.34}$$

i.e.,

$$\chi_c^{(1)} = -\frac{\partial^2 E_0}{\partial \epsilon_f^2} = \frac{\mu}{(1+\mu)^3}\frac{1}{T_A}$$
$$= (\pi/N\Gamma)[n_f^{(1)}]^2[1 - n_f^{(1)}] . \tag{2.35}$$

The charge susceptibility vanishes in the integral-valent limit $n_f \to 1$.

The magnetic susceptibility follows by a similar calculation. For simplicity we assume that the g factors of the f and conduction electrons are the same. (This assumption is dubious in real systems.) Note first that

$$\chi^{(1)} = \frac{\mu}{1+\mu}\frac{\mu_j^2}{3T_A} = n_f^{(1)}\frac{\mu_j^2}{3T_A} . \tag{2.38}$$

Finally, the specific heat follows from

$$-\frac{\partial E_0}{\partial T} = \frac{N\Gamma}{\pi}\int_{-D}^{D} d\varepsilon \left[-\frac{\partial f(\varepsilon)}{\partial T}\frac{1}{E_0 - \epsilon_f + \varepsilon} + \frac{f(\varepsilon)}{(E_0 - \epsilon_f + \varepsilon)^2}\frac{\partial E_0}{\partial T}\right]$$
$$= \frac{\pi^2}{3}\mu\frac{T}{T_A} + \mu\frac{\partial E_0}{\partial T} , \tag{2.39}$$

applying Sommerfeld's expansion (Ashcroft and Mermin, 1976). Thus

$$\gamma^{(1)}=\frac{\mu}{1+\mu}\frac{\pi^2}{3T_A}=n_f^{(1)}\frac{\pi^2}{3T_A}\ . \tag{2.40}$$

The Sommerfeld ratio R, i.e., the ratio of the zero-temperature susceptibility and specific-heat coefficient, has the value

$$R^{(1)}=\frac{\pi^2/3}{\mu_j^2/3}\frac{\chi^{(1)}}{\gamma^{(1)}}=1 \tag{2.41}$$

at $O(1)$ in the large-degeneracy expansion. This is the result expected for a noninteracting Fermi gas of quasiparticles.

In order to extend the expansion to $O(1/N)$, it is necessary to extract the contribution to the free energy from Eq. (2.25). As before, this contribution arises from the most negative poles of the integrand; the contribution from branch cuts is exponentially small in the limit $T\to 0$. The poles appear in the factors $[z-\Sigma_0^{(1)}(z)]^{-1}$ and $[z+\varepsilon_k-\varepsilon_{k'}-\Sigma_0^{(1)}(z+\varepsilon_k-\varepsilon_{k'})]^{-1}$ at $z=E_0$ and $z+\varepsilon_k-\varepsilon_{k'}=E_0$, with $E_0(T)$ the solution to Eq. (2.26) found previously. Since

$$Z=Z^{(1)}\left[1+\frac{Z^{(1/N)}}{Z^{(1)}}\right]+O(1/N^2)\ ,$$

the free energy may be written

$$F-F_{\rm band}=-\frac{1}{\beta}\left[\ln\left[\frac{Z^{(1)}}{Z_{\rm band}}\right]+\frac{Z^{(1/N)}}{Z^{(1)}}\right]\ . \tag{2.42}$$

When the expression for $Z^{(1/N)}$ in Eq. (2.25) is substituted, and the pole contributions extracted, the result for the excess free energy in a finite magnetic field is

$$F-F_{\rm band}=E_0(T)+\tfrac{1}{2}Z(E_0)V^4\sum_{kk'm}\left[f_k(1-f_{k'})\frac{1}{(E_0+\varepsilon_k-\varepsilon_{fm})^2}\frac{1}{E_0+\varepsilon_k-\varepsilon_{k'}-\Sigma_0^{(1)}(E_0+\varepsilon_k-\varepsilon_{k'})}+(k\leftrightarrow k')\right]\ ,$$
$$Z(E_0)=\left[1-\frac{\partial\Sigma_0^{(1)}}{\partial z}\right]^{-1}\Bigg|_{z=E_0}\ , \tag{2.43}$$

where $\varepsilon_{fm}=\varepsilon_f-mg\mu_B H$, and $\varepsilon_k,\varepsilon_{k'}$ depend on the field in the same manner. We intentionally retain a form symmetric in the indices k and k'. The denominator containing $\Sigma_0^{(1)}$ becomes singular for $\varepsilon_k\to\varepsilon_{k'}$; nevertheless, the sum of terms in large parentheses remains nonsingular in this limit. (This is an important point in the derivation of $\chi^{(1/N)}$ and $\gamma^{(1/N)}$.)

The second term in (2.43) contains several field- and temperature-dependent factors, each of which must be differentiated in calculating zero-temperature properties. The evaluation of the susceptibility and specific heat is summarized in Appendix A.

To $O(1/N)$, the susceptibility and specific heat coefficient for a flat band density of states take the form

$$\chi^{(1)}+\chi^{(1/N)}=\frac{\mu_j^2}{3}\frac{n_f^{(1)}}{T_A}\left\{1+\frac{\mu^2}{(1+\mu)N}\left[\frac{2(1+\mu)}{\mu}L_3-L_2-M-\left[2-\frac{\mu}{1+\mu}\right]L_1\right]\right\}\ ,$$
$$\gamma^{(1)}+\gamma^{(1/N)}=\frac{\pi^2/3}{\mu_j^2/3}\left[\chi^{(1)}+\chi^{(1/N)}-\frac{\chi^{(1)}}{N}\left[1-\frac{1}{(1+\mu)^2}\right]\right]\ , \tag{2.44a}$$

where

$$L_n=\int_0^{D/T_A}\frac{dy}{y+\mu\ln(1+y)}\left[1-\frac{1}{(1+y)^n}\right]\ ,$$
$$M=\int_0^{D/T_A}\frac{dy}{[y+\mu\ln(1+y)]^2}\frac{y^2(2+\mu+y)}{(1+y)^3}\ . \tag{2.44b}$$

The f valence (Rasul and Hewson, 1984b) may be written

$$n_f^{(1)}+n_f^{(1/N)}=\frac{\mu}{1+\mu}\left[1+\frac{\mu}{(1+\mu)N}\left[L_2-\mu K-\frac{\mu}{1+\mu}L_1\right]\right]\ , \tag{2.45a}$$

with

$$K=\int_0^{D/T_A}\frac{dy}{[y+\mu\ln(1+y)]^2}\frac{y^2}{(1+y)^2}\ . \tag{2.45b}$$

These results are valid to terms of relative order T_A/D when the impurity level ε_f lies within the conduction band. When the level lies outside the band, extra terms arise in the simplification of the two-dimensional integrals derived in Appendix A. (See also the discussion of this point in Sec. II.E.)

From Eq. (2.44), the Sommerfeld ratio at this order is

$$R=\frac{\pi^2/3}{\mu_j^2/3}\frac{\chi}{\gamma}=1+\frac{1}{N}\left[1-\frac{1}{(1+\mu)^2}\right]+O(1/N^2)\ . \tag{2.46}$$

This may be compared with an exact Ward identity, or Fermi liquid relation, connecting the magnetic suscepti-

bility, charge susceptibility, and specific heat of the degenerate Anderson model (Yamada, 1975; Yosida and Yamada, 1975; Yoshimori, 1976):

$$R=\frac{N}{N-1}\left[1-\frac{1}{N}\frac{\pi^2}{3}\frac{\chi_c}{\gamma}\right]$$
$$=1+\frac{1}{N}\left[1-\frac{\pi^2}{3}\frac{\chi_c^{(1)}}{\gamma^{(1)}}\right]+O(1/N^2)\,. \tag{2.47}$$

It is easy to check using Eqs. (2.35), (2.40), (2.46), and (2.47) that the Fermi liquid relation is satisfied within the large-N expansion at $O(1/N)$. Bickers (1987) has extended this conclusion to $O(1/N^2)$.

The source of Fermi-liquid-like corrections in the Sommerfeld ratio beyond $O(1)$ is the appearance of singlet electron-hole pairs in the perturbative ground state. Such a pair appears in the rightmost diagram of Fig. 5: a horizontal line cutting the $O(1)$ empty-state propagator intersects a rising band line (an electron) and a falling band line (a hole). The electron and hole lie within the same angular momentum channel and carry no net spin. Hence the pair excitation does not couple to an applied magnetic field. Nevertheless, the presence of electron-hole pairs in the interacting ground state alters the effective density of states probed by the low-temperature specific heat, increasing the Sommerfeld ratio from its Fermi-gas value of unity.

The fact that Eq. (2.47), a nontrivial identity connecting three thermodynamic properties, is satisfied order by order is one of the strongest indications that the zero-temperature $1/N$ expansion is convergent (or at least asymptotic). It is not clear *a priori* that this should be the case. If, for example, the exact expressions for n_f, χ, γ, and χ_c were nonanalytic in $1/N$ after setting NV^2 constant, infinite-order resummations of large-N perturbation theory would be required. (This is just the case for perturbation theory in the hybridization width Γ.) The fact that the Sommerfeld ratio emerges correctly does not *prove* that the ground-state expansions are convergent, but it strongly favors this possibility.

Further evidence for the validity of the zero-temperature expansions has been presented by Rasul and Hewson (1984b). After obtaining an exact relation between the band cutoffs in large-N perturbation theory and the Bethe ansatz, these authors were able to compare results for χ and n_f within the two techniques. The comparisons demonstrate agreement at $O(1)$ and $O(1/N)$ for the full range of ε_f. These results are discussed at greater length in Sec. II.F.

The convergence of systematic expansions for finite-temperature properties like $n_f(T)$ and $\chi(T)$ remains uncertain. Comparison with exact results requires the solution of the finite-temperature Bethe ansatz integral equations within an $O(1/N)$ approximation and the calculation of complicated branch-cut integrals from large-N perturbation theory. The convergence of the ground-state expansion suggests that a systematic approach may succeed at finite temperatures as well. However, at the present time, approximate infinite-order resummations of large-N perturbation theory (see Sec. V) provide a simpler route for computing finite-temperature properties.

D. Propagator for f electrons

The perturbation theory for the partition function described in Sec. II.B may be extended to correlation functions as well. The derivation of correlation functions for general many-particle systems with strong local correlations is described in Appendix B, following a treatment by Keiter and Morandi (1984). Here we state only the required result for the finite-temperature f-electron propagator $G_f(i\omega_n)$:

$$G_f(i\omega_n)=\int_0^\beta d\tau\, e^{i\omega_n\tau}G_f(\tau)\,,$$
$$G_f(\tau)\equiv-\langle T_\tau F_m(\tau)F_m^\dagger(0)\rangle\,, \tag{2.48a}$$

with

$$F_m=|0\rangle\langle m|\,, \tag{2.48b}$$

an f-orbital projection operator. In terms of the eigenstates of the unperturbed Hamiltonian $|N\rangle$,

$$G_f(i\omega_n)=\frac{1}{Z/Z_{\rm band}}\sum_{NM_i}\int_\Gamma\frac{dz}{2\pi i}\frac{e^{-\beta z}}{z}\frac{e^{-\beta E_N}}{Z_{\rm band}}\sum_{l,m=0}^{\infty}\langle N|[V(z+E_N-H_0)^{-1}]^l|M_3\rangle$$
$$\times\langle M_3|F_m|M_2\rangle\langle M_2|[(z+E_N+i\omega_n-H_0)^{-1}V]^m|M_1\rangle$$
$$\times(z+E_N-E_{M_1}+i\omega_n)^{-1}\langle M_1|F_m^\dagger|N\rangle\,. \tag{2.49}$$

This complicated expression may be simplified and given a diagrammatic interpretation using the techniques of Sec. II.B. Diagrams for the f Green's function have a simple form. The right-hand side of Eq. (2.49) closely resembles the expression for the empty-state contribution to the partition function [see Eq. (2.14)]. G_f resembles the empty-state contribution to $Z/Z_{\rm band}$ since necessarily the f configuration in the initial state $|N\rangle$ is empty. The expressions for $Z/Z_{\rm band}$ and G_f differ in the following ways: (a) only one factor of $1/z$ appears in the integral representing G_f; (b) in G_f, factors of V are at two points replaced by factors of F_m and $F_m^\dagger$; (c) in all energy denominators to the right of F_m, an additional factor of $i\omega_n$ appears.

TABLE V. Diagrammatic rules for evaluating the f Green's function $G_f(i\omega_n)$.

To compute a general contribution to $G_f(i\omega_n)$ of $O(V^{2n})$, $n \geq 0$:

(a) Set down $2n+2$ vertices (solid dots) in a vertical line. Beginning at the bottom with a dashed line, connect the vertices with alternating dashed and wavy lines (all ascending), finally leaving the top vertex on a wavy line. (A total of $2n+2$ lines now appear.)

(b) Counting from the bottom, convert the first vertex to an open circle (to represent the operator $F_m^\dagger$); convert an even-numbered vertex to an open circle (to represent the operator F_m).

(c) Always working to the right of the vertical line, connect the remaining $2n$ vertices with full lines in all possible ways that maintain the direction of the dashed line at each vertex.

(d) Working on the left side of the diagram, connect the open circles with a dash-dotted "external line," carrying energy $i\omega_n$ from top to bottom.

(e) Assign quantum numbers km (m) to full lines (dashed lines), conserving angular momentum at each vertex.

(f) Assign to ascending band lines a factor $1-f_{km}$ and to descending band lines a factor f_{km}, with f the Fermi function.

(g) Draw a perpendicular to each local configuration line and assign to it an energy denominator $(z-E_\alpha)^{-1}$, where E_α is found by adding the energies of ascending lines intersected by the perpendicular and subtracting the energies of descending lines intersected.

(h) Multiply the product of energy denominators and Fermi factors by $V^{2n}(-)^c$. Here c is the number of line crossings on the right side of the diagram. Sum on conduction momenta and internal angular momenta.

(i) Compute the contour integral

$$\frac{1}{Z_f}\int_\Gamma \frac{dz}{2\pi i} e^{-\beta z} R(z) ,$$

where R is the result of the preceding operations, Z_f is the system partition function, and Γ encircles all singularities of R in a countercloskwise fashion.

Points (b) and (c) may be implemented in each empty-state partition function diagram by replacing the band electron line which enters the lowest vertex with an "external line" of frequency $i\omega_n$. See Fig. 7. (In the figure the external line is dash-dotted and drawn to the left of the diagram to prevent confusion with conduction lines.) This means that contributions to the Green's function may trivially be obtained from diagrams for the partition function by applying the rules outlined in Table III, making the necessary replacement of a single line, and finally dividing through by Z/Z_{band}. We display the rules explicitly in Table V.

We proceed to compute contributions to G_f at $O(1)$ and $O(1/N)$, following the work of Brandt, Keiter, and Liu (1985). The diagrams contributing to G_f at $O(1)$ are displayed in Fig. 8. Summing this series gives

$$G_f^{(1)}(i\omega_n)=\frac{1}{Z^{(1)}/Z_{\text{band}}}\int_\Gamma \frac{dz}{2\pi i}\frac{e^{-\beta z}}{z}\sum_{n=0}^{\infty}\left[\frac{\Sigma_0^{(1)}(z)}{z}\right]^n \frac{1}{z+i\omega_n-\varepsilon_f}=\frac{1}{Z^{(1)}/Z_{\text{band}}}\int_\Gamma \frac{dz}{2\pi i}\frac{e^{-\beta z}}{z-\Sigma_0^{(1)}(z)}\frac{1}{z+i\omega_n-\varepsilon_f} . \tag{2.50}$$

For $T\to 0$, only the lowest pole of the integrand contributes, and

$$G_f^{(1)}(i\omega_n)=\frac{Z(E_0)}{i\omega_n-T_A},\quad Z(E_0)=\left[1-\frac{\partial\Sigma_0^{(1)}}{\partial E_0}\right]^{-1} . \tag{2.51}$$

Note that $Z^{(1)}/Z_{\text{band}}$ cancels the factor of $e^{-\beta E_0}$ at the pole. The corresponding spectral density is

$$\rho_f(\omega)\equiv-\frac{1}{\pi}\,\text{Im}G_f^{(1)}(\omega+i0^+)=Z(E_0)\delta(\omega-T_A)=[1-n_f^{(1)}]\delta(\omega-T_A) . \tag{2.52}$$

The delta function simply represents the process of adding an f electron to the ground state with energy T_A. $Z(E_0)$ may be interpreted as a quasiparticle renormalization factor, reflecting the small admixture of the empty state in the $O(1)$ ground state. The delta function is the lowest-order approximation for a narrow Fermi-surface resonance (the so-called Kondo-Abrikosov-Suhl, or Kondo, resonance). The resonance appears as a delta function in $O(1)$ treatments, since its half-width is of order $\pi T_A/N$. Low-temperature electronic transport properties are controlled by the growth of the Kondo resonance (since the conduction-electron scattering rate is directly proportional to the f spectral density).

At $O(1/N)$, a large set of contributions to G_f appear. The three types of contribution are the following: (a) self-energy insertions which lie entirely above the external ($i\omega_n$) line [see Fig. 9(a)]; (b) self-energy insertions parallel to the external line [see Fig. 9(b)]; and (c) additional contributions to Z/Z_{band} in the denominator of Eq. (2.49). Note that no contributions arise at this order from diagrams with crossing conduction lines. All contributions may be obtained by expanding the expression

$$G_f^{(1)}(i\omega_n)+G_f^{(1/N)}(i\omega_n)\sim\frac{Z_{\rm band}}{Z^{(1)}+Z^{(1/N)}}\int_\Gamma\frac{dz}{2\pi i}e^{-\beta z}\frac{1}{z-\Sigma_0^{(1)}(z)-\Sigma_0^{(1/N)}(z)}$$
$$\times\left[\frac{1}{z+i\omega_n-\varepsilon_f}+\frac{1}{(z+i\omega_n-\varepsilon_f)^2}V^2\sum_k\frac{1-f_k}{z+i\omega_n-\varepsilon_k-\Sigma_0^{(1)}(z+i\omega_n-\varepsilon_k)}\right] \tag{2.53}$$

to $O(1/N)$. This gives immediately

$$G_f^{(1/N)}(i\omega_n)=-\frac{Z^{(1/N)}}{Z^{(1)}}G_f^{(1)}(i\omega_n)+\frac{1}{Z^{(1)}/Z_{\rm band}}\int_\Gamma\frac{dz}{2\pi i}\frac{e^{-\beta z}}{(z+i\omega_n-\varepsilon_f)[z-\Sigma_0^{(1)}(z)]}$$
$$\times\left[\frac{V^2}{z+i\omega_n-\varepsilon_f}\sum_k\frac{1-f_k}{z+i\omega_n-\varepsilon_k-\Sigma_0^{(1)}(z+i\omega_n-\varepsilon_k)}+\frac{\Sigma_0^{(1/N)}(z)}{z-\Sigma_0^{(1)}(z)}\right]. \tag{2.54}$$

In this expression, $\Sigma_0^{(1/N)}$ is given by Eq. (2.23). The first term in (2.54) is a renormalization of the $O(1)$ result. The other terms may be evaluated at zero temperature by considering only pole contributions. The zero-temperature form of $G_f^{(1/N)}$ is worked out explicitly in Appendix C. Here we only quote the result:

$$G_f^{(1)}(i\omega_n)+G_f^{(1/N)}(i\omega_n)=Q(i\omega_n)+B_1(i\omega_n)+B_2(i\omega_n) \tag{2.55a}$$

with

$$Q(i\omega_n)=\frac{1}{i\omega_n-T_A}\left[Z(E_0)+\frac{\partial}{\partial z}\left[\Sigma_0^{(1/N)}(z)\frac{(z-E_0)^2}{[z-\Sigma_0^{(1)}(z)]^2}\right]_{E_0}\right],$$
$$B_1(i\omega_n)=\frac{1}{(i\omega_n-T_A)^2}Z(E_0)\left[V^2\sum_k\frac{1-f_k}{i\omega_n+E_0-\varepsilon_k-\Sigma_0^{(1)}(i\omega_n+E_0-\varepsilon_k)}-Z(E_0)\Sigma_0^{(1/N)}(E_0)\right],$$
$$B_2(i\omega_n)=-Z(E_0)V^2\sum_k\frac{f_k}{(\varepsilon_k-T_A)^2}\left[\frac{1}{-i\omega_n+E_0+\varepsilon_k-\Sigma_0^{(1)}(-i\omega_n+E_0+\varepsilon_k)}\right.$$
$$\left.-NV^2\sum_{k'}\frac{1-f_{k'}}{i\omega_n+\varepsilon_k-\varepsilon_{k'}-T_A}\frac{1}{[E_0+\varepsilon_k-\varepsilon_{k'}-\Sigma_0^{(1)}(E_0+\varepsilon_k-\varepsilon_{k'})]^2}\right], \tag{2.55b}$$
$$Z(E_0)\equiv\left[1-\frac{\partial\Sigma_0^{(1)}}{\partial E_0}\right]^{-1}.$$

The term Q is formally a quasiparticlelike propagator with excitation energy T_A, while B_1 and B_2 are background contributions singular near T_A. Closer examination (see Appendix C) reveals that Q has a logarithmically divergent quasiparticle renormalization constant. The divergence arises from soft electron-hole pairs in $\Sigma_0^{(1/N)}$. Retaining only the leading term and the most singular correction, the renormalization constant takes the form

$$(1-n_f^{(1)})\left[1+\frac{1}{N}[n_f^{(1)}]^2\ln\Lambda\right]+(\text{nonsingular}), \tag{2.56}$$

with Λ a formal infrared cutoff, i.e., a minimum electron-hole excitation energy at the Fermi surface. Remarkably, this infrared divergence is canceled by a compensating logarithm from the second term in B_2. The real and imaginary parts of the Green's function are finite for all $\omega\neq T_A$.

As shown in Appendix C both the compensating divergent contributions arise from the diagram in Fig. 9(a). This diagram represents the $O(1)$ Green's function, dressed by the lowest-order correction $\Sigma_0^{(1/N)}$ to the empty-state propagator G_0. The propagator G_0 is not itself physically measurable; however, as shown in Sec. II.B, its spectral density may be interpreted as an overlap function for eigenstates of the noninteracting and interacting Hamiltonians. If the empty-state propagator exhibited an isolated pole at the energy of the interacting ground state E_G, the residue at this pole would be precisely $|\langle 0;\Omega\,|\,\Phi_0\rangle|^2$, the overlap of the noninteracting and interacting ground states [cf. Eq. (2.18)]. Within the large-N expansion, the empty-state propagator exhibits such a pole at $O(1)$ [cf. Eq. (2.26)]. The residue is $Z(E_0)=1-n_f^{(1)}$, the quasiparticle renormalization factor introduced previously. In carrying the expansion to higher order, one implicitly assumes that this pole shifts,

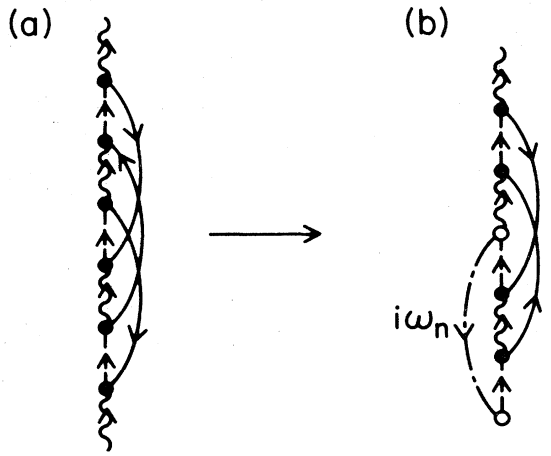

FIG. 7. Diagrammatic relation between the partition function and f Green's function. (a) An $O(1/N^2)$ empty-state contribution to Z/Z_{band} in the representation of Eq. (2.14). (b) The $O(1/N^2)$ contribution to $G_f(i\omega_n)$ analogous to diagram (a). Diagram (b) is obtained from (a) by excising the bottom empty-state line, replacing the lowest conduction line with a dash-dotted external line of "energy" $i\omega_n$, and replacing the interaction vertices at the ends of the external line with open circles, representing the operators F_m and $F_m^\dagger$.

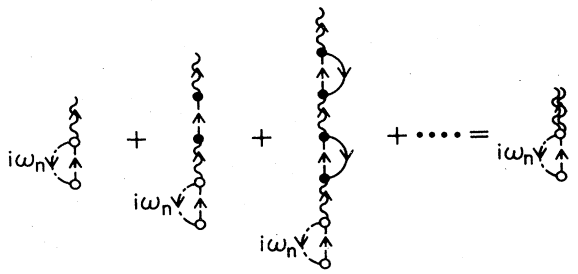

FIG. 8. Diagrams contributing to the f Green's function at $O(1)$. All contributions may be obtained by dressing the empty-state line at $O(1)$.

but remains isolated. [The shift in the pole is just the order-by-order correction to the ground-state energy, found using Eq. (2.21) or alternatively Eq. (2.16). Corrections to the quasiparticle renormalization factor do not appear explicitly in expansions based on Eq. (2.21), and cancel from expansions based on Eq. (2.16).] In fact, the quasiparticle renormalization constant diverges logarithmically when computed, order by order, in a large-N expansion. The expression for $Z(E_G)$ at $O(1/N)$ is precisely the quasiparticle renormalization constant in Q above. Read (1985) has conjectured that the logarithmic divergences in $Z(E_G)$ may be resummed as a geometric series, and that the ground-state overlap vanishes as $\Lambda^{n_f^2/N}$, with n_f the exact f valence. Such an infrared overlap catastrophe is expected on general grounds (Anderson, 1967) whenever a Fermi sea is subjected to a localized perturbation. The noninteracting ground state is effectively "lost" in a cascade of soft electron-hole pairs. The conjectured overlap exponent assumes the form expected (Nozières and de Dominicis, 1969) for N-channel scattering by a Fermi-surface resonance. The remarkable success of the large-N expansion is based on the fact that divergences due to the overlap catastrophe cancel in physical results (such as the f Green's function above).

The f-electron spectral density assumes a much simpler form at $O(1/N)$ than the full Green's function. As shown in Appendix C, for a flat density of states,

$$\rho_f^{(1/N)}(\omega)=\frac{1}{N}Z^2(E_0)\frac{N\Gamma}{\pi}\frac{1}{(\omega-T_A)^2}+R(\omega)\theta(-\omega-T_A)\ ,$$
$$R(\omega)=\frac{1}{N}Z(E_0)\left[\frac{N\Gamma}{\pi}\right]^2\int_{T_A}^{-\omega}\frac{d\varepsilon}{(\omega+\varepsilon-T_A)^2}\frac{1}{[\varepsilon-(N\Gamma/\pi)\ln(\varepsilon/T_A-1)]^2+(N\Gamma)^2},\quad -D<\omega<T_A\ . \tag{2.57a}$$

This relation was first derived by Gunnarsson and Schönhammer (1983b) within an alternate approach (see Sec. IV.B). The first contribution, which diverges quadratically at T_A, is just the lowest-order term in the expansion of the Lorentzian function

$$Z\frac{Z\Gamma/\pi}{(\omega-T_A)^2+(Z\Gamma)^2}\sim Z\frac{T_A/N}{(\omega-T_A)^2+(\pi T_A/N)^2} \tag{2.57b}$$

in powers of $1/N$. Hence, at this order, the large-N expansion is consistent with the appearance of a Fermi-surface "Kondo resonance" with excitation energy T_A, half-width $Z(E_0)\Gamma$, and weight $Z(E_0)=1-n_f^{(1)}$.

The value of the spectral density at zero frequency, i.e.,

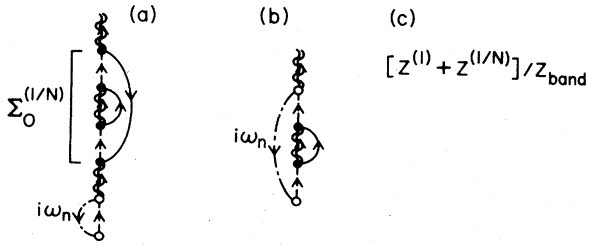

FIG. 9. Diagrams contributing to the f Green's function at $O(1/N)$. (a) Contribution from the $O(1/N)$ empty-state self-energy. Note that this correction to the $O(1)$ diagram appears above the external line. (b) Contribution from the $O(1/N)$ occupied-state self-energy. This correction appears parallel to the external line. (c) Contribution from the $O(1/N)$ term in the partition function.

at the Fermi energy, is just

$$\rho_f^{(1/N)}(0)=\frac{1}{N}\frac{\mu}{(1+\mu)^2}\frac{1}{T_A},\quad \mu=\frac{N\Gamma}{\pi T_A}\ . \tag{2.58}$$

This result satisfies the Friedel-Langreth sum rule (Friedel, 1952; Langreth, 1966), a nonperturbative relation connecting the f valence and spectral density, to $O(1/N)$. The sum rule states

$$\begin{aligned}\rho_f(0)&=\frac{1}{\pi\Gamma}\sin^2\left[\frac{\pi n_f}{N}\right]\\&=\frac{1}{N}\frac{\mu^2}{(1+\mu)^2}\frac{\pi}{N\Gamma}+O(1/N^2)\\&=\frac{1}{N}\frac{\mu}{(1+\mu)^2}\frac{1}{T_A}+O(1/N^2)\ .\end{aligned} \tag{2.59}$$

It is encouraging that the perturbative expansion satisfies an exact relation between static and dynamic quantities. This constitutes additional strong evidence that the expansion is actually convergent (at least for $T\to 0$).

For $|\omega|$, $|\varepsilon_f|$, and $N\Gamma\gg T_A$, the integral contribution to ρ_f in Eq. (2.57) may be simplified. Note that the largest contribution to the integral arises for $\varepsilon\sim-\omega$. Thus

$$\begin{aligned}R(\omega)&\sim n_f^{(1)}\frac{1}{N}\frac{N\Gamma/\pi}{[-\omega-(N\Gamma/\pi)\ln(-\omega/T_A-1)]^2+(N\Gamma)^2}\\&\quad\times\int_{T_A}^{-\omega}\frac{T_A d\varepsilon}{(\omega+\varepsilon-T_A)^2}\\&\sim n_f^{(1)}\frac{1}{N}\frac{N\Gamma/\pi}{[-\omega+\varepsilon_f-(N\Gamma/\pi)\ln(-\omega/D)]^2+(N\Gamma)^2}\ ,\end{aligned} \tag{2.60}$$

dropping terms of relative order $T_A/N\Gamma$ and $T_A/|\varepsilon_f|$. This contribution to the spectral density is a broad resonance (half-width $\sim N\Gamma$) with weight $\sim n_f^{(1)}/N$ per angular momentum channel; the resonance peaks at $\tilde{\varepsilon}_f=\varepsilon_f-\Delta\varepsilon_f$ with $\Delta\varepsilon_f$ the highest-energy solution of

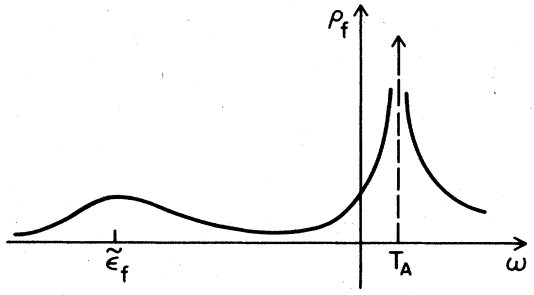

FIG. 10. Single-channel spectral density for f electrons ρ_f at $O(1/N)$. A δ function with weight $1-n_f^{(1)}+O(1/N)$ appears at $\omega=T_A$. An infinite-order summation in $1/N$ is required to smear this δ function into a true "Kondo resonance" (with half-width of order $\pi T_A/N$). A broad, nearly Lorentzian resonance (half-width of order $N\Gamma$) appears at $\tilde{\varepsilon}_f\sim\varepsilon_f$. The weight of this resonance is approximately $n_f^{(1)}/N$. The spectral weight at the Fermi energy is finite and in agreement with the Friedel-Langreth sum rule.

$$\omega=\Sigma_0^{(1)}(\omega)=\frac{N\Gamma}{\pi}\ln\left[\frac{\omega-\varepsilon_f}{D}\right]\ . \tag{2.61}$$

The characteristic two-peaked form for the $O(1/N)$ spectral density is sketched in Fig. 10.

It should be noted that the large-N expansion for G_f breaks down near $\omega=T_A$. This is because the imaginary part of the f-electron self-energy is $O(1/N)$ for all values of ω. Since the imaginary part vanishes at $O(1)$, a zero-width resonance (i.e., a delta function) appears in the spectral density at this order. The singularity at $\omega=T_A$ cannot be removed by expanding G_f and ρ_f in powers of $1/N$: at lowest order, a simple pole appears at T_A, at $O(1/N)$ a double pole [cf. Eq. (2.55b)], and so forth. The $1/N$ expansion for G_f is *nonuniform* in frequency. A nonuniform expansion may nevertheless converge pointwise at all points (except singular points like $\omega=T_A$). In particular, the singularity at T_A does not rule out the existence of a convergent expansion for G_f near zero frequency. Furthermore, a large-N expansion may still be generated for low-temperature transport properties (which depend only on the form of the f spectral density near the Fermi energy). [Transport properties in the Fermi-liquid regime have been investigated using the equivalent techniques of Sec. VI (Houghton, Read, and Won, 1987).]

E. $1/N$ perturbation theory for the Coqblin-Schrieffer model

Up to this point we have limited our discussion to techniques for treating the infinite-U Anderson model. In this section we show how these techniques may be adapted to treat the Coqblin-Schrieffer model (Coqblin and Schrieffer, 1969).

Recall from Sec. I.B that the Coqblin-Schrieffer Hamiltonian takes the form

$$\begin{aligned}&H_{\rm CS}=H_{\rm band}+H_{\rm int},\quad H_{\rm band}=\sum_{km}\varepsilon_k n_{km}\ ,\\&H_{\rm int}=-J\sum_{kk'mm'}c^\dagger_{k'm'}\,|\,m\rangle\langle m'\,|\,c_{km}\ .\end{aligned} \tag{2.62}$$

The projection operator acts within the impurity Hilbert space $\{|\,m\rangle\colon m=-j,\ldots,j\}$. We shall find it convenient to rewrite the interaction as

$$H_{\rm int}=J\sum_{kk'mm'}c_{km}\,|\,m\rangle\langle m'\,|\,c^\dagger_{k'm'}-J\sum_k 1\ . \tag{2.63}$$

The constant term may be disregarded. In this form the interaction operator resembles a product of interaction terms from the infinite-U Anderson model:

$$(c_{km}\,|\,m\rangle\langle 0\,|\,)(\,|\,0\rangle\langle m'\,|\,c^\dagger_{k'm'})\ . \tag{2.64}$$

This correspondence may be exploited to derive a simple set of perturbative rules for computing the partition function.

The coupling-constant representation for the partition function from Eq. (2.10) is

$$Z/Z_{\text{band}}=N-\beta\int_0^1\frac{dg}{g}\int_\Gamma\frac{dz}{2\pi i}\frac{e^{-\beta z}}{z}\sum_N\frac{e^{-\beta E_N}}{Z_{\text{band}}}\sum_{n=1}^{\infty}\langle N\,|\,gH_{\text{int}}\{[z-(H_{\text{band}}-E_N)]^{-1}gH_{\text{int}}\}^{n-1}\,|\,N\rangle\ . \tag{2.65}$$

A sample diagram which appears at $O(J^3)$ is shown in Fig. 11(a). The dashed lines represent states of the impurity and the solid lines band electrons; the square dots are interaction vertices. [It is easy to find the term in Eq. (2.65) which generates this diagram. We temporarily postpone the enumeration of systematic rules.] Note that two impurity lines and two band lines are attached at each vertex. Diagrams become easier to interpret if the vertices are "exploded" into wavy lines, as shown in Fig. 11(b). The wavy lines do not represent empty impurity states; they serve as a bookkeeping device. The wavy lines serve another purpose, however: when drawn in this way, the Coqblin-Schrieffer diagrams are formally identical to occupied-state partition function diagrams for the infinite-U Anderson model [cf. Eq. (2.20)]. Contributions to the Coqblin-Schrieffer partition function may be obtained from Anderson model diagrams by a graphical Schrieffer-Wolff (Schrieffer and Wolff, 1966; Keiter and Kimball, 1971) transformation. If the integration variable z in Eq. (2.18) is shifted by $z\to z+\varepsilon_f$, wavy lines in the Anderson diagrams correspond to energy denominators of the form

$$\frac{1}{z+\varepsilon_f+\sum_i\varepsilon_{k_i}}\ . \tag{2.66}$$

Each denominator may be combined with two factors of V from neighboring vertices. In the limit

$$V^2\to\infty,\quad \varepsilon_f\to-\infty,\quad V^2/\varepsilon_f=J<0\ , \tag{2.67}$$

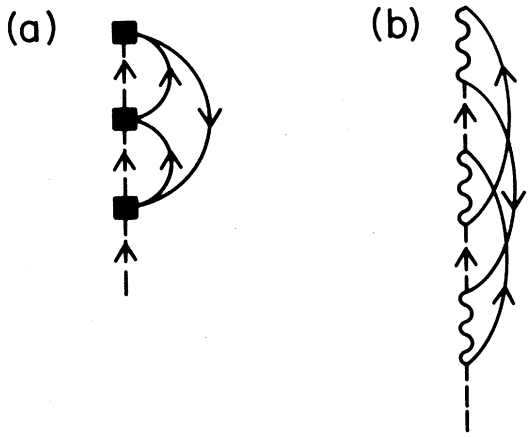

FIG. 11. Diagrams for the Coqblin-Schrieffer partition function in the representation of Eq. (2.65). (a) An $O(J^3)$ contribution to Z/Z_{band}. The local f state is represented by dashed lines and conduction electrons by solid lines. A shaded square represents the four-fermion interaction vertex; a factor gJ is associated with each vertex. (b) The same diagram shown in (a) redrawn with "exploded" vertices. This diagram closely resembles the first contribution to the Anderson partition function in Fig. 3.

every product of V^2 and an empty-state energy denominator is replaced by J. In this limit, occupied-state Anderson diagrams are mapped onto Coqblin-Schrieffer diagrams order by order in perturbation theory. The existence of such a transformation might have been anticipated from the form of the interaction in Eq. (2.63).

It is possible to write down diagrammatic rules for evaluating the partition function using Eq. (2.65). It is more convenient to introduce additional simplifications based on analogy with the Anderson model. It was demonstrated in Sec. II.B that perturbation theory for the Anderson partition function may be streamlined by computing only empty-state diagrams, then multiplying by a factor of 2; it is relatively simple to develop a $1/N$ expansion for the empty-state self-energy. The same concept may be invoked to simplify perturbation theory for the Coqblin-Schrieffer model, even though no empty state appears in the Hilbert space. The reason is that every occupied-state diagram for the infinite-U Anderson model is related by a cyclic vertex permutation to an empty-state diagram: the two diagrams contribute equally to Z. Hence contributions to the Coqblin-Schrieffer partition function may be obtained by considering either occupied- or empty-state Anderson diagrams in the limit of Eq. (2.67). If the latter choice is made, the rules in Table IV, based on the empty-state self-energy, may be adapted for the Coqblin-Schrieffer model: in Eq. (2.15), it is only necessary to shift the variable of integration z by $z\to z+\varepsilon_f$ before passing to the Coqblin-Schrieffer limit. This ensures that ε_f shows up only in empty-state denominators (which are to be converted to vertices). In addition, note that empty-state self-energy contributions enter the Coqblin-Schrieffer partition function with multiplicative factor 1, not 2. Empty-state self-energy diagrams for the Anderson model may be reinterpreted as "irreducible polarization" diagrams for the four-fermion interaction in the Coqblin-Schrieffer model. We shall generally refer to them by this name.

Perturbative rules for Z based on irreducible polarization diagrams are listed in Table VI and illustrated by an example in Fig. 12. The irreducible polarization to $O(1)$ is shown in Fig. 13(a). Thus

$$\Pi^{(1)}(z,g)\equiv g\Pi^{(1)}(z)=g(NJ)\sum_k\frac{f_k}{z+\varepsilon_k}$$
$$=-gN\gamma\int_{-D}^{D}\frac{d\varepsilon}{z+\varepsilon}f(\varepsilon)\ , \tag{2.68}$$

with

$$\gamma\equiv N(0)\,|\,J\,|\ .$$

The associated contribution to the partition function is

TABLE VI. Diagrammatic rules for evaluating the Coqblin-Schrieffer partition function using the irreducible polarization Π.

To compute a general contribution to Z of $O(J^n)$, $n \geq 1$:
(a) Set down $n+1$ short wavy lines (vertices) in a vertical line, identifying the top and bottom vertices as one. Connect the vertices with ascending dashed lines. (A total of n dashed lines appear.)
(b) Always working to the right of the vertical line, connect the vertices with full (conduction) lines in all possible ways that maintain the direction of the dashed line at each vertex. Disregard diagrams that may be disconnected by cutting a single wavy line—they do not contribute to the irreducible polarization.
(c) Assign quantum numbers km (m) to full lines (dashed lines), conserving angular momentum at each vertex.
(d) Assign to ascending conduction lines a factor $1-f_{km}$ and to descending conduction lines a factor f_{km}, with f the Fermi function. Draw a perpendicular to each impurity line and assign to it an energy denominator $(z-E_\alpha)^{-1}$, where E_α is found by adding the energies of ascending lines intersected by the perpendicular and subtracting the energies of descending lines intersected.
(e) Multiply the product of energy denominators and Fermi factors by $(gJ)^n(-)^c$, where c is the number of conduction line crossings. Sum on all internal variables. Compute the contour integral

$$Z(g)=-\beta\int_\Gamma \frac{dz}{2\pi i}e^{-\beta z}\frac{\Pi(z,g)}{1-\Pi(z,g)} ,$$

where Π is the full irreducible polarization to the required order, including the result of the previous steps, and Γ encircles all singularities of the integrand in a counterclockwise fashion. Compute the coupling-constant integral

$$\frac{Z}{Z_{\text{band}}}=\int_0^1 \frac{dg}{g}Z(g) .$$

$$\begin{aligned} Z^{(1)}/Z_{\text{band}} &= \int_0^1 \frac{dg}{g}-\beta\int_\Gamma \frac{dz}{2\pi i}e^{-\beta z}\frac{g\Pi^{(1)}(z)}{1-g\Pi^{(1)}(z)} \\ &= \beta\int_\Gamma \frac{dz}{2\pi i}e^{-\beta z}\ln[1-\Pi^{(1)}(z)] \\ &= \int_\Gamma \frac{dz}{2\pi i}e^{-\beta z}\frac{-\partial\Pi^{(1)}(z)/\partial z}{1-\Pi^{(1)}(z)} . \end{aligned} \tag{2.69}$$

This form is quite similar to that for the Anderson model [Eq. (2.24b)]. As before, in the limit $T\to 0$, the integral is dominated by an isolated pole $E_0(T)<0$ at the solution of the equation

$$\text{Re}\Pi^{(1)}(\omega)=1 . \tag{2.70}$$

(The branch cut along the positive real axis has terminus at the origin.) At $T=0$, this equation may be reduced (assuming a flat density of states) to

$$-N\gamma\ln(-E_0/D)=1 ,$$

i.e.,

$$E_0=-T_{\text{CS}} , \tag{2.71}$$

with

$$T_{\text{CS}}=De^{-1/N\gamma} .$$

This result is completely analogous to Eq. (2.27) for the infinite-U Anderson model. In the Anderson model, the

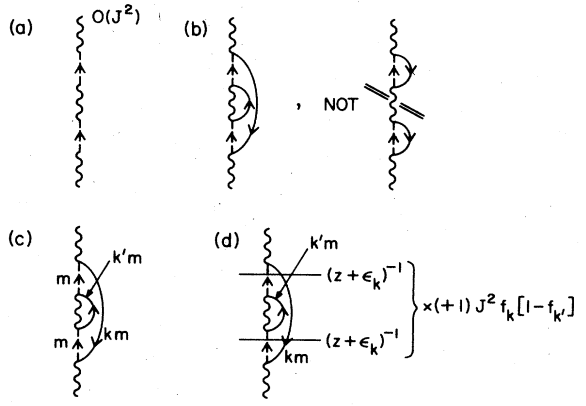

FIG. 12. Illustration of diagrammatic perturbation theory for the irreducible polarization $\Pi(z,g)$. The diagram constructed here is $O(J^2)$. (a) Vertices and f-electron lines. Three vertices appear, but the top and bottom are to be identified as one. Dashed lines represent the singly occupied f level. (b) Addition of conduction electrons (solid lines). (c) Assignment of quantum numbers. (d) Assignment of Fermi factors, energy denominators, factors of J, and an overall sign. This diagram contributes to the polarization

$$\frac{1}{N}(gNJ)^2\sum_{kk'}f_k(1-f_{k'})\frac{1}{(z+\varepsilon_k)^2} .$$

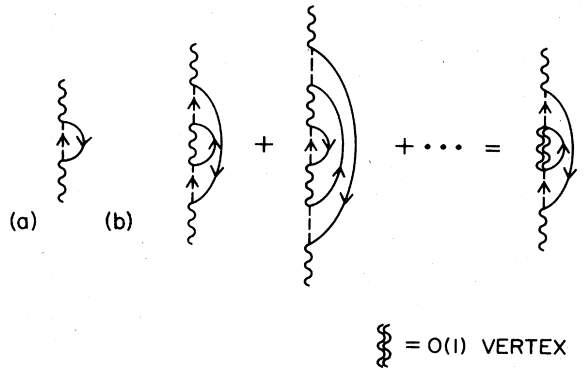

FIG. 13. Irreducible polarization for the Coqblin-Schrieffer model. (a) $O(1)$ contribution, $\Pi^{(1)}(z,g)$. (b) $O(1/N)$ contribution, $\Pi^{(1/N)}(z,g)$. The dressed $O(1)$ vertex, $gJ/[1-\Pi^{(1)}(z,g)]$ is denoted by a double wavy line.

ground-state energy is lowered by T_A at $O(1)$; in the Coqblin-Schrieffer model, the ground-state energy is lowered by T_{CS}.

The zero-temperature susceptibility and specific-heat coefficient follow by differentiating $E_0(T)$ as in Sec. II.C. One finds in this case

$$\chi^{(1)}=-\frac{\partial^2 E_0}{\partial H^2}=\frac{\mu_j^2}{3T_{CS}},\quad \mu_j^2\equiv j(j+1)(g\mu_B)^2 ,$$
$$\gamma^{(1)}=-\frac{\partial^2 E_0}{\partial T^2}=\frac{\pi^2}{3T_{CS}} , \tag{2.72}$$

and

$$R^{(1)}=\frac{\pi^2/3}{\mu_j^2/3}\frac{\chi^{(1)}}{\gamma^{(1)}}=1 .$$

These are the analogs of the results (2.38)–(2.41) for the infinite-U Anderson model. The Coqblin-Schrieffer results may be obtained from the Anderson results in the limit

$$V^2\to\infty,\quad \varepsilon_f\to-\infty,\quad \Gamma/\pi\varepsilon_f=\gamma . \tag{2.73}$$

At $O(1/N)$, the polarization diagram that must be considered is that shown in Fig. 13(b):

$$\Pi^{(1/N)}(z,g)=gJ\sum_{kk'}\frac{f_k(1-f_{k'})}{(z+\varepsilon_k)^2}\frac{gJ}{1-\Pi^{(1)}(z+\varepsilon_k-\varepsilon_{k'},g)} . \tag{2.74}$$

The contribution to $Z^{(1/N)}/Z_{\text{band}}$ analogous to that in Eq. (2.25) may be found by performing the coupling-constant integration and combining terms:

$$Z^{(1/N)}/Z_{\text{band}}=-\beta\int_\Gamma\frac{dz}{4\pi i}e^{-\beta z}\frac{1}{N}(NJ)^2\sum_{kk'}\frac{f_k(1-f_{k'})}{(z+\varepsilon_k)^2}\frac{1}{1-\Pi^{(1)}(z)}\frac{1}{1-\Pi^{(1)}(z+\varepsilon_k-\varepsilon_{k'})} . \tag{2.75}$$

Note that, in the presence of a field,

$$\frac{1}{N}(NJ)^2\sum_{kk'}\to J^2\sum_{kk'm}\quad\text{and}\quad \varepsilon_k\to\varepsilon_{km}=\varepsilon_k-mg\mu_B H . \tag{2.76}$$

From the pole contributions in the zero-temperature limit, the free-energy correction is

$$\Delta F^{(1/N)}=\tfrac{1}{2}J^2(-\partial\Pi^{(1)}/\partial E_0)^{-1}\sum_{kk'm}\left[f_k(1-f_{k'})\frac{1}{(\varepsilon_k+E_0)^2}\frac{1}{1-\Pi^{(1)}(E_0+\varepsilon_k-\varepsilon_{k'})}+(k\leftrightarrow k')\right] . \tag{2.77}$$

This expression may be differentiated with respect to field and temperature to obtain $\chi^{(1/N)}$ and $\gamma^{(1/N)}$; the derivation is parallel to that in Appendix A. In this case, some additional care is required to simplify the resulting double integrals over the conduction band. (The same care is required for the Anderson model in the Coqblin-Schrieffer limit $-\varepsilon_f\gg D$.) Omitting terms of relative order T_{CS}/D and $N\gamma$, the results are

$$\chi=\chi^{(1)}+\chi^{(1/N)}$$
$$=\frac{\mu_j^2}{3T_{CS}}\left[1+\frac{1}{N}(2\bar{L}_3-\bar{L}_1-\bar{L}_2-\bar{M}-1)\right] ,$$
$$\gamma=\gamma^{(1)}+\gamma^{(1/N)}=\frac{\pi^2/3}{\mu_j^2/3}\left[\chi^{(1)}\left[1-\frac{1}{N}\right]+\chi^{(1/N)}\right] , \tag{2.78a}$$
$$R=1+\frac{1}{N}+O\left[\frac{1}{N^2}\right] ,$$

with

$$\bar{L}_n=\int_0^{D/T_{CS}}\frac{dy}{\ln(1+y)}\left[1-\frac{1}{(1+y)^n}\right] ,$$
$$\bar{M}=\int_0^{D/T_{CS}}\frac{dy}{\ln^2(1+y)}\frac{y^2}{(1+y)^3} . \tag{2.78b}$$

As in the case of the infinite-U Anderson model, the nontrivial Sommerfeld ratio at $O(1/N)$ arises from the temperature dependence of Bose-type electron-hole pairs which do not couple to the magnetic field.

The integrals $\bar{L}_n$ and $\bar{M}$ may be evaluated analytically in this case (Rasul and Hewson, 1984a). The final expression for the magnetic susceptibility is

$$\chi=\chi^{(1)}+\chi^{(1/N)}=\frac{\mu_j^2}{3T_{CS}}\left[1-\frac{1}{N}(1-C+\ln N\gamma)+O(T_{CS}/D)+O(N\gamma)\right] , \tag{2.79}$$

where Euler's constant $C=0.577\,216$.

We emphasize again that the results above may alternately be obtained directly from the Anderson model results of Appendix A in the Coqblin-Schrieffer limit [Eq. (2.73)]. However, a simple limiting procedure in Eq. (2.44) does not yield all the terms in Eq. (2.78): this is because some of the steps in deriving (2.44) assume that $D\gg-\varepsilon_f$, rather than $-\varepsilon_f\gg D$ (see Appendix A). Also note that these results may be obtained from a pseudo-Hamiltonian approach analogous to that discussed in Sec. III for the Anderson model. In this case the pseudo-Hamiltonian takes the form

$$H_{\text{pseudo}}=H_{\text{band}}+H_{\text{int}} ,$$
$$H_{\text{band}}=\sum_{km}\varepsilon_k n_{km} , \tag{2.80}$$
$$H_{\text{int}}=-J\sum_{kk'mm'} c^{\dagger}_{k'm'}f^{\dagger}_{m}f_{m'}c_{km} \quad (J<0) .$$

The pseudo-Hamiltonian is equivalent to the Coqblin-Schrieffer Hamiltonian within the restricted Hilbert space with

$$\sum_m n_m=\sum_m f^{\dagger}_m f_m=1 . \tag{2.81}$$

Finally, it is possible to derive a functional integral representation for the Coqblin-Schrieffer partition based on Eqs. (2.80) and (2.81); using this representation, one may generate the large-N expansion for Z without introducing a coupling-constant integration (cf. Sec. III.B).

F. Comparison of large-N and Bethe ansatz results

In this section we compare the results of large-N perturbation theory at zero temperature with results of the Bethe ansatz (Andrei *et al.*, 1983; Tsvelick and Wiegmann, 1983). This comparison provides strong evidence that the large-N expansion for low-temperature thermodynamic properties is convergent, or at least asymptotic in $1/N$. The Bethe ansatz technique is a diagonalization scheme for many-particle Hamiltonians which yields exact solutions for the equilibrium properties of the infinite-U Anderson and Coqblin-Schrieffer models. These solutions serve as a benchmark with which approximate treatments, such as large-N perturbation theory, may be compared. (As yet, the Bethe ansatz has not provided solutions for dynamic properties, such as the f spectral density.) The most subtle aspect of such comparisons is the relationship between low-temperature scales in the Bethe ansatz and conventional solutions. The Bethe ansatz requires a "relativistic" spectrum for band electrons, i.e., a dispersion law $\varepsilon_k=vk$, $-\infty\le k\le\infty$, with v constant; a band cutoff at $-D_{\text{BA}}$ must be imposed on the charge-excitation spectrum of the interacting system after the fact. In contrast, conventional treatments start from a noninteracting conduction band with finite cutoffs at $\pm D$. The expressions for characteristic energy scales in the two methods consequently vary.

The relationship between energy scales in Bethe ansatz and finite-bandwidth treatments of the infinite-U Anderson model has been extensively studied by Rasul and Hewson (1984a, 1984b). It is possible to relate the cutoffs D and D_{BA} for arbitrary N by expanding Bethe ansatz and perturbative results for χ and n_f in some parameter *other than* $1/N$. It is necessary to choose another parameter since the Bethe ansatz results for these properties are not analytic in $1/N$. The general zero-temperature expressions derived by Ogievetskii, Tsvelick, and Wiegmann (1983) and by Schlottmann (1982, 1983) take the form

$$\chi=\frac{\mu_j^2}{3}\left[\frac{e^{-A}}{\Gamma(1+1/N)}+\frac{1}{2\pi}\int_{-\infty}^{\infty}d\omega\frac{\Gamma(1+i\omega)(-i\omega+0^+)^{-i\omega(N-1)/N}}{\Gamma(1+i\omega/N)(1-i\omega)}\exp(-i\omega A-\pi|\omega|/N)\right] ,$$
$$n_f=1-\frac{i}{2\pi}\int_{-\infty}^{\infty}\frac{d\omega}{\omega+i0^+}\frac{\Gamma(1+i\omega)(-i\omega+0^+)^{-i\omega(N-1)/N}}{\Gamma(1+i\omega/N)}\exp(-i\omega A-\pi|\omega|/N) , \tag{2.82}$$
$$A\equiv\pi\varepsilon_f/N\Gamma+[(N-1)/N]\ln(D_{\text{BA}}/e\Gamma)+\ln N/N .$$

The expressions in Eqs. (2.44), (2.45), and (2.82) may each be expanded in powers of $N\Gamma/\pi\varepsilon_f$ in the "empty-impurity limit," $\varepsilon_f\to\infty$. Rasul and Hewson (1984b) have demonstrated that

$$n_f=\frac{N\Gamma}{\pi\varepsilon_f}-\left[\frac{N\Gamma}{\pi\varepsilon_f}\right]^2\left[\frac{\ln N}{N}+\left[1-\frac{1}{N}\right]\ln(ND_{\text{BA}}/e\pi\varepsilon_f)\right]+O(N\Gamma/\pi\varepsilon_f)^3 \quad \text{(Bethe ansatz)} ,$$

(2.83a)

$$n_f=\frac{N\Gamma}{\pi\varepsilon_f}+\left[\frac{N\Gamma}{\pi\varepsilon_f}\right]^2\left[1-\frac{1}{N}\right][1+\ln(D/\varepsilon_f)]+O(N\Gamma/\pi\varepsilon_f)^3 \quad \text{(large-}N\text{ expansion)} ,$$

while

$$\frac{\chi}{\mu_j^2/3}=\frac{\pi}{N\Gamma}\left\{\left[\frac{N\Gamma}{\pi\varepsilon_f}\right]^2-\left[\frac{N\Gamma}{\pi\varepsilon_f}\right]^3\left[\left[1-\frac{3}{N}\right]+\frac{2\ln N}{N}+2\left[1-\frac{1}{N}\right]\ln(ND_{\text{BA}}/e\pi\varepsilon_f)\right]+O(N\Gamma/\pi\varepsilon_f)^4\right\} \quad \text{(Bethe ansatz)} ,$$

(2.83b)

$$\frac{\chi}{\mu_j^2/3}=\frac{\pi}{N\Gamma}\left\{\left[\frac{N\Gamma}{\pi\varepsilon_f}\right]^2-\left[\frac{N\Gamma}{\pi\varepsilon_f}\right]^3\left[\left[1-\frac{3}{N}\right]+2\left[1-\frac{1}{N}\right]\ln(D/\varepsilon_f)\right]+O(N\Gamma/\pi\varepsilon_f)^4\right\} \quad \text{(large-}N\text{ expansion)} .$$

[Note that all terms of $O(N\Gamma/\pi\varepsilon_f)^2$ are included in the large-N expansion for n_f at $O(1/N)$. This is because all diagrams of $O(V^4)$ enter the partition function at $O(1)$ or $O(1/N)$. A similar argument holds for the expansion of χ.] The expressions for n_f and χ above agree provided

$$D_{\mathrm{BA}}=\frac{\pi e}{N^{N/(N-1)}}D\ . \tag{2.84}$$

This is the necessary identification of cutoffs. Note that this identification does not depend on the validity of the large-N expansion. The expansion parameter is $N\Gamma/\pi\varepsilon_f$. The terms in Eq. (2.82) which prevent a series expansion in powers of $1/N$ are eliminated when D_{BA} is replaced by D; note, for instance, that

$$A=\frac{\pi\varepsilon_f}{N\Gamma}+\left[1-\frac{1}{N}\right]\ln(\pi D/N\Gamma)\ . \tag{2.85}$$

Equation (2.84) serves as the basis for comparisons of Bethe ansatz and large-N results for arbitrary ε_f (since the cutoff parameters cannot depend on the position of the f level). It has been established analytically that the expressions for n_f and χ in Eqs. (2.44), (2.45), and (2.82) agree at $O(1)$ for all values of ε_f. Further, this equivalence has been established numerically at $O(1/N)$.

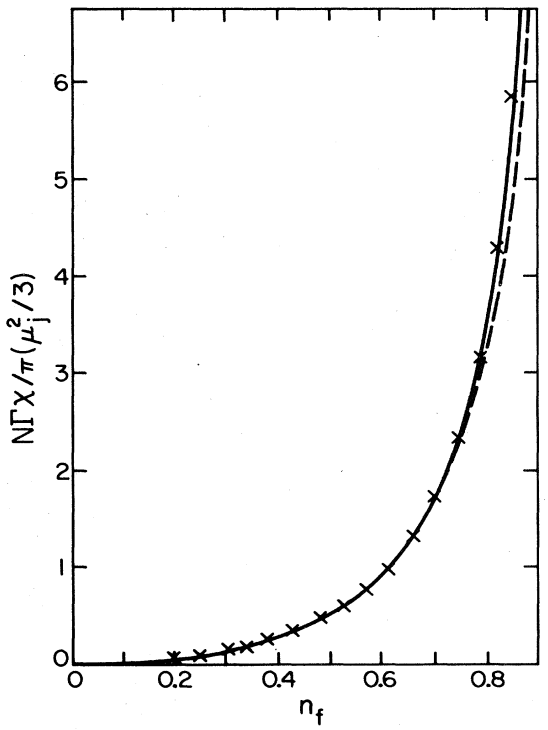

FIG. 14. Comparison of zero-temperature large-N and Bethe ansatz results for the f valence and magnetic susceptibility. The curve above is reproduced from Rasul and Hewson, 1984b. Results are shown for $N=8$, $N\Gamma/\pi D=0.01$. The full curve is the large-N result to $O(1/N)$, the dashed curve the large-N result to $O(1)$. The crosses are results of the Bethe ansatz (in terms of the conventional cutoff D) expanded to $O(1/N)$. The large-N results are in excellent agreement with the Bethe ansatz.

This requires expanding the exact Bethe ansatz results for n_f and χ to $O(1/N)$. Results for χ as a function of n_f to $O(1/N)$ are reproduced from the work of Rasul and Hewson (1984b) in Fig. 14. The curves generated by the two methods are identical within numerical accuracy. More detailed comparisons for the valence and susceptibility as functions of ε_f are contained in Rasul and Hewson (1984b).

We may summarize the logic establishing the validity of a perturbative large-N expansion at zero temperature: (i) the Bethe ansatz expressions for n_f and χ, when rewritten in terms of the cutoff D, possess a convergent (or asymptotic) expansion in $1/N$; (ii) the agreement of Bethe ansatz and perturbative results at $O(1)$ and $O(1/N)$ establishes the validity of perturbation theory. As discussed in Secs. II.C and II.D, the perturbative expansion also satisfies an exact Ward identity, or Fermi-liquid relation (Yamada, 1975; Yosida and Yamada, 1975; Yoshimori, 1976) and obeys the Friedel-Langreth sum rule (Friedel, 1952; Langreth, 1966) to $O(1/N)$. Taken together, these facts indicate that, at zero temperature and frequency, $1/N$ perturbation theory leads to convergent (or asymptotic) expansions. It is much more difficult to establish convergence at finite T or ω, but it is reasonable to believe that the expansion remains valid over a finite range.

The zero-temperature large-degeneracy expansion has been of importance in establishing the universality of Bethe ansatz and conventional (finite-bandwidth) approaches to the Coqblin-Schrieffer model (Rasul and Hewson, 1984a). For $N=2$ (the spin-$\frac{1}{2}$ Kondo model), a nonperturbative proof of universality has been provided by Andrei and Lowenstein (1981). [See also Andrei *et al.* (1983).] The proof consists of showing that the same ratio of characteristic high- and low-temperature scales is obtained in renormalization-group (finite-bandwidth) and Bethe ansatz studies. The low-temperature scale T_L is defined by the relation

$$\chi=\frac{\mu_j^2}{3}\frac{1}{T_L},\quad \mu_j^2\equiv j(j+1)(g\mu_B)^2\ . \tag{2.86}$$

The high-temperature scale has a more technical definition: at high temperature, the impurity susceptibility approaches Curie behavior with logarithmic corrections. As shown by Rasul and Hewson (1984a), the exact behavior for arbitrary N is

$$\chi(T)=\frac{\mu_j^2}{3T}\left[1-\frac{2}{N\ln(T/T_K)}-\frac{2}{N^2}\frac{\ln[\ln(T/T_K)]}{[\ln(T/T_K)]^2}+O(\ln^{-3}(T/T_K))\right]\ . \tag{2.87}$$

T_K is defined (Wilson, 1975) so that no terms of $O[\ln^{-2}(T/T_K)]$ appear in this high-temperature expansion. Rasul and Hewson (1984a) have computed T_K for the Coqblin-Schrieffer model by direct perturbation theory:

$$T_K=\frac{D}{2\pi}\exp\left[1+C-\frac{1}{2N}\right](N\gamma)^{1/N}e^{-1/N\gamma}\ , \quad (2.88)$$

with $\gamma=N(0)\,|J|$ and Euler's constant $C=0.577\,216$.

The Wilson number (Wilson, 1975), which relates high- and low-temperature scales, is by definition

$$W(N)=T_K/T_L\ . \quad (2.89)$$

This number has not been computed rigorously for arbitrary N. While the value of T_K is known within the finite-bandwidth scheme [Eq. (2.88)] and T_L is known within the Bethe ansatz (Andrei *et al.*, 1983; Tsvelick and Wiegmann, 1983), it has not been possible (for technical reasons) to derive the exact relation of the cutoffs D and $D_{\rm BA}$. (This relation *is* known for the infinite-U Anderson model [Eq. (2.84)].)

The large-N expansion for the Coqblin-Schrieffer model may be employed to derive $W(N)$ perturbatively. From Eq. (2.79), it follows that

$$T_L=D\left[1+\frac{1}{N}(1-C+\ln N\gamma)\right]e^{-1/N\gamma}+O(1/N^2)\ , \quad (2.90)$$

with C Euler's constant. Combining this result with Eq. (2.88) gives

$$\begin{aligned}W(N)&=\frac{e^{1+C}}{2\pi}\left[1-\frac{1}{N}\left[\frac{1}{2}-\ln N\gamma\right]\right]\\&\quad\times\left[1-\frac{1}{N}(1-C+\ln N\gamma)\right]+O(1/N^2)\\&=\frac{e^{1+C}}{2\pi}\left[1-\frac{1}{N}\left[\frac{3}{2}-C\right]\right]+O(1/N^2)\ . \quad (2.91)\end{aligned}$$

The Wilson number has also been calculated by a numerical technique within the Bethe ansatz for the Coqblin-Schrieffer model (Hewson and Rasul, 1983). The result postulated for arbitrary N is

$$W(N)=\frac{e^{1+C-3/2N}}{2\pi\Gamma(1+1/N)}\ . \quad (2.92)$$

This coincides exactly to $O(1/N)$ with the result above from large-N perturbation theory for the finite-bandwidth model. From the postulated exact value of $W(N)$ and the exact expression for T_K in Eq. (2.88) an exact expression for T_L (and hence χ) in the finite-bandwidth scheme may be derived:

$$\begin{aligned}&\chi=\frac{\mu_j^2}{3T_L}\ ,\\&T_L/D=\Gamma(1+1/N)e^{1/N}(N\gamma)^{1/N}e^{-1/N\gamma}\ .\end{aligned} \quad (2.93)$$

Since $W(N)$ has been established perturbatively, the arguments above do not constitute a proof of the universality of the two approaches; however, the agreement is compelling evidence in this direction. For completeness, we note that $W(N)$ for the infinite-U Anderson Hamiltonian has been derived nonperturbatively (Rasul and Hewson, 1984b) by combining (a) the Bethe ansatz result for T_L, (b) the relation (2.84) between D and $D_{\rm BA}$ (necessary for translating T_L to the finite-bandwidth scheme), and (c) results of a high-temperature expansion in the finite-bandwidth scheme. Results of the Bethe ansatz and finite-bandwidth approaches may be combined provided $D\gg|\varepsilon_f|\gg N\Gamma$ (this is required since in the Bethe ansatz approach $D_{\rm BA}\gg|\varepsilon_f|$). We list the values of T_L, T_K, and $W(N)$ for the Coqblin-Schrieffer and infinite-U Anderson models in Table VII.

TABLE VII. Temperature scales in the Coqblin-Schrieffer and infinite-U Anderson models with conventional band cutoffs. The characteristic low- and high-temperature scales in the Coqblin-Schrieffer model and the infinite-U Anderson model (for $N\Gamma\ll-\varepsilon_f\ll D$) are listed below. A flat conduction-band profile with half-width D is assumed.

Definitions

$$\chi=\frac{\mu_j^2}{3T_L}\quad(T=0)$$

$$\chi=\frac{\mu_j^2}{3T}\left[1-\frac{2}{N\ln(T/T_K)}+O\left[\frac{\ln[\ln(T/T_K)]}{[\ln(T/T_K)]^2}\right]\right]\quad(T\to\infty)$$

$$W=\frac{T_K}{T_L}$$

	Coqblin-Schrieffer	Infinite-U Anderson
T_L	$D\Gamma\left[1+\frac{1}{N}\right]e^{1/N}(N\gamma)^{1/N}e^{-1/N\gamma}$	$D\Gamma\left[1+\frac{1}{N}\right]\left[\frac{N\Gamma}{\pi D}\right]^{1/N}\exp\left[\frac{\pi\varepsilon_f}{N\Gamma}\right]$
T_K	$\frac{D}{2\pi}\exp\left[1+C-\frac{1}{2N}\right](N\gamma)^{1/N}e^{-1/N\gamma}$	$\frac{D}{2\pi}\exp\left[1+C-\frac{3}{2N}\right]\left[\frac{N\Gamma}{\pi D}\right]^{1/N}\exp\left[\frac{\pi\varepsilon_f}{N\Gamma}\right]$
W	$\frac{\exp\left[1+C-\frac{3}{2N}\right]}{2\pi\Gamma\left[1+\frac{1}{N}\right]}$	$\frac{\exp\left[1+C-\frac{3}{2N}\right]}{2\pi\Gamma\left[1+\frac{1}{N}\right]}$

III. AUXILIARY BOSON TECHNIQUE IN LARGE-N EXPANSIONS FOR THE INFINITE-U ANDERSON MODEL

In this section we discuss an alternate approach to the large-N expansion for the infinite-U Anderson model. This approach is the auxiliary boson (or slave boson) technique introduced by Barnes (1976) and Coleman (1984). This approach does not require the machinery developed in Sec. II.A and Appendix B for treating systems with strong local correlations. It instead makes use of the Feynman formulation for imaginary-time Green's functions. The two methods yield equivalent results and differ only at the formal level. The technique in Sec. II.A is, perhaps, more direct and physically motivated; on the other hand, the auxiliary boson formalism is more closely related to conventional many-body techniques based on free-particle propagators. Furthermore, the auxiliary boson approach allows the introduction of saddle-point approximations and an all-orders rearrangement of perturbation theory for the Fermi-liquid regime (see Sec. VI).

We introduce the auxiliary boson technique in Sec. III.A. To illustrate this technique, we rederive the $O(1)$ and $O(1/N)$ contributions to the partition function in Sec. III.B, employing a functional integral formalism. Finally, in Sec. III.C, we sketch the derivation of the f-electron Green's function using auxiliary bosons. The reader interested in the use of saddle-point approximations for the functional integral may wish to read Sec. III.A, then proceed directly to Sec. VI.

A. Auxiliary boson representation for the Anderson Hamiltonian

The infinite-U Anderson Hamiltonian takes the form

$$\begin{aligned} &H=H_{\rm band}+H_f+H_{\rm mix},\quad H_{\rm band}=\sum_{km}\varepsilon_k n_{km}\ , \\ &H_f=\varepsilon_f\sum_m |m\rangle\langle m|\ , \\ &H_{\rm mix}=V\sum_{km}(c_{km}^\dagger |0\rangle\langle m| +\text{H.c.})\ . \end{aligned} \tag{3.1}$$

The states $|0\rangle$ and $|m\rangle$ $(m=-j,\ldots,j)$ represent the empty and singly occupied configurations of an impurity f level. In the presence of an infinite on-site Coulomb energy, these are the only possible configurations. The occupied-state degeneracy is just $N=2j+1$. The presence of projection operators $|m\rangle\langle 0|$ and $|0\rangle\langle m|$ prevents the straightforward use of diagrammatic techniques based on free fermions. Nevertheless, the infinite-U Hamiltonian may be identified with an equivalent operator acting within a *restricted* Hilbert space of free-particle states. The use of equivalent representations of this type dates from the work of Abrikosov (1965) on the Kondo model. The complicating feature in the Kondo model is the presence of ionic spin operators. Abrikosov replaced these operators with fermion bilinears acting within a restricted Hilbert space; since the fermions that appear in perturbation theory may not be interpreted as physical particles, this approach has been termed a *pseudofermion* technique. The same type of representation for the infinite-U Anderson model was introduced by Barnes (1976) and later by Coleman (1984). In this case, projection operators may be replaced by bilinears acting within a mixed Hilbert space of Fermi and Bose states:

$$\begin{aligned} &|0\rangle\langle m|\rightarrow b^\dagger f_m,\quad |m\rangle\langle 0|\rightarrow f_m^\dagger b\ , \\ &|m\rangle\langle m|\rightarrow f_m^\dagger f_m\ . \end{aligned} \tag{3.2}$$

Here f_m and b are Fermi and Bose destruction operators. A pseudo-Hamiltonian may be defined on the full Hilbert space. It takes the form

$$H_{\rm pseudo}=H_{\rm band}+H_f+H_{\rm mix}\ ,$$

where $H_{\rm band}$ is as before and now

$$H_f=\varepsilon_f\sum_m f_m^\dagger f_m,\quad H_{\rm mix}=V\sum_{km}(c_{km}^\dagger b^\dagger f_m+\text{H.c.})\ . \tag{3.3}$$

The restricted space of physical states is the subspace for which

$$b^\dagger b+\sum_m f_m^\dagger f_m\equiv Q=1\ . \tag{3.4}$$

Within this restricted space, the properties of the pseudo-Hamiltonian are identical with those of the initial Hamiltonian (3.1). This approach has been termed an auxiliary boson technique, since a boson is introduced to represent a system that previously contained only fermions. Hereafter we drop the subscript "pseudo" in describing the auxiliary boson Hamiltonian.

The identifications in Eq. (3.2) do not constitute a unique representation. One may equally well choose the representation

$$\begin{aligned} &|0\rangle\langle m|\rightarrow f^\dagger b_m,\quad |m\rangle\langle 0|\rightarrow b_m^\dagger f\ , \\ &|m\rangle\langle m|\rightarrow b_m^\dagger b_m\ , \end{aligned} \tag{3.5}$$

with b_m and f Bose and Fermi operators. Even more general representations are possible, since the pseudo-Hamiltonian's form outside the restricted Hilbert space is completely arbitrary (Kotliar and Ruckenstein, 1986). Note, however, that this equivalence of representations generally breaks down when approximations are employed that introduce matrix elements beyond the restricted space. In this section we do not consider such approximations; the representation in (3.2) is then perfectly adequate for all derivations. [A particular saddle-point approach, which violates the rigid occupancy constraint in Eq. (3.3), becomes exact in the Fermi-liquid regime. This approach is reviewed at length in Sec. VI.]

B. Derivation of the partition function to $O(1/N)$

The auxiliary boson approach allows the exact representation of the Anderson partition function by a thermal functional integral. In this section we demonstrate how this representation may be employed to derive the Ander-

son partition function to $O(1/N)$.

The functional representation may be derived rigorously using a Trotter-type limiting procedure (Bickers, 1986). Here we merely explain the rationale for this representation and quote the result. The partition function takes the form

$$Z=\mathrm{Tr}_1 e^{-\beta H}, \tag{3.6}$$

where H is the pseudo-Hamiltonian of Eq. (3.3) and the trace is restricted to the subspace of states with $Q=1$. The trace may be extended to the full Hilbert space if an "operator delta function," which projects out the $Q=1$ subspace, is inserted. Such an operator is

$$\int_{-\pi T}^{\pi T}\frac{\beta d\lambda}{2\pi}e^{-i\beta\lambda(Q-1)}. \tag{3.7a}$$

Thus

$$Z=\int_{-\pi T}^{\pi T}\frac{\beta d\lambda}{2\pi}e^{i\beta\lambda}\mathrm{Tr}e^{-\beta H(\lambda)},\quad H(\lambda)=H+i\lambda Q. \tag{3.7b}$$

Since the trace is now performed over the full Hilbert space of Fermi and Bose states, a relatively compact functional representation is possible. In the conventional continuum notation, the partition function may be written

$$Z=\int_{-\pi T}^{\pi T}\frac{\beta d\lambda}{2\pi}e^{i\beta\lambda}\int_{cf\xi}e^{-S},\quad S=\int_0^\beta d\tau L(\tau), \tag{3.8a}$$

$$L(\tau)=\sum_{km}\bar{c}_{km}\left[\frac{\partial}{\partial\tau}+\varepsilon_{km}\right]c_{km}+\sum_m\bar{f}_m\left[\frac{\partial}{\partial\tau}+\varepsilon_{fm}+i\lambda\right]f_m+\bar{\xi}\left[\frac{\partial}{\partial\tau}+i\lambda\right]\xi+V\sum_{km}(\bar{\xi}\bar{c}_{km}f_m+\xi\bar{f}_m c_{km}),$$

with τ-dependent Grassmann fields c and f and complex field ξ. The Grassmann fields enter quadratically and may be eliminated, or traced over, in the usual way. The resulting expression involves only the complex field ξ and the time-independent "constraint field" λ. In a frequency representation, the partition function becomes

$$Z/Z_{\mathrm{band}}=\int_{-\pi T}^{\pi T}\frac{\beta d\lambda}{2\pi}e^{i\beta\lambda}(1+e^{-\beta(\varepsilon_f+i\lambda)})^N\int_\xi e^{-S}, \tag{3.8b}$$

$$S=-N\,\mathrm{Tr}\ln\left[1-V^2\sum_k\mathbf{G}(\varepsilon_f+i\lambda)\mathbf{X}\mathbf{G}(\varepsilon_k)\mathbf{X}^\dagger\right]-\beta\sum_m|\xi_m|^2D_0^{-1}(i\nu_m,i\lambda),$$

where

$$\mathbf{G}(\varepsilon_k)_{nn'}\equiv G_k(i\omega_n)\delta_{nn'}=\frac{\delta_{nn'}}{i\omega_n-\varepsilon_k},\quad \mathbf{G}(\varepsilon_f+i\lambda)_{nn'}\equiv G_f^\lambda(i\omega_n)\delta_{nn'}=\frac{\delta_{nn'}}{i\omega_n-\varepsilon_f-i\lambda}, \tag{3.8c}$$

$$D_0(i\nu_m,i\lambda)\equiv D_0^\lambda(i\nu_m)=\frac{1}{i\nu_m-i\lambda},\quad \mathbf{X}_{nn'}=\xi_{n-n'},\quad \int_\xi\equiv\int\prod_m d\bar{\xi}_m d\xi_m=\int\prod_m\frac{d(\mathrm{Re}\xi_m)d(\mathrm{Im}\xi_m)}{\pi}.$$

As always, ω_n and ν_m are Fermi and Bose Matsubara frequencies. Note that the Bose propagator is written with subscript "0." We reserve the notation D^λ for a dressed Bose propagator that appears at a later stage of the derivation. [The inverse Bose propagator that appears in the action S should strictly remain in a discretized form. We regard the form in Eq. (3.8) as a notational shorthand.]

Equation (3.8) provides a straightforward means for approximating the partition function within a large-N expansion. Before proceeding we mention an alternate form for Z/Z_{band} discussed in the literature (Coleman, 1984); this form is not so amenable to a systematic expansion in $1/N$. Instead of employing the operator delta function in Eq. (3.7a) to restrict the trace over states to the subspace with $Q=1$, one may write

$$Z=\mathrm{Tr}_1 e^{-\beta H}=\lim_{\mu\to\infty}e^{\beta\mu}\mathrm{Tr}e^{-\beta H(\mu)}Q \tag{3.9a}$$

with

$$H(\mu)=H+\mu Q.$$

The presence of Q in the trace eliminates the contribution from the subspace with $Q=0$, and contributions from subspaces with $Q>1$ are eliminated in the limit $\mu\to\infty$. It follows that

$$Z/Z_{\mathrm{band}}=\lim_{\mu\to\infty}\frac{e^{\beta\mu}\mathrm{Tr}e^{-\beta H(\mu)}Q}{\mathrm{Tr}e^{-\beta H(\mu)}}\equiv\lim_{\mu\to\infty}e^{\beta\mu}\langle Q\rangle^\mu. \tag{3.9b}$$

The operator expectation value $\langle Q\rangle^\mu$ may be evaluated by standard Feynman techniques, including the use of the linked cluster theorem. This approach is somewhat difficult to implement in large-N perturbation theory beyond $O(1)$; contributions to both $\sum_m\langle n_m\rangle$ and $\langle b^\dagger b\rangle$ must be computed at each order, and the number of diagrams that arise quickly becomes unmanageable. It is much simpler to work with Eq. (3.8). In this expression the fermions have already been eliminated, and relatively few Bose diagrams are generated at each order. This is quite analogous to the procedure in Sec. IIB. In that case, the num-

ber of partition function diagrams was reduced by considering an expansion based on the "empty-state self-energy."

We now proceed with the derivation of $Z^{(1)}$ and $Z^{(1/N)}$. The quantity NV^2 is to be treated as a constant of $O(1)$. To obtain all terms of $O(1)$, it is only necessary to retain terms of order $|\xi_m|^2$ in the action S; terms of quartic and higher order, which follow from the expansion of the logarithm in Eq. (3.8), enter with coefficients of $O(1/N^l)$, $l \geq 1$. Thus

$$S^{(1)} = -\beta \sum_m |\xi_m|^2 [D_0^{-1}(i\nu_m, i\lambda) - \Pi^\lambda(i\nu_m)] , \tag{3.10}$$

$$\Pi^\lambda(i\nu_m) \equiv NV^2 \frac{1}{\beta} \sum_{kn} G_f^\lambda(i(\omega_n + \nu_m)) G_k(i\omega_n)$$

$$= NV^2 \sum_k \frac{f(\varepsilon_k) - f(\varepsilon_f + i\lambda)}{i\nu_m - i\lambda + \varepsilon_k - \varepsilon_f} .$$

The term Π^λ follows from expanding the logarithm to lowest order, then explicitly writing out the frequency trace.

The Gaussian integral over the fluctuating fields ξ_m, assuming the $O(1)$ action, is

$$\int_\xi e^{-S^{(1)}} = (1 - e^{-i\beta\lambda})^{-1} \times \exp\left[- \sum_m \ln[1 - D_0^\lambda(i\nu_m)\Pi^\lambda(i\nu_m)] \right] . \tag{3.11}$$

The sum in the exponential may be transformed to an integral over the contour Γ_1 surrounding the imaginary axis in Fig. 15(a):

$$\sum_m \ln[1 - D_0^\lambda(i\nu_m)\Pi^\lambda(i\nu_m)] = \beta \int_{\Gamma_1} \frac{dz}{2\pi i} b(z) \ln[1 - D_0^\lambda(z)\Pi^\lambda(z)] , \tag{3.12}$$

with b the Bose function. [This step actually requires some care. For λ a real variable (as we have assumed to this point), the principal branch of the logarithm has a cut along the line $\mathrm{Im} z = \lambda$ with branch point at $E_0 + i\lambda$, $E_0 < 0$. The contour of integration Γ_1 must not cross this cut. The solution to this technical difficulty is simple: the representation in (3.8) continues to hold if the λ integration is shifted into the complex plane by $\lambda \to \lambda - i\lambda_0$, with constant λ_0. With this shift, the branch point in the logarithm is displaced to $(E_0 + \lambda_0) + i\lambda$. By choosing $E_0 + \lambda_0 > 0$, the cut may be located entirely in the right half-plane, and the step in Eq. (3.12) is allowed. We shall implicitly employ this procedure whenever necessary.] The complex integration variable may trivially be shifted by

$$z \to z + i\lambda$$

giving

$$\sum_m \ln[1 - D_0^\lambda(i\nu_m)\Pi^\lambda(i\nu_m)] = \beta \int_{\Gamma_1} \frac{dz}{2\pi i} b(z + i\lambda) \ln\left[1 - \frac{\overline{\Pi}^\lambda(z)}{z}\right] , \tag{3.13}$$

with

$$\overline{\Pi}^\lambda(z) \equiv NV^2 \sum_k \frac{f(\varepsilon_k) - f(\varepsilon_f + i\lambda)}{z + \varepsilon_k - \varepsilon_f}$$

and Γ_2 as in Fig. 15(b).

The Bose and Fermi functions may be expanded as

$$b(z + i\lambda) = e^{-\beta(z + i\lambda)} + O(e^{-2i\beta\lambda}) ,$$
$$f(\varepsilon_f + i\lambda) = e^{-\beta(\varepsilon_f + i\lambda)} + O(e^{-2i\beta\lambda}) . \tag{3.14}$$

It follows that

$$\sum_m \ln[1 - D_0^\lambda(i\nu_m)\Pi^\lambda(i\nu_m)] = \beta e^{-i\beta\lambda} \int_{\Gamma_1} \frac{dz}{2\pi i} e^{-\beta z} \ln\left[1 - \frac{\Sigma_0^{(1)}(z)}{z}\right] + O(e^{-2i\beta\lambda})$$
$$= -\beta e^{-i\beta\lambda} \int_{\Gamma} \frac{dz}{2\pi i} e^{-\beta z} \ln\left[1 - \frac{\Sigma_0^{(1)}(z)}{z}\right] + O(e^{-2i\beta\lambda}) ,$$

where

$$\Sigma_0^{(1)}(z) \equiv NV^2 \sum_k \frac{f_k}{z + \varepsilon_k - \varepsilon_f} \tag{3.15}$$

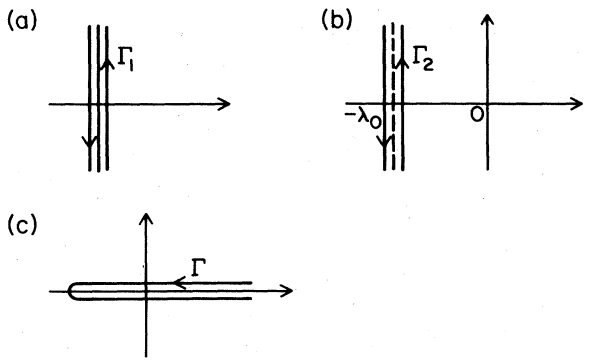

FIG. 15. Contours of integration for frequency sums. (a) Contour of integration Γ_1 for performing the Bose frequency sum in Eq. (3.12). (b) Contour of integration Γ_2 after the variable shift $z \to z + i\lambda$, with $\lambda_0 = \mathrm{Im}\lambda$. The quantity λ_0 may be chosen sufficiently negative to ensure that Γ_2 lies entirely to the left of the singularities of the logarithm in Eq. (3.13). (c) Contour of integration Γ encircling the singularities of the logarithm in a counterclockwise fashion.

and Γ is the contour illustrated in Fig. 18(c) below. (The expansion of the Bose and Fermi functions within the λ integral may be simply justified. It was already noted that λ should strictly contain a negative imaginary part. The expansions in Eq. (3.14) are then uniformly convergent for $\mathrm{Re}\lambda \in [-\pi T, \pi T]$. Note that $\Sigma_0^{(1)}$ is exactly the empty-state self-energy that appears in the treatment of Sec. II.B.)

Finally, the $O(1)$ partition function is

$$Z^{(1)} = \int_{-\pi T}^{\pi T} \frac{\beta d\lambda}{2\pi} e^{i\beta\lambda}(1+e^{-\beta(\varepsilon_f + i\lambda)})^N \frac{1}{1-e^{-i\beta\lambda}} \left[1+\beta e^{-i\beta\lambda} \int_\Gamma \frac{dz}{2\pi i} e^{-\beta z} \ln\left[1-\frac{\Sigma_0^{(1)}(z)}{z} \right] + O(e^{-2i\beta\lambda}) \right]$$

$$= N e^{-\beta\varepsilon_f} + 1 + \beta \int_\Gamma \frac{dz}{2\pi i} e^{-\beta z} \ln\left[1-\frac{\Sigma_0^{(1)}(z)}{z} \right] . \tag{3.16}$$

Integrating by parts on z gives

$$Z^{(1)} = N e^{-\beta\varepsilon_f} + \int_\Gamma \frac{dz}{2\pi i} e^{-\beta z} \frac{1-\partial\Sigma_0^{(1)}(z)/\partial z}{z-\Sigma_0^{(1)}(z)} . \tag{3.17}$$

This is precisely the expression derived for the partition function at $O(1)$ in Sec. II.B [see Eq. (2.24)]. With somewhat more effort, the $O(1/N)$ correction may be obtained. The additional term appearing in the action at $O(1/N)$ is just the second-order term in the expansion of the logarithm in Eq. (3.8):

$$S^{(1/N)} = \frac{1}{2} \frac{(NV^2)^2}{N} \sum_{kk'} \mathrm{Tr}\mathbf{G}(\varepsilon_f + i\lambda)\mathbf{X}\mathbf{G}(\varepsilon_k)\mathbf{X}^\dagger \mathbf{G}(\varepsilon_f + i\lambda)\mathbf{X}\mathbf{G}(\varepsilon_{k'})\mathbf{X}^\dagger . \tag{3.18}$$

The partition function to $O(1/N)$ becomes

$$Z = Z^{(1)} + Z^{(1/N)} = Z^{(1)} + \int_{-\pi T}^{\pi T} \frac{\beta d\lambda}{2\pi} e^{i\beta\lambda}(1+e^{-\beta(\varepsilon_f + i\lambda)})^N \int_\xi (-S^{(1/N)}) e^{-S^{(1)}}$$

with

$$S^{(1)} = -\beta \sum_m |\xi_m|^2 D^\lambda(i\nu_m), \quad D^\lambda(i\nu_m)^{-1} \equiv i\nu_m - i\lambda - \Pi^\lambda(i\nu_m) . \tag{3.19}$$

Here, D^λ is a dressed Bose propagator.

The $O(1/N)$ action may now be written out explicitly by applying the definitions of the frequency-space matrices in Eq. (3.8). The integral over ξ_m takes the form

$$\int_\xi (-S^{(1/N)}) e^{-S^{(1)}} = -\frac{1}{2} \frac{(NV^2)^2}{N} F_{m_1 m_2 m_3 m_4} \int_\xi \xi_{m_1} \bar{\xi}_{m_2} \xi_{m_3} \bar{\xi}_{m_4} e^{-S^{(1)}} , \tag{3.20a}$$

where a sum on m_i is implied, and F is an expression involving Fermi Green's functions that we do not write out explicitly. This integral may be simply evaluated by recalling the general Gaussian integral formula

$$\int d\bar{\mathbf{z}}\, d\mathbf{z}\, z_i z_j \bar{z}_k \bar{z}_l e^{-\bar{\mathbf{z}}\mathbf{A}\mathbf{z}} = (\det\mathbf{A})^{-1}[(\mathbf{A}^{-1})_{ik}(\mathbf{A}^{-1})_{jl} + (\mathbf{A}^{-1})_{il}(\mathbf{A}^{-1})_{jk}] . \tag{3.20b}$$

In this case, $\mathbf{A}^{-1}$ takes the form $-\beta^{-1}\mathbf{D}^\lambda$, i.e., it is proportional to the dressed propagator; the factor $(\det\mathbf{A})^{-1}$ is then exactly the expression which resulted from the ξ integrations in the $O(1)$ calculation [see Eq. (3.11)]. Since the dressed propagator is diagonal in frequency, the indices m_i in Eq. (3.20a) must be equal in pairs. It is straightforward to show that the resulting expression for the $1/N$ correction to Z is

$$Z^{(1/N)} = -\frac{1}{2} \frac{(NV^2)^2}{N} \int_{-\pi T}^{\pi T} \frac{\beta d\lambda}{2\pi} e^{i\beta\lambda}[1+O(e^{-i\beta\lambda})][S_1(\lambda)+S_2(\lambda)] ,$$

where

$$S_1(\lambda) = \beta^{-2} \sum_{kk'mm'n} D^\lambda(i\nu_m) D^\lambda(i\nu_{m'}) G_f^\lambda(i\omega_n) G_k(i(\omega_n - \nu_m)) G_f^\lambda(i\omega_n) G_{k'}(i(\omega_n - \nu_{m'}))$$

and

$$S_2(\lambda) = \beta^{-2} \sum_{kk'mm'n} D^\lambda(i\nu_m) D^\lambda(i\nu_{m'}) G_f^\lambda(i\omega_n) G_k(i(\omega_n - \nu_m)) G_f^\lambda(i(\omega_n - \nu_m + \nu_{m'})) G_{k'}(i(\omega_n - \nu_m)) . \tag{3.21}$$

The frequency sums S_1 and S_2 have the simple diagrammatic representation shown in Fig. 16. The only part of these sums that contribute to $Z^{(1/N)}$, i.e, the only part that survives the λ integration, is the part proportional to $e^{-i\beta\lambda}$.

It may be checked that S_2 is $O(e^{-2i\beta\lambda})$. Thus only S_1 contributes to the partition function. This frequency sum may be simply evaluated:

$$\beta^{-1}\sum_{k'm'} D^{\lambda}(i\nu_{m'})G_{k'}(i(\omega_n-\nu_{m'}))=-\sum_{k'}(1-f_{k'})D^{\lambda}(i\omega_n-\varepsilon_{k'})+O(e^{-i\beta\lambda})$$

and

$$-\beta^{-1}\sum_{k'}(1-f_{k'})\sum_{kn} D^{\lambda}(i\omega_n-\varepsilon_{k'})G_f^{\lambda}(i\omega_n)^2 G_k(i(\omega_n-\nu_m))$$
$$=-\sum_{kk'} f_k(1-f_{k'})D^{\lambda}(i\nu_m+\varepsilon_k-\varepsilon_{k'})G_f^{\lambda}(i\nu_m+\varepsilon_k)^2+O(e^{-i\beta\lambda})\ . \quad (3.22)$$

The remaining sum over m in Eq. (3.21) may be converted to a contour integral over the path Γ_1 illustrated in Fig. 15(a). Thus, finally,

$$S_1(\lambda)=-\beta\sum_{kk'} f_k(1-f_{k'})\int_{\Gamma_1}\frac{dz}{2\pi i}\frac{b(z)}{[z+\varepsilon_k-(\varepsilon_f+i\lambda)]^2}D^{\lambda}(z)D^{\lambda}(z+\varepsilon_k-\varepsilon_{k'})+O(e^{-2i\beta\lambda})\ . \quad (3.23)$$

Shifting the variable of integration along the imaginary axis, dropping higher-order contributions in $e^{-i\beta\lambda}$, and deforming the integration contour into the path in Fig. 15(c) [cf. Eqs. (3.13)—(3.15)] gives

$$S_1(\lambda)=\beta e^{-i\beta\lambda}\int_{\Gamma}\frac{dz}{2\pi i}e^{-\beta z}\sum_{kk'} f_k(1-f_{k'})\frac{1}{(z+\varepsilon_k-\varepsilon_f)^2}\frac{1}{z-\Sigma_0^{(1)}(z)}\frac{1}{z+\varepsilon_k-\varepsilon_{k'}-\Sigma_0^{(1)}(z+\varepsilon_k-\varepsilon_{k'})}+O(e^{-2i\beta\lambda})\ . \quad (3.24)$$

When the λ integral in Eq. (3.21) is finally evaluated, the result takes the form

$$Z^{(1/N)}=-\beta\int_{\Gamma}\frac{dz}{4\pi i}e^{-\beta z}\frac{1}{N}(NV^2)^2\sum_{kk'} f_k(1-f_{k'})\frac{1}{(z+\varepsilon_k-\varepsilon_f)^2}\frac{1}{[z-\Sigma_0^{(1)}(z)][z+\varepsilon_k-\varepsilon_{k'}-\Sigma_0^{(1)}(z+\varepsilon_k-\varepsilon_{k'})]}\ . \quad (3.25)$$

This is exactly the result derived in Sec. II [see Eq. (2.25)]. The chief technical advantage of the auxiliary boson approach at this order is that it eliminates the need for a coupling-constant integration; the chief disadvantage is the presence of the projection integral over λ. The derivation of thermodynamic properties from the expression for the partition function in Eqs. (3.16) and (3.25) has been carried out in Sec. II.C. Corrections to the partition function at $O(1/N^2)$ have been computed by Bickers (1987) using the approach above.

C. Auxiliary boson approach for the f-electron Green's function

To illustrate the auxiliary boson technique for computing correlation functions, we sketch below the derivation of the f-electron Green's function. Recall from Eq. (2.48) that

$$G_f(i\omega_n)=\int_0^{\beta} d\tau e^{i\omega_n\tau}G_f(\tau)\ ,$$
$$G_f(\tau)=-\langle T_\tau F_m(\tau)F_m^{\dagger}(0)\rangle\ ,$$

with

$$F_m\equiv|0\rangle\langle m|\ . \quad (3.26)$$

In the equivalent auxiliary boson representation,

$$F_m\to b^{\dagger}f_m$$

and

$$G_f(\tau)=\frac{1}{Z}\mathrm{Tr}_1 e^{-\beta H}[-T_\tau b^{\dagger}(\tau)f_m(\tau)f_m^{\dagger}(0)b(0)]\ . \quad (3.27)$$

As shown in detail in Appendix D, this expression may be evaluated in two equivalent ways:

$$G_f(\tau)=\frac{1}{Z/Z_{\mathrm{band}}}\int_{-\pi T}^{\pi T}\frac{\beta d\lambda}{2\pi}e^{i\beta\lambda}\frac{1}{Z^{\lambda}}\mathrm{Tr}e^{-\beta H(\lambda)}(-T_\tau e^{\tau H(\lambda)}b^{\dagger}f_m e^{-\tau H(\lambda)}f_m^{\dagger}b),\quad H(\lambda)\equiv H+i\lambda Q\ ,$$

or (3.28)

$$G_f(\tau)=\frac{1}{Z/Z_{\mathrm{band}}}\lim_{\mu\to\infty}e^{\beta\mu}\frac{1}{Z^{\mu}}\mathrm{Tr}e^{-\beta H(\mu)}(-T_\tau e^{\tau H(\mu)}b^{\dagger}f_m e^{-\tau H(\mu)}f_m^{\dagger}b),\quad H(\mu)\equiv H+\mu Q\ .$$

In these expressions, the functions of λ and μ obey linked cluster theorems (i.e., only connected diagrams need to be considered in perturbation theory). Note, however, that the prefactor $(Z/Z_{\mathrm{band}})^{-1}$ must be evaluated separately order by order.

To maintain continuity with Sec. III.B, we employ the first expression above. There is in this case no advantage to be gained from working with a functional integral representation in which fermions have been eliminated [see Eq. (3.8)]. Instead, we summarize in Table VIII the Feyn-

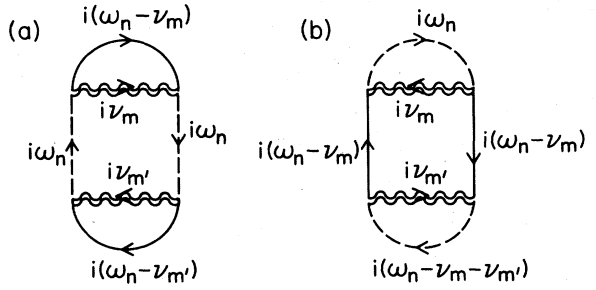

FIG. 16. Diagrammatic representation of the frequency sums in $Z^{(1/N)}$ [cf. Eq. (3.21)]. Double wavy lines represent dressed Bose propagators D^{λ} and dashed lines Fermi propagators G_f^{λ}. Solid lines represent conduction-electron propagators G_k. Each line carries a Bose or Fermi frequency, and frequency is conserved at the vertices. (a) Representation of $S_1(\lambda)$. (b) Representation of $S_2(\lambda)$.

man rules for evaluating $G_f(i\omega_n)$. These rules may be derived from a mixed Fermi-Bose functional integral or by a more conventional route. A step-by-step illustration of the rules for a specific diagram is shown in Fig. 17. Note that the Fermi and Bose propagators in every allowed diagram form a single continuous loop of Q "charge." Diagrams with multiple Q loops need not be considered, since each loop is $O(e^{-i\beta\lambda})$, and such contributions are projected away in step (h).

The frequency sums may be performed in a way that makes transparent the connection of this treatment with that in Sec. II.D. To do this, it is convenient to follow the supplemental rules below.

(e′) When labeling lines with frequency, let the Bose line that leaves the top of the diagram (and enters the bottom) carry frequency $i\nu_m$. Let this frequency and the external frequency $i\omega_n$ appear only on Fermi and Bose lines. Associate independent frequencies $i\omega_{n'}$ with conduction lines. Label the remaining lines obeying frequency conservation. An example of this labeling scheme is shown in Fig. 17.

(f′) Perform first the sums on conduction-electron frequencies (associating a factor $1/\beta$ with each sum). Each ascending line produces a sum

$$\frac{1}{\beta}\sum_{n'}\frac{1}{i\omega_{n'}-\varepsilon_k}F_A(i\nu_m-i\omega_{n'}) = -(1-f_k)F_A(i\nu_m-\varepsilon_k)+O(e^{-i\beta\lambda}) , \quad (3.29a)$$

with F_A the product of all Fermi and Bose propagators to the left of the ascending line. Each descending line produces a sum

$$\frac{1}{\beta}\sum_{n'}\frac{1}{i\omega_{n'}-\varepsilon_k}F_D(i\nu_m+i\omega_{n'})=f_kF_D(i\nu_m+\varepsilon_k) +O(e^{-i\beta\lambda}) , \quad (3.29b)$$

TABLE VIII. Diagrammatic rules for evaluating $G_f(i\omega_n)$ in the auxiliary boson formalism.

To compute a general contribution to $G_f(i\omega_n)$ of $O(V^{2n})$, $n\geq 0$:
(a) Set down $2n+2$ vertices (solid dots) in a vertical line.
(b) Beginning at the bottom with a dashed line, connect the vertices with alternating dashed (Fermi) and wavy (Bose) lines (all ascending), finally leaving the highest vertex on a wavy line. Connect this outgoing wavy line with the lowest vertex (either implicitly, or by explicitly drawing in a line). A total of $2n+2$ lines now appear.
(c) Replace the lowest vertex and another vertex directly above a dashed line with open circles, to represent the operators $b^{\dagger}f_m$ and $f_m^{\dagger}b$. To the left of the lower circle, draw an incoming (source) arrow and to the left of the upper circle, an outgoing (sink) arrow.
(d) On the right of the diagram, draw solid (conduction-electron) lines connecting the remaining solid dots (vertices). The solid lines must maintain the direction of the dashed lines entering or leaving each vertex.
(e) Assign quantum numbers km (m) to conduction (Fermi) lines, conserving angular momentum at each vertex. Assume that frequency $i\omega_n$ and angular momentum m enter the diagram through the source arrow and leave through the sink.
(f) Assign to each line a propagator, conserving frequency at each solid dot or open circle:

$$\text{Bose}\rightarrow\frac{1}{i\nu_m-i\lambda} ,$$

$$\text{Fermi}\rightarrow\frac{1}{i\omega_{n'}-(\varepsilon_f+i\lambda)} ,$$

$$\text{conduction electron}\rightarrow\frac{1}{i\omega_{n'}-\varepsilon_k} .$$

(g) Sum on internal frequencies (associating a factor $1/\beta$ with each sum), conduction-electron momenta, and angular momentum indices. (Each angular momentum sum furnishes a factor N.) Multiply the diagram by $V^{2n}(-)^{a+c+1}$, with a the number of ascending conduction lines and c the number of conduction line crossings.
(h) Perform the projection to the $Q=1$ subspace:

$$G_f(i\omega_n)=\frac{1}{Z_f}\int_{-\pi T}^{\pi T}\frac{\beta\, d\lambda}{2\pi}e^{i\beta\lambda}G_f^{\lambda}(i\omega_n) ,$$

where $G_f^{\lambda}(i\omega_n)$ is the result of the preceding operations.

with F_D the analog of F_A. *Drop* the terms of $O(e^{-i\beta\lambda})$ from the expansion, since these contributions vanish when the projection is performed. Perform the sum on ν_m (with its associated factor of $1/\beta$) last.

When these rules are applied in conjunction with those listed previously, the result takes the form

$$\frac{(NV^2)^n}{N^q}(-)^{c+1}\int_{\Gamma_2}\frac{dz}{2\pi i}e^{-\beta z}S(z)\,, \tag{3.30}$$

where c is the number of conduction line crossings [a minus sign arises for each ascending line from Eq. (3.29a)], q is the order of the diagram in $1/N$, and the contour Γ_2 is that shown in Fig. 15(b). $S(z)$ is an expression containing (i) one momentum sum for each conduction line; (ii) a factor of $1-f_k$ for each ascending conduction line and f_k for each descending conduction line; and (iii) a product of energy denominators, one for each Fermi and Bose line. From Eq. (3.29), it is easy to show that a given Fermi (Bose) denominator takes the form

$$\begin{aligned}&\frac{1}{z-\varepsilon_f-(\Sigma_a\varepsilon_{k_a}-\Sigma_d\varepsilon_{k_d})}\,,\quad\text{Fermi}\,,\\&\frac{1}{z-(\Sigma_a\varepsilon_{k_a}-\Sigma_d\varepsilon_{k_d})}\,,\quad\text{Bose}\,,\end{aligned} \tag{3.31}$$

where the sums run over all ascending and descending conduction lines to the right of the Fermi (Bose) line. Deforming the path of integration into the contour Γ shown in Fig. 15(c) gives

$$\frac{(NV^2)^n}{N^q}(-)^c\int_{\Gamma}\frac{dz}{2\pi i}e^{-\beta z}S(z)\,. \tag{3.32}$$

This expression is precisely the result for a general contribution to the f Green's function derived in Sec. II.D.

Since the Feynman rules outlined above produce results equivalent to those in Sec. II.D we shall only indicate the auxiliary boson diagrams that contribute to G_f at O(1) and $O(1/N)$. These are shown in Fig. 18 (the line connecting the highest and lowest vertices is not drawn in explicitly). The resemblance to the diagrams in Figs. 8 and 9 is obvious. Note that the rules for computing the finite-temperature Green's function in Table V are considerably more direct than those in Table VIII. The auxiliary boson approach requires an unnecessary calculation of Feynman frequency sums. The true versatility of the auxiliary boson approach is realized in the Fermi-liquid regime ($T\to 0$): in this limit, exact large-N expansions for the partition function and correlation functions may be obtained by evaluating the constraint integral over λ in an

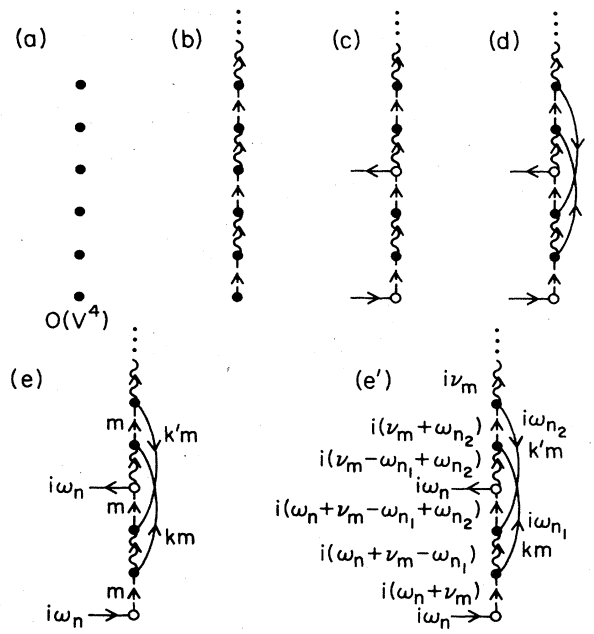

FIG. 17. Illustration of diagrammatic perturbation theory for the f Green's function using the auxiliary boson representation. The diagram constructed above is $O(V^4)$ and $O(1/N^2)$. (a) Vertices. Six solid dots are set down initially (though two will be altered shortly). (b) Local Fermi and Bose lines. A dashed line represents a local fermion and a wavy line a local boson. A dashed line flows up from the bottom vertex, then wavy and dashed lines alternate, with a wavy line flowing out of the top. The ellipsis indicates that the top line is implicitly connected to the bottom vertex as well. (c) Introduction of external lines. The bottom vertex and another, directly above a dashed line, are replaced by open circles with attached external lines, representing the operators $b^\dagger f_m$ and $f_m^\dagger b$; no factors of V are associated with the open circles. (d) Addition of conduction electrons (solid lines). (e) Assignment of quantum numbers and frequencies. The external lines introduce angular momentum m and Fermi frequency $i\omega_n$. (e') Assignment of frequencies for simple evaluation of Matsubara sums associated with conduction lines.

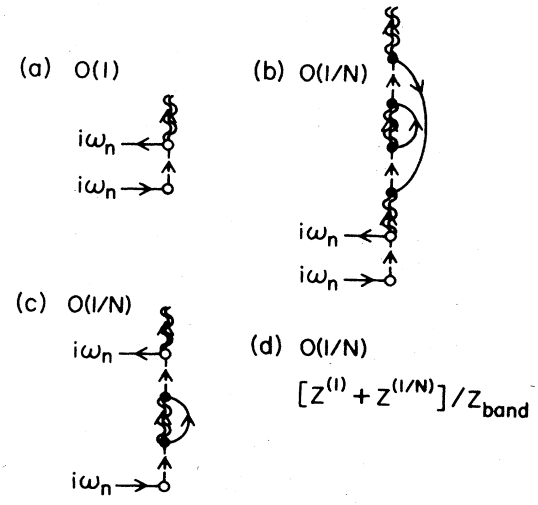

FIG. 18. Contributions to the f Green's function in the auxiliary boson representation. (a) $O(1)$ contribution. The Bose propagator is dressed to $O(1)$ using the self-energy computed in Eq. (3.30). This diagram should be compared with that in Fig. 8. (b) $O(1/N)$ contribution from a single Bose self-energy insertion; cf. Fig. 9(a). (c) $O(1/N)$ contribution from a single Fermi self-energy insertion; cf. Fig. 9(b). (d) $O(1/N)$ contribution from the partition function; cf. Fig. 9(c).

order-by-order saddle-point approximation. We discuss this powerful approach in Sec. VI.

IV. ZERO-TEMPERATURE VARIATIONAL APPROACH TO THE $1/N$ EXPANSION

The treatments of the Anderson and Coqblin-Schrieffer models reviewed in Secs. II and III are in principle valid for arbitrary temperatures. In fact, these methods have been applied almost exclusively in the zero-temperature limit. In this section we review an alternate approach for calculating zero-temperature properties of the Anderson model, the variational method of Gunnarsson and Schönhammer (1983a, 1983b, 1985, 1986). This treatment provides results for the f valence and magnetic susceptibility (both static and dynamic) and the f Green's function. The method is particularly suited to realistic calculations of the f Green's function. Calculations have been performed for various conduction electron densities of states and for finite, as well as infinite, U (Gunnarsson and Schönhammer, 1985). However, as a variational method, the technique cannot be trivially extended to finite temperatures.

In Sec. IV.A we discuss the determination of the ground-state energy and wave function, valence, and static susceptibility for the infinite-U model to $O(1)$. The extension of the calculation to $O(1/N)$ is briefly treated in Appendix E. In Sec. IV.B we discuss the calculation of the f spectral density to $O(1)$ and $O(1/N)$. In Appendix F we discuss the generalization of these techniques to finite U.

A. Zero-temperature thermodynamics within the variational approach

The Anderson model for rare-earth impurities takes the form

$$H = H_{\text{band}} + H_f + H_{\text{mix}}, \quad H_{\text{band}} = \sum_{km} \varepsilon_k n_{km} ,$$
$$H_f = \varepsilon_f \sum_m n_m + U \sum_{m>m'} n_m n_{m'} , \tag{4.1}$$
$$H_{\text{mix}} = V \sum_{km} (c_{km}^\dagger f_m + \text{H.c.}) ,$$

where $f_m^\dagger$ creates an f electron in magnetic channel m and $c_{km}^\dagger$ creates a conduction electron of wave number $k = |\mathbf{k}|$ in channel m. The ground-state energy E_G and properties that depend on it, such as the valence and magnetic susceptibility, may be computed by introducing a variational wave function $|\phi_0\rangle$. The true ground state may be denoted $|\psi_0\rangle$. In the infinite-U limit, only states with empty or singly occupied impurity orbitals contribute to $|\phi_0\rangle$ and $|\psi_0\rangle$. The simplest such states are the noninteracting vacuum $|\Omega\rangle$, i.e., a filled Fermi sea of band electrons with Fermi energy ε_F, and

$$|\varepsilon_f \varepsilon_k m\rangle = f_m^\dagger c_{km} |\Omega\rangle . \tag{4.2}$$

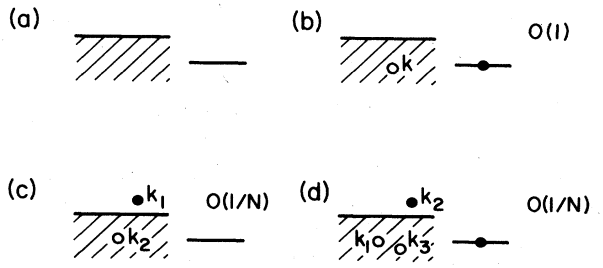

FIG. 19. Pictorial representation for components of the variational ground state. The shaded rectangle denotes the Fermi sea of conduction electrons and the adjacent line the localized f orbital. Electrons are represented by solid circles and holes by open circles. The order in $1/N$ at which each state couples to the first is indicated. (a) $|\Omega\rangle$, the filled Fermi sea and an empty f orbital; this is the simplest component of the ground state. (b) $|\varepsilon_f \varepsilon_k m\rangle$, a state containing one f electron and one conduction hole of energy ε_k, both in magnetic channel m. This set of states couples to $|\Omega\rangle$ at $O(1)$. States $|\Omega\rangle$ and $|\varepsilon_f \varepsilon_k m\rangle$ are the only states that must be considered in an $O(1)$ calculation. (c) $|E_{k_1} \varepsilon_{k_2} m\rangle$, a state containing one conduction electron and one conduction hole. The states in (b) and (c) couple at $O(1/N)$. (d) $|(\varepsilon_f \varepsilon_{k_1} m)(E_{k_2} \varepsilon_{k_3} m')\rangle$, a state containing one f electron, one conduction electron, and two conduction holes. The states in (c) and (d) couple at $O(1)$. States (a)—(d) must all be considered in an $O(1/N)$ calculation of the ground-state energy and wave function.

For convenience, throughout this section the energy of a band hole is denoted by lower-case epsilon and the energy of a band electron by upper-case E.

In general, states that couple to $|\Omega\rangle$ may be indicated pictorially. In Fig. 19, electrons are represented by filled circles and holes by empty circles; the shaded rectangle represents the filled Fermi sea, and the adjacent line the localized f level. The noninteracting vacuum $|\Omega\rangle$ is indicated in 19(a) and the f-electron—band-hole state $|\varepsilon_f \varepsilon_k m\rangle$ in 19(b). A band-electron—band-hole state

$$|E_{k_1} \varepsilon_{k_2} m\rangle = c_{k_1 m}^\dagger c_{k_2 m} |\Omega\rangle \tag{4.3}$$

is indicated in 19(c), and so on.

Since the true ground state is an angular momentum singlet, the noninteracting vacuum provides a valid starting point for a variational calculation. Further, only singlet contributions to $|\phi_0\rangle$ need be considered. Singlets may be constructed from the antisymmetrized electron-hole wave functions in Fig. 19 by summing symmetrically on all magnetic quantum numbers. The resulting wave functions may be classified by the order in $1/N$ at which they couple to $|\Omega\rangle$. As always (see Sec. I.C), it must be assumed that

$$NV^2 = O(1) \tag{4.4}$$

for $N \to \infty$. Brillouin-Wigner perturbation theory to determine the energy of state $|\Omega\rangle$ in the presence of interactions gives rise to terms of the form

$$\sum_{N_1 N_2 \cdots} \frac{\langle \Omega \mid H_{\rm mix} \mid N_1 \rangle \langle N_1 \mid H_{\rm mix} \mid N_2 \rangle \langle N_2 \cdots H_{\rm mix} \mid \Omega \rangle}{\text{energy denominator}} . \tag{4.5}$$

A given electron-hole singlet may be classified by counting powers of $1/N$ in the product of matrix elements that contains that state at lowest order. Note that by electron number conservation, all contributions to Eq. (4.5) contain even powers of $H_{\rm mix}$. For example, the normalized f-electron—band-hole state

$$\frac{1}{\sqrt{N}} \sum_m \mid \varepsilon_f \varepsilon_k m \rangle$$

couples at $O(1)$, since

$$\frac{1}{N} \left| \sum_m \langle \Omega \mid H_{\rm mix} \mid \varepsilon_f \varepsilon_k m \rangle \right|^2 = NV^2 . \tag{4.6}$$

Since

$$\frac{1}{N} \left| \sum_m \langle \Omega \mid H_{\rm mix} \mid \varepsilon_f \varepsilon_{k_2} m \rangle \langle \varepsilon_f \varepsilon_{k_2} m \mid H_{\rm mix} \mid E_{k_1} \varepsilon_{k_2} m \rangle \right|^2 = NV^4 = \frac{1}{N}(NV^2)^2 , \tag{4.7}$$

the state

$$\frac{1}{\sqrt{N}} \sum_m \mid E_{k_1} \varepsilon_{k_2} m \rangle$$

couples at $O(1/N)$ and may be neglected in an $O(1)$ calculation. The order at which other states couple is indicated in Fig. 19.

It follows that to compute the ground-state energy exactly to $O(1)$ it is only necessary to consider variational states of the form

$$\mid \phi_0^{(1)} \rangle = A \left[\mid \Omega \rangle + \frac{1}{\sqrt{N}} \sum_{km}^{\rm occ} \alpha_k \mid \varepsilon_f \varepsilon_k m \rangle \right] , \tag{4.8}$$

where the superscript "occ" indicates that the k sum is restricted to occupied states with $\varepsilon_k < \varepsilon_F$. As usual, the noninteracting Fermi sea $\mid \Omega \rangle$ sets the zero of energy:

$$\langle \Omega \mid H \mid \Omega \rangle \equiv 0 . \tag{4.9}$$

The variational solution may be found by minimizing the quantity

$$\langle \phi_0^{(1)} \mid H \mid \phi_0^{(1)} \rangle - E_0 (\langle \phi_0^{(1)} \mid \phi_0^{(1)} \rangle - 1) = A^2 \left[\sum_k^{\rm occ} \alpha_k^2 (\varepsilon_f - \varepsilon_k) + 2\sqrt{N} V \sum_k^{\rm occ} \alpha_k \right] - E_0 \left[A^2 \left[1 + \sum_k^{\rm occ} \alpha_k^2 \right] - 1 \right] , \tag{4.10}$$

with E_0 a Lagrange multiplier. [E_0 is just the $O(1)$ approximation for the ground-state energy E_G.] The variational equations take the form

$$\begin{aligned} &\partial/\partial A^2 : \; E_0 = \frac{\langle \phi_0^{(1)} \mid H \mid \phi_0^{(1)} \rangle}{\langle \phi_0^{(1)} \mid \phi_0^{(1)} \rangle} , \\ &\partial/\partial \alpha_k : \; (E_0 - \varepsilon_f + \varepsilon_k) \alpha_k = \sqrt{N} V , \\ &\partial/\partial \lambda : \; A^2 \left[1 + \sum_k^{\rm occ} \alpha_k^2 \right] = 1 . \end{aligned} \tag{4.11}$$

From the second equation,

$$\alpha_k = \frac{\sqrt{N} V}{E_0 - \varepsilon_f + \varepsilon_k} . \tag{4.12}$$

Writing out the first equation explicitly and substituting for α_k gives

$$E_0 = NV^2 \sum_k^{\rm occ} \frac{1}{E_0 - \varepsilon_f + \varepsilon_k} = \Sigma_0^{(1)}(E_0) \mid_{T=0} = \frac{N\Gamma}{\pi} \ln \left| \frac{\varepsilon_f - E_0}{D} \right| \tag{4.13}$$

employing the notation of Sec. II.B; the last line holds assuming a flat density of conduction states. This is precisely the equation for the ground-state energy at $O(1)$ derived previously [cf. Eq. (2.26)]. A^2 may be interpreted as a wave function renormalization constant, since

$$\mid \langle \Omega \mid \phi_0^{(1)} \rangle \mid^2 = A^2 . \tag{4.14a}$$

Note also that

$$A^2 = \left[1 + \sum_k^{\rm occ} \alpha_k^2 \right]^{-1} = (1 - \partial \Sigma_0^{(1)} / \partial E_0)^{-1} . \tag{4.14b}$$

The corresponding f valence is

$$\begin{aligned} &n_f^{(1)} = \sum_{km}^{\rm occ} \mid \langle \varepsilon_f \varepsilon_k m \mid \phi_0^{(1)} \rangle \mid^2 = \frac{\mu}{1+\mu} , \\ &\mu = NV^2 \sum_k \frac{1}{(\varepsilon_k - T_A)^2} = \frac{N\Gamma}{\pi T_A} , \\ &T_A \equiv \varepsilon_f - E_0 . \end{aligned} \tag{4.15}$$

This result has also been derived previously [cf. Eq. (2.32)].

The magnetic susceptibility χ may be calculated from the ground-state energy as in Sec. II.C. It is easy to show that

$$\chi^{(1)} = n_f^{(1)} \frac{\mu_j^2}{3T_A} , \quad \mu_j^2 \equiv j(j+1)(g\mu_B)^2 . \tag{4.16}$$

This calculation of E_0, n_f, and χ may be extended to $O(1/N)$ by including states (c) and (d) from Fig. 19 in the variational ground state. We sketch the derivation in Appendix E.

B. Spectral density for f electrons within the variational approach

In this section we derive expressions for the f-electron spectral density using the variational method. The spectral density may be measured experimentally using valence-band x-ray photoemission and inverse photoemission. Gunnarsson and Schönhammer (1983b, 1986) have performed extensive comparisons of experimental spectra with $1/N$ results, obtaining good agreement for a variety of materials. The variational method has in addition been applied to describe x-ray core spectra, x-ray absorption spectra, and the dynamic susceptibility. In this section we emphasize analytical results for the f-electron spectral density and demonstrate their connection to results from other approaches. For a complete discussion of numerical calculations and the comparison of theory and experiment, the reader should consult the extensive review article by Gunnarsson and Schönhammer (1986).

At zero temperature, the f Green's function takes the form

$$G_f(t)=-i\theta(t)\langle\psi_0|\{f_m(t),f_m^\dagger(0)\}|\psi_0\rangle\ , \tag{4.17}$$

where $|\psi_0\rangle$ is the full interacting ground state. Inserting a complete set of eigenstates of the interacting Hamiltonian gives

$$G_f(t)=-i\theta(t)\left[\sum_N e^{i(E_N-E_G)t}\langle\psi_0|f_m^\dagger|N\rangle\langle N|f_m|\psi_0\rangle+\sum_N e^{i(E_G-E_N)t}\langle\psi_0|f_m|N\rangle\langle N|f_m^\dagger|\psi_0\rangle\right]\ . \tag{4.18}$$

This expression may be Fourier transformed in the upper half-plane:

$$\begin{aligned}G_f(z)&=\int_{-\infty}^{\infty}dt\,e^{izt}G_f(t)\\&=-i\sum_N\int_0^\infty dt\,e^{i(z+E_N-E_G)t}\langle\psi_0|f_m^\dagger|N\rangle\langle N|f_m|\psi_0\rangle-i\sum_N\int_0^\infty dt\,e^{i(z+E_G-E_N)t}\langle\psi_0|f_m|N\rangle\langle N|f_m^\dagger|\psi_0\rangle\\&=\left\langle\psi_0\left|f_m^\dagger\frac{1}{z-E_G+H}f_m\right|\psi_0\right\rangle+\left\langle\psi_0\left|f_m\frac{1}{z+E_G-H}f_m^\dagger\right|\psi_0\right\rangle\\&\equiv G_f^<(z)+G_f^>(z)\ .\end{aligned} \tag{4.19}$$

The imaginary part of this Green's function is just the f spectral density, i.e., the energy distribution for adding or removing one f electron from the system:

$$\rho_f(\omega)=-\frac{1}{\pi}\mathrm{Im}G_f(\omega+i0^+)=\sum_N|\langle N|f_m|\psi_0\rangle|^2\delta(\omega-E_G+E_N)+\sum_N|\langle N|f_m^\dagger|\psi_0\rangle|^2\delta(\omega+E_G-E_N)\ . \tag{4.20}$$

The first term in this equation is the spectra for removing an f electron from the system. Since $E_G-E_N<0$, this spectrum is nonzero for $\omega<0$. To an excellent approximation, this spectrum may be measured experimentally by valence-band x-ray photoemission (XPS). In order to compute

$$\rho_f(\omega)=-\frac{1}{\pi}\mathrm{Im}\left\langle\psi_0\left|f_m^\dagger\frac{1}{\omega+i0^+-E_G+H}f_m\right|\psi_0\right\rangle$$

directly, it is necessary to (a) solve variationally for the ground state, then (b) invert the operator $\omega-E_G+H$ within a suitably restricted subspace. The XPS spectral density is actually $O(1/N)$ for all $\omega<0$. This follows by noting that the valence n_f is just

$$n_f=N\int_{-\infty}^0 d\omega\,\rho_f(\omega)=O(1)\ . \tag{4.21}$$

The total weight of the negative-energy spectrum in a single m channel is then $O(1/N)$. To compute $\rho_f(\omega<0)$ to $O(1/N)$, the leading-order approximation

$$|\psi_0\rangle\simeq|\phi_0^{(1)}\rangle=A\left[|\Omega\rangle+\frac{1}{\sqrt{N}}\sum_{km}^{\mathrm{occ}}\alpha_k|\varepsilon_f\varepsilon_k m\rangle\right] \tag{4.22}$$

of Eq. (4.8) is adequate. This is because the resolvent $(\omega-E_0+H)^{-1}$ is itself $O(1/N)$. α_k and A are as in Eqs. (4.12) and (4.14). Thus

$$f_m|\psi_0\rangle\simeq\frac{A}{\sqrt{N}}\sum_k\alpha_k c_{km}|0\rangle\ . \tag{4.23}$$

At $O(1)$, the one-hole state $c_{k'm'}|0\rangle\equiv|\varepsilon_{k'}m'\rangle$ is coupled by H_{mix} to the two-hole, one-f states

$$|(\varepsilon_f\varepsilon_k m)(\varepsilon_{k'}m')\rangle = f_m^\dagger c_{km} c_{k'm'}|0\rangle \ . \tag{4.24}$$

(For $m=m'$, it is necessary to set $\varepsilon_k < \varepsilon_k'$ to prevent overcompleteness.)

To calculate $\rho_f(\omega)$ at $O(1)$, it suffices to invert $\omega - E_0 + H$ in the subspace spanned by $|\varepsilon_k m\rangle$ and $|(\varepsilon_f\varepsilon_k m)(\varepsilon_{k'}m')\rangle$. The pertinent matrix elements are

$$\langle \varepsilon_k m | \omega - E_0 + H | \varepsilon_{k'} m' \rangle = (\omega - E_0 - \varepsilon_k)\delta_{kk'}\delta_{mm'} \ ,$$

$$\langle (\varepsilon_f\varepsilon_k m)(\varepsilon_{k'}m') | \omega - E_0 + H | (\varepsilon_f\varepsilon_{k_1}m_1)(\varepsilon_{k_2}m_2)\rangle = (\omega - E_0 - \varepsilon_k - \varepsilon_{k'} + \varepsilon_f)\delta_{kk_1}\delta_{k'k_2}\delta_{mm_1}\delta_{m'm_2} \ ,$$

and

$$\langle (\varepsilon_f\varepsilon_k m)(\varepsilon_{k'}m') | \omega - E_0 + H | \varepsilon_{k''}m''\rangle = V(\delta_{k'k''} - \delta_{kk''}\delta_{mm'})\delta_{m'm''} = V\delta_{k'k''}\delta_{m'm''} + O(1/N) \ . \tag{4.25}$$

The simplification of the last matrix element is allowed in an $O(1)$ calculation. The only matrix element of the resolvent required is

$$\langle \varepsilon_k m | (\omega - E_0 + H)^{-1} | \varepsilon_{k'} m' \rangle \ .$$

A general matrix identity (Gunnarsson and Schönhammer, 1983b) may be invoked to find this element: for a matrix $\mathbf{A}$ with blocks $\mathbf{B}$, $\mathbf{C}$, and $\mathbf{D}$,

$$\mathbf{A} = \begin{bmatrix} \mathbf{B} & \mathbf{C} \\ \mathbf{C} & \mathbf{D} \end{bmatrix} , \tag{4.26a}$$

the inverse of $\mathbf{A}$ in the $\mathbf{B}$ subspace takes the form

$$(A^{-1})_{bb'} = (E^{-1})_{bb'}, \quad E_{bb'} = B_{bb'} - \sum_{dd'} C_{bd} D_{dd'}^{-1} C_{d'b} \ , \tag{4.26b}$$

where index b is restricted to the $\mathbf{B}$ subspace, and so on. This "folding-down relation" implies that

$$\langle \varepsilon_k m | (\omega - E_0 + H)^{-1} | \varepsilon_{k'} m' \rangle = \delta_{kk'}\delta_{mm'} \left[(\omega - E_0 - \varepsilon_k) - NV^2 \sum_{k'}^{\text{occ}} \frac{1}{\omega - E_0 - \varepsilon_k - \varepsilon_{k'} + \varepsilon_f} \right]^{-1}$$

$$= -\frac{\delta_{kk'}\delta_{mm'}}{-\omega + E_0 + \varepsilon_k - \Sigma_0^{(1)}(-\omega + E_0 + \varepsilon_k)} \tag{4.27a}$$

with

$$\Sigma_0^{(1)}(z) = NV^2 \sum_k^{\text{occ}} \frac{1}{z + \varepsilon_k - \varepsilon_f} \ . \tag{4.27b}$$

Substituting Eqs. (4.23) and (4.27) into (4.19) gives finally

$$G_f^<(z) = -\frac{A^2}{N} \sum_k^{\text{occ}} \frac{\alpha_k^2}{-z + E_0 + \varepsilon_k - \Sigma_0^{(1)}(-z + E_0 + \varepsilon_k)}$$

$$= -Z(E_0)\frac{NV^2}{N} \sum_k^{\text{occ}} \frac{1}{(\varepsilon_k - T_A)^2} \frac{1}{-z + E_0 + \varepsilon_k - \Sigma_0^{(1)}(-z + E_0 + \varepsilon_k)} \ ,$$

$$Z(E_0) = \left[1 - \frac{\partial \Sigma_0^{(1)}}{\partial E_0} \right]^{-1} . \tag{4.28}$$

The spectral density $\rho_f(\omega)$ takes a simple form for $-T_A < \omega \leq 0$. The function

$$\frac{1}{-\omega - E_0 + \varepsilon - \Sigma_0^{(1)}(-\omega + E_0 + \varepsilon)} \tag{4.29a}$$

has a pole at $\varepsilon = \omega$ with ε-residue $Z(E_0)$, and a branch cut along the real axis for $\varepsilon > \omega + T_A$. Thus, for $-T_A < \omega \leq 0$,

$$\rho_f(\omega) = \frac{1}{N} Z(E_0) \frac{N\Gamma}{\pi^2} \operatorname{Im} \int_{-D}^{0} \frac{d\varepsilon}{(\varepsilon - T_A)^2} \frac{1}{-\omega + E_0 + \varepsilon - \Sigma_0^{(1)}(-\omega + E_0 + \varepsilon) - i0^+}$$

$$= \frac{1}{N} Z^2(E_0) \frac{N\Gamma}{\pi} \frac{1}{(\omega - T_A)^2} \ . \tag{4.29b}$$

Note also that for general $\omega < 0$ [the case in which the branch cut in Eq. (4.29a) contributes], the spectral density assumes

the form found previously using the diagrammatic approach [Eq. (2.57)]. We shall have more to say about the equivalence of these techniques after deriving the positive-energy spectral density.

The quantity $\rho_f(\omega>0)$ is the spectrum for adding an f electron to the system. This spectrum may be measured experimentally by inverse photoemission, or bremsstrahlung isochromat spectroscopy (BIS). While the spectrum is $O(1/N)$ for negative energies, it is in fact $O(1)$ for positive energies. This is because

$$n_f = N\int_0^\infty d\omega\,\rho_f(\omega) = \begin{cases} N-n_f, & U<\infty\ , \\ N(1-n_f), & U=\infty\ . \end{cases} \tag{4.30}$$

(In the latter case the missing spectral weight lies at infinite energy.) Thus the total weight of the positive-energy spectrum in a single m channel is $O(1)$. In this case it is necessary to compute

$$\rho_f(\omega) = \sum_N |\langle N|f_m^\dagger|\psi_0\rangle|^2\delta(\omega+E_G-E_N) = -\frac{1}{\pi}\mathrm{Im}\left\langle\psi_0\left|f_m\frac{1}{\omega+i0^+ +E_G-H}f_m^\dagger\right|\psi_0\right\rangle\ . \tag{4.31}$$

Within the lowest-order approximation applied to this point, the state

$$f_m^\dagger|\psi_0\rangle = Af_m^\dagger|\Omega\rangle \equiv |\varepsilon_f m\rangle\ , \tag{4.32}$$

with A as in Eq. (4.14). Recall that for the negative-energy spectrum, an $O(1)$ approximation for the ground state is sufficient, since the matrix elements of the resolvent are of leading order $1/N$. In this case, the resolvent has matrix elements of $O(1)$; hence the $O(1/N)$ expression for the ground state must be used to obtain $1/N$ accuracy for general $\omega>0$. Despite this fact, it turns out that the $O(1)$ ground state is sufficient to obtain $O(1/N)$ accuracy for all $\omega\in(0,T_A)$. [This may be seen from the full expression for $G_f(\omega+i0^+)$ in Appendix C.] We reproduce only this partial calculation below.

The required matrix element of the resolvent is

$$\left\langle\varepsilon_f m\left|\frac{1}{z+E_0-H}\right|\varepsilon_f m\right\rangle\ .$$

Note that $|\varepsilon_f m\rangle$ is coupled by H to

$$c_{km}^\dagger|0\rangle \equiv |E_K m\rangle \tag{4.33}$$

at $O(1/N)$ (since $|\langle E_K m|H_{\rm mix}|\varepsilon_f m\rangle|^2 = V^2$) and that $|E_K m\rangle$ is coupled to the states

$$c_{Km}^\dagger f_{m'}^\dagger c_{k'm'}|0\rangle \equiv |(E_K m)(\varepsilon_f\varepsilon_{k'}m')\rangle \tag{4.34}$$

at $O(1)$. The required matrix element may now be computed to terms of $O(1/N)$ as before. For convenience, let

$$\overline{H} = z+E_0-H\ . \tag{4.35}$$

Applying the folding-down procedure of Eq. (4.26) twice gives

$$\langle\varepsilon_f m|\overline{H}^{-1}|\varepsilon_f m\rangle = \left[\langle\varepsilon_f m|\overline{H}|\varepsilon_f m\rangle - \sum_K^{\rm unocc}\langle\varepsilon_f m|\overline{H}|E_K m\rangle\langle E_K m|\overline{H}^{-1}|E_K m\rangle\langle E_K m|\overline{H}|\varepsilon_f m\rangle\right]^{-1}$$

with

$$\begin{aligned}\langle E_K m|\overline{H}^{-1}|E_K m\rangle &= \Bigg[\langle E_K m|\overline{H}|E_K m\rangle \\ &\quad - \sum_{k'm'}^{\rm occ}\langle E_K m|\overline{H}|(E_K m)(\varepsilon_f\varepsilon_{k'}m')\rangle \\ &\quad\quad \times\langle(E_K m)(\varepsilon_f\varepsilon_{k'}m')|\overline{H}|(E_K m)(\varepsilon_f\varepsilon_{k'}m')\rangle^{-1}\langle(E_K m)(\varepsilon_f\varepsilon_{k'}m')|\overline{H}|E_K m\rangle\Bigg]^{-1} \\ &= \left[z+E_0-E_K-NV^2\sum_{k'}^{\rm occ}\frac{1}{z+E_0-E_K-\varepsilon_f+\varepsilon_{k'}}\right]^{-1} = [z+E_0-E_K-\Sigma_0^{(1)}(z+E_0-E_K)]^{-1}\ .\end{aligned} \tag{4.36}$$

Thus

$$\langle \varepsilon_f m \mid \bar{H}^{-1} \mid \varepsilon_f m \rangle = [z + E_0 - \varepsilon_f - \Sigma_m(z+E_0)]^{-1} , \tag{4.37}$$

$$\Sigma_m(z) = V^2 \sum_K^{\text{unocc}} \frac{1}{z - E_K - \Sigma_0^{(1)}(z - E_K)} = \frac{\Gamma}{\pi} \int_0^D \frac{dE}{z - E - \Sigma_0^{(1)}(z-E)} .$$

The last line assumes a flat density of states.

The resulting expression for the propagator is

$$G_f^>(z) = \frac{A^2}{z - T_A - \Sigma_m(z+E_0)} = Z(E_0) \left[\frac{1}{z - T_A} + \frac{1}{(z-T_A)^2} \Sigma_m(z+E_0) \right] + O(1/N^2) . \tag{4.38}$$

The quantity Σ_m is $O(1/N)$, so the leading-order result for the spectral density is simply

$$\rho_f(\omega > 0) = Z(E_0)\delta(\omega - T_A) = (1 - n_f^{(1)})\delta(\omega - T_A) . \tag{4.39}$$

This delta function is the only feature of the spectrum at $O(1)$.

At $O(1/N)$, an additional background appears. The integrand in the expression for $\Sigma_m(\omega + E_0)$ has a pole at $E = \omega$ with E-residue $-Z(E_0)$, and a branch cut along the real E axis for $E < \omega - T_A$. Thus, for $0 \le \omega < T_A$,

$$\mathrm{Im}\Sigma_m(\omega + E_0 + i0^+) = -Z(E_0)\Gamma = -(1 - n_f^{(1)})\Gamma , \tag{4.40a}$$

and to $O(1/N)$,

$$\rho_f(\omega) = -\frac{1}{\pi}\mathrm{Im}G_f(\omega + i0^+) = \frac{1}{N} Z^2(E_0) \frac{N\Gamma}{\pi} \frac{1}{(\omega - T_A)^2}, \quad 0 \le \omega < T_A . \tag{4.40b}$$

For $\omega > T_A$, the continuum part of $\mathrm{Im}\Sigma_m(\omega + E_0 + i0^+)$ contributes. This is not the only contribution to ρ_f for $\omega > T_A$. A contribution also arises from the $1/N$ correction to the ground-state wave function, which has been neglected in this treatment. [This contribution may easily be derived from the full $1/N$ expression for $G_f(\omega)$ in Appendix C.]

The spectral density expansion clearly breaks down at $\omega = T_A$, where a pole occurs at lowest order. As discussed in Sec. II.D, the functions G_f and ρ_f do not possess uniformly convergent expansions in $1/N$ on the full real line. In particular, a convergent expansion is impossible at $\omega = T_A$. Nevertheless, a systematic $1/N$ expansion of the spectral density is expected to be *pointwise* convergent. A corollary of this pointwise convergence is that the expansions of ρ_f for negative and positive energies must match at $\omega = 0$ order by order. Equations (4.29) and (4.40) illustrate this matching property. Throughout the region $-T_A < \omega < T_A$, the spectral density has a simple analytic form to order $1/N$. As discussed previously the validity of the expansion is also confirmed by the Friedel-Langreth sum rule (see Sec. II.D).

Despite the pointwise convergence of the expansion, an infinite-order approximation is necessary to obtain a smooth spectrum in the vicinity of the singular point $\omega = T_A$. The simplest infinite-order approximation is that in Eq. (4.38) before expansion in powers of Σ_m. The spectrum near $\omega = T_A$ takes on a finite width due to the imaginary part of Σ_m (which is proportional to $1/N$). While this infinite-order summation in $1/N$ ensures a smooth spectrum near $\omega = T_A$, it alters the analytic properties of the spectrum near $\omega = 0$: the function

$$\frac{1}{z - T_A - \Sigma_m(z + E_0)}$$

exhibits an undamped pole just below $z = 0$. The energy of the pole does not have an expansion analytic in $1/N$. The pole occurs where

$$\omega - T_A - \mathrm{Re}\Sigma_m(\omega + E_0) = 0, \quad \omega < 0 . \tag{4.41}$$

Recall that

$$\Sigma_m(\omega + E_0) = \frac{\Gamma}{\pi} \int_0^D \frac{dE}{\omega + E_0 - E - \Sigma_0^{(1)}(\omega + E_0 - E)} = Z(E_0)\frac{\Gamma}{\pi} \int_0^D dE \left[\frac{1}{\omega - E} + F(\omega - E) \right] ,$$

with F nonsingular at $\omega = E$. Thus

$$\Sigma_m(\omega + E_0) = -Z(E_0)\frac{\Gamma}{\pi}\ln(-D/\omega) + \text{nonsingular terms} \simeq \frac{T_A}{N}\ln(-\omega/D) + \text{nonsingular terms} , \tag{4.42}$$

for $N\Gamma \gg T_A$. Ignoring the nonsingular contribution gives

$$\omega - T_A = \frac{T_A}{N}\ln(-\omega/D), \text{ i.e., } \omega \simeq -De^{-N} \text{ for } N \to \infty . \tag{4.43}$$

The presence of this anomalous energy scale and its implications for infinite-order partial resummations in $1/N$ were first emphasized by Krishna-murthy (1984). We discuss such resummations in detail in Sec. V.

Finally, note that the quantity

$$G_f(i\omega_n) = G_f^<(i\omega_n) + G_f^>(i\omega_n) \tag{4.44}$$

obtained by adding Eqs. (4.28) and (4.38) is precisely the contribution $G_A(i\omega_n)$ found in Appendix C [cf. Eq. (C4)].

This contribution arises diagrammatically (see Sec. II.D) from self-energy insertions parallel to the line carrying external frequency $i\omega_n$. In the language of this section, these contributions are corrections to the f resolvent; self-energy insertions that lie entirely above the external line are corrections to the ground-state wave function. In the language of Sec. III, corrections to the f resolvent take the form of self-energy insertions on the fermion lines; ground-state wave-function corrections are self-energy insertions on the boson lines. At zero temperature the three approaches are completely equivalent. The physical content is arguably clearest in the variational approach, since the form of the ground-state wave function is explicitly exhibited; however, this approach is limited to zero temperature, while the other approaches are not.

V. SELF-CONSISTENT DIAGRAMMATIC EXPANSIONS

It was noted in preceding sections that, in a perturbative $1/N$ expansion, the f-electron spectral density exhibits a singularity at $\omega=T_A$, with T_A the solution of Eqs. (2.26) and (2.27). This singularity remains order by order, preventing a complete description of f photoemission and electronic transport. In order to remove this singularity, it is necessary to perform an infinite-order resummation in $1/N$. Resummations have been investigated within a variety of contexts, including the variational approach of Sec. IV (Gunnarsson and Schönhammer, 1983b) and the saddle-point approach of Sec. VI. In this section we review partial resummations of diagrammatic perturbation theory (Keiter and Kimball, 1972; Inagaki, 1979; Grewe, 1982; Keiter and Czycholl, 1983; Kuramoto, 1983; Coleman, 1984; Kuramoto and Kojima, 1984; Müller-Hartmann, 1984; Zhang and Lee, 1984; Bickers *et al.*, 1985, 1987; Maekawa *et al.*, 1985a, 1985b). Partial resummations incorporate many desirable features of low-order perturbative expansions, provide a more satisfactory treatment of dynamic properties, and are simple to apply in finite-temperature calculations. In contrast, partial resummations are *not* appropriate in the Fermi-liquid regime, where a systematic treatment of low-energy electron-hole processes is essential. In this sense, the approaches discussed below serve a function complementary to that of the approaches in Secs. II–IV and VI.

The simplest thermodynamically self-consistent approximation for the Anderson and Coqblin-Schrieffer models has appeared in the literature under a number of names. These include the "noncrossing approximation" or NCA (Kuramoto, 1983), the "self-consistent ladder approximation" (Maekawa *et al.*, 1985a, 1985b), and the "self-consistent large-N expansion" (Bickers *et al.*, 1987). For brevity we shall generally refer to this approach as the NCA. In Sec. V.A we describe the NCA for the infinite-U Anderson model. The thermodynamic self-consistency of this approach and its higher-order generalizations is discussed at length in Appendix G. In Appendix H we summarize a number of exact sum rules for the Anderson model and show that they are satisfied within the NCA. Analytical solutions of the NCA equations at zero temperature are reviewed in Sec. V.B. In Sec. V.C we describe the NCA for the Coqblin-Schrieffer model. Finally, in Sec. V.D we provide an overview of finite-temperature NCA results.

A. Noncrossing approximation for the infinite-U Anderson model

Recall the alternate representations for the partition function of the infinite-U Anderson model derived in Sec. II.B:

$$Z_f \equiv Z/Z_{\rm band} = \int_\Gamma \frac{dz}{2\pi i} e^{-\beta z} \mathrm{Tr}_f \frac{1}{z - H_f - \hat{\Sigma}_f(z)} \tag{5.1a}$$

and

$$Z_f = 1 + N e^{-\beta\varepsilon_f} - \beta \int_0^1 \frac{dg}{g} \int_\Gamma \frac{dz}{2\pi i} e^{-\beta z} \mathrm{Tr}_f \frac{\hat{\Sigma}_f(z,g)}{z - H_f - \hat{\Sigma}_f(z,g)} . \tag{5.1b}$$

The low-order expansions in $1/N$ derived in Sec. II were based on the second representation; for present purposes the first representation is considerably easier to manipulate. The diagrams contributing to the partition function at $O(1)$ are those shown in Fig. 20(a). Note that the empty and occupied states are necessarily treated asymmetrically. The diagrams contributing to Z_f at $O(1/N)$ are those shown in Fig. 20(b). All the diagrams that enter at $O(1)$ and $O(1/N)$ have noncrossing conduction lines. There are, of course, a host of other diagrams with the same noncrossing property. A few are illustrated in Fig. 20(c). *All* diagrams with noncrossing conduction lines may be summed by solving the coupled equations in Fig. 21. The equations for the self-energy may be written out simply using the rules of Table IV:

$$\begin{aligned} \Sigma_0^{(1)}(z) &= NV^2 \sum_k \frac{f_k}{z + \varepsilon_k - \varepsilon_f} \\ &\rightarrow \Sigma_0(z) = NV^2 \sum_k f_k G_m(z + \varepsilon_k) , \\ \Sigma_m^{(1/N)}(z) &= V^2 \sum_k \frac{1 - f_k}{z - \varepsilon_k} \\ &\rightarrow \Sigma_m(z) = V^2 \sum_k (1 - f_k) G_0(z - \varepsilon_k) , \end{aligned} \tag{5.2}$$

where

$$G_0(z) = \frac{1}{z - \Sigma_0(z)}$$

and

$$G_m(z) = \frac{1}{z - \varepsilon_f - \Sigma_m(z)} . \tag{5.3}$$

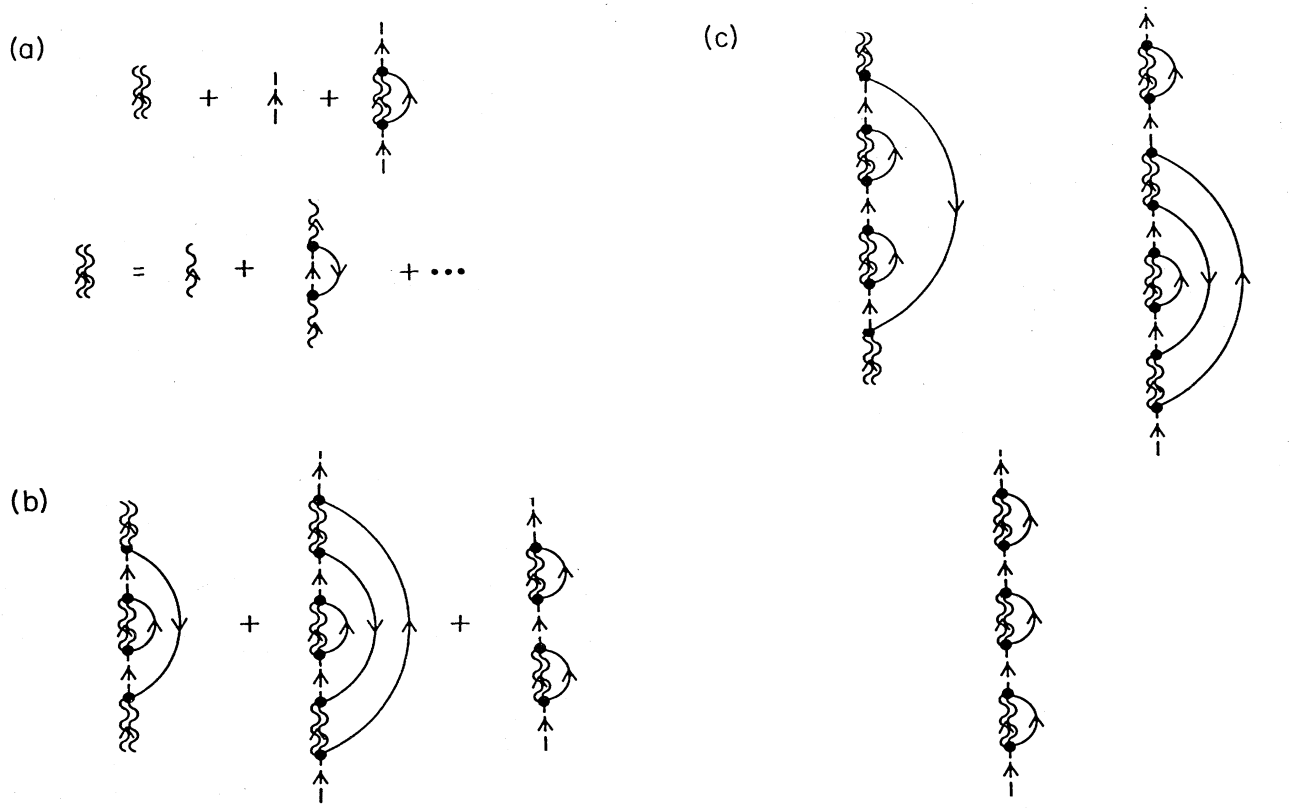

FIG. 20. Diagrams contributing to the infinite-U Anderson partition function in the representation of Eq. (5.1a). (a) Empty- and occupied-state contributions at $O(1)$. The empty state is indicated by a wavy line and the occupied states by dashed lines. The double wavy line indicates an empty-state propagator dressed to $O(1)$ (see Sec. II). (b) Empty- and occupied-state contributions at $O(1/N)$. (c) Some empty- and occupied-state contributions with noncrossing conduction lines at $O(1/N^2)$. Note that contributions with crossing lines begin to enter at this same order.

It is convenient at this point to define the spectral densities

$$\rho_0(\omega)=-\frac{1}{\pi}\mathrm{Im}G_0(\omega+i0^+)\,,$$
$$\rho_m(\omega)=-\frac{1}{\pi}\mathrm{Im}G_m(\omega+i0^+)\,. \tag{5.4}$$

This approximate solution for the Anderson partition function has been named the noncrossing approximation, or NCA (Kuramoto, 1983), to emphasize the class of perturbative diagrams retained. It may be shown (Kuramoto, 1983; see Appendix G) that this approximate solution is thermodynamically self-consistent. By this we mean that various exact expressions for the partition function which follow from integrating thermodynamic derivatives (such as the valence or magnetization) remain consistent when the noncrossing approximation is introduced. The NCA is the simplest approximation in a hierarchy of self-consistent solutions (Kuramoto, 1983).

Simple expressions for the f-electron Green's function and dynamic susceptibility may also be obtained within the NCA. The Green's function diagrams are illustrated in Fig. 22. Applying the rules of Sec. II.D gives

$$G_f(i\omega_n)=\frac{1}{Z_f}\int_\Gamma\frac{dz}{2\pi i}e^{-\beta z}G_0(z)G_m(z+i\omega_n)$$
$$=\frac{1}{Z_f}\int_{-\infty}^{\infty}d\varepsilon\,e^{-\beta\varepsilon}[\rho_0(\varepsilon)G_m(\varepsilon+i\omega_n)$$
$$-\rho_m(\varepsilon)G_0(\varepsilon-i\omega_n)]\,. \tag{5.5}$$

The resulting spectral density is

$$\rho_f(\omega)=\frac{1}{Z_f}(1+e^{-\beta\omega})\int_{-\infty}^{\infty}d\varepsilon\,e^{-\beta\varepsilon}\rho_0(\varepsilon)\rho_m(\varepsilon+\omega)\,. \tag{5.6}$$

The dynamic susceptibility $\chi(\omega)$ also has a simple form within the NCA. The f contribution to the magnetic susceptibility may be written

$$\chi(i\nu_m)=-\int_0^\beta d\tau e^{i\nu_m\tau}M(\tau)$$

with

$$M(\tau)=-\langle T_\tau \hat{M}(\tau)\hat{M}(0)\rangle ,$$
$$\hat{M}=g\mu_B\sum_m m\,|m\rangle\langle m| . \tag{5.7}$$

The diagrammatic representation of $\chi(i\nu_m)$ within the NCA is shown in Fig. 23. Applying the general expression for correlation functions derived in Appendix B gives

$$\chi(i\nu_m)=-\frac{N\mu_j^2}{3}\frac{1}{Z_f}\int_\Gamma\frac{dz}{2\pi i}e^{-\beta z}G_m(z)G_m(z+i\nu_m)=-\frac{N\mu_j^2}{3}\frac{1}{Z_f}\int_{-\infty}^{\infty}d\varepsilon\, e^{-\beta\varepsilon}\rho_m(\varepsilon)[G_m(\varepsilon+i\nu_m)+G_m(\varepsilon-i\nu_m)] , \tag{5.8}$$

$\mu_j^2=j(j+1)(g\mu_B)^2$.

The magnetic spectral density becomes

$$\mathrm{Im}\chi(\omega+i0^+)=\frac{N\mu_j^2}{3}\frac{\pi}{Z_f}\int_{-\infty}^{\infty}d\varepsilon\, e^{-\beta\varepsilon}\rho_m(\varepsilon)[\rho_m(\varepsilon+\omega)-\rho_m(\varepsilon-\omega)] . \tag{5.9}$$

The expression for the static susceptibility $\chi(\omega=0)$ obtained by this approach is the same as that which follows from differentiating Z_f directly with respect to the field; for a proof see the end of Appendix G.

B. Analytical solutions of the NCA equations for zero temperature

Although the NCA is a thermodynamically consistent approximation, it does not obey a number of exact Fermi-liquid relations that connect static and dynamic properties. Kuramoto and Kojima (1984) and Müller-Hartmann (1984) have investigated the NCA in the zero-temperature limit. At zero temperature, the coupled NCA integral equations derived in the previous section may be converted to differential equations (Inagaki, 1979), and analytical results, which clarify the limitations of the approach, may be extracted. In addition, the differential equations provide yet another way to generate perturbative expansions for zero-temperature properties up to $O(1/N)$ [recall that the NCA omits terms of $O(1/N^2)$]. We review this approach in detail below, following the treatments of Kuramoto and Kojima (1984) and Müller-Hartmann (1984).

1. NCA differential equations

At zero temperature, the NCA integral equations take the form

$$\Sigma_0(\omega+i0^+)=\frac{N\Gamma}{\pi}\int_{-D}^{D}d\varepsilon f(\varepsilon)G_m(\omega+\varepsilon+i0^+)$$
$$=\frac{N\Gamma}{\pi}\int_{-D+\omega}^{\omega}d\varepsilon\, G_m(\varepsilon+i0^+) ,$$
$$\Sigma_m(\omega+i0^+)=\frac{\Gamma}{\pi}\int_{-D}^{D}d\varepsilon[1-f(\varepsilon)]G_0(\omega-\varepsilon+i0^+) \tag{5.10}$$
$$=\frac{\Gamma}{\pi}\int_{-D+\omega}^{\omega}d\varepsilon\, G_0(\varepsilon+i0^+) .$$

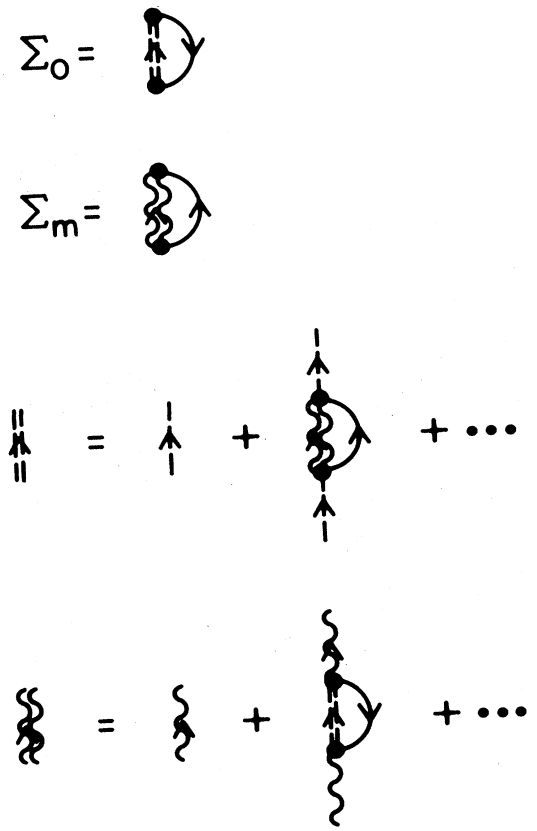

FIG. 21. Pictorial representation of the coupled integral equations for summing diagrams with noncrossing lines (the NCA integral equations). Σ_0 and Σ_m are the empty- and occupied-state self-energies. The empty state is indicated by a wavy line and the occupied states by dashed lines; double lines indicate self-consistently dressed propagators. These integral equations incorporate all contributions of $O(1)$ and $O(1/N)$ in the large-N expansion.

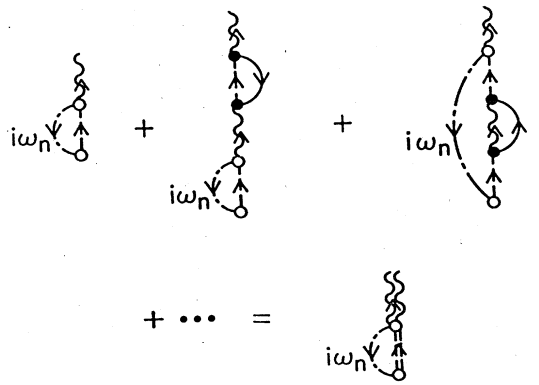

FIG. 22. Diagrammatic form of the f Green's function within the noncrossing approximation for the infinite-U Anderson model. The notation is as in Sec. II.D. The f Green's function is expressed as a convolution of the self-consistently dressed empty- and occupied-state propagators.

So long as $D \gg N\Gamma$, the ω dependence of the lower limit of integration may be ignored. Differentiating with respect to ω gives immediately

$$\frac{\partial \Sigma_0}{\partial \omega}=\frac{N\Gamma}{\pi}G_m(\omega), \quad \frac{\partial \Sigma_m}{\partial \omega}=\frac{\Gamma}{\pi}G_0(\omega) \tag{5.11}$$

(the $i0^+$ is not written explicitly hereafter). The initial conditions consistent with neglecting ω in the lower integration bound are

$$\Sigma_0(-D)=\Sigma_m(-D)=0 . \tag{5.12}$$

Following Kuramoto and Kojima (1984) and Müller-Hartmann (1984), we introduce a notation for the inverse propagators:

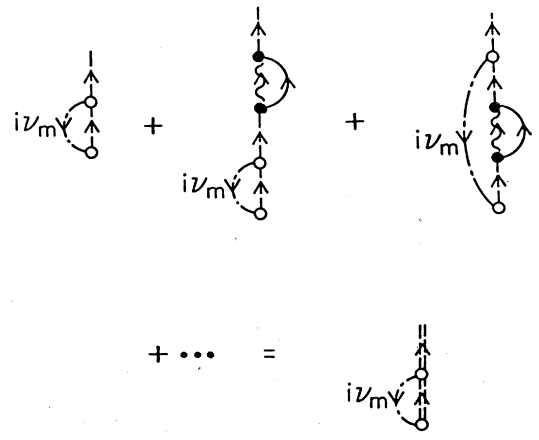

FIG. 23. Diagrammatic form of the dynamic susceptibility within the noncrossing approximation for the infinite-U Anderson model. $\chi(i\nu_m)$ is expressed as a convolution of two occupied-state propagators.

$$Y_0(\omega)=-G_0^{-1}(\omega), \quad Y_m(\omega)=-G_m^{-1}(\omega) . \tag{5.13}$$

These quantities obey the coupled equations

$$\frac{d}{d\omega}Y_0(\omega)=-1-\frac{N\Gamma}{\pi}Y_m^{-1}(\omega) , \tag{5.14a}$$

$$\frac{d}{d\omega}Y_m(\omega)=-1-\frac{\Gamma}{\pi}Y_0^{-1}(\omega) , \tag{5.14b}$$

with

$$Y_0(-D)=D, \quad Y_m(-D)=D+\varepsilon_f . \tag{5.15}$$

2. Some preliminaries on the zero-temperature limit

An important step in solving for zero-temperature static and dynamic properties is the determination of the propagators G_0 and G_m. This step alone is not sufficient, however; special care is necessary to evaluate thermally weighted sums for $T\to 0$. Consider, for example, the empty-state spectral density ρ_0. As shown in Sec. II.B, ρ_0 may be decomposed by introducing a complete set of energy eigenstates $|\Phi\rangle$ of the Anderson Hamiltonian. At zero temperature,

$$\rho_0(\omega)=\sum_{\Phi} |\langle \Phi | 0;\Omega\rangle|^2 \delta(\omega-E_\Phi) , \tag{5.16}$$

with $|0;\Omega\rangle$ the noninteracting empty state and filled Fermi sea. The function ρ_0 vanishes below E_G, the exact ground-state energy. The occupied-state distribution function $\rho_m(\omega)$ exhibits the same threshold. [It may be established rigorously that *above* the threshold E_G the spectral densities exhibit power-law singularities, indicative of an infrared overlap catastrophe. A proof has been provided by Kuramoto and Kojima (1984).]

At finite temperature, excited states of the noninteracting conduction-electron system contribute to the thermal averages defining ρ_0 and ρ_m (see Sec. II.B). This implies that, for $T>0$, ρ_0 and ρ_m possess exponentially damped tails extending *below* the exact ground-state energy E_G. On the other hand, the factor $e^{-\beta\omega}/Z_f$ grows exponentially for $\omega<E_G$ in the zero-temperature limit. Thus, in expressions such as

$$\rho_f(\omega)=\frac{1}{Z_f}(1+e^{-\beta\omega})\int_{-\infty}^{\infty} d\varepsilon\, e^{-\beta\varepsilon}\rho_0(\varepsilon)\rho_m(\varepsilon+\omega) , \tag{5.17}$$

a zero-temperature limit must be sought for the composite factors

$$\bar{\rho}_0(\varepsilon)\equiv Z_f^{-1}e^{-\beta\varepsilon}\rho_0(\varepsilon)$$

and

$$\bar{\rho}_m(\varepsilon)\equiv Z_f^{-1}e^{-\beta\varepsilon}\rho_m(\varepsilon) . \tag{5.18}$$

These quantities are spectral densities for a pair of (unphysical) propagators analogous to G_0 and G_m. It is easy to show that $\bar{\rho}_0$ and $\bar{\rho}_m$ vanish above the exact ground-state energy E_G.

NCA equations for $\bar{\rho}_0$ and $\bar{\rho}_m$ may be obtained at finite temperature by multiplying the imaginary part of Eq. (5.10) by $-e^{-\beta\omega}/\pi Z_f$. Thus

$$Z_f^{-1}e^{-\beta\omega}\left[-\frac{1}{\pi}\mathrm{Im}\Sigma_0(\omega+i0^+)\right] = \bar{\rho}_0(\omega)\,|\,G_0(\omega)\,|^{-2} = \frac{N\Gamma}{\pi}\int_{-D}^{D} d\varepsilon[1-f(\varepsilon)]\bar{\rho}_m(\varepsilon+\omega) \tag{5.19}$$

and

$$Z_f^{-1}e^{-\beta\omega}\left[-\frac{1}{\pi}\mathrm{Im}\Sigma_m(\omega+i0^+)\right] = \bar{\rho}_m(\omega)\,|\,G_m(\omega)\,|^{-2} = \frac{\Gamma}{\pi}\int_{-D}^{D} d\varepsilon[1-f(\varepsilon)]\bar{\rho}_0(\varepsilon+\omega)\,.$$

In terms of these new quantities, the f spectral density becomes

$$\rho_f(\omega) = \int_{-\infty}^{\infty} d\varepsilon[\bar{\rho}_0(\varepsilon)\rho_m(\varepsilon+\omega)+\rho_0(\varepsilon)\bar{\rho}_m(\varepsilon+\omega)]\,. \tag{5.20}$$

3. Solution of the NCA differential equations

The coupled equations (5.14) may be solved in two steps (Inagaki, 1979): (a) Y_m may be determined as a function of Y_0, then (b) the frequency corresponding to each value of Y_0 may be found. To implement step (a), the second equation may be divided by the first:

$$\left[1+\frac{N\Gamma}{\pi}Y_m^{-1}\right]dY_m = \left[1+\frac{\Gamma}{\pi}Y_0^{-1}\right]dY_0\,. \tag{5.21}$$

Integrating this equation gives

$$Y_m+\frac{N\Gamma}{\pi}\ln(Y_m/D)+C = Y_0+\frac{\Gamma}{\pi}\ln(Y_0/D)\,, \tag{5.22a}$$

with C a constant of integration. Since $Y_0(-D) = Y_m(-D)-\varepsilon_f = D$ and $D \gg \varepsilon_f$, the integration constant is simply

$$C = -\varepsilon_f\,. \tag{5.22b}$$

Step (b) may now be implemented by integrating Eq. (5.14a) [or (5.14b)] with respect to Y_0 (or Y_m) to determine $\omega(Y_0)$ [or $\omega(Y_m)$]. Integrating up from the lower band edge gives

$$\int_{-D}^{\omega} d\varepsilon = -\int_{D}^{Y_0}\frac{dx}{1+(N\Gamma/\pi)Y_m^{-1}(x)} = \frac{N\Gamma}{\pi}\int_{D}^{Y_0}\frac{dx}{(N\Gamma/\pi)+Y_m(x)} - (Y_0-D)\,, \tag{5.23}$$

i.e.,

$$\omega = -Y_0-\frac{N\Gamma}{\pi}\int_{Y_0}^{D}\frac{dx}{(N\Gamma/\pi)+Y_m(x)}\,.$$

The arguments in Sec. V.B.2 imply that the exact Y_0 and Y_m vanish at the ground-state energy of the interacting system and are real for $\omega < E_G$. One might reasonably assume that this exact behavior is preserved by the NCA, i.e., that there exists an energy E_G^{NCA} at which the inverse propagators Y_0 and Y_m vanish, and below which they are pure real. We know of no rigorous proof that this ansatz is correct; however, the ansatz is consistent with extensive numerical investigations by Kuramoto and Kojima (1984), and its validity seems firmly established.

With this ansatz, Eq. (5.23) yields immediately an expression for E_G^{NCA}:

$$E_G^{\mathrm{NCA}} = -\frac{N\Gamma}{\pi}\int_0^D\frac{dx}{(N\Gamma/\pi)+Y_m(x)}\,. \tag{5.24a}$$

Further, replacing $-D$ and $Y_0(-D)=D$ with E_G^{NCA} and $Y_0(E_G^{\mathrm{NCA}})=0$ in the first line of Eq. (5.23) gives

$$\omega-E_G^{\mathrm{NCA}} = -\int_0^{Y_0}dx\frac{Y_m(x)}{(N\Gamma/\pi)+Y_m(x)},\quad \omega<E_G^{\mathrm{NCA}}\,. \tag{5.24b}$$

The analogous expressions which follow from integrating Eq. (5.10b) are

$$E_G^{\mathrm{NCA}} = \varepsilon_f-\frac{\Gamma}{\pi}\int_0^D\frac{dx}{(\Gamma/\pi)+Y_0(x)} \tag{5.25a}$$

and

$$\omega-E_G^{\mathrm{NCA}} = -\int_0^{Y_m}dx\frac{Y_0(x)}{(\Gamma/\pi)+Y_0(x)}\,. \tag{5.25b}$$

Since E_G^{NCA} is the approximate ground-state energy, Eqs. (5.24) and (5.25) may be used to calculate the zero-temperature thermodynamic properties n_f, χ_c, and χ. Differentiating Eq. (5.22) with respect to ε_f at fixed Y_0 gives

$$\frac{\partial Y_m}{\partial\varepsilon_f}\left[1+\frac{N\Gamma}{\pi}Y_m^{-1}\right]-1=0\,, \tag{5.26}$$

i.e.,

$$\frac{\partial Y_m}{\partial\varepsilon_f} = \frac{Y_m}{(N\Gamma/\pi)+Y_m}\,.$$

Thus differentiating Eq. (5.24a) gives

$$n_f^{\mathrm{NCA}} = \frac{\partial E_G^{\mathrm{NCA}}}{\partial\varepsilon_f} = \frac{N\Gamma}{\pi}\int_0^D dx\frac{Y_m(x)}{[(N\Gamma/\pi)+Y_m(x)]^3}\,. \tag{5.27}$$

By the same approach

$$\chi_c^{\mathrm{NCA}} = -\frac{\partial^2 E_G^{\mathrm{NCA}}}{\partial\varepsilon_f^2} = -\frac{N\Gamma}{\pi}\int_0^D dx\frac{(N\Gamma/\pi)Y_m(x)-2Y_m^2(x)}{[(N\Gamma/\pi)+Y_m(x)]^5}\,. \tag{5.28}$$

To compute χ, one requires the generalization of Eq.

(5.22) for occupied f states split by a field. The resulting expression for $\chi^{\rm NCA}$ is

$$\chi^{\rm NCA}=\frac{\mu_j^2}{3}\int_0^D dx\frac{(N\Gamma/\pi)[(N\Gamma/\pi)+2Y_m(x)]}{Y_m(x)[(N\Gamma/\pi)+Y_m(x)]^3}\ . \tag{5.29}$$

If now the NCA differential equations are not solved exactly, but perturbatively in $1/N$, the expressions for $n_f^{(1)}$, $\chi_c^{(1)}$, and $\chi^{(1)}$ first derived in Sec. II.C may be recovered (Kuramoto and Müller-Hartmann, 1985). For example, at $O(1)$, Eq. (5.22) becomes

$$Y_m+\frac{N\Gamma}{\pi}\ln(Y_m/D)-\varepsilon_f=Y_0 \tag{5.30a}$$

and

$$\frac{\partial Y_0}{\partial Y_m}=Y_m^{-1}\left[\frac{N\Gamma}{\pi}+Y_m\right]\ . \tag{5.30b}$$

Changing variables in (5.27) gives immediately

$$n_f^{(1)}=\frac{N\Gamma}{\pi}\int_{T_A}^D\frac{dY_m}{[(N\Gamma/\pi)+Y_m]^2}=\frac{\mu}{1+\mu}\ ,$$
$$\mu=\frac{N\Gamma}{\pi T_A}\ , \tag{5.31a}$$

with ε_f-T_A the lowest energy solution of

$$\omega=\frac{N\Gamma}{\pi}\ln\left|\frac{\varepsilon_f-\omega}{D}\right|\ . \tag{5.31b}$$

(It is amusing that the low-temperature scale T_A emerges in this case as an integration limit after a change of variables.) Likewise,

$$\chi_c^{(1)}=-\frac{N\Gamma}{\pi}\int_{T_A}^D dY_m\frac{(N\Gamma/\pi)-2Y_m}{[(N\Gamma/\pi)+Y_m]^4}$$
$$=\frac{1}{T_A}\frac{\mu}{(1+\mu)^3}=\frac{\pi}{N\Gamma}(n_f^{(1)})^2(1-n_f^{(1)}) \tag{5.32}$$

and

$$\chi^{(1)}=\frac{\mu_j^2}{3}\frac{N\Gamma}{\pi}\int_{T_A}^D\frac{dY_m}{Y_m^2}\frac{(N\Gamma/\pi)+2Y_m}{[(N\Gamma/\pi)+Y_m]^2}$$
$$=n_f^{(1)}\frac{\mu_j^2}{3T_A}\ . \tag{5.33}$$

Results for n_f, χ_c, and χ at $O(1/N)$ can also be rederived by this approach. Results at $O(1/N^2)$ cannot, since the NCA equations omit terms of this order.

4. Zero-temperature limit for propagators and spectral densities

The propagators G_0 and G_m near the ground-state energy $E_G^{\rm NCA}$ may be obtained from Eqs. (5.22)—(5.25) (Müller-Hartmann, 1984). Equation (5.22) may be rewritten

$$\ln\left[\frac{\pi Y_m/\Gamma}{(\pi Y_0/\Gamma)^{1/N}}\right]=\frac{\pi\varepsilon_f}{N\Gamma}+\left[1-\frac{1}{N}\right]\ln\left[\frac{\pi D}{\Gamma}\right]$$
$$-\frac{\pi}{N\Gamma}(Y_m-Y_0)\ ,$$

i.e.,

$$\frac{\pi Y_m/\Gamma}{(\pi Y_0/\Gamma)^{1/N}}=\frac{\pi T_{\rm NCA}}{\Gamma}\exp[-\pi(Y_m-Y_0)/N\Gamma]\ , \tag{5.34a}$$

with

$$T_{\rm NCA}\equiv D(\Gamma/\pi D)^{1/N}\exp(\pi\varepsilon_f/N\Gamma)\ .$$

For Y_0 and $Y_m\ll N\Gamma/\pi$, this expression reduces to

$$Y_0=\frac{\Gamma}{\pi}(Y_m/T_{\rm NCA})^N\ . \tag{5.34b}$$

Thus, from Eq. (5.24b),

$$E_G^{\rm NCA}-\omega\sim\frac{\pi}{N\Gamma}\int_0^{Y_0}dx\,T_{\rm NCA}(\pi x/\Gamma)^{1/N}\ ,$$

i.e.,

$$Y_0(\omega)\sim\frac{\Gamma}{\pi}\left[\frac{(N+1)(E_G^{\rm NCA}-\omega)}{T_{\rm NCA}}\right]^{N/(N+1)}\ ,$$
$$\omega<E_G^{\rm NCA}\ . \tag{5.35}$$

Similarly,

$$Y_m(\omega)\sim T_{\rm NCA}\left[\frac{(N+1)(E_G^{\rm NCA}-\omega)}{T_{\rm NCA}}\right]^{1/(N+1)}\ ,$$
$$\omega<E_G^{\rm NCA}\ . \tag{5.36}$$

Propagators G_0 and G_m valid on both sides of the threshold $E_G^{\rm NCA}$ may be found immediately by analytic continuation:

$$G_0(\omega\pm i0^+)=-\frac{\pi}{\Gamma}e^{\pm i\pi N/(N+1)}\left[\frac{(N+1)(\omega-E_G^{\rm NCA})}{T_{\rm NCA}}\right]^{-N/(N+1)}\ ,$$
$$\rho_0(\omega)=\theta(\omega-E_G^{\rm NCA})\frac{1}{\Gamma}\sin\left[\frac{\pi N}{N+1}\right]\left[\frac{(N+1)(\omega-E_G^{\rm NCA})}{T_{\rm NCA}}\right]^{-N/(N+1)} \tag{5.37}$$

and

$$G_m(\omega\pm i0^+)=-\frac{1}{T_{\rm NCA}}e^{\pm i\pi/(N+1)}\left[\frac{(N+1)(\omega-E_G^{\rm NCA})}{T_{\rm NCA}}\right]^{-1/(N+1)},$$
$$\rho_m(\omega)=\theta(\omega-E_G^{\rm NCA})\frac{1}{\pi T_{\rm NCA}}\sin\left[\frac{\pi}{N+1}\right]\left[\frac{(N+1)(\omega-E_G^{\rm NCA})}{T_{\rm NCA}}\right]^{-1/(N+1)}. \tag{5.38}$$

Within the NCA, the spectral densities ρ_0 and ρ_m exhibit power-law threshold singularities with exponents dependent only on the degeneracy N. More systematic treatments of the threshold behavior (see, for example, Sec. II.D) suggest that the exact exponents depend on the f valence as well.

To compute the f spectral density within the NCA, it remains to calculate $\bar\rho_0$ and $\bar\rho_m$ [cf. Eq. (5.18)]. From Eq. (5.19), these quantities satisfy the equations

$$\frac{\partial}{\partial\omega}[\bar\rho_0(\omega)Y_0^2(\omega)]=-\frac{N\Gamma}{\pi}\bar\rho_m(\omega),$$
$$\frac{\partial}{\partial\omega}[\bar\rho_m(\omega)Y_m^2(\omega)]=-\frac{\Gamma}{\pi}\bar\rho_0(\omega), \tag{5.39}$$

with

$$\bar\rho_0(\omega)Y_0^2(\omega)\,|_{E_G^{\rm NCA}}=\bar\rho_m(\omega)Y_m^2(\omega)\,|_{E_G^{\rm NCA}}=0.$$

These equations assume the same form in the asymptotic region $\omega\to E_G^{\rm NCA}$ as the equations for Y_0 and Y_m [see Eq. (5.15)], if one makes the ansatz

$$\bar\rho_0(\omega)\sim\alpha Y_0^{-1}(\omega),$$
$$\bar\rho_m(\omega)\sim\alpha Y_m^{-1}(\omega),\quad \omega\to E_G^{\rm NCA}. \tag{5.40}$$

The value of α may be determined using an identity due to Müller-Hartmann (1984). Note that

$$\frac{d}{d\omega}[\bar\rho_0(\omega)Y_0(\omega)+N\bar\rho_m(\omega)Y_m(\omega)]=\bar\rho_0(\omega)+N\bar\rho_m(\omega). \tag{5.41}$$

Hence

$$\int_{-\infty}^{\infty}d\omega\frac{d}{d\omega}[\bar\rho_0(\omega)Y_0(\omega)+N\bar\rho_m(\omega)Y_m(\omega)]=\int_{-\infty}^{\infty}d\omega[\bar\rho_0(\omega)+N\bar\rho_m(\omega)]=1,$$

i.e.,

$$[\bar\rho_0(\omega)Y_0(\omega)+N\bar\rho_m(\omega)Y_m(\omega)]\,|_{E_G^{\rm NCA}}=1, \tag{5.42}$$

giving immediately

$$\alpha=\frac{1}{N+1}. \tag{5.43}$$

Finally, the f Green's function may be computed. Recall that in the NCA

$$G_f(\omega\pm i0^+)=\frac{1}{Z_f}\int_{-\infty}^{\infty}d\varepsilon\,e^{-\beta\varepsilon}[\rho_0(\varepsilon)G_m(\varepsilon+\omega\pm i0^+)-G_0(\varepsilon-\omega\mp i0^+)\rho_m(\varepsilon)]$$
$$=-\int_{-\infty}^{E_G^{\rm NCA}}d\varepsilon[\bar\rho_0(\varepsilon-\omega)Y_m^{-1}(\varepsilon)-Y_0^{-1}(\varepsilon-\omega)\bar\rho_m(\varepsilon)]+\int_{E_G^{\rm NCA}}^{E_G^{\rm NCA}+\omega}d\varepsilon\,\bar\rho_0(\varepsilon-\omega)G_m(\varepsilon\pm i0^+). \tag{5.44}$$

The first integral is real and may be neglected if only the spectral density is required. It may, however, be computed exactly using an identity (Müller-Hartmann, 1984) analogous to Eq. (5.42):

$$-\bar\rho_0(\varepsilon)Y_m^{-1}(\varepsilon)+Y_0^{-1}(\varepsilon)\bar\rho_m(\varepsilon)=\frac{\pi}{\Gamma}\frac{\partial}{\partial\varepsilon}[\bar\rho_m(\varepsilon)Y_m(\varepsilon)]-\frac{\pi}{\Gamma}\bar\rho_m(\varepsilon). \tag{5.45}$$

Applying the identity in Eq. (5.44) gives for $\omega=0$

$$-\int_{-\infty}^{E_G^{\rm NCA}}d\varepsilon[\bar\rho_0(\varepsilon)Y_m^{-1}(\varepsilon)-Y_0^{-1}(\varepsilon)\bar\rho_m(\varepsilon)]=\frac{\pi}{\Gamma}[\bar\rho_m(\varepsilon)Y_m(\varepsilon)]\Big|_{E_G^{\rm NCA}}-\frac{\pi}{\Gamma}\int_{-\infty}^{E_G^{\rm NCA}}d\varepsilon\,\bar\rho_m(\varepsilon)=\frac{\pi}{(N+1)\Gamma}\left[1-\frac{N+1}{N}n_f\right]. \tag{5.46}$$

Finally, for $\omega\to0$,

$$\int_{E_G^{\rm NCA}}^{E_G^{\rm NCA}+\omega}d\varepsilon\,\bar\rho_0(\varepsilon-\omega)G_m(\varepsilon\pm i0^+)=-\frac{1}{T_{\rm NCA}}e^{\pm i\pi/(N+1)}\frac{\pi}{(N+1)^2\Gamma}$$
$$\times\int_{E_G^{\rm NCA}}^{E_G^{\rm NCA}+\omega}d\varepsilon\left[\frac{\varepsilon-E_G^{\rm NCA}}{T_{\rm NCA}}\right]^{-1/(N+1)}\left[\frac{E_G^{\rm NCA}+\omega-\varepsilon}{T_{\rm NCA}}\right]^{-N/(N+1)}$$
$$=-\frac{\pi}{(N+1)^2\Gamma}e^{\pm i\pi/(N+1)}\int_0^1dx\,x^{-1/(N+1)}(1-x)^{-N/(N+1)}$$
$$=-\frac{\pi}{(N+1)^2\Gamma}e^{\pm i\pi/(N+1)}\pi\csc\frac{\pi}{N+1}. \tag{5.47}$$

Thus the f Green's function at the Fermi surface becomes

$$G_f(\pm i0^+)=\frac{\pi}{(N+1)\Gamma}\left[1-\frac{N+1}{N}n_f-\frac{\pi}{N+1}\cot\frac{\pi}{N+1}\mp\frac{i\pi}{N+1}\right]. \tag{5.48}$$

This analysis is only sufficient to find the Green's function at $\omega=0$. Müller-Hartmann (1984) has extended this analysis by retaining the next-leading corrections to the singular functions Y_0^{-1}, Y_m^{-1}, $\bar{\rho}_0$, and $\bar{\rho}_m$ for $\omega\to E_G^{\rm NCA}$. The result obtained for G_f is, in our notation,

$$\begin{aligned}G_f(\omega\pm i0^+)-G_f(\pm i0^+)=&\frac{\pm i\pi}{(N+1)^2\Gamma}4\sin\left[\frac{\pi}{N+1}\right]\left[\frac{1}{N+2}B_1\frac{T_{\rm NCA}}{\Gamma/\pi}\left[\frac{(N+1)\omega}{T_{\rm NCA}}\right]^{1/(N+1)}\right.\\&\left.+\frac{1}{2N+1}B_2\left[\frac{(N+1)\omega}{T_{\rm NCA}}\right]^{N/(N+1)}\right],\\B_1=B\left[\frac{2}{N+1},\frac{N}{N+1}\right],&\quad B_2=B\left[\frac{1}{N+1},\frac{2N}{N+1}\right],\end{aligned} \tag{5.49}$$

with B the beta function. We comment on this form below.

The leading term in the magnetic spectral density, i.e., the imaginary part of the magnetic susceptibility, may also be obtained for $\omega\to 0$. The calculation exactly parallels that in Eq. (5.47), and we only quote the result:

$$\mathrm{Im}\chi(\omega+i0^+)\sim\frac{\mu_j^2}{3}\frac{N}{N+1}B_3\sin\frac{\pi}{N+1}\frac{\omega}{T_{\rm NCA}^2}\left[\frac{(N+1)|\omega|}{T_{\rm NCA}}\right]^{-2/(N+1)},\quad B_3=B\left[\frac{N}{N+1},\frac{N}{N+1}\right]. \tag{5.50}$$

Equations (5.48)–(5.50) allow the direct comparison of NCA results with exact Fermi-liquid relations for the Anderson model. Four Fermi-liquid relations are listed in Table IX (Langreth, 1966; Shiba, 1975). The first two relations state that the character of the f-electron self-energy at zero energy is unchanged by the presence of Coulomb correlations (even in the limit $U\to\infty$). Within the NCA,

$$\mathrm{Im}\Sigma_f(i0^+)=-\mathrm{Im}G_f^{-1}(i0^+)=-\Gamma\left[\left[1-\frac{N+1}{N}n_f-\frac{\pi}{N+1}\cot\frac{\pi}{N+1}\right]^2+\frac{\pi^2}{(N+1)^2}\right]^{-1}. \tag{5.51a}$$

The first relation is clearly violated in general; for $N\to\infty$,

$$\mathrm{Im}\Sigma_f^{\rm NCA}(i0^+)\sim-\frac{\Gamma}{n_f^2}, \tag{5.51b}$$

and the approximate form deteriorates with decreasing valence. The second Fermi-liquid relation is also violated, since the NCA Green's function is nonanalytic at $\omega=0$. The spectral density exhibits a slightly asymmetric and very sharp cusp ($\sim|\omega|^{1/(N+1)}$) at $\omega=0$.

The third and fourth Fermi-liquid relations connect thermodynamic derivatives with low-energy dynamic properties. The third relation is violated since

$$\rho_f^{\rm NCA}(0)=\frac{\pi}{(N+1)^2\Gamma}, \tag{5.52}$$

a value independent of the valence; once again, the correct value is approached in the integral-valent limit for large N. The NCA fails most severely for the fourth relation: the quantity $\omega^{-1}\mathrm{Im}\chi^{\rm NCA}(\omega)$ actually diverges for $\omega\to 0$.

These shortcomings of the NCA prevent its application for $T\to 0$. However, the method's failure in the Fermi-liquid regime does not invalidate its application at finite temperature and frequency. The failure is due to an improper treatment of high-order perturbative processes involving low-energy electron-hole pairs. As the temperature (or probe energy) is raised, contributions from these high-order processes are quickly outweighed in thermal averages by low-order processes requiring higher-energy transfer. For example, the sharp cusp that dominates $\rho_f(\omega)$ for $\omega\to 0$ falls off rapidly; for larger ω (still in the asymptotic regime), the dominant contribution to the spectral density varies as $|\omega|^{N/(N+1)}$. For large N this term becomes indistinguishable from a linear contribution. Thus on a coarse-grained frequency scale, the spectral density appears smooth down to an energy of the order of $T_{\rm NCA}^*$, a characteristic crossover energy for the two asymptotic contributions in Eq. (5.49). We define $T_{\rm NCA}^*$ as the energy $\omega>0$ at which these contributions to ρ_f are equal. By a short computation,

$$T_{\rm NCA}^*=\frac{T_{\rm NCA}}{N+1}\left[\frac{2N+1}{N+2}\frac{B_1}{B_2}\frac{T_{\rm NCA}}{\Gamma/\pi}\sec\left[\frac{\pi}{N+1}\right]\right]^{(N+1)/(N-1)}\to\frac{T_{\rm NCA}}{N+1}\left[\frac{T_{\rm NCA}}{\Gamma/\pi}+O\left[\frac{1}{N}\right]\right]^{(N+1)/(N-1)}, \tag{5.53}$$

TABLE IX. Fermi-liquid relations for the f Green's function and dynamic susceptibility. We list below four Fermi-liquid relations involving dynamic properties of the degenerate-orbital Anderson model. These relations have been established by all-orders perturbation theory in U (Yamada, 1975) and remain valid in the limit $U\to\infty$. Σ_f is the f-electron self-energy, ρ_f the f density of states, and $\chi(\omega)$ the dynamic susceptibility.

1. $\mathrm{Im}\Sigma_f(i0^+)\,|_{T=0}=-\Gamma$.
2. $\left.\frac{\partial}{\partial\omega}\mathrm{Im}\Sigma_f(\omega+i0^+)\right|_{\omega=T=0}=0$.
3. $\rho_f(0)\,|_{T=0}=\frac{1}{\pi\Gamma}\sin^2\left[\left.\frac{\pi n_f}{N}\right]\right|_{T=0}$ (Friedel-Langreth).
4. $\left.\frac{\mu_j^2}{3}\frac{\mathrm{Im}\chi(\omega)}{\omega}\right|_{\omega=T=0}=\left.\frac{\pi}{N}\chi^2\right|_{T=0}$ (Korringa-Shiba).

with B_1 and B_2 as in Eq. (5.49). The height of the cusp above its value at the crossover energy is

$$\frac{\rho_f(0)-\rho_f(T^*_{\mathrm{NCA}})}{\rho_f(T^*_{\mathrm{NCA}})}=O\left[\left[\frac{T_{\mathrm{NCA}}}{\Gamma/\pi}\right]^{N/(N-1)}\right]. \quad (5.54)$$

This demonstrates analytically that the cusp anomaly has a sizable effect only in the mixed-valent regime, where $T_{\mathrm{NCA}}\sim\Gamma$; in the Kondo regime, where $T_{\mathrm{NCA}}\ll\Gamma$, the crossover scale T^*_{NCA} is tiny $[O(T_{\mathrm{NCA}}/\Gamma)]$ in comparison with T_{NCA}, and the relative height of the cusp above background at $\omega=T^*_{\mathrm{NCA}}$ is equally small. At finite temperature, thermal smearing prevents the observation of zero-temperature spectral features with energy scales smaller than T; the temperature acts as a natural coarse-graining scale. This means that, in the Kondo regime, finite-temperature NCA calculations should not produce an anomalous zero-frequency feature for $T>T^*_{\mathrm{NCA}}$. In particular, if the *onset* of a Fermi-liquid regime (in which properties vary with simple power-law temperature dependences) occurs at $T>T^*_{\mathrm{NCA}}$ one expects extrapolations of NCA calculations to zero temperature, or frequency, to be reliable.

C. NCA for the Coqblin-Schrieffer model

1. NCA integral equations for the Coqblin-Schrieffer model

The noncrossing approximation for the Anderson model partition function may be simply extended to the Coqblin-Schrieffer model. In this case, the fundamental quantities are the irreducible polarization and the occupied-state self-energy (see Sec. II.E). Recall from Sec. V.A the NCA equations for the Anderson model:

$$\begin{aligned}\Sigma_0(z)&=NV^2\sum_k f_k G_m(z+\varepsilon_k)\,,\\ \Sigma_m(z)&=V^2\sum_k(1-f_k)G_0(z-\varepsilon_k)\,,\end{aligned} \quad (5.55)$$

with

$$G_0(z)=\frac{1}{z-\Sigma_0(z)}$$

and

$$G_m(z)=\frac{1}{z-\varepsilon_f-\Sigma_m(z)}\,.$$

The Coqblin-Schrieffer NCA equations may be derived by a Schrieffer-Wolff transformation (Schrieffer and Wolff, 1966; Keiter and Kimball, 1971). The prescription is the following.

(1) Write down the Anderson model NCA equations with $z\to z+\varepsilon_f$.

(2) Pass to the Coqblin-Schrieffer limit

$$V^2\to\infty,\quad \varepsilon_f\to-\infty,\quad V^2/\varepsilon_f=J\,. \quad (5.56)$$

It is convenient to let

$$\begin{aligned}\lim_{\mathrm{CS}}\frac{1}{\varepsilon_f}\Sigma_0(z+\varepsilon_f)&=\Pi^{\mathrm{CS}}(z)\,,\\ \lim_{\mathrm{CS}}\Sigma_m(z+\varepsilon_f)&=\Sigma_m^{\mathrm{CS}}(z)\,,\\ \lim_{\mathrm{CS}}G_m(z+\varepsilon_f)&=G_m^{\mathrm{CS}}(z)\,.\end{aligned} \quad (5.57)$$

By inspection, the Coqblin-Schrieffer NCA equations are

$$\begin{aligned}\Pi^{\mathrm{CS}}(z)&=NJ\sum_k f_k G_m^{\mathrm{CS}}(z+\varepsilon_k)\,,\\ \Sigma_m^{\mathrm{CS}}(z)&=J\sum_k\frac{1-f_k}{1-\Pi^{\mathrm{CS}}(z-\varepsilon_k)}\,,\\ G_m^{\mathrm{CS}}(z)&=\frac{1}{z-\Sigma_m^{\mathrm{CS}}(z)}\,.\end{aligned} \quad (5.58)$$

The Coqblin-Schrieffer NCA has been investigated extensively by Maekawa and collaborators (1985a, 1985b), who refer to it as the "self-consistent ladder approximation," or SCLA. The integral equations treated by these authors take the form

$$\begin{aligned}\Pi^{\mathrm{SCLA}}(z)&=NJ\sum_k f_k G_m^{\mathrm{SCLA}}(z+\varepsilon_k)\,,\\ \Sigma_m^{\mathrm{SCLA}}(z)&=J\sum_k(1-f_k)\frac{\Pi^{\mathrm{SCLA}}(z)}{1-\Pi^{\mathrm{SCLA}}(z-\varepsilon_k)}\\ &=J\sum_k(1-f_k)\left[\frac{1}{1-\Pi^{\mathrm{SCLA}}(z-\varepsilon_k)}-1\right],\\ G_m^{\mathrm{SCLA}}(z)&=\frac{1}{z-\varepsilon_f-\Sigma_m^{\mathrm{SCLA}}(z)}\,.\end{aligned} \quad (5.59)$$

The term

$$J\sum_k(1-f_k)(-1)\equiv\Delta\varepsilon_f \quad (5.60)$$

is a temperature-independent constant; without loss, it may be absorbed into the f-level energy by letting

$$\varepsilon_f\to\tilde{\varepsilon}_f=\varepsilon_f+\Delta\varepsilon_f\,. \quad (5.61)$$

(This step remains valid in the presence of a magnetic field, provided $g\mu_B h \ll D$.) The energy $\tilde{\varepsilon}_f$ itself cannot appear in any physically measurable quantity. This is because the f orbital remains singly occupied at all times. Equations (5.59) are precisely the NCA equations with

$$G_m^{\mathrm{SCLA}}(z)\leftrightarrow G_m^{\mathrm{CS}}(z-\tilde{\varepsilon}_f)\ , \qquad \Pi^{\mathrm{SCLA}}(z)\leftrightarrow \Pi^{\mathrm{CS}}(z-\tilde{\varepsilon}_f)\ . \tag{5.62}$$

The SCLA partition function takes the form

$$Z^{\mathrm{SCLA}}=\sum_m \int_\Gamma \frac{dz}{2\pi i}\frac{e^{-\beta z}}{z-\varepsilon_f-\Sigma_m^{\mathrm{SCLA}}(z)} =e^{-\beta\tilde{\varepsilon}_f}\sum_m \int_\Gamma \frac{dz}{2\pi i}\frac{e^{-\beta z}}{z-\Sigma_m^{\mathrm{CS}}(z)}=e^{-\beta\tilde{\varepsilon}_f}Z^{\mathrm{CS}}\ . \tag{5.63}$$

The intermediate step follows by the variable shift $z\to z+\tilde{\varepsilon}_f$.

The name "self-consistent ladder approximation" is derived from an alternate pictorial representation of the Coqblin-Schrieffer diagrams [see the treatment by Maekawa *et al.* (1985a)]. Furthermore, Maekawa and collaborators (1985a, 1985b) employ a pseudo-Hamiltonian approach (see Sec. III) analogous to Abrikosov's treatment (Abrikosov, 1965) of the Kondo Hamiltonian (see Sec. III). Such an approach is completely equivalent to the diagrammatic technique described in Sec. II.E.

2. NCA expressions for dynamic properties

The impurity t matrix and dynamic susceptibility of the Coqblin-Schrieffer model have been studied by Maekawa and collaborators (1985a, 1985b). Both quantities may be simply obtained by a Schrieffer-Wolff transformation (1966) from the analogous quantities in the Anderson model. From an equation of motion treatment, the Anderson model t matrix is found to be

$$T_{kk'}(i\omega_n)=V^2G_f(i\omega_n) =\frac{1}{Z_f}\int_\Gamma \frac{dz}{2\pi i}e^{-\beta z}G_m(z+i\omega_n)G_0(z)$$

with

$$Z_f=\int_\Gamma \frac{dz}{2\pi i}e^{-\beta z}[G_0(z)+NG_m(z)]\ . \tag{5.64}$$

The contour Γ encircles the singularities of the integrands in a counterclockwise fashion. Performing the shift $z\to z+\varepsilon_f$ in both integrals, then passing to the Coqblin-Schrieffer limit gives immediately

$$T_{kk'}^{\mathrm{CS}}(i\omega_n)=J\frac{1}{Z^{\mathrm{CS}}}\int_\Gamma \frac{dz}{2\pi i}e^{-\beta z}G_m^{\mathrm{CS}}(z+i\omega_n)\frac{1}{1-\Pi^{\mathrm{CS}}(z)}\ , \tag{5.65a}$$

with

$$Z^{\mathrm{CS}}=N\int_\Gamma \frac{dz}{2\pi i}e^{-\beta z}G_m^{\mathrm{CS}}(z)\ . \tag{5.65b}$$

Here G_m^{CS} and Π^{CS} are as in Eq. (5.57). This may be rewritten as

$$T_{kk'}^{\mathrm{CS}}(i\omega_n)=J\frac{1}{Z^{\mathrm{CS}}}\int_\Gamma \frac{dz}{2\pi i}e^{-\beta z}G_m^{\mathrm{CS}}(z+i\omega_n)\left[\frac{\Pi^{\mathrm{CS}}(z)}{1-\Pi^{\mathrm{CS}}(z)}+1\right]=-\frac{J}{N}+J\frac{1}{Z^{\mathrm{CS}}}\int_\Gamma \frac{dz}{2\pi i}e^{-\beta z}G^{\mathrm{CS}}(z+i\omega_n)\frac{\Pi^{\mathrm{CS}}(z)}{1-\Pi^{\mathrm{CS}}(z)}\ . \tag{5.66}$$

The first term is energy independent and real valued. Such contributions always arise from nonmagnetic impurity scattering. This term may be removed by redefining the nonmagnetic impurity t matrix. The function

$$\frac{\Pi^{\mathrm{CS}}(z)}{1-\Pi^{\mathrm{CS}}(z)}$$

is analytic in the upper and lower half-planes and decays as z^{-1} at infinity. Hence it has the spectral representation

$$\frac{\Pi^{\mathrm{CS}}(z)}{1-\Pi^{\mathrm{CS}}(z)}=\int_{-\infty}^{\infty}d\varepsilon\frac{\eta(\varepsilon)}{z-\varepsilon},\quad \eta(\varepsilon)=-\frac{1}{\pi}\mathrm{Im}\frac{\Pi^{\mathrm{CS}}(\varepsilon+i0^+)}{1-\Pi^{\mathrm{CS}}(\varepsilon+i0^+)}\ . \tag{5.67}$$

The t matrix may then be rewritten

$$T_{kk'}^{\mathrm{CS}}(i\omega_n)=-\frac{J}{N}-J\frac{1}{Z^{\mathrm{CS}}}\int_{-\infty}^{\infty}d\varepsilon\, e^{-\beta\varepsilon}\left[\rho_m^{\mathrm{CS}}(\varepsilon)\frac{\Pi^{\mathrm{CS}}(\varepsilon-i\omega_n)}{1-\Pi^{\mathrm{CS}}(\varepsilon-i\omega_n)}-G_m^{\mathrm{CS}}(\varepsilon+i\omega_n)\eta(\varepsilon)\right]; \tag{5.68a}$$

hence

$$\mathrm{Im}\,T_{kk'}^{\mathrm{CS}}(\omega+i0^+)=-\frac{\pi J}{Z^{\mathrm{CS}}}(1+e^{-\beta\omega})\int_{-\infty}^{\infty}d\varepsilon\, e^{-\beta\varepsilon}\rho_m(\varepsilon+\omega)\eta(\varepsilon)\ . \tag{5.68b}$$

This t matrix (generalized to include crystal-field split f levels) has been employed to calculate the resistivity of model Ce systems (Maekawa *et al.*, 1985a, 1985b).

The dynamic susceptibility may also be derived by a Schrieffer-Wolff transformation from the Anderson result [Eq. (5.8)]. Recall that for the Anderson model

$$\chi(i\nu_m)=-\frac{N\mu_j^2}{3}\frac{1}{Z_f}\int_\Gamma \frac{dz}{2\pi i}e^{-\beta z}G_m(z)G_m(z+i\nu_m)\ . \tag{5.69}$$

Again shifting the variable of integration by $z\to z+\varepsilon_f$ and passing to the Coqblin-Schrieffer limit gives

$$\chi^{\rm CS}(i\nu_m)=-\frac{N\mu_j^2}{3}\frac{1}{Z^{\rm CS}}\int_\Gamma \frac{dz}{2\pi i}e^{-\beta z}G_m^{\rm CS}(z)G_m^{\rm CS}(z+i\nu_m)$$

$$=-\frac{N\mu_j^2}{3}\frac{1}{Z^{\rm CS}}\int_{-\infty}^{\infty}d\varepsilon\, e^{-\beta\varepsilon}\rho_m^{\rm CS}(\varepsilon)[G_m^{\rm CS}(\varepsilon+i\nu_m)+G_m^{\rm CS}(\varepsilon-i\nu_m)]\ ,$$

with

$$\mu_j^2=j(j+1)(g\mu_B)^2\ . \tag{5.70a}$$

The absorptive part of the susceptibility is then

$$\mathrm{Im}\chi^{\rm CS}(\omega+i0^+)=\frac{N\mu_j^2}{3}\frac{\pi}{Z^{\rm CS}}\int_{-\infty}^{\infty}d\varepsilon\, e^{-\beta\varepsilon}\rho_m^{\rm CS}(\varepsilon)[\rho_m^{\rm CS}(\varepsilon+\omega)-\rho_m^{\rm CS}(\varepsilon-\omega)]\ . \tag{5.70b}$$

The static susceptibility may be obtained directly from Eq. (5.70a) as

$$\chi^{\rm CS}(\omega=0)=-\frac{N\mu_j^2}{3}\frac{1}{Z^{\rm CS}}$$

$$\times\int_{-\infty}^{\infty}d\varepsilon\, e^{-\beta\varepsilon}\rho_m^{\rm CS}(\varepsilon)\cdot 2\,\mathrm{Re}G_m^{\rm CS}(\varepsilon)\ .$$

These expressions have been employed by Maekawa and collaborators (1985a, 1985b) to study the static and dynamic susceptibility in a model Ce compound ($CeCu_2Si_2$).

D. NCA results at finite temperature

The failure of the NCA in the Fermi-liquid regime (Sec. V.B) is balanced by its success in calculations at finite temperature. The NCA provides a conceptually simple approach for treating static and dynamic properties above the characteristic anomaly temperature $T^*_{\rm NCA}$ introduced in Sec. V.B. In this sense, the NCA is largely complementary to the approaches discussed in Secs. II–IV and VI. The variational approach (Sec. IV) is expressly formulated for the zero-temperature limit. The powerful saddle-point approximations discussed in Sec. VI are valid throughout the Fermi-liquid regime, but not at higher temperatures. The diagrammatic expansions of Secs. II and III are, in principle, valid at arbitrary temperature, but are, in practice, awkward to apply outside the Fermi-liquid regime.

In view of the NCA's behavior for $T\to 0$, its reliability at finite temperature must be established by comparing results for static properties (specific heat and magnetic susceptibility) with "exact" results from the Bethe ansatz or numerical renormalization group. Comparisons for systems with angular momentum degeneracy $N=4$ and $N=6$ (Bickers, Cox, and Wilkins, 1987) are shown in Fig. 24. (Since different conduction-electron band structures are assumed in the NCA and Bethe ansatz, the low-temperature scales have been adjusted to give identical magnetic susceptibilities at high temperature.) The NCA results are in good agreement with the exact treatment and improve slightly with increasing degeneracy. As shown in Fig. 25 the NCA remains an excellent approximation in systems with N as small as 2 (Zhang and Lee, 1984). The success of the NCA at small magnetic degeneracy has important implications for the modeling of more realistic systems. When impurity levels are split by a strong crystalline electric field (CEF) or a finite magnetic field, N does not formally remain an expansion parameter. Nevertheless, on the basis of results for $N=2$, one expects the NCA to retain much of its quantitative validity in these cases.

Since the NCA yields reliable results for static properties outside the Fermi-liquid regime, it is reasonable to assume dynamic properties are accurately represented as well. Bickers, Cox, and Wilkins (1985, 1987) have studied the temperature dependence of the impurity valence, magnetic susceptibility, specific heat, resistivity, thermopower, and thermal conductivity over a wide range of parameters in the so-called Kondo regime. In this regime, the degenerate impurity configuration lies far below the nondegenerate configuration ($-\varepsilon_f \gg \Gamma$). Most dilute intermetallic alloys of Ce and Yb are now believed to lie in this parameter range of the Anderson model rather than in the strongly mixed valent regime (where $|\varepsilon_f| \leq \Gamma$). In Ce alloys (Yb alloys), the degenerate impurity configuration is f^1 (f^{13}) and the nondegenerate configuration f^0 (f^{14}). Strong spin-orbit interactions reduce the impurity degeneracy from 14 to 6 (Ce) and 8 (Yb). Crystalline electric field (CEF) splitting may further reduce the effective degeneracy in some alloys. Systems may be conveniently

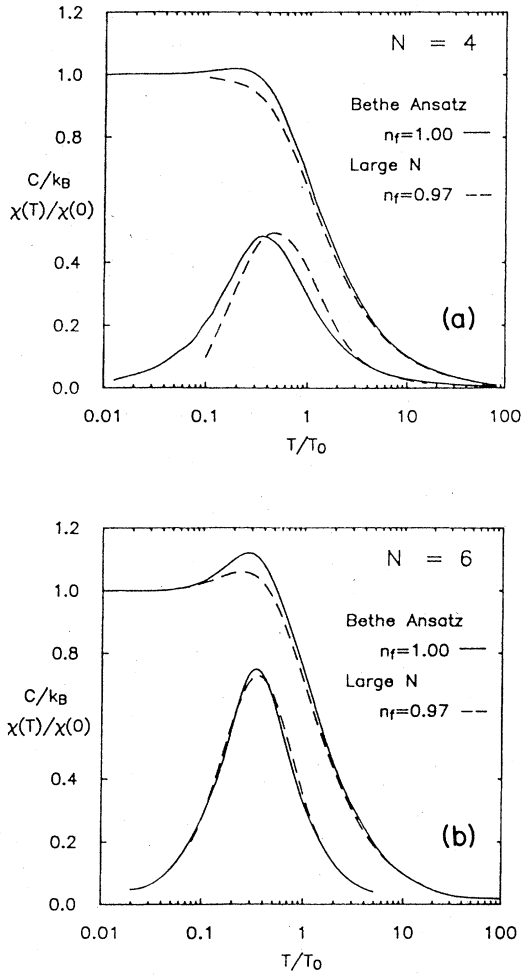

FIG. 24. Comparison of large-N and Bethe ansatz results for finite-temperature thermodynamics (Bickers, Cox, and Wilkins, 1987). (a) Specific heat C and magnetic susceptibility χ for $N=4$. (b) Specific heat and susceptibility for $N=6$. In both cases, Bethe ansatz results for the Coqblin-Schrieffer model are compared with large-N results for the Anderson model in the scaling regime.

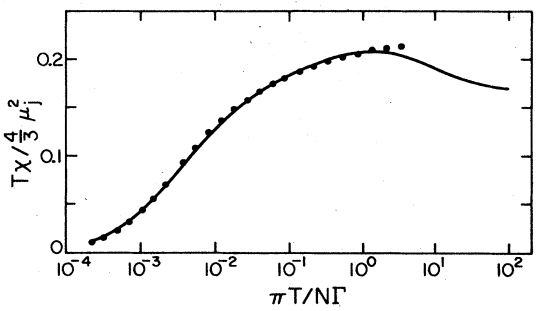

FIG. 25. Comparison of large-N and renormalization-group results for the magnetic susceptibility of the $N=2$ Anderson model (Zhang and Lee, 1984). The solid line shows large-N results for a flat conduction band of half-width D, with $\Gamma/D=0.016$ and $\varepsilon_f/D=-0.075$. The dots represent the Kondo model susceptibility curve deduced by the numerical renormalization group (Krishna-murthy, Wilkins, and Wilson, 1980a).

characterized by values of the ground-state energy scale T_A and the zero-temperature valence. [In this context, the valence $n_f(T)$ is defined as the fractional occupancy of the degenerate configuration at temperature T.] Finite-temperature properties assume approximate scaling forms as functions of the reduced parameter T/T_A in the valence range $n_f(0)=0.7-1.0$. Representative results for $N=6$ are shown in Fig. 26. This approximate universality within the Kondo regime allows robust comparisons with experiment. The precise values of the configuration splitting ε_f and the hybridization width Γ are not crucial, so long as the valence is sufficiently large. The only fitting parameter remaining is the low-energy scale itself. The most thoroughly characterized dilute alloy of Ce is (La,Ce)B_6. As shown in Fig. 27 the susceptibility, specific heat, resistivity, and thermopower of this system are consistently described by the NCA over ranges of two to four temperature decades.

Maekawa, Kashiba, Takahashi, and Tachiki (1985a, 1985b) have studied the magnetic susceptibility and resistivity of Ce impurities within the Coqblin-Schrieffer NCA (unit impurity valence). These authors modeled the anisotropic properties of $CeCu_2Si_2$ by incorporating CEF splitting of the Ce $j=\frac{5}{2}$ term (Fig. 28). Cox (1987a) has used the Anderson model NCA to study the static and dynamic properties of a proposed single-impurity model for UBe_{13}.

In addition to thermodynamic and transport properties, the NCA has been used to study dynamic correlation functions at finite temperature. The impurity electron density of states $\rho_f(\omega)$ and the dynamic magnetic susceptibility $\mathrm{Im}\chi(\omega)$ have simple expressions within the NCA (see Secs. V.A and V.C). The density of states may, in principle, be probed directly by x-ray photoemission (f-electron removal) and inverse photoemission (f-electron addition). Anderson model studies have concentrated on the Kondo parameter regime (see above), which is believed to be most relevant to experiment. As discussed in Secs. II.D and IV.B, the f density of states has two prominent features in the simplest infinite-U approximation (see Fig. 29): a broad charge-excitation resonance (half-width $\sim N\Gamma$) near ε_f, the position of the unhybridized degenerate configuration; and a narrow Kondo-Abrikosov-Suhl resonance near the Fermi level. In Ce alloys, the charge-excitation resonance measures the weight for $f^1\rightarrow f^0$ transitions, while the Kondo resonance reflects $f^0\rightarrow f^1$ transitions: hence, the charge-excitation resonance is probed primarily by photoemission and the Kondo resonance by inverse photoemission. In Yb alloys, these roles are reversed: photoemission probes the $f^{14}\rightarrow f^{13}$ Kondo resonance, while inverse photoemission probes the $f^{13}\rightarrow f^{14}$ charge-excitation resonance.

The scaling properties of the Kondo resonance at low temperatures and energies have been investigated by Bick-

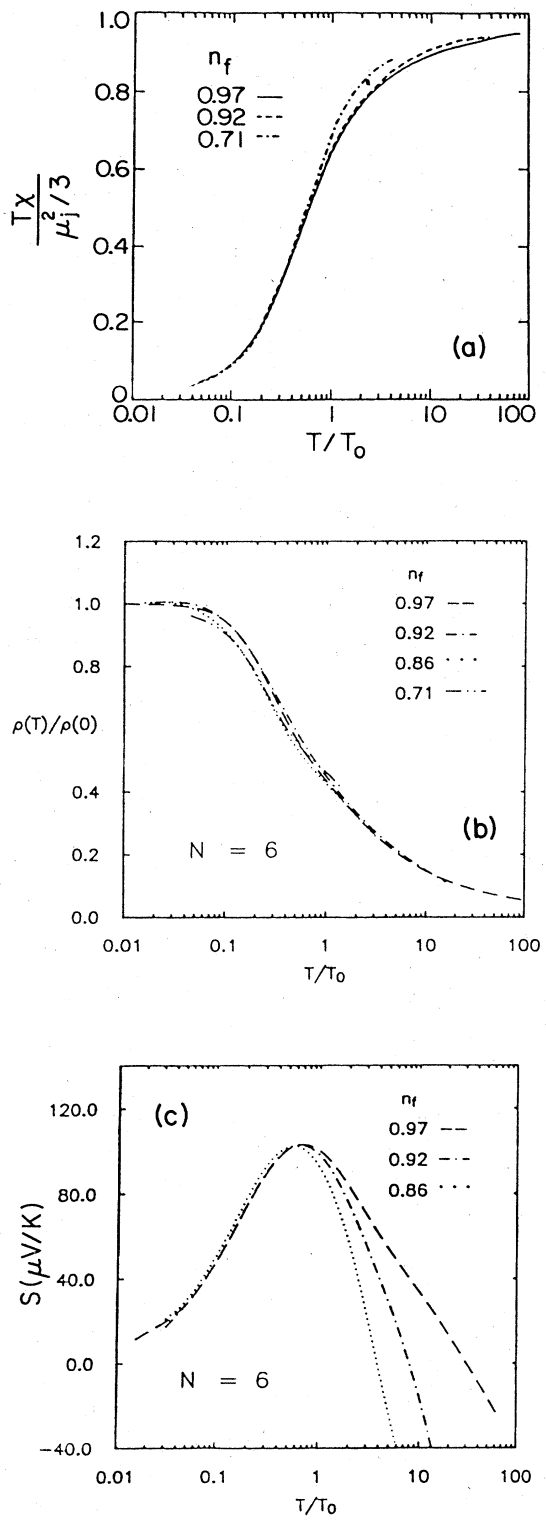

FIG. 26. Scaling of thermodynamic and transport properties for the $N=6$ Anderson model (Bickers, Cox, and Wilkins, 1987). (a) Effective magnetic moment $T\chi(T)$. (b) Electrical resistivity. (c) Thermopower. Results are shown for an f valence varying between 0.97 and 0.71.

ers, Cox, and Wilkins (1985, 1987). The resonance shows approximate scaling with reduced parameters T/T_A and ω/T_A (see Fig. 30) over a wide range of impurity valences. This scaling behavior is directly reflected in low-temperature transport properties, which measure weighted averages of the conduction-electron lifetime $\tau(\omega)\propto\rho_f^{-1}(\omega)$. As the temperature is increased through $T\sim T_A$, the Kondo resonance melts away (see Fig. 31). At finite temperature, ρ_f measures the density of states for changing the f-electron count, thermally averaged over all many-body eigenstates. The Kondo resonance is due to a small admixture of the nondegenerate configuration in the ground state and low-lying excited states. Hence, when higher-lying eigenstates with negligible admixtures of this configuration become appreciably populated, the unique ground-state signature disappears.

More realistic generalizations of the simplest infinite-U Anderson model lead to a richer structure in the f density of states. Bickers, Cox, and Wilkins (1985, 1987) have investigated the photoemission and inverse photoemission spectra for model Ce and Yb alloys with two spin-orbit multiplets.

The dynamic susceptibility $\mathrm{Im}\chi(\omega)$ has also been studied extensively within the NCA. This spectrum may be probed directly by neutron scattering (see, for example, Holland-Moritz, Wohlleben, and Loewenhaupt, 1982). The temperature dependence of $\mathrm{Im}\chi(\omega)$ for the infinite-U Anderson model has been investigated by Kuramoto and Kojima (1984) and by Cox, Bickers, and Wilkins (1985). Using a single-impurity approximation, the latter authors obtained good agreement with neutron scattering experiments on $CePd_3$ (see Fig. 32). The behavior of inelastic lines in systems with more complex multiplet structure has been investigated by Maekawa, Kashiba, Takahashi, and Tachiki (1985a, 1985b).

A number of other properties have been investigated within the NCA for the Anderson model. The behavior of the magnetization $M(H)$ in high fields has been investigated by Cox (1987b). Cox (1987c) has applied NCA results to a discussion of NMR linewidths in the heavy-electron metals. Finally, the NCA for the Anderson model has been employed in an investigation of pair breaking by magnetic impurities in BCS superconductors (Bickers and Zwicknagl, 1987).

VI. LARGE-N SADDLE-POINT APPROXIMATIONS IN THE FUNCTIONAL INTEGRAL APPROACH

A. Introduction

In this section we discuss saddle-point approximations (Read and Newns, 1983a, 1983b; Coleman, 1985a, 1985b, 1987; Read, 1985) based on functional integral representations for the Coqblin-Schrieffer and infinite-U Anderson models. Such approaches rely on pseudo-Hamiltonians, which we first discussed in Sec. III.A. The pseudo-Hamiltonians conventionally studied are

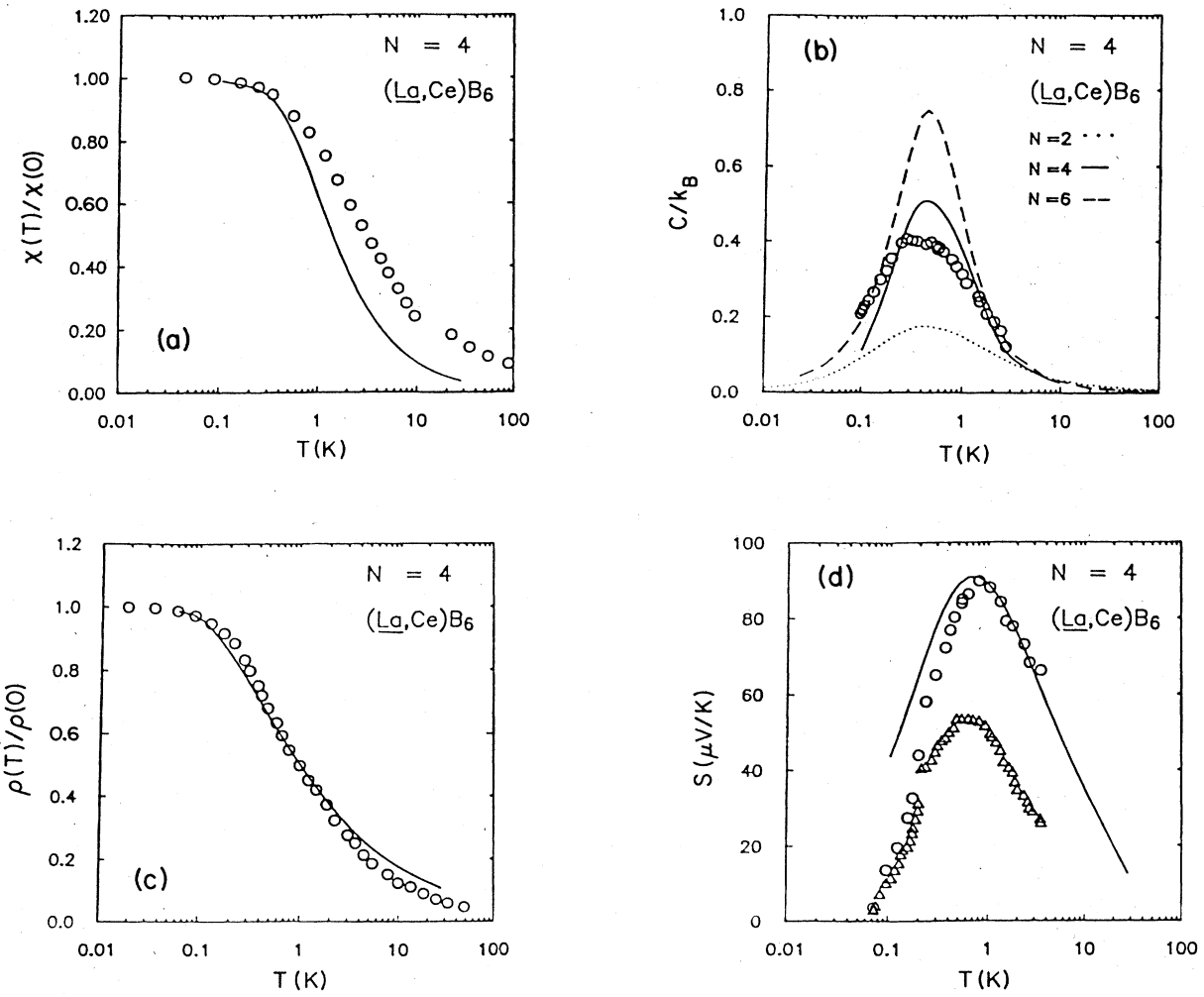

FIG. 27. Comparison of large-N theory (Bickers, Cox, and Wilkins, 1987) and experiment for (La,Ce)B_6. A quartet f ground state is assumed. All theoretical results (solid lines) assume a low-temperature scale $T_0=1$ K. (a) Magnetic susceptibility (Felsch, 1978). (b) Specific heat (Ernst, Grühl, Krug, and Winzer, 1984). (c) Electrical resisitivity (Winzer, 1975). (d) Thermopower (Ernst *et al.*, 1984).

$$H^{\rm CS}_{\rm pseudo}=H_{\rm band}+H_{\rm int}\ ,$$

where

$$H_{\rm band}=\sum_{km}\varepsilon_k c^\dagger_{km}c_{km}\ ,$$
$$H_{\rm int}=-J\sum_{kk'mm'}c^\dagger_{k'm'}f^\dagger_m f_{m'}c_{km}\ , \tag{6.1}$$

subject to

$$\sum_m f^\dagger_m f_m=1 \tag{6.2}$$

and

$$H^{A}_{\rm pseudo}=H_{\rm band}+H_f+H_{\rm mix},\quad H_f=\varepsilon_f\sum_m f^\dagger_m f_m\ ,$$
$$H_{\rm mix}=V\sum_{km}(c^\dagger_{km}b^\dagger f_m+\text{H.c.})\ , \tag{6.3}$$

subject to

$$\sum_m f^\dagger_m f_m+b^\dagger b=1\ . \tag{6.4}$$

The operators $f^\dagger_m$ and $b^\dagger$ create fermions and bosons, respectively. The pseudo-Hamiltonians are equivalent to the Coqblin-Schrieffer and infinite-U Anderson models within the restricted Hilbert spaces satisfying the occupancy constraints (6.2) and (6.4).

It is possible to derive rigorous functional integral representations for these models based on Eqs. (6.1)–(6.4). In Sec. III.B functional integrals were used to derive the first two terms in the expansion of the Anderson partition function in powers of $1/N$ for arbitrary temperature T. Recall that results obtained in this way may alternately be derived by the methods of Sec. II. Functional integral methods may also be used to derive expansions for the

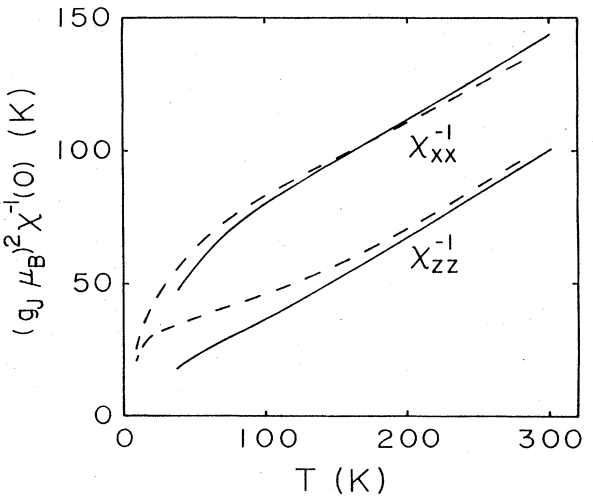

FIG. 28. Comparison of large-N theory and experiment for $CeCu_2Si_2$ (Maekawa, Kashiba, Takahashi, and Tachiki, 1986). Experimental results (dashed lines) for the anisotropic magnetic susceptibility in the heavy-electron compound $CeCu_2Si_2$ (Onuki, Furukawa, and Komatsubara, 1983) are compared with theoretical results (solid lines) for the $N=6$ Coqblin-Schrieffer model with crystal-field splitting

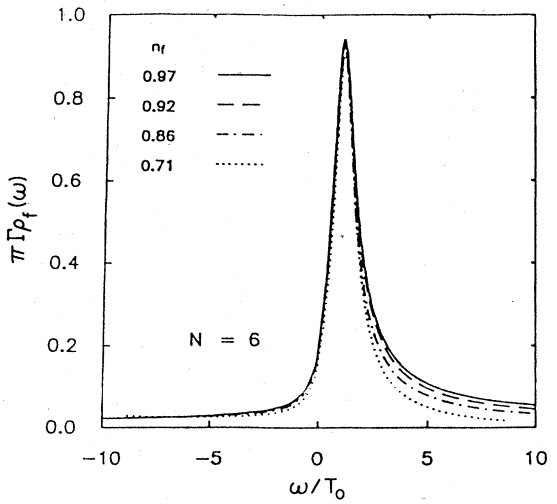

FIG. 30. Approximate scaling for the low-temperature f spectral density ρ_f of the Anderson model (Bickers, Cox, and Wilkins, 1987). Results are shown for four values of the f valence n_f. The low-energy Kondo resonance assumes a nearly universal form within this parameter range. This universality is reflected directly in electronic transport properties.

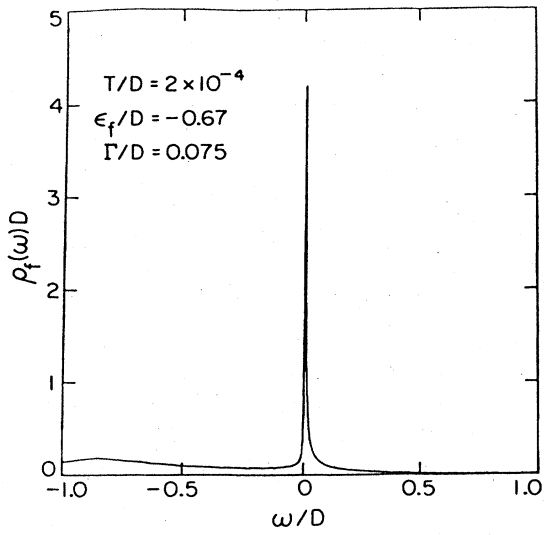

FIG. 29. NCA result for the low-temperature f spectral density ρ_f of the $N=6$ Anderson model (Bickers, Cox, and Wilkins, 1987). A Lorentzian conduction density of states with half-width D is assumed. The f spectral density exhibits two peaks: a broad (half-width $\sim N\Gamma$) charge-excitation resonance near ε_f, the position of the unhybridized f level; and an extremely sharp "Kondo resonance" just above the Fermi surface. For the parameters chosen, the Kondo resonance lies at $\omega/D = T_0/D \sim 5.3\times10^{-3}$. (For finite U, an additional resonance would appear near energy $\varepsilon_f + U$.) The nonanalyticity of the NCA spectral density at the Fermi surface is not visible for the temperature shown.

Coqblin-Schrieffer partition function and correlation functions of the two models. In all such calculations the occupancy constraints (6.2) and (6.4) play an important role: the full pseudo-Hamiltonian Hilbert spaces contain "ghost" states, which should not contribute to physical properties.

Whenever functional integrals over real or complex spaces are introduced, nonperturbative saddle-point ap-

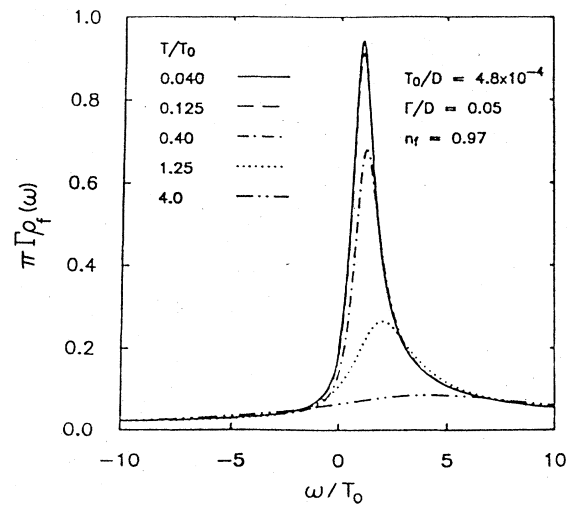

FIG. 31. Temperature dependence of the f spectral density ρ_f for the $N=6$ Anderson model (Bickers, Cox, and Wilkins, 1987). The Kondo resonance rapidly drops in height and shifts as excited states with small f^0 admixture become thermally populated. Nevertheless, the resonance has an important effect at temperatures up to $\sim 10T_0$.

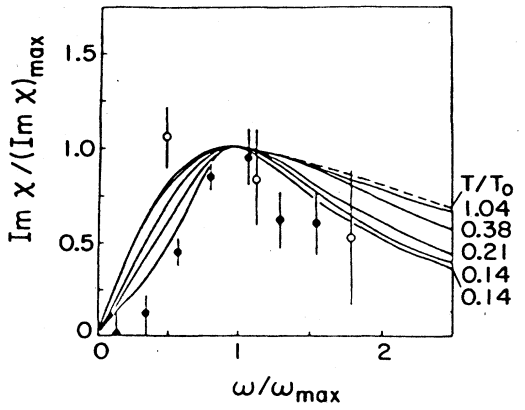

FIG. 32. Comparison of large-N theory and experiment for the dynamic susceptibility $\mathrm{Im}\chi(\omega)$ of $CePd_3$ (Bickers, Cox, and Wilkins, 1987). The dashed line shows a simple quasielastic line shape. Finite-temperature results (solid lines) for the $N=6$ Anderson model in the scaling regime are compared with experimental neutron spectra (Galera *et al.*, 1985) measured at 5 K (solid circles) and 280 K (open circles).

proximations become possible. Such approximations are common in the description of phase transitions and other collective behavior. For example, the BCS theory of superconductivity may be formulated as a saddle-point approximation with fluctuation corrections [see, for example, Popov, 1983)]. Saddle-point approximations have also been introduced in treatments of the Anderson and Coqblin-Schrieffer models (Read and Newns, 1983a, 1983b; Coleman, 1985a, 1985b, 1987; Read, 1985; Kotliar and Ruckenstein, 1986). [Mean-field treatments of the magnetic impurity problem actually have a longer history, dating from a study of the Kondo model by Takano and Ogawa (1966).] Since saddle-point approximations are in this case based on pseudo-Hamiltonians with enlarged Hilbert spaces, a cause for concern is the fate of the occupancy constraints (6.2) and (6.4). The exact role of these constraints in saddle-point treatments has been (and remains, to some extent) a point of controversy.

Constraints on particle number arise in statistical mechanics within the canonical ensemble. In the thermodynamic limit, canonical and grand canonical treatments are equivalent, and exact constraints on particle number are not crucial. It is only necessary that constraints be satisfied on average, since relative fluctuations are inversely proportional to the total particle number. The occupancy constraints (6.2) and (6.4) are qualitatively different in character. Only one local Fermi or Bose particle may be present in the system at any time, even if the magnetic degeneracy $N\to\infty$ (the large-N limit is *not* a thermodynamic limit). For this reason the occupancy constraints in magnetic alloy models are qualitatively different from those that arise in the statistical mechanics of macroscopic systems. At finite temperature, a saddle-point treatment of the occupancy constraints introduces errors formally of $O(1)$ in a large-N expansion. These errors arise partially from the inclusion of unphysical states in the pseudo-Hamiltonian Hilbert space.

The degree of violation of the occupancy constraints is, however, highly temperature dependent. (A failure to realize this fact has been the source of much of the controversy surrounding the saddle-point approach.) In the Fermi-liquid regime, i.e., for temperatures much less than the characteristic low-energy scales T_{CS} and T_A, the constraints are violated by an exponentially small amount [$\propto \exp(-T_{CS}/T)$ or $\exp(-T_A/T)$]. For this reason, expressions for the *low-temperature* free energy and correlation functions derived by other methods (Secs. II—IV) may be recovered from a saddle-point analysis in which the constraints are enforced approximately. (This statement has not, in fact, been established to all orders in perturbation theory, but now seems clear from examination of low orders in the large-N expansion.) The basis for this unusual behavior in the zero-temperature limit is not entirely clear, but may be related to the integrability of the Coqblin-Schrieffer and Anderson models [in this regard, see Coleman and Andrei (1986)].

Since the occupancy constraints need only be treated *perturbatively* in the Fermi-liquid regime, the Coqblin-Schrieffer and Anderson models may be reanalyzed using the full array of methods for treating quantum field theories near a saddle point. Such methods, which may alternately be phrased in purely diagrammatic terms ('t Hooft and Veltman, 1974), allow all-orders resummations of perturbation theory. Assuming suitable convergence properties for the diagrammatic sums before and after such a transformation, this amounts to a *nonperturbative* reinterpretation of the underlying degrees of freedom in the theory. The infrared divergences that arise from dressing the $O(1)$ magnetic alloy ground state with electron-hole pairs (see Sec. II.D) may be eliminated by such a transformation (Read and Newns, 1983; Read, 1985; Coleman, 1987). [While such divergences are automatically eliminated from measurable properties by the large-N expansions of Secs. II—IV, they remain order by order in other properties, such as the overlap between the noninteracting and interacting ground states (see Sec. II.D).] The resulting Fermi degrees of freedom may be interpreted as weakly interacting "quasiparticles," coupled by excitations of a Bose background field. [These are not quite the quasiparticles of Nozière's Fermi-liquid theory (Nozières, 1974). In Nozière's theory the specific heat γT is completely determined by the quasiparticle density of states; in the present case, the Bose degrees of freedom also contribute to γ.] The quasiparticle transformation is a crucial conceptual advance which allows a possible extension in periodic systems.

Generalizations of the Coqblin-Schrieffer and Anderson models for which the large-N limit is a thermodynamic limit have been proposed (Coleman, 1985a, 1985b, 1987). In such treatments the impurity level is assumed to hold up to N fermions or bosons, and the filling is fixed at some integer value $Q=qN$; the case $q=1/N$ is physically relevant. For fixed q, a thermodynamic-limit saddle-point expansion is expected to converge asymptoti-

cally for $N\to\infty$ at all temperatures. The small parameter in such an expansion is $(qN)^{-1}$. In the physical limit, this parameter tends to 1, and the treatment amounts to a saddle-point expansion based on the number of Bose loops, rather than the small parameter $1/N$. Such an expansion is poorly behaved at finite temperature, but remains well controlled in the Fermi-liquid regime. (The number of Bose loops in a diagram and its order in $1/N$ are closely related: for this reason, results from a loop expansion may subsequently be reexpanded in $1/N$.) A saddle-point expansion based on the number of Bose loops was first discussed by Read and Newns (1983). We describe the Bose loop expansion in parallel with our discussion of the saddle-point $1/N$ expansions for the Coqblin-Schrieffer and Anderson models.

The remainder of this section is organized as follows: In Sec. VI.B we describe the saddle-point approximation for the Coqblin-Schrieffer and Anderson models. We discuss in parallel the $O(1)$ approximation in the large-N expansion and the tree-level approximation in the Bose loop expansion. In Appendix I we discuss the saddle-point approximation for two "toy models," again distinguishing the results of $O(1)$ and tree-level approximations. This discussion illustrates many features of the full magnetic alloy analysis in a simpler context; in particular, the quantitative success of saddle-point approximations in the zero-temperature limit and their qualitative breakdown at finite temperature may be simply understood for the toy models. In Appendix J we discuss the calculation of $O(1/N)$ corrections to zero-temperature properties within the saddle-point approach. In Sec. VI.C we discuss the nonperturbative transformation introduced by Read and Newns (1983) for treating quasiparticle degrees of freedom in the Fermi-liquid regime. Finally, in Sec. VI.D, we make some additional comments on the Bose loop expansion for the magnetic impurity models.

B. Saddle-point approximations for magnetic impurity models

In this section we derive saddle-point approximations for the Coqblin-Schrieffer and infinite-U Anderson models. We consider in parallel a mathematical generalization of these models: for each value of N, the pseudo-Hamiltonians in Eqs. (6.1) and (6.3) describe a hierarchy of models with different local-level occupancies. The models describing the magnetic impurity problem correspond to the constraints

$$\sum_m f_m^\dagger f_m = 1, \quad \sum_m f_m^\dagger f_m + b^\dagger b = 1 . \tag{6.5}$$

Well-defined (but unphysical) models correspond to the constraints

$$\sum_m f_m^\dagger f_m = Q, \quad \sum_m f_m^\dagger f_m + b^\dagger b = Q \quad (Q<N) , \tag{6.6}$$

with $f_m^\dagger$ and $b^\dagger$ Fermi and Bose operators. In particular, models with simple thermodynamic limits are obtained for

$$\sum_m f_m^\dagger f_m = qN, \quad \sum_m f_m^\dagger f_m + b^\dagger b = qN , \tag{6.7}$$

with q a constant and qN integral. As we emphasized in Sec. III.A and Appendix I, such generalizations are not mathematically unique. The levels $|m\rangle$ and $|0\rangle$ in the magnetic impurity problem have neither Fermi nor Bose character. The generalization in Eq. (6.7) has particularly nice properties, however. In this case, the large-N expansion is equivalent to a Bose loop expansion (Coleman, 1985a, 1985b, 1987). The loop expansion is well controlled in the Fermi-liquid regime (Read, 1985), and results derived by other large-N techniques may be recovered by expanding in $q=1/N$ *after* expanding in the number of Bose loops. [Outside the Fermi-liquid regime, i.e., for temperatures of order T_A and T_{CS}, the loop expansion introduces errors due to violation of the level occupancy constraint in Eq. (6.5).] In the course of our treatment we compare lowest-order results from the large-N expansion and the Bose loop expansion.

The success of the saddle-point approach at zero temperature may be interpreted using the language of Sec. II. For $T\to 0$, thermodynamic properties are dominated by the lowest-energy singularities in the quantities $(1-\Pi^{(1)}(z))^{-1}$ (the polarization function for the Coqblin-Schrieffer model) and $(z-\Sigma_0^{(1)}(z))^{-1}$ (the empty-state propagator for the Anderson model). The saddle-point prescription amounts to locating these singularities. At finite temperature, properties may no longer be expressed as contributions from a single singularity. The agreement between the saddle-point treatment and alternative approaches worsens with increasing T. The occupancy constraints (6.2) and (6.4) are "effectively" enforced at zero temperature; at finite temperature, the constraints cannot be enforced within a saddle-point approximation.

1. Coqblin-Schrieffer model

We consider first the Coqblin-Schrieffer model [Eq. (6.1)] and its generalization (Read and Newns, 1983a). The partition function for arbitrary qN takes the form

$$Z=\int_{-\pi T}^{\pi T}\frac{\beta d\lambda}{2\pi}e^{i\beta\lambda(qN)}(1+e^{-i\beta\lambda})^N\int_\xi e^{-S} ,$$

with

$$S=\beta\sum_m |\xi_m|^2 - N\,\mathrm{Tr}\ln\left[1+J\sum_k \mathbf{G}(i\lambda)\mathbf{X}^\dagger\mathbf{G}(\varepsilon_k)\mathbf{X}\right] \quad (J<0) ,$$

$$\mathbf{X}_{nn'}=\xi_{n-n'}, \quad \mathbf{G}(E)_{nn'}=\delta_{nn'}\frac{1}{i\omega_n-E} , \tag{6.8}$$

$$\int_\xi=\int\prod_m d\bar{\xi}_m d\xi_m .$$

The value of the partition function is unchanged if λ is shifted into the complex plane by

$$\lambda \to \lambda + i\varepsilon_{\rm MF} \,. \tag{6.9}$$

It is convenient to perform this shift at the outset, since the saddle-point value of λ is imaginary. Mean-field equations may be obtained by (a) ignoring finite-frequency fluctuations (the variables ξ_m with $m \neq 0$) and (b) evaluating the static integrals over λ and ξ_0 by a saddle-point approximation. [We review the inclusion of lowest-order fluctuation corrections (Read, 1985) in Appendix J.] The partition function may be divided into mean-field and fluctuation components:

$$\begin{aligned} &Z = Z_{\rm MF} Z_{\rm fluct}, \quad Z_{\rm MF} = e^{-\beta F_{\rm MF}} \,, \\ &F_{\rm MF} = \varepsilon_{\rm MF}(qN) - NT \ln(1 + e^{\beta \varepsilon_{\rm MF}}) + \langle \xi_0 \rangle^2 \\ &\qquad + L(\varepsilon_{\rm MF}, \langle \xi_0 \rangle) \,, \\ &L = -N \frac{1}{\beta} {\rm Tr} \ln \left[1 + J \langle \xi_0 \rangle^2 \sum_k {\bf G}(-\varepsilon_{\rm MF}) {\bf G}(\varepsilon_k) \right] , \\ &Z_{\rm fluct} = Z / Z_{\rm MF} \,. \end{aligned} \tag{6.10}$$

Note that when $\langle \xi_0 \rangle$ vanishes, $F_{\rm MF}$ reduces to the mean-field free energy for the first toy model in Appendix I (with ε_f set to zero).

For $N = q^{-1}$ (the "physical limit"), the logarithmic trace L may be expanded to $O(1)$ as

$$\begin{aligned} L &\simeq -NJ \langle \xi_0 \rangle^2 \frac{1}{\beta} \sum_{kn} \frac{1}{i\omega_n + \varepsilon_{\rm MF}} \frac{1}{i\omega_n - \varepsilon_k} \\ &= -NJ \langle \xi_0 \rangle^2 \sum_k \frac{f(\varepsilon_k) - f(-\varepsilon_{\rm MF})}{\varepsilon_k + \varepsilon_{\rm MF}} \\ &\to -\langle \xi_0 \rangle^2 {\rm Re} \Pi^{(1)}(\varepsilon_{\rm MF}) \,, \end{aligned} \tag{6.11a}$$

with $\Pi^{(1)}$ the $O(1)$ polarization introduced in Eq. (2.68). The identification in the last line holds rigorously assuming a flat density of band states, and to terms of $O(1/D)$ for any band with characteristic energy D. Recall that for a flat density of states

$$\begin{aligned} &\Pi^{(1)}(z) = -N\gamma \ln \left[\frac{-z}{D} \right] \quad (T=0) \,, \\ &\gamma = N(0) |J| \,. \end{aligned} \tag{6.11b}$$

Within a Bose loop expansion, the logarithmic trace representing Fermi degrees of freedom may *not* be expanded. Fermi contributions to the free energy must be included to all orders even at mean-field or tree level. Alternatively, within a large-N expansion about the thermodynamic limit (fixed q), $\langle \xi_0 \rangle^2$ is itself $O(N)$. In this case, L may be rewritten exactly as a contour integral, and the contour distorted onto the real axis. The resulting expression is

$$L = N \int_{-\infty}^{\infty} \frac{d\varepsilon}{\pi} f(\varepsilon) {\rm Im} \ln \left[1 + J \langle \xi_0 \rangle^2 \sum_k \frac{1}{\varepsilon - \varepsilon_k + i0^+} \frac{1}{\varepsilon + \varepsilon_{\rm MF} + i0^+} \right] . \tag{6.12a}$$

Assuming a flat density of band states,

$$L = N \int_{-D}^{D} \frac{d\varepsilon}{\pi} f(\varepsilon) \tan^{-1} \left[\frac{\Delta}{\varepsilon + \varepsilon_{\rm MF}} \right], \quad \Delta = \pi\gamma \langle \xi_0 \rangle^2 \,. \tag{6.12b}$$

This is the partition function for an effective resonant level model. The resonance position and hybridization widths are just $-\varepsilon_{\rm MF} > 0$ and Δ. (Note that the inverse tangent is restricted to the interval $[-\pi/2, \pi/2]$, changing discontinuously from $-\pi/2$ to $\pi/2$ as ε increases through $-\varepsilon_{\rm MF}$.)

We discuss first the saddle-point solution within the "physical" $1/N$ expansion [Eq. (6.11)]. The mean-field equations to $O(1)$ are in this case

$$\begin{aligned} &\frac{\partial}{\partial \langle \xi_0 \rangle^2} : \ {\rm Re} \Pi^{(1)}(\varepsilon_{\rm MF}) = 1 \,, \\ &\frac{\partial}{\partial \varepsilon_{\rm MF}} : \ \langle \xi_0 \rangle^2 = Z(\varepsilon_{\rm MF})[1 - Nf(-\varepsilon_{\rm MF})] \,, \\ &Z(\varepsilon_{\rm MF}) = \left[\frac{\partial \, {\rm Re} \Pi^{(1)}(z)}{\partial z} \right]^{-1} \Bigg|_{z=\varepsilon_{\rm MF}} . \end{aligned} \tag{6.13}$$

At zero temperature the first equation has the solution

$$\varepsilon_{\rm MF} = -T_{\rm CS} = -De^{-1/N\gamma} \,, \tag{6.14}$$

assuming a flat band profile. Substituting in Eq. (6.10) gives immediately

$$E_0 = F(T=0) = -T_{\rm CS} \,. \tag{6.15}$$

This is exactly the result for the ground-state energy derived in Sec. II.E. Previous results for the magnetic susceptibility and specific-heat coefficient at $O(1)$ may also be reproduced. For a general external field x (h or T), the required thermodynamic derivative is $\partial E_0 / \partial x$. Differentiating the equality

$$\Pi^{(1)}(E_0) = 1 \tag{6.16a}$$

with respect to x gives

$$\frac{\partial \Pi^{(1)}(E_0)}{\partial E_0} \frac{\partial E_0}{\partial x} + \frac{\partial \Pi^{(1)}(E_0)}{\partial x} = 0 \,. \tag{6.16b}$$

Thus

$$\frac{\partial E_0}{\partial x} = -\left[\frac{\partial \Pi^{(1)}(E_0)}{\partial E_0} \right]^{-1} \frac{\partial \Pi^{(1)}(E_0)}{\partial x} \,, \tag{6.16c}$$

and, by Eqs. (6.13),

$$\frac{\partial E_0}{\partial x} = -\langle \xi_0 \rangle^2 \frac{\partial \Pi^{(1)}(E_0)}{\partial x} \ . \tag{6.16d}$$

This last form guarantees that $\partial E_0/\partial x$ may be obtained simply by differentiating $F_{\rm MF}$ [Eq. (6.10)] with respect to x, disregarding the implicit dependence of $\varepsilon_{\rm MF}$ and $\langle \xi_0 \rangle$ on x. The results in Eq. (2.74) follow immediately.

At finite temperature, the saddle-point partition function takes the form

$$\begin{aligned} Z_{\rm MF} &= e^{-\beta \varepsilon_{\rm MF}(T)}(1+e^{\beta \varepsilon_{\rm MF}(T)})^N, \quad T<T_c \\ &= N + e^{-\beta \varepsilon_{\rm MF}(T)}[1+O(e^{2\beta \varepsilon_{\rm MF}(T)})] \ , \end{aligned} \tag{6.17}$$

with $\varepsilon_{\rm MF}(T)$ the solution of the first equation in (6.13). In comparison, the $O(1)$ result from Sec. II.E is

$$Z^{(1)}/Z_{\rm band} = N + \int_\Gamma \frac{dz}{2\pi i} e^{-\beta z} \frac{-\partial \Pi^{(1)}(z)/\partial z}{1-\Pi^{(1)}(z)} \ , \tag{6.18}$$

where Γ encircles the singularities of the integrand in a counterclockwise fashion. Up to terms of $O(e^{2\beta \varepsilon_{\rm MF}})$, the saddle-point result may be obtained from the rigorous $O(1)$ result by approximating the integrand in Eq. (6.18) by an undamped pole at the lowest solution of $\mathrm{Re}\Pi^{(1)}(\omega)=1$. The terms of $O(e^{2\beta \varepsilon_{\rm MF}})$, which vanish for $T \to 0$, but become large for $T \sim T_{\rm CS}$, reflect explicitly a violation of the occupancy constraint in the saddle-point treatment; the neglect of $\mathrm{Im}\Pi^{(1)}$ is a second approximation, which worsens with increasing temperature.

It is interesting to compare the results obtained above with results from the Bose loop expansion. Assuming a flat density of states, the mean-field equations for arbitrary temperature take the form

$$\begin{aligned} \frac{\partial}{\partial \langle \xi_0 \rangle^2}: \ & -N\gamma \int_{-D}^{D} d\varepsilon f(\varepsilon) \frac{\varepsilon + \varepsilon_{\rm MF}}{(\varepsilon+\varepsilon_{\rm MF})^2+\Delta^2} = 1 \ , \\ \frac{\partial}{\partial \varepsilon_{\rm MF}}: \ & \frac{\Delta}{\pi} \int_{-D}^{D} d\varepsilon f(\varepsilon) \frac{1}{(\varepsilon+\varepsilon_{\rm MF})^2+\Delta^2} = q - f(-\varepsilon_{\rm MF}) \ . \end{aligned} \tag{6.19}$$

(The integrals may be expressed in terms of the digamma function if desired.) At zero temperature these equations reduce to

$$\begin{aligned} & (\varepsilon_{\rm MF}^2+\Delta^2)^{1/2} = T_{\rm CS} = D e^{-1/N\gamma} \ , \\ & \frac{1}{\pi} \tan^{-1}\left[\frac{\Delta}{-\varepsilon_{\rm MF}}\right] = q \ . \end{aligned} \tag{6.20}$$

For fixed q and $N\gamma = O(1)$, these equations contain no quantities of $O(1/N)$, and no further reduction is permitted. In the thermodynamic limit, relative fluctuations are suppressed by factors of $1/N$ at all temperatures. Hence the mean-field equations constitute a rigorous solution of the model in the limit $N \to \infty$ (cf. the discussion of the toy models in Appendix I). In this thermodynamic limit, the system exhibits a continuous transition from a high-temperature phase with $\langle \xi_0 \rangle = 0$ to a low-temperature condensate phase with $\langle \xi_0 \rangle \neq 0$. The high-temperature free energy is the same as that for toy model (i) [Eq. (6.12)]: the system corresponds to a set of N noninteracting fermion levels, each with probability q for occupancy. The high-temperature solution becomes unstable (and the phase transition occurs) at T_c, where

$$\begin{aligned} \mathbf{P} \int_{-D}^{D} \frac{d\varepsilon}{e^{\beta_c \varepsilon}+1} \frac{1}{\varepsilon+\varepsilon_{\rm MF}} &= -\frac{1}{N\gamma} \\ &\Leftrightarrow \mathrm{Re}\Pi^{(1)}(\varepsilon_{\rm MF})\,|_{T_c} = 1 \ , \end{aligned}$$

with

$$\frac{1}{\varepsilon^{-\beta_c \varepsilon_{\rm MF}}+1} = q \ , \tag{6.21a}$$

i.e., $\varepsilon_{\rm MF} = -T_c \ln(q^{-1}-1)$. Approximating the Fermi function in the first equation with its zero-temperature value gives

$$T_c \sim \frac{T_{\rm CS}}{\ln(q^{-1}-1)} \ . \tag{6.21b}$$

As in Appendix I, finite-temperature results obtained in the thermodynamic limit become unreliable when extrapolated to $N = q^{-1}$. The violation of the occupancy constraint at high temperature is the same as that for the toy models (see Table XII below). Further, the continuous phase transition is an artifact of the saddle-point solution with no analog in the Coqblin-Schrieffer model. Nevertheless, for the physical limit $N = q^{-1}$, the zero-temperature solution obtained by the Bose loop expansion reduces to the $O(1)$ result of Eq. (6.15) upon expansion to leading order in q. Since this property persists at higher orders, the loop expansion (or thermodynamic-limit expansion) is well controlled throughout the Fermi-liquid regime.

2. Infinite-U Anderson model

The generalized Anderson partition function for arbitrary qN takes the form

$$\begin{aligned} Z &= \int_{-\pi T}^{\pi T} \frac{\beta d\lambda}{2\pi} e^{i\beta\lambda(qN)} (1+e^{-\beta(\varepsilon_f + i\lambda)})^N \int_\xi e^{-S} \ , \\ S &= -N \,\mathrm{Tr} \ln \left[1 - V^2 \sum_k \mathbf{G}(\varepsilon_f + i\lambda) \mathbf{X} \mathbf{G}(\varepsilon_k) \mathbf{X}^\dagger \right] \\ &\quad - \beta \sum_m |\xi_m|^2 D^{-1}(i\nu_m, i\lambda) \ , \end{aligned}$$

where

$$\begin{aligned} & \mathbf{G}(E)_{nn'} = \frac{\delta_{nn'}}{i\omega_n - E}, \quad D(i\nu_m, i\lambda) = \frac{1}{i\nu_m - i\lambda} \ , \\ & \mathbf{X}_{nn'} = \xi_{n-n'}, \quad \int_\xi = \int \prod_m d\bar{\xi}_m d\xi_m \ . \end{aligned} \tag{6.22}$$

The variable λ may conveniently be shifted off the real axis as in Eq. (6.9). In this case, the mean-field partition function (Read and Newns, 1983b; Coleman, 1985a) takes the form

$$Z_{\rm MF}=e^{-\beta F_{\rm MF}},$$

$$F_{\rm MF}=\varepsilon_{\rm MF}(qN)-NT\ln(1+e^{\beta(\varepsilon_{\rm MF}-\varepsilon_f)})-\varepsilon_{\rm MF}\langle\xi_0\rangle^2 +L'(\varepsilon_{\rm MF},\langle\xi_0\rangle), \tag{6.23}$$

$$L'=-N\frac{1}{\beta}\mathrm{Tr}\ln\left[1-V^2\langle\xi_0\rangle^2\sum_k \mathbf{G}(\varepsilon_f-\varepsilon_{\rm MF})\mathbf{G}(\varepsilon_k)\right].$$

This saddle-point free energy is quite similar to that for the Coqblin-Schrieffer model [Eq. (6.10)]. For $qN=1$, L' may be simplified by inspection:

$$L'\simeq NV^2\langle\xi_0\rangle^2\sum_k\frac{f(\varepsilon_k)-f(\varepsilon_f-\varepsilon_{\rm MF})}{\varepsilon_k+\varepsilon_{\rm MF}-\varepsilon_f}+O(1/N)$$

$$=\langle\xi_0\rangle^2\mathrm{Re}\Sigma_0^{(1)}(\varepsilon_{\rm MF})+O(1/N), \tag{6.24a}$$

with $\Sigma_0^{(1)}$ the $O(1)$ empty-state self-energy introduced in Eq. (2.15). Note again that this correspondence holds rigorously for a flat band, and to terms of $O(1/D)$ for an arbitrary band. For the flat band,

$$\mathrm{Re}\Sigma_0^{(1)}(z)=\frac{N\Gamma}{\pi}\ln\left|\frac{\varepsilon_f-z}{D}\right| \quad (T=0). \tag{6.24b}$$

Within the loop expansion, the $O(1)$ approximation for L' above is not sufficient. It is easy to check that more generally

$$L'=N\int_{-D}^{D}\frac{d\varepsilon}{\pi}f(\varepsilon)\tan^{-1}\left[\frac{\Delta}{\varepsilon+\varepsilon_{\rm MF}-\varepsilon_f}\right],$$

$$\Delta=\Gamma\langle\xi_0\rangle^2, \tag{6.25}$$

assuming a flat band profile. Note that, as in Eq. (6.12b), the inverse tangent lies in $[-\pi/2,\pi/2]$.

We discuss first the $O(1)$ solution. The mean-field equations take the form

$$\frac{\partial}{\partial\langle\xi_0\rangle^2}:\ \varepsilon_{\rm MF}-\mathrm{Re}\Sigma_0^{(1)}(\varepsilon_{\rm MF})=0,$$

$$\frac{\partial}{\partial\varepsilon_{\rm MF}}:\ \langle\xi_0\rangle^2\left[1-\frac{\partial}{\partial\varepsilon_{\rm MF}}\Sigma_0^{(1)}(\varepsilon_{\rm MF})\right]=1-Nf(\varepsilon_f-\varepsilon_{\rm MF}). \tag{6.26}$$

At zero temperature, the minimum-energy solution of the first equation is just

$$\varepsilon_{\rm MF}=E_0=\varepsilon_f-T_A, \tag{6.27}$$

with E_0 the ground-state energy of Sec. II.C. Furthermore, for $T=0$,

$$\langle\xi_0\rangle^2=Z(E_0),$$

$$Z(E_0)=\left[1-\frac{\partial\Sigma_0^{(1)}(E_0)}{\partial E_0}\right]^{-1}. \tag{6.28}$$

Since the coefficient of $\langle\xi_0\rangle^2$ in $F_{\rm MF}$ [Eq. (6.23)] vanishes, the ground-state energy becomes

$$F_{\rm MF}(T=0)=E_0, \tag{6.29}$$

as in Secs. II–V.

The zero-temperature thermodynamic properties $n_f^{(1)}$, $\chi_c^{(1)}$, $\chi^{(1)}$, and $\gamma^{(1)}$ may be computed by differentiating $F_{\rm MF}$ with respect to the appropriate field, ignoring the implicit field dependence of $\varepsilon_{\rm MF}$ and $\langle\xi_0\rangle^2$ [the argument used to validate this procedure in part (a) may be trivially extended to the Anderson model]. The results obtained in previous sections at $O(1)$ may be reproduced in this way.

As in our discussion of the Coqblin-Schrieffer model we may compare the saddle-point and $O(1)$ treatments at finite temperature. The finite-temperature saddle-point partition function takes the form

$$Z_{\rm MF}=e^{-\beta\varepsilon_{\rm MF}(T)}(1+e^{\beta[\varepsilon_{\rm MF}(T)-\varepsilon_f]})^N,\quad T<T_c$$

$$=Ne^{-\beta\varepsilon_f}+e^{-\beta\varepsilon_{\rm MF}(T)}[1+O(e^{2\beta[\varepsilon_{\rm MF}(T)-\varepsilon_f]})], \tag{6.30}$$

with $\varepsilon_{\rm MF}(T)$ the solution of Eq. (6.26). The rigorous $O(1)$ result [Eq. (2.24)] is

$$Z^{(1)}/Z_{\rm band}=Ne^{-\beta\varepsilon_f}+\int_\Gamma\frac{dz}{2\pi i}e^{-\beta z}\frac{1-\partial\Sigma_0^{(1)}/\partial z}{z-\Sigma_0^{(1)}(z)}. \tag{6.31}$$

The saddle-point result may be obtained from Eq. (6.31), to terms of $O(e^{2\beta(\varepsilon_{\rm MF}-\varepsilon_f)})$, by approximating the integral by its lowest pole and neglecting $\mathrm{Im}\Sigma_0^{(1)}$. The additional terms of $O(e^{2\beta(\varepsilon_{\rm MF}-\varepsilon_f)})$ in Eq. (6.30) represent a violation of the occupancy constraint. The inclusion of these terms and the neglect of $\mathrm{Im}\Sigma_0^{(1)}$ represent approximations in the finite-temperature saddle-point treatment, which deteriorate with increasing T.

Finally, we compare the $O(1)$ results with results from the tree-level loop expansion (Coleman, 1985a). In the latter case, the saddle-point equations for a flat band profile take the form

$$\frac{\partial}{\partial\langle\xi_0\rangle^2}:\ \frac{N\Gamma}{\pi}\int_{-D}^{D}d\varepsilon f(\varepsilon)\frac{\varepsilon+\varepsilon_{\rm MF}-\varepsilon_f}{(\varepsilon+\varepsilon_{\rm MF}-\varepsilon_f)^2+\Delta^2}=\varepsilon_{\rm MF},$$

$$\frac{\partial}{\partial\varepsilon_{\rm MF}}:\ \frac{\Delta}{\pi}\int_{-D}^{D}d\varepsilon f(\varepsilon)\frac{1}{(\varepsilon+\varepsilon_{\rm MF}-\varepsilon_f)^2+\Delta^2} =q-\left[f(\varepsilon_f-\varepsilon_{\rm MF})+\frac{\Delta}{N\Gamma}\right]. \tag{6.32}$$

In the zero-temperature limit, these equations reduce to

$$[(\varepsilon_f-\varepsilon_{\rm MF})^2+\Delta^2]^{1/2}=\exp\left[\frac{\pi\varepsilon_{\rm MF}}{N\Gamma}\right],$$

$$\frac{1}{\pi}\tan^{-1}\left[\frac{\Delta}{\varepsilon_f-\varepsilon_{\rm MF}}\right]=q-\frac{\Delta}{N\Gamma}. \tag{6.33}$$

Equations (6.32) and (6.33) are analogous to Eqs. (6.19) and (6.20) for the thermodynamic-limit Coqblin-Schrieffer model. As before, the mean-field equations become exact in the limit $N\to\infty$. In this limit the system exhibits a continuous phase transition. The high-temperature phase again corresponds to a set of noninteracting fermion levels with probability q for occupancy.

The transition temperature T_c follows from Eq. (6.32):

$$\mathbf{P}\int_{-D}^{D}\frac{d\varepsilon}{e^{\beta_c\varepsilon}+1}\frac{1}{\varepsilon+\varepsilon_{\rm MF}-\varepsilon_f}=\frac{\pi\varepsilon_{\rm MF}}{N\Gamma}$$

$$\Longleftrightarrow \varepsilon_{\rm MF}=\mathrm{Re}\Sigma_0^{(1)}(\varepsilon_{\rm MF})\,|_{T_c}$$

with

$$\varepsilon_{\rm MF}=\varepsilon_f-T_c\ln(q^{-1}-1)\ . \tag{6.34a}$$

Approximating the Fermi function by its zero-temperature value gives

$$T_c\sim\frac{T_A}{\ln(q^{-1}-1)}\ . \tag{6.34b}$$

The extrapolation from the thermodynamic limit to $N=q^{-1}$ is unreliable at finite temperature for the same reasons raised in the discussion of the Coqblin-Schrieffer model. The expansion about the thermodynamic limit is an asymptotic expansion for $qN\to\infty$ with q fixed. The point $N=q^{-1}$ lies far outside the range of validity of the expansion. Despite this breakdown of the loop expansion at finite temperature, reliable results may be obtained throughout the Fermi-liquid regime with exponentially small errors: in particular, results of systematic large-N perturbation theory may be recovered by expanding the Bose loop free energy in powers of the small parameter $q=1/N$.

The saddle-point approach has been used to calculate a number of properties besides n_f, χ, χ_c, and γ. Houghton, Read, and Won (1987) have extensively treated the large-N expansion for the $T\to0$ resistivity and thermopower. Coleman (1987) has computed the zero-temperature f spectral density and dynamic susceptibility to $O(1/N)$. Read (1984) has calculated the coefficients for T^2 terms in the low-temperature magnetic susceptibility and specific-heat coefficient and H^2 terms in the susceptibility to $O(1)$. Withoff and Fradkin (1986) have computed the zero-temperature field-dependent magnetization $M(H)$ and susceptibility $\chi(H)$ to $O(1)$.

We briefly discuss the effect of fluctuations in the thermodynamic-limit models in Sec. VI.D. In Appendix J we discuss a method for extending the $O(1)$ calculation of Eq. (6.26) to $O(1/N)$. In the next section we discuss an all-orders rearrangement of perturbation theory which furnishes a new interpretation for alloy physics in the Fermi-liquid limit.

C. Nonperturbative transformation to quasiparticle modes

As mentioned in Sec. VI.A, the functional integral provides a powerful tool for reorganizing perturbation theory in the zero-temperature limit. In this limit, the constraint integral (see Sec. VI.C) which eliminates unphysical states from the analysis need not be performed exactly, but may be treated in a saddle-point approximation. The formal perturbative series that arises from fluctuations about the saddle point may be transformed to an equivalent series by applying the following theorem of 't Hooft and Veltman (1974).

Theorem. Let $\varphi=\chi+R(\chi)$ be any transformation (local or nonlocal) invertible in the vicinity of $\varphi=0$. Then the partition function

$$Z=\int_\varphi e^{-S(\varphi)}$$

and all φ Green's functions, defined by their perturbative expansions, remain invariant when Z is rewritten as

$$\begin{aligned}&Z(\chi)=\int_\chi e^{-S'(\chi)}\ ,\\ &S'(\chi)=S[\chi+R(\chi)]-\mathrm{Tr}\ln\left[1+\frac{\delta R}{\delta\chi}\right]\ .\end{aligned} \tag{6.35}$$

The logarithmic trace is the formal Jacobian of the variable transformation. $Z(\chi)$, like $Z(\varphi)$, is defined by its diagrammatic expansion and may be obtained formally by performing Gaussian integrations over the full real line or complex plane.

This is a truly remarkable theorem. Its proof (see 't Hooft and Veltman, 1974) relies only on the combinatoric properties of diagrams. Several points should be stressed in connection with this theorem. (a) Variable transformations in functional integrals defined in this formal way are even simpler than transformations in ordinary integrals; it is not necessary to keep track of the domain of integration. (b) The condition that the transformation be invertible is crucial. If the transformation were singular in the vicinity of $\varphi=0$, it would be impossible to define a propagator for χ, and $Z(\chi)$ would be ill defined. For example, the transformation

$$(\bar\xi,\xi)\to(r,\theta) \tag{6.36}$$

is not permitted in the neighborhood of $\xi=0$. (c) The theorem expresses the equivalence of formal series summed to infinite order. In some cases a nonlinear variable transformation may complicate a small-parameter expansion. An infinite number of diagrams in χ perturbation theory may be required to reproduce a finite number of diagrams in φ perturbation theory. Further, new divergences (which ultimately cancel, if treated properly) may appear in the resummation of a convergent series. (d) The theorem is purely perturbative in character. The nonperturbative features of the actions $S(\varphi)$ and $S'(\chi)$ are not guaranteed to be identical.

In the magnetic alloy problem, nonlinear variable transformations are allowed in the vicinity of the $T\to0$ saddle point, since all modes, including the "constraint field," may be treated perturbatively. At higher temperatures such transformations neglect nonperturbative contributions from values of the constraint field near $\pm\pi T$. These contributions are essential for eliminating ghost states from the calculation at finite temperature. As discovered by Read and Newns (1983), a particular transformation leads to an elegant new interpretation for degrees of freedom in the Fermi-liquid regime: the physics may be formulated in terms of Fermi quasiparticles which interact weakly through the exchange of Bose-type

excitations. Effects of the "infrared catastrophe" (Anderson, 1967), which ensures that noninteracting and interacting ground states have zero overlap, may be bypassed in this way.

The Read-Newns transformation entails a change to polar coordinates in the Bose (or Stratonovich-Hubbard) field $\xi(\tau)$ [see Eq. (3.8a)] and a subsequent ξ-dependent gauge transformation on the local Fermi fields. For simplicity we restrict the following discussion to the Anderson model; for the analogous treatment of the Coqblin-Schrieffer model, see Read and Newns (1983). Recall that the Anderson partition function may be written in

$$Z_A=\int_{-\pi T}^{\pi T}\frac{\beta d\lambda}{2\pi}\int_{cf\xi}e^{-S},\quad S=\int_0^\beta d\tau L(\tau)\,,$$
$$L(\tau)=\sum_{km}\bar{c}_{km}\left[\frac{\partial}{\partial\tau}+\varepsilon_{km}\right]c_{km}+\sum_m\bar{f}_m\left[\frac{\partial}{\partial\tau}+\varepsilon_{fm}+i\lambda\right]f_m+\bar{\xi}\left[\frac{\partial}{\partial\tau}+i\lambda\right]\xi+V\sum_{km}(\bar{\xi}\bar{c}_{km}f_m+\xi\bar{f}_m c_{km})-i\lambda\,, \tag{6.37}$$

with τ-dependent fields c, f, and ξ. By the theorem of 't Hooft and Veltman, the transformation

$$\xi(\tau)\to r(\tau)e^{i\theta(\tau)},\quad \bar{\xi}(\tau)\to r(\tau)e^{-i\theta(\tau)}\,, \tag{6.38}$$

is allowed for $T\to 0$. (The Jacobian at the saddle point is just $r_0\neq 0$.) Note that two independent *real* fields appear before and after the transformation. Since r and θ are real, their formal frequency decompositions are

$$r(\tau)=\beta^{-1/2}\sum_m r_m e^{i\nu_m\tau},\quad \theta(\tau)=\beta^{-1/2}\sum_m\theta_m e^{i\nu_m\tau},\quad r_m=r^*_{-m},\quad \theta_m=\theta^*_{-m}\,. \tag{6.39}$$

Having introduced r and θ, one may perform the field-dependent gauge transformation

$$f_m(\tau)\to e^{i\theta(\tau)}f_m(\tau),\quad \bar{f}_m(\tau)\to e^{-i\theta(\tau)}\bar{f}_m(\tau)\,. \tag{6.40}$$

The Jacobian of this transformation is unity. As before, the transformation expresses the equality of two infinite perturbative series.

The transformed action may be written

$$S'=\int_0^\beta d\tau\left[r\frac{\partial}{\partial\tau}r+i\frac{\partial\theta}{\partial\tau}\right]+\int_0^\beta d\tau L'(\tau)-\prod_\tau \ln r(\tau)\,,$$
$$L'(\tau)=\sum_{km}\bar{c}_{km}\left[\frac{\partial}{\partial\tau}+\varepsilon_{km}\right]c_{km}+\sum_m\bar{f}_m\left[\frac{\partial}{\partial\tau}+\varepsilon_{fm}+i\lambda+i\frac{\partial\theta}{\partial\tau}\right]f_m+ir\left[\lambda+\frac{\partial\theta}{\partial\tau}\right]r+Vr\sum_{km}(\bar{c}_{km}f_m+\bar{f}_m c_{km})$$
$$-i\left[\lambda+\frac{\partial\theta}{\partial\tau}\right]. \tag{6.41}$$

The transformed action contains no static θ component. This reflects the invariance of the original action to simultaneous changes in phase of the Fermi and Bose fields. The phase variable is a Nambu-Goldstone mode, which decouples completely from physical modes of the theory. The Gaussian integral over the static phase yields a formally infinite (but harmless) contribution to the partition function.

The transformation

$$\lambda+\frac{\partial}{\partial\tau}\theta(\tau)=\lambda(\tau) \tag{6.42}$$

may now be applied to replace the static constraint field and purely dynamic components of the θ field with a new τ-dependent variable. In this case, the Jacobian is formally infinite, but field and parameter independent. It may be dropped, with the understanding that it formally cancels a second infinity elsewhere in the expansion. Finally, note that the term

$$\int_0^\beta d\tau\left[r\frac{\partial}{\partial\tau}r+i\frac{\partial\theta}{\partial\tau}\right]=0\,. \tag{6.43}$$

Thus the Fermi-liquid action becomes

$$S=\int_0^\beta d\tau L(\tau)-\prod_\tau r(\tau)\,,$$
$$L(\tau)=\sum_{km}\bar{c}_{km}\left[\frac{\partial}{\partial\tau}+\varepsilon_{km}\right]c_{km}+\sum_m\bar{f}_m\left[\frac{\partial}{\partial\tau}+\varepsilon_{fm}+i\lambda\right]f_m+i\lambda r^2+Vr\sum_{km}(\bar{c}_{km}f_m+\bar{f}_m c_{km})\,, \tag{6.44}$$

with τ-dependent fields c, f, r, and λ. Note that saddle-point expansions in the old and new variables remain equivalent at finite temperature, so long as the saddle point occurs away from the origin. It is the saddle-point approximation itself that eventually breaks down due to large-scale fluctuations in the constraint field. These nonperturbative corrections may only be recovered in the original variables. (If the theorem relating formal perturbative series is not sufficiently convincing, the reader may demonstrate explicitly at Gaussian order that diagrammatic expansions based on the original "Cartesian" coordinates and the new polar, or quasiparticle, coordinates

are equivalent.)

Previous large-N results for static and dynamic properties in the Fermi-liquid regime may be rederived by an expansion in the quasiparticle coordinates. As shown by Read and Newns (1983), it is advantageous to sum Fermi loops to all orders by integrating out the fields c and f, then to perform a loop expansion in the Bose fields. The position of the saddle point in r and λ shifts, order by order (cf. the treatment in Appendix I). The loop expansion and large-N expansion are *not* equivalent. Results of the loop expansion (which partially sums contributions of all orders in $1/N$ even at tree level) may subsequently be expanded in $1/N$, if desired. To obtain all contributions of $O(1/N)$, a one-loop calculation is sufficient; the connection between the loop expansion and $1/N$ expansion at higher orders has not been investigated. [Note that for the thermodynamic-limit generalizations of the Coqblin-Schrieffer and Anderson models (Coleman, 1985, 1987), the Bose loop expansion and large-N expansion are identical. In the physical limit these generalized expansions reduce to the loop expansion of Read and Newns.]

The conceptual advantage of the quasiparticle loop expansion, which mixes all orders in the small parameter $1/N$, is that it provides a microscopic justification for the local Fermi-liquid theory of Newns and Hewson (1980). At tree level the Anderson model thermodynamics is governed by the resonant level partition function of Eq. (6.25) with ε_{MF} and Δ given by Eqs. (6.32) and (6.33). At higher orders in the expansion this basic picture of an underlying resonant level remains. The parameters ε_{MF} and Δ change, order by order, but only by finite amounts. These parameters completely determine the zero-temperature magnetic susceptibility χ; at higher orders in the expansion, the specific-heat coefficient γ contains additional contributions from fluctuations of the background Bose field. Within the quasiparticle framework, it is these fluctuations which alter the Sommerfeld ratio from the Fermi-gas value of unity.

Only at tree level does this simple picture of an effective level model emerge in saddle-point expansions based on the original degrees of freedom (see Appendix I). At this order the parameter Δ/Γ may be viewed as a finite wave-function renormalization constant measuring the overlap between the noninteracting and interacting ground states (see also the discussion in Sec. IV.A). The low-energy thermodynamics may be expressed in terms of Fermi-type excitations above this ground state. Beyond this order the presence of electron-hole excitations with arbitrarily small energy gives rise to infrared divergences in the wave-function renormalization constant. These are the signal of the well-known infrared catastrophe (Anderson, 1967): the noninteracting ground state has zero overlap with the interacting ground state. In principle, the interacting ground state resembles the tree-level ground state, but dressed by an infinite cascade of electron-hole pairs. The elementary Fermi excitations above this ground state must also incorporate the effects of pair creation. The quasiparticle transformation alters the character of the tree-level ground state and the excitations above it. The new tree-level ground state is expected to have finite overlap with the full interacting ground state, and a consistent resonant level description is possible. It is this feature which makes the extension of the quasiparticle transformation to lattice models so attractive. The picture of hybridized quasiparticle bands, built from conduction electrons and local Fermi excitations, emerges at tree level in a loop expansion.

Rather than computing the effective resonant level parameters ε_{MF} and Δ in perturbation theory, one may regard the position of the local quasiparticle pole ε_{MF} and the value of the quasiparticle-conduction electron hybridization width Δ as *physical,* or fully renormalized, parameters of the interacting system. (These parameters follow from knowledge of the magnetic susceptibility and some other measurable property.) The values of the physical parameters may then, in principle, be maintained, order by order, in a loop expansion (or large-N expansion) by altering the input parameters of the theory. Such a renormalization scheme has been discussed at one-loop order by Read and Newns (1983a).

D. Further comments on the zero-temperature limit for magnetic alloy models

As discussed in the previous section the Fermi-liquid physics of the Coqblin-Schrieffer and Anderson models may be reinterpreted by introducing an all-orders transformation of perturbation theory. This "quasiparticle transformation" eliminates the ground-state overlap catastrophe in conventional expansions by proceeding from a new zeroth-order ground state. Coleman (1985a, 1987) has emphasized that the Fermi-liquid physics may be alternatively viewed within the original Hilbert state basis as a case of "almost-broken symmetry." In this context the Coqblin-Schrieffer and Anderson models may be viewed as members of an infinite hierarchy of Fermi-Bose models (see Sec. VI.B) with varying local level occupancy. In the thermodynamic limit the generalized models exhibit a true broken symmetry at low temperature. In this section we comment on the sense in which the physical Coqblin-Schrieffer and Anderson models exhibit an almost-broken symmetry.

As first emphasized by Coleman (1985a), $1/N$ expansions about the thermodynamic limit have the character of loop expansions in field theory. Loop expansions are generally attractive in Lagrangian field theory, since they preserve characteristic symmetries order by order. For a theory whose commutation relations depend on $\hbar$, a loop expansion may be shown to be an expansion in $\hbar$. A tree-level (no loops) calculation reproduces the theory's classical limit ($\hbar \to 0$), and the inclusion of fluctuations constitutes a semiclassical expansion in powers of $\hbar$. For the generalized magnetic alloy models, the limit $qN \to \infty$ with fixed q is also a classical limit, in which operator commutators may be replaced by Poisson brackets, and a classical phase space may (in principle) be defined. Yaffe has reviewed this approach to large degeneracy expansions in a general context (1982).

Coleman and Andrei (1986) have derived the Bethe ansatz equations describing the thermodynamic-limit Anderson model

$$H=H_{\rm band}+H_f+H_{\rm mix},\quad H_{\rm band}=\sum_{km}\varepsilon_k c_{km}^\dagger c_{km}\ ,$$
$$H_f=\varepsilon_f\sum_m f_m^\dagger f_m,\quad H_{\rm mix}=V\sum_{km}(c_{km}^\dagger b^\dagger f_m+{\rm H.c.})\ , \tag{6.45}$$
$$\sum_m f_m^\dagger f_m+b^\dagger b=qN\ ,$$

for arbitrary N and have explicitly verified that the mean-field solution of Sec. VI.B becomes exact for $N\to\infty$. In this limit the model exhibits a finite-temperature continuous phase transition. Fluctuation corrections for finite N have been investigated using perturbation theory. In the high-temperature phase, the calculation of Gaussian corrections is quite similar to that for toy model (ii) (Appendix I). The resulting expression for the partition function is

$$Z=\frac{Z_{\rm MF}}{[2\pi q(1-q)N]^{1/2}}\frac{1}{1-e^{\beta\varepsilon_{\rm MF}}}e^{-\beta F_{\rm mix}}\ ,$$
$$F_{\rm mix}=\int_{-D}^{D}\frac{d\varepsilon}{\pi}b(\varepsilon)\tan^{-1}\left[\frac{{\rm Im}\Sigma_{\rm MF}(\varepsilon-i0^+)}{\varepsilon+\varepsilon_{\rm MF}-{\rm Re}\Sigma_{\rm MF}(\varepsilon)}\right]\ , \tag{6.46}$$
$$\Sigma_{\rm MF}(z)=NV^2\sum_k\frac{f(\varepsilon_k)-q}{z+\varepsilon_k+\varepsilon_{\rm MF}-\varepsilon_f}\ .$$

[The fact that $f(\varepsilon_f-\varepsilon_{\rm MF})=q$ in the high-temperature phase has been used to simplify the last equation.]

As mentioned in Sec. VI.B, the high-temperature solution becomes unstable with respect to Gaussian fluctuations at T_c, where

$${\rm Re}\Sigma_{\rm MF}(0)={\rm Re}\Sigma_0^{(1)}(\varepsilon_{\rm MF})=\varepsilon_{\rm MF}\ , \tag{6.47}$$

with

$$\varepsilon_{\rm MF}=\varepsilon_f-T_c\ln(q^{-1}-1)\ .$$

At this point, Bose condensation occurs and the mean-field equations develop a broken-symmetry solution. As for toy model (ii) in Appendix I, the broken symmetry is invariance under a static rotation of phase in the Bose and Fermi fields:

$$b(\tau)\to e^{i\theta}b(\tau),\quad f(\tau)\to e^{i\theta}f(\tau)\ . \tag{6.48}$$

For q fixed and N large, but finite, fluctuations about the saddle-point solution destroy the broken symmetry. Mathematically, the broken-symmetry order parameter $|\langle\xi_0\rangle|^2$ exhibits logarithmic divergences order by order in perturbation theory. Infrared divergences of this type are familiar from studies of fluctuation corrections to mean-field theory in low-dimensional systems. The divergence of fluctuations in low-frequency (or low-momentum) modes is the basis for the Mermin-Wagner argument (Mermin and Wagner, 1966) against long-range order in one- and two-dimensional systems.

It is helpful to develop further this analogy between the partition function in Eqs. (6.8) and (6.22) and the partition function of a two-dimensional x-y spin system. The spin partition function takes the form

$$Z(s)=\int\prod_{i=1}^{N}ds_i e^{-\beta H(s)}\ . \tag{6.49}$$

Note that the temperature appears only as a multiplicative factor (or coupling constant). In a suggestive continuum notation,

$$Z(s)\sim\int_s e^{-S},\quad S=\beta\int d^2x\,\mathscr{H}[s(x)]\ , \tag{6.50}$$

with $\mathscr{H}$ an appropriate energy density.

The functional integral representation of the spin partition function closely resembles the representations of the thermodynamic-limit alloy models. Various analogies are listed in Table X. Since the spin propagator behaves as $1/k^2$ at low momentum, fluctuations about a broken-symmetry solution in an infinite two-dimensional system lead to logarithmic divergences (recall $\int d^2k\sim\int k\,dk$); likewise, since the Bose propagator in the Anderson model behaves as $1/\omega$ at low frequency, fluctuations diverge logarithmically for $\beta=\infty$ (an infinite one-dimensional system). In both cases, infinite fluctuations imply the absence of long-range order, i.e.,

$$\lim_{x\to\infty}\langle s(x)\cdot s(0)\rangle=0,\quad \lim_{\tau\to\infty}\langle b(\tau)b^\dagger(0)\rangle=0\ . \tag{6.51}$$

Despite this fact, it is well known that two-dimensional x-y spin systems display a form of "almost-long-range order" over a finite range of temperature. Spin-correlation functions decay algebraically, rather than exponentially fast. It has been argued (Coleman, 1985a; Read, 1985) that $\langle b(\tau)b^\dagger(0)\rangle$ exhibits the same algebraic decay at large imaginary times for $T=0$. Extrapolating from a perturbative analysis at one-loop order, Read (1985) has proposed that the exponent for decay at long times is n_f^2/N, with n_f the exact impurity valence [this result may be interpreted as a Nozières–de Dominicis (1968) infrared exponent for N-channel impurity scattering].

For $L<\infty$ or $\beta<\infty$, there is by definition no infinite-range order. Nevertheless, slowly decaying correlations in the corresponding infinite system have a residual effect. Large correlations remain between points separated by any distance shorter than the correlation length in the infinite system. If the correlations are infinite range (remain finite or decay algebraically), correlations remain

TABLE X. Analogies between the thermodynamic-limit Anderson model and a two-dimensional x-y spin system.

Anderson model	Spin Hamiltonian
Imaginary time	Distance
β	Size of system L
Parameters ε_f, Γ	β, other parameters
$\langle b(\tau)b^\dagger(0)\rangle$	$\langle s(x)\cdot s(0)\rangle$
Low-frequency propagator $\sim 1/\omega$	Low-momentum propagator $\sim 1/k^2$

on all length scales in the finite system. In the thermodynamic-limit Anderson model, treated at mean-field level, the magnitude of the long-range order parameter $\langle b \rangle$ decreases with increasing temperature (decreasing β). If the system actually exhibits no long-range order, but only algebraically decaying correlations at zero temperature, one expects slowly decaying correlations to remain for large finite β; as β decreases, the correlations should smoothly cross over from long-range to short-range behavior. Note, however, that as the correlations change, the dimension of the system (β) shrinks as well. Inverse temperature plays the role of an adjustable parameter in the classical x-y spin system, but acts as the system dimension in the thermodynamic-limit magnetic alloy models.

Is the development of almost-long-range order in the Bose field a distinguishing feature of the thermodynamic-limit models *and* the physical models with $N=q^{-1}$? Certainly such behavior is reasonable in the thermodynamic limit. For $qN\to\infty$, canonical and grand canonical treatments become equivalent—the Fermi-Bose occupancy constraint of Eq. (6.45) need not be satisfied exactly to obtain correct results. At zero temperature (the analog of infinite L in a spin system), algebraically decaying off-diagonal order in the Bose field is entirely plausible. At finite temperature, a remnant of this behavior is expected (the quantum system is analogous to a classical spin system with finite dimension L). On the other hand, in the limit $N=q^{-1}$, canonical and grand canonical treatments are definitely not equivalent. Strictly speaking, the quantities $\langle b(\tau)b^{\dagger}(0)\rangle$ and $\langle b \rangle$ *vanish identically* when the occupancy constraint is imposed (cf. Appendix D). Nonzero contributions to these quantities arise from ghost states within an enlarged Hilbert space. Nevertheless, in the Fermi-liquid regime, it is unnecessary to impose occupancy constraints rigidly to obtain exact results for physical properties. In this limit the Coqblin-Schrieffer and Anderson models are *equivalent* to models exhibiting almost-long-range order. [This statement has been established to $O(1/N)$. Its extension to all orders in perturbation theory now appears compelling.] Since the rigid constraint is physically immaterial at zero temperature, the Fermi-liquid physics may be rigorously interpreted within the framework of an almost-broken symmetry. Such an interpretation remains valid at finite temperature if one neglects *nonperturbative* corrections (i.e., terms arising from fluctuations in the constraint field far from the saddle point). These large-scale fluctuations, which are not governed by a small parameter, dominate the physics for temperatures of order T_{CS} or T_A and become essential for a correct description of the crossover to free-moment behavior at high temperature.

In conclusion, the Coqblin-Schrieffer and infinite-U Anderson models may be said to display an almost-broken symmetry in the Fermi-liquid limit. The correlation function $\langle b(\tau)b^{\dagger}(0)\rangle$, exhibits algebraic decay at long times for all model parameters within the Kondo and mixed-valent regimes. The decay exponent is parameter-dependent and has been conjectured to be n_f^2/N. This behavior is the analog of the Kosterlitz-Thouless phenomenon in two-dimensional x-y spin systems [in the spin analog, the correlation function $\langle s(x)\cdot s(0)\rangle$ decays algebraically in space with a temperature-dependent exponent over a finite range of temperature]. In a renormalization-group sense, the zero-temperature magnetic alloy models may be said to exhibit a continuous set of critical points in parameter space (J, or ε_f and Γ, *not* T). As explained long ago by Anderson, Yuval, and Hamann (1970), this critical behavior is governed by a strong-coupling fixed point. The Bose field b provides an explicit realization of a correlation function with strong-coupling exponents.

VII. CONCLUSIONS

We have attempted to emphasize throughout this review the essential unity of various approaches to the large-N expansion for magnetic alloys. To aid in comparison with the literature, a translation table of symbols for various quantities introduced in the previous six sections is provided at the end of this section (Table XI). Diagrammatic perturbation theory, the variational ground-state method, the integral equation method, and the functional integral saddle-point expansion all lead to equivalent zero-temperature results at $O(1)$ and $O(1/N)$. Despite this fact, the methods may be distinguished by their strengths and weaknesses in higher-order approximations and in calculations at finite temperatures.

Diagrammatic methods provide the most straightforward means to extend systematic ground-state *and* finite-temperature calculations to higher order in $1/N$. Nevertheless, systematic expansions of frequency-dependent functions are, in general, nonuniform and exhibit singular points order by order in perturbation theory. Furthermore, the convergence of systematic expansions for static properties at finite temperature is, at this time, largely unstudied.

The variational ground-state method provides a particularly clear physical picture of the many-particle correlations underlying the Kondo effect. Since this method may be readily extended to include realistic effects like spin-orbit coupling and a finite Coulomb energy, it provides a particularly promising route for calculations in materials applications. The method cannot, by its nature, be extended to treat finite-temperature properties.

The integral equation method, or NCA, has been the subject of extensive study at finite temperature. This method is conceptually simple to apply, leads to smoothly varying frequency-dependent properties, and allows the incorporation of realistic effects like spin-orbit and crystal-field splitting. Results for static properties are in excellent agreement with exact Bethe ansatz results, and a large number of comparisons with experiment have been possible. The principal weakness of this approach is its failure in the Fermi-liquid regime ($T\to 0$, $\omega\to 0$). Although the NCA diagrammatic summation includes all

contributions of $O(1)$ and $O(1/N)$, the omission of high-order electron-hole excitations near the Fermi energy introduces large errors at zero temperature. The expansion of frequency-dependent properties remains nonuniform in this limit.

Saddle-point approximations provide an intuitively attractive and mathematically rigorous reinterpretation of magnetic alloy physics in the Fermi-liquid regime. In particular, the quasiparticle transformation of Read and Newns (1983) formalizes the phenomenological picture of localized quasiparticles (Newns and Hewson, 1980), weakly hybridized with conduction electrons and interacting through the exchange of Bose-type excitations. The possible applicability of the saddle-point approximation in concentrated alloys (including the heavy-electron systems) is currently a subject of great interest (see Table II). The saddle-point approximation breaks down outside the Fermi-liquid regime, where it leads to a number of spurious features, including a continuous phase transition. In this sense, the method is largely complementary to the NCA, which deteriorates in the Fermi-liquid regime.

We have reviewed the evidence for the existence of convergent or asymptotic expansions in $1/N$ for the ground state. Agreement with exact Fermi-liquid relations and with Bethe ansatz results strongly supports the existence of such expansions for both static and dynamic properties. Further numerical convergence studies for finite-temperature properties are required.

One of the most striking results of large-N studies is the perturbative derivation of the Sommerfeld ratio, which relates the low-temperature susceptibility and specific heat (see Sec. II.C). In contrast with most strongly interacting Fermi systems, the development of a Fermi-liquid ground state in the Coqblin-Schrieffer and Anderson models may be studied analytically. At $O(1/N)$ the Sommerfeld ratio differs from unity due to the appearance in the ground state of singlet electron-hole pairs. These Bose-type excitations alter the density of states sampled by the specific heat, but do not couple to a magnetic field. It would be of interest to pursue the study

TABLE XI. Translation guide for $1/N$ notation. Below we list some of the more common notation found in the literature for quantities in the $1/N$ expansion. The first column lists symbols in this review. The second column lists the equations in which the adjacent symbols are introduced. The remaining columns list the corresponding symbols in other treatments. In cases where no special symbol is introduced, a blank appears.

Symbol	Eq.	BKL	Coleman	Cox	GS	KKT	MKTT	M-H	RH	Read	RN
N	(1.4b)	N	N	N_f	N_f	$[J]$	$2j+1$	N	N	N	N
Γ	(1.3)	Δ	Δ	Γ	Δ	πW_0		$\Delta=\pi\tilde{\Delta}$	Δ	Δ_0	
ε_{fm}	(1.4a)	E_m	E_{fm}	ε_{fm}	ε_{fm}	ε_{fm}	E_m	E_{fm}	ε_{fm}	E_{0m}	
D	(1.9)	D		D	B	D	D	W	D	D	D
$N(0)$	(1.3)		ρ	$N(0)$			ρ		ρ_0	ρ	ρ
$G_f(z)$	(2.48)	$G(z)$	$G(z)$	$G_{4f}(z)$	$g(z)$	$G_{4f}(z)$		$G(z)$			
$\rho_f(\omega)$	(2.52)		$\rho(\omega)$	$\pi^{-1}\rho_{4f}(\omega)$		$\rho_{4f}(\omega)$		$\rho(\omega)$			
$G_0(z)$	(2.17a)	$(z-\Sigma_0)^{-1}$	$D(z)$	$D(z)$	$-g(-z+\varepsilon_f)$	$R_0(z)$		$D(z)$			
$\rho_0(\omega)$	(2.17b)		$B(\omega)$	$\pi^{-1}B(\omega)$				$B(\omega)$			
$G_m(z)$	(2.17a)		$G_{fm}(z)$	$G_m(z)$	$(G^>)_{00}(z-\Delta E)$	$R_{jm}(z)$		$G_{fm}(z)$			
$\rho_m(\omega)$	(2.17b)		$A_{fm}(\omega)$	$\pi^{-1}A_m(\omega)$				$A_m(\omega)$			
$\bar{\rho}_0(\omega)$	(2.19a)		$b(\omega)$	$\pi^{-1}A_b(\omega)$		$\xi_0(\omega)$		$b(\omega)$			
$\bar{\rho}_m(\omega)$	(2.19b)		$a_{fm}(\omega)$	$\pi^{-1}a_m(\omega)$		$\xi_{jm}(\omega)$		$A_m(\omega)$			
$\Sigma_0^{(1)}(z)$	(2.22)	$\Sigma_{00}(z)$			$-N\tilde{\Gamma}(-z+\varepsilon_f)$				$NV^2\chi(z)$		
E_0	(2.27)	E_0			ΔE				E_0	E_G	
T_A	(2.27)	T_A			δ				T_A	T_A	
$-G_m^{-1}(\omega)$	(5.13)							$d(\omega)$			
$-G_m^{-1}(\omega)$	(5.13)							$g(\omega)$			
J	(1.8)						J				$-J_0/N$
$\Delta=\pi\gamma\langle\xi_0\rangle^2$	(6.12)										Δ
$\Delta=\Gamma\langle\xi_0\rangle^2$	(6.25)									Δ	
$\varepsilon_{\mathrm{MF}}$	(6.9)										$-\varepsilon_f$
$\varepsilon_{\mathrm{MF}}$	(6.23)									$E_0-\varepsilon_f$	

BKL—Brandt, Keiter, and Liu, 1985.
Coleman—Coleman, 1984.
Cox—Cox, 1985.
GS—Gunnarsson and Schönhammer, 1983b.
KKT—Kuramoto, 1983; Kojima, Kuramoto, and Tachiki, 1984; Kuramoto and Kojima, 1984.
MKTT—Maekawa *et al.*, 1985a, 1985b.
M-H—Müller-Harmann, 1984.
RH—Rasul and Hewson, 1984a, 1984b.
Read—Read, 1985.
RN—Read and Newns, 1983a.

of the Fermi-liquid ground state to higher order in $1/N$. It is conceivable that the Sommerfeld ratio could be established to all orders in $1/N$ by careful analysis of the perturbation series. Even if this is not feasible, a great deal more might be learned about the strongly correlated ground state.

The large-N expansion has, in addition, provided the most powerful approach now available for computing dynamic properties of magnetic alloys, such as the f-electron spectral density and the dynamic susceptibility. Although the existence of "Kondo resonances" in dynamic spectra has been known for many years [see, for example, the review by Grüner and Zawadowski (1974)], the first reliable techniques for computing these resonances rely on the large-N expansion. This perturbative approach has provided a unifying framework within which static and dynamic properties may be viewed on the same footing.

In conclusion, the large-N expansion for magnetic alloys furnishes new insight in a number of areas. The expansion allows the comparison of a well-controlled perturbation theory with exact Bethe ansatz results. Further study of this correspondence might furnish information on the all-orders convergence of a nontrivial perturbation expansion or the calculation of dynamical correlation functions within the Bethe ansatz. The various techniques employed to generate the large-N expansion are in principle applicable to other condensed matter problems involving strong local correlations. Finally, the expansion allows the calculation of both static and dynamic properties, providing one of the most complete approaches to the magnetic alloy problem now available.

ACKNOWLEDGMENTS

The author has benefited from helpful discussion or correspondence with P. Coleman, B. Jones, H. Keiter, T. K. Lee, A. Millis, E. Müller-Hartmann, N. Read, F. C. Zhang, and G. E. Zwicknagl. The author especially thanks D. L. Cox and J. W. Wilkins for continuous discussion and suggestions. This work was supported by NSF Grant No. DMR-83-14764 at Cornell University and by NSF Grant No. PHY82-17853 and funds from NASA at the Institute for Theoretical Physics, Santa Barbara.

APPENDIX A: DERIVATION OF χ AND γ TO $O(1/N)$ IN PERTURBATION THEORY

In this appendix we derive expressions for the zero-temperature magnetic susceptibility and specific-heat coefficient of the infinite-U Anderson model to $O(1/N)$. The susceptibility has been previously derived by Rasul and Hewson (1984a, 1984b), whose notation we employ at various stages; a partial result for the specific-heat coefficient has been obtained by Brandt, Keiter, and Liu (1985). A flat conduction density of states is assumed for simplicity. We begin with the expression for the $1/N$ contribution to the free energy in the zero-temperature limit [see Eq. (2.43)]:

$$\Delta F^{(1/N)}=\tfrac{1}{2}Z(E_0)V^4\sum_{kk'm}\left[f_k(1-f_{k'})\frac{1}{(E_0+\varepsilon_k-\varepsilon_{fm})^2}\frac{1}{E_0+\varepsilon_k-\varepsilon_{k'}-\Sigma_0^{(1)}(E_0+\varepsilon_k-\varepsilon_{k'})}+(k\leftrightarrow k')\right],$$
$$Z(E_0)=\left[1-\frac{\partial\Sigma_0^{(1)}}{\partial z}\right]^{-1}\Bigg|_{z=E_0}. \tag{A1a}$$

The energies ε_{fm}, ε_k, and $\varepsilon_{k'}$ contain a contribution $-mg\mu_B H$ in the presence of a magnetic field. The empty-state self-energy $\Sigma_0^{(1)}$ is

$$\Sigma_0^{(1)}(E)=\frac{\Gamma}{\pi}\sum_m\int_{-D}^{0}d\varepsilon\frac{f(\varepsilon-mg\mu_B H)}{E-\varepsilon_f+\varepsilon}. \tag{A1b}$$

Note that the expression for $\Delta F^{(1/N)}$ is symmetric in the indices k and k'. Even though the denominator containing $\Sigma_0^{(1)}$ becomes singular for $\varepsilon_k\to\varepsilon_{k'}$, the sum of terms in large parentheses remains nonsingular in this limit. In expressions for χ and γ we combine terms resulting from this expression whenever possible; we do not combine terms at the outset, since the treatment of the singularity requires some care at a later stage. The $1/N$ contributions to χ and γ may be found using

$$-\frac{\partial\Delta F^{(1/N)}}{\partial H}\Bigg|_{H\to 0}\sim\chi^{(1/N)}H,$$
$$-\frac{\partial\Delta F^{(1/N)}}{\partial T}\Bigg|_{T\to 0}\sim\gamma^{(1/N)}T. \tag{A2}$$

We first compute the magnetic susceptibility.

The magnetic field appears in four places in Eq. (A1): (a) in the "quasiparticle renormalization factor" $Z(E_0)$; (b) in E_0, which occurs in the energy denominators; (c) in the self-energy $\Sigma_0^{(1)}$; and (d) in the arguments of the Fermi functions. The individual contributions are derived below. Recall from Eqs. (2.27) and (2.33) the definitions

$$T_A\equiv\varepsilon_f-E_0,\quad \mu\equiv\frac{N\Gamma}{\pi T_A}. \tag{A3}$$

Also note the $O(1)$ result from Eq. (2.39) that

$$-\frac{\partial E_0}{\partial H}=\chi^{(1)}H,\quad \chi^{(1)}=\frac{\mu}{1+\mu}\frac{\mu_j^2}{3T_A}\ . \tag{A4}$$

(a) First of all,

$$\begin{aligned}\partial\Sigma_0^{(1)}(E_0)/\partial E_0\,|_{T=0}&=\frac{\partial}{\partial E_0}\frac{\Gamma}{\pi}\sum_m\int_{-\infty}^{0}d\varepsilon\frac{f(\varepsilon-mg\mu_BH)}{E_0-\varepsilon_f+\varepsilon}\\&=\frac{N\Gamma}{\pi}(E_0-\varepsilon_f)^{-1}+\frac{N\Gamma}{\pi}\frac{\mu_j^2}{3}H^2(E_0-\varepsilon_f)^{-3}\\&\quad+O(H^4)\ .\end{aligned} \tag{A5}$$

The second term follows from expanding the Fermi function to second order in the field, then integrating by parts. Thus, for $H\to 0$,

$$\begin{aligned}-\frac{\partial}{\partial H}\left[1-\frac{\partial\Sigma_0^{(1)}}{\partial E_0}\right]^{-1}&=-\left[1-\frac{\partial\Sigma_0^{(1)}}{\partial E_0}\right]^{-2}\frac{\partial}{\partial H}\left[\frac{\partial\Sigma_0^{(1)}}{\partial E_0}\right]\\&=\frac{1}{(1+\mu)^2}\left[\frac{\mu}{T_A}\chi^{(1)}H+\frac{2\mu_j^2}{3}\frac{\mu}{T_A^2}H\right]\\&=\frac{\chi^{(1)}H}{(1+\mu)T_A}\left[2-\frac{\mu}{1+\mu}\right]\ .\end{aligned} \tag{A6}$$

The accompanying contribution to $\chi^{(1/N)}$ follows by substituting the last result in Eq. (A2):

$$\chi_a^{(1/N)}=\frac{\chi^{(1)}}{T_A}\left[2-\frac{\mu}{1+\mu}\right]\frac{N\Gamma^2}{\pi^2(1+\mu)}\times\int_{-D}^{0}d\varepsilon_1\int_0^D d\varepsilon_2\frac{1}{(\varepsilon_1-T_A)^2D(\varepsilon_2-\varepsilon_1)}\ , \tag{A7}$$

where

$$D(\varepsilon)\equiv E_0-\varepsilon-\Sigma_0^{(1)}(E_0-\varepsilon)\ . \tag{A8}$$

(b) Differentiating the quadratic energy denominator in (A1) gives

$$\begin{aligned}-\frac{\partial}{\partial H}\frac{1}{(E_0+\varepsilon_1-\varepsilon_f)^2}&=\frac{-2}{(E_0+\varepsilon_1-\varepsilon_f)^3}\left[-\frac{\partial E_0}{\partial H}\right]\\&=\frac{-2}{(\varepsilon_1-T_A)^3}\chi^{(1)}H\ .\end{aligned} \tag{A9}$$

The corresponding contribution to the susceptibility is

$$\chi_{b1}^{(1/N)}=\chi^{(1)}\left[\frac{-2\mu}{1+\mu}\frac{T_A\Gamma}{\pi}\int_{-D}^{0}d\varepsilon_1\int_0^D d\varepsilon_2\frac{1}{(\varepsilon_1-T_A)^3D(\varepsilon_2-\varepsilon_1)}\right]\ . \tag{A10}$$

Differentiating the linear energy denominator gives

$$-\frac{\partial}{\partial H}D(\varepsilon_2-\varepsilon_1)^{-1}=\frac{-\chi^{(1)}H}{D(\varepsilon_2-\varepsilon_1)^2}\left[1-\frac{\partial\Sigma_0^{(1)}(E_0+\varepsilon_1-\varepsilon_2)}{\partial E_0}\right]\ . \tag{A11}$$

The contribution to the susceptibility is

$$\chi_{b2}^{(1/N)}=\chi^{(1)}\left[\frac{-\mu}{1+\mu}\frac{T_A\Gamma}{\pi}\int_{-D}^{0}d\varepsilon_1\int_0^D d\varepsilon_2\frac{1+N\Gamma/\pi(\varepsilon_2-\varepsilon_1+T_A)}{(\varepsilon_1-T_A)^2[D(\varepsilon_2-\varepsilon_1)]^2}\right]\ . \tag{A12}$$

(c) From Eq. (A1b), the explicit dependence of $\Sigma_0^{(1)}$ on H (as distinguished from the implicit dependence through E_0) gives

$$-\frac{\partial\Sigma_0^{(1)}(E_0+\varepsilon_1-\varepsilon_2)}{\partial H}=\frac{N\Gamma}{\pi}\frac{\mu_j^2H}{3}\frac{1}{(\varepsilon_1-\varepsilon_2-T_A)^2}\ . \tag{A13}$$

The corresponding contribution to the susceptibility from this dependence in the linear energy denominator is

$$\chi_c^{(1/N)}=\chi^{(1)}\frac{N\Gamma^2T_A^2}{\pi^2}\int_{-D}^{0}d\varepsilon_1\int_0^D d\varepsilon_2\frac{1}{(\varepsilon_1-T_A)^2[D(\varepsilon_2-\varepsilon_1)]^2(\varepsilon_1-\varepsilon_2-T_1)^2}\ . \tag{A14}$$

(d) The only H dependence remaining to be accounted for is in the arguments of the Fermi functions. Thus

$$\chi_d^{(1/N)}=-\frac{\partial^2}{\partial H^2}\frac{1}{1+\mu}\frac{1}{N}\left[\frac{N\Gamma}{\pi}\right]^2\frac{1}{2N}\times\sum_m\int d\varepsilon_1d\varepsilon_2\left[f(\varepsilon_1-mg\mu_BH)[1-f(\varepsilon_2-mg\mu_BH)]\frac{1}{(\varepsilon_1-T_A)^2D(\varepsilon_2-\varepsilon_1)}+(1\leftrightarrow 2)\right]\ . \tag{A15}$$

Note that

$$-\frac{\partial^2}{\partial H^2}\sum_m f(\varepsilon_1-mg\mu_B H)[1-f(\varepsilon_2-mg\mu_B H)]\Big|_{H=0}=-\frac{N\mu_j^2}{3}\left[\frac{\partial}{\partial\varepsilon_1}+\frac{\partial}{\partial\varepsilon_2}\right]^2 f(\varepsilon_1)[1-f(\varepsilon_2)]\ . \tag{A16}$$

The preceding double integral contains no singularities, and an integration by parts is allowed. Substituting Eq. (A16) in (A15), integrating twice by parts, then combining terms gives

$$\chi_d^{(1/N)}=-\frac{1}{N}\left[\frac{N\Gamma}{\pi}\right]^2\frac{\mu_j^2/3}{1+\mu}\int d\varepsilon_1 d\varepsilon_2 f(\varepsilon_1)[1-f(\varepsilon_2)]\left[\frac{\partial^2}{\partial\varepsilon_1^2}\frac{1}{(\varepsilon_1-T_A)^2}\right]D(\varepsilon_2-\varepsilon_1)^{-1}\ , \tag{A17}$$

since $\partial/\partial\varepsilon_1+\partial/\partial\varepsilon_2$ applied to the last factor is 0. Finally,

$$\chi_d^{(1/N)}=\chi^{(1)}\left[-\frac{6}{N}\left[\frac{N\Gamma}{\pi}\right]^2\frac{T_A}{\mu}\int_{-D}^{0}d\varepsilon_1\int_0^D d\varepsilon_2\frac{1}{(\varepsilon_1-T_A)^4 D(\varepsilon_2-\varepsilon_1)}\right]\ . \tag{A18}$$

The complicated double integrals that appear in (a)—(d) above may be simplified to dimensionless single integrals in the limit of large D. Specifically, consider the change of variables from $\varepsilon_1,\varepsilon_2$ to

$$x=\varepsilon_1/T_A,\quad -D/T_A\le x\le 0,\quad y=(\varepsilon_2-\varepsilon_1)/T_A,\quad -x\le y\le D/T_A-x\ . \tag{A19}$$

If the impurity level lies well within the band ($D\gg|\varepsilon_f|$), the range of integration for y may be restricted to $[-x,D/T_A]$ with errors of order T_A/D. A slightly more careful treatment is required when the impurity level lies outside the band. If this possibility is ignored, the region of integration becomes

$$0\le y\le D/T_A,\quad -y\le x\le 0\ . \tag{A20}$$

Note further that $D(\varepsilon)$ takes the form

$$D(\varepsilon)=E_0-\varepsilon-\frac{N\Gamma}{\pi}\int_{-D}^{0}\frac{d\varepsilon'}{\varepsilon'-\varepsilon-T_A}=E_0-\varepsilon+\frac{N\Gamma}{\pi}\ln\left[\frac{D+T_A+\varepsilon}{T_A+\varepsilon}\right]\approx-\varepsilon-\frac{N\Gamma}{\pi}\ln\left[1+\frac{\varepsilon}{T_A}\right]\ . \tag{A21}$$

The double integrals encountered above may be reduced to the following simplified forms:

$$\int_{-D}^{0}d\varepsilon_1\int_0^D d\varepsilon_2\frac{1}{(\varepsilon_1-T_A)^{n+1}D(\varepsilon_2-\varepsilon_1)}=\frac{(-)^n}{nT_A^n}\int_0^{D/T_A}\frac{dy}{y+\mu\ln(1+y)}\left[1-\frac{1}{(1+y)^n}\right]\equiv\frac{(-)^n}{nT_A^n}L_n\ , \tag{A22a}$$

$$\int_{-D}^{0}d\varepsilon_1\int_0^D d\varepsilon_2\frac{1}{(\varepsilon_1-T_A)^2[D(\varepsilon_2-\varepsilon_1)]^2(\varepsilon_2-\varepsilon_1+T_A)^2}=T_A^{-4}\int_0^{D/T_A}\frac{dy}{[y+\mu\ln(1+y)]^2}\frac{1}{(1+y)^2}\left[1-\frac{1}{1+y}\right]\ , \tag{A22b}$$

$$\int_{-D}^{0}d\varepsilon_1\int_0^D d\varepsilon_2\frac{1}{(\varepsilon_1-T_A)^2[D(\varepsilon_2-\varepsilon_1)]^2}=T_A^{-2}\int_0^{D/T_A}\frac{dy}{[y+\mu\ln(1+y)]^2}\left[1+\frac{\mu}{1+y}\right]\left[1-\frac{1}{1+y}\right]\ . \tag{A22c}$$

The expressions for $\chi_{b2}^{(1/N)}$ and $\chi_c^{(1/N)}$ may be combined using the last two results:

$$\chi_{b2}^{(1/N)}+\chi_c^{(1/N)}=\chi^{(1)}\frac{\mu^2}{(1+\mu)N}\left[(1+\mu)\int_0^{D/T_A}\frac{dy}{[y+\mu\ln(1+y)]^2}\frac{y}{(1+y)^3}\right.$$
$$\left.-\int_0^{D/T_A}\frac{dy}{[y+\mu\ln(1+y)]^2}\left[1+\frac{\mu}{1+y}\right]\left[1-\frac{1}{1+y}\right]\right]=-\chi^{(1)}\frac{\mu^2}{(1+\mu)N}M\ , \tag{A23}$$

where

$$M=\int_0^{D/T_A}\frac{dy}{[y+\mu\ln(1+y)]^2}\frac{y^2(2+\mu+y)}{(1+y)^3}\ .$$

Finally, the complete expression for χ in terms of convergent one-dimensional integrals is

$$\chi=\chi^{(1)}\left\{1+\frac{\mu^2}{(1+\mu)N}\left[\frac{2(1+\mu)}{\mu}L_3-L_2-M-\left[2-\frac{\mu}{1+\mu}\right]L_1\right]\right\}\ . \tag{A24}$$

This expression was first derived by Rasul and Hewson (1984a, 1984b).

Next, we derive the specific-heat coefficient γ, following the treatment by Brandt, Keiter, and Liu (1985). The procedure is essentially the same as that above; it is necessary to consider temperature dependence from the same sources (a)—(d). The contributions to $\gamma^{(1/N)}$ from (a)—(c) may be obtained from Eqs. (A7), (A10), (A12), and (A14) by making

the trivial replacement

$$\chi^{(1)}\to\gamma^{(1)}\,. \tag{A25}$$

This follows from the simple relationship between temperature and field derivatives of E_0 and of the Fermi function. The temperature dependence from source (d), i.e., the explicit temperature dependence of the Fermi functions in (A1a), is more subtle. It is this term which accounts for the nontrivial Sommerfeld ratio obtained in Eq. (2.46) at $O(1/N)$.

The quantity that must be evaluated is

$$\gamma_d^{(1/N)}=\frac{-\partial^2}{\partial T^2}\frac{1}{1+\mu}\frac{1}{N}\left[\frac{N\Gamma}{\pi}\right]^2\tfrac{1}{2}\int d\varepsilon_1 d\varepsilon_2\left[f(\varepsilon_1)[1-f(\varepsilon_2)]\frac{1}{(\varepsilon_1-T_A)^2 D(\varepsilon_2-\varepsilon_1)}+(1\leftrightarrow 2)\right], \tag{A26}$$

where only the explicit temperature dependence of the Fermi functions is to be considered. Both of the terms in large parentheses become singular for $\varepsilon_1\to\varepsilon_2$; the sum is nonsingular. It is convenient to isolate the singularity by changing to variables $\varepsilon=\varepsilon_1-\varepsilon_2$, ε_2, and noting that

$$f(\varepsilon_1)[1-f(\varepsilon_2)]=-[f(\varepsilon_1)-f(\varepsilon_2)]b(\varepsilon_1-\varepsilon_2)=-[f(\varepsilon_2+\varepsilon)-f(\varepsilon_2)]b(\varepsilon)\,, \tag{A27}$$

with b the Bose function. The integral over ε may be saved for last. In these new variables,

$$\gamma_d^{(1/N)}=\frac{-\partial^2}{\partial T^2}\frac{1}{1+\mu}\frac{-1}{N}\left[\frac{N\Gamma}{\pi}\right]^2\int d\varepsilon\tfrac{1}{2}b(\varepsilon)\int d\varepsilon_2[f(\varepsilon_2+\varepsilon)-f(\varepsilon_2)]\left[\frac{1}{(\varepsilon_2+\varepsilon-T_A)^2}\frac{1}{D(-\varepsilon)}+\frac{e^{\beta\varepsilon}}{(\varepsilon_2-T_A)^2}\frac{1}{D(\varepsilon)}\right]. \tag{A28a}$$

The integral over ε takes the form

$$\tfrac{1}{2}\int d\varepsilon\left[\frac{b(\varepsilon)G(\varepsilon)}{D(-\varepsilon)}+\frac{b(-\varepsilon)G(-\varepsilon)}{D(\varepsilon)}\right]=\mathbf{P}\int d\varepsilon\frac{b(\varepsilon)G(\varepsilon)}{D(-\varepsilon)},\quad G(\varepsilon)=\int d\varepsilon_2\frac{f(\varepsilon_2+\varepsilon)-f(\varepsilon_2)}{(\varepsilon_2+\varepsilon-T_A)^2}\,, \tag{A28b}$$

with $\mathbf{P}$ the principal value; this follows by noting $e^{\beta\varepsilon}b(\varepsilon)=-b(-\varepsilon)$, then shifting variables in the last term of Eq. (A28a) by $\varepsilon_2\to\varepsilon_2-\varepsilon$. Hence

$$\gamma_d^{(1/N)}=\frac{-\partial^2}{\partial T^2}\frac{1}{1+\mu}\frac{-1}{N}\left[\frac{N\Gamma}{\pi}\right]^2\mathbf{P}\int d\varepsilon\frac{b(\varepsilon)G(\varepsilon)}{D(-\varepsilon)}\,. \tag{A28c}$$

To isolate behavior in the neighborhood of $\varepsilon=0$, the range of the ε integral may conveniently be divided into three parts $[-D,-\bar{E}]$, $[-\bar{E},\bar{E}]$, and $[\bar{E},D]$, where $\bar{E}$ is a small energy that may be sent to zero *after* letting $T\to 0$. The temperature dependence of the factor G follows by a Sommerfeld expansion:

$$G(\varepsilon)=\frac{1}{\varepsilon-T_A}+\frac{1}{T_A}+\frac{\pi^2T^2}{6}\left[\frac{2}{T_A^3}+\frac{2}{(\varepsilon-T_A)^3}\right]+O(T^4)\,. \tag{A29}$$

The integral of the T^2 term over $[-\bar{E},\bar{E}]$ is nonsingular (even in the limit $T\to 0$) and vanishes for $\bar{E}\to 0$. For $T\to 0$, the Bose function becomes

$$b(\varepsilon)=\begin{cases}-1, & \varepsilon<-\bar{E}\,,\\ 0, & \varepsilon>\bar{E}\,.\end{cases} \tag{A30}$$

Thus the contribution to $\gamma^{(1/N)}$ from G is

$$\begin{aligned}\gamma_{d1}^{(1/N)}&=-\frac{2\pi^2}{3(1+\mu)}\frac{1}{N}\left[\frac{N\Gamma}{\pi}\right]^2\lim_{\bar{E}\to 0}\int_{-D}^{-\bar{E}}d\varepsilon\left[\frac{1}{T_A^3}+\frac{1}{(\varepsilon-T_A)^3}\right]D^{-1}(-\varepsilon)\\&=\frac{2\pi^2}{3(1+\mu)}\frac{1}{N}\left[\frac{N\Gamma}{\pi}\right]^2\int_0^D d\varepsilon\left[\frac{1}{(\varepsilon+T_A)^3}-\frac{1}{T_A^3}\right]D^{-1}(\varepsilon)\,.\end{aligned} \tag{A31}$$

The only contribution to $\gamma^{(1/N)}$ from the Bose function in Eq. (A28c) arises from the interval $[-\bar{E},\bar{E}]$. The temperature-independent part of G may be employed in deriving the T^2 contribution from $b(\varepsilon)$. Thus

$$\mathbf{P}\int d\varepsilon\frac{b(\varepsilon)G(\varepsilon)}{D(-\varepsilon)}\to\mathbf{P}\int_{-\bar{E}}^{\bar{E}}d\varepsilon\, b(\varepsilon)F(\varepsilon) \tag{A32}$$

with

$$F(\varepsilon)=\left[\frac{1}{\varepsilon-T_A}+\frac{1}{T_A}\right]\frac{1}{D(-\varepsilon)} .$$

The integrand varies as $1/\varepsilon$ for $\varepsilon\to 0$, but the singularity is removed by the principal value; hence the integral has a valid Sommerfeld expansion. The T^2 term is just

$$\frac{\pi^2T^2}{3}F'(0)=-\frac{\pi^2T^2}{3}\frac{1}{T_A^2(1-\partial\Sigma_0^{(1)}/\partial E_0)}\left[\frac{1}{T_A}+\frac{\partial^2\Sigma_0^{(1)}/\partial E_0^2}{2(1-\partial\Sigma_0^{(1)}/\partial E_0)}\right]=-\frac{\pi^2T^2}{6T_A}\frac{1}{T_A^2(1+\mu)}\left[2-\frac{\mu}{1+\mu}\right] . \tag{A33}$$

The resulting contribution to $\gamma^{(1/N)}$ is

$$\gamma_{d2}^{(1/N)}=-\frac{\pi^2}{3T_A}\frac{1}{N}\left[\frac{\mu}{1+\mu}\right]^2\left[2-\frac{\mu}{1+\mu}\right]=-\frac{\pi^2}{3T_A}\frac{1}{N}\frac{\mu}{1+\mu}\left[1-\frac{1}{(1+\mu)^2}\right] . \tag{A34}$$

This contribution to γ has no analog in the expression for χ [Eq. (A24)] derived previously. It is this term which makes the Sommerfeld ratio differ from 1, the value for a noninteracting Fermi gas of quasiparticles, at $O(1/N)$. Note that the correction term $\gamma_{d2}^{(1/N)}$ arises from Bose-type electron-hole excitations that do not couple to the magnetic field. To summarize, the complete expression for the specific-heat coefficient to $O(1/N)$ is

$$\gamma=\gamma^{(1)}\left\{1+\frac{\mu^2}{(1+\mu)N}\left[\frac{2(1+\mu)}{\mu}L_3-L_2-M-\left[2-\frac{\mu}{1+\mu}\right]L_1\right]-\frac{1}{N}\left[1-\frac{1}{(1+\mu)^2}\right]\right\} , \tag{A35}$$

with L_n and M as in Eqs. (A22a) and (A23).

APPENDIX B: DERIVATION OF CORRELATION FUNCTIONS FOR SYSTEMS WITH STRONG LOCAL CORRELATIONS

In this appendix we derive a general expression for the correlation functions of a many-particle Hamiltonian, using the same approach applied to the partition function in Sec. II.A. We follow precisely the procedure outlined by Keiter and Morandi (1984).

Consider the correlation function

$$G_{AB}(\tau)=-\langle T_\tau A(\tau)B\rangle . \tag{B1a}$$

The operators A and B may have Fermi or Bose character. The Fourier transform has a simple representation,

$$G_{AB}(i\omega_n)=\int_0^\beta d\tau e^{i\omega_n\tau}G_{AB}(\tau)=-\frac{1}{Z}\int_0^\beta d\tau e^{i\omega_n\tau}\int_\Gamma\frac{dz}{2\pi i}e^{-(\beta-\tau)z}\int_\Gamma\frac{dz'}{2\pi i}e^{-\tau z'}\mathrm{Tr}(z-H)^{-1}A(z'-H)^{-1}B ,$$
$$\omega_n=\begin{cases}(2n+1)\pi T & \text{(Fermi)} ,\\ 2n\pi T & \text{(Bose)} .\end{cases} \tag{B1b}$$

Here the contour Γ encloses all singularities of the resolvent $(z-H)^{-1}$ in a counterclockwise fashion. Performing the Fourier transform gives

$$G_{AB}=-\frac{1}{Z}\int_\Gamma\frac{dz}{2\pi i}\int_\Gamma\frac{dz'}{2\pi i}\frac{\mp e^{-\beta z'}-e^{-\beta z}}{i\omega_n+z-z'}\mathrm{Tr}(z-H)^{-1}A(z'-H)^{-1}B . \tag{B2}$$

One of the contour integrals may be performed by residues:

$$G_{AB}=\mp\frac{1}{Z}\int_\Gamma\frac{dz'}{2\pi i}e^{-\beta z'}\mathrm{Tr}(z'-i\omega_n-H)^{-1}A(z'-H)^{-1}B+\frac{1}{Z}\int_\Gamma\frac{dz}{2\pi i}e^{-\beta z}\mathrm{Tr}(z-H)^{-1}A(z+i\omega_n-H)^{-1}B . \tag{B3}$$

Finally, shifting the contour in the first integral by $z'\to z'+i\omega_n$ and combining terms gives

$$G_{AB}=\frac{1}{Z}\int_C\frac{dz}{2\pi i}e^{-\beta z}\mathrm{Tr}(z-H)^{-1}A(z+i\omega_n-H)^{-1}B , \tag{B4}$$

where now C is a counterclockwise contour enclosing all singularities of the two resolvents $(z-H)^{-1}$ and $(z+i\omega_n-H)^{-1}$ (see Fig. 33).

As in Sec. II.A, a perturbative expansion may be generated by dividing H into an unperturbed part and a perturbation

$$H=H_0+V \tag{B5}$$

and rewriting the resolvents:

$$G_{AB}=\frac{1}{Z}\int_C \frac{dz}{2\pi i}e^{-\beta z}\mathrm{Tr}\left[(z-H_0)^{-1}\sum_{l=0}^{\infty}[V(z-H_0)^{-1}]^l A\sum_{m=0}^{\infty}[(z+i\omega_n-H_0)^{-1}V]^m(z+i\omega_n-H_0)^{-1}B\right]. \tag{B6}$$

Inserting a complete set of eigenstates of the unperturbed Hamiltonian and shifting the integration variable by $z\to z+E_N$ gives

$$\begin{aligned}G_{AB}=\frac{1}{Z}\sum_{NM_i}\int_C\frac{dz}{2\pi i}\frac{e^{-\beta z}}{z}e^{-\beta E_N}\sum_{l,m=0}^{\infty}&\langle N\,|\,[V(z+E_N-H_0)^{-1}]^l\,|\,M_3\rangle\\ &\times\langle M_3\,|\,A\,|\,M_2\rangle\langle M_2\,|\,[(z+E_N+i\omega_n-H_0)^{-1}V]^m\,|\,M_1\rangle\\ &\times(z+E_N-E_{M_1}+i\omega_n)^{-1}\langle M_1\,|\,B\,|\,N\rangle\,.\end{aligned} \tag{B7}$$

This expression is employed in Sec. II.D to investigate the f-electron Green's function for the infinite-U Anderson model.

APPENDIX C: 1/N CORRECTIONS TO THE ZERO-TEMPERATURE f GREEN'S FUNCTION FOR THE INFINITE-U ANDERSON MODEL

In this appendix we derive an expression for the zero-temperature f-electron Green's function (see Sec. II.D) to $O(1/N)$, following in part a treatment by Brandt, Keiter, and Liu (1985). The Green's function was reduced to contour integrals in Eqs. (2.51) and (2.54):

$$\begin{aligned}&G_f(i\omega_n)=G_f^{(1)}(i\omega_n)+G^{(1/N)}(i\omega_n),\quad G_f^{(1)}(i\omega_n)=Z(E_0)\frac{1}{i\omega_n-T_A}\,,\\ &G_f^{(1/N)}(i\omega_n)=-\frac{Z^{(1/N)}}{Z^{(1)}}G_f^{(1)}(i\omega_n)+G_A(i\omega_n)+G_B(i\omega_n)\,,\end{aligned} \tag{C1a}$$

with

$$\begin{aligned}G_A(i\omega_n)&=\frac{1}{Z^{(1)}/Z_{\text{band}}}\int_\Gamma\frac{dz}{2\pi i}\frac{e^{-\beta z}}{(z+i\omega_n-\varepsilon_f)^2[z-\Sigma_0^{(1)}(z)]}V^2\sum_k\frac{1-f_k}{z+i\omega_n-\varepsilon_k-\Sigma_0^{(1)}(z+i\omega_n-\varepsilon_k)}\,,\\ G_B(i\omega_n)&=\frac{1}{Z^{(1)}/Z_{\text{band}}}\int_\Gamma\frac{dz}{2\pi i}\frac{e^{-\beta z}\Sigma_0^{(1/N)}(z)}{(z+i\omega_n-\varepsilon_f)[z-\Sigma_0^{(1)}(z)]^2}\,.\end{aligned} \tag{C1b}$$

At $T=0$, the first term in $G_f^{(1/N)}$ is [see Eqs. (2.24), (2.25), and (2.51)]

$$\begin{aligned}-\frac{Z^{(1/N)}}{Z^{(1)}}G_f^{(1)}(i\omega_n)&=\frac{1}{i\omega_n-T_A}\frac{\beta(NV^2)^2}{N}Z^2(E_0)\sum_{kk'}f_k(1-f_{k'})\frac{1}{(\varepsilon_k-T_A)^2}\frac{1}{E_0+\varepsilon_k-\varepsilon_{k'}-\Sigma_0^{(1)}(E_0+\varepsilon_k-\varepsilon_{k'})}\\ &=\frac{\beta}{i\omega_n-T_A}Z^2(E_0)\Sigma_0^{(1/N)}(E_0)\,.\end{aligned} \tag{C2}$$

The next term G_A has pole contributions at

$$z=E_0\ \text{ and }\ z=E_0+\varepsilon_k-i\omega_n\,. \tag{C3}$$

Noting that $Z^{(1)}/Z_{\text{band}}\to e^{-\beta E_0}$ at zero temperature, one finds

$$\begin{aligned}G_A(i\omega_n)\to&\frac{1}{(i\omega_n-T_A)^2}\frac{NV^2}{N}Z(E_0)\sum_k\frac{1-f_k}{i\omega_n+E_0-\varepsilon_k-\Sigma_0^{(1)}(i\omega_n+E_0-\varepsilon_k)}\\ &-\frac{NV^2}{N}Z(E_0)\sum_k\frac{f_k}{(\varepsilon_k-T_A)^2}\frac{1}{-i\omega_n+E_0+\varepsilon_k-\Sigma_0^{(1)}(-i\omega_n+E_0+\varepsilon_k)}\,.\end{aligned} \tag{C4}$$

Finally, consider the last term G_B. It is useful to write out explicitly $\Sigma_0^{(1/N)}$ to examine its pole structure:

$$\Sigma_0^{(1/N)}(z)=\frac{(NV^2)^2}{N}\sum_{k_1k_2}\frac{f_{k_1}(1-f_{k_2})}{(z+\varepsilon_1-\varepsilon_f)^2}\frac{1}{z+\varepsilon_1-\varepsilon_2-\Sigma_0^{(1)}(z+\varepsilon_1-\varepsilon_2)}\,. \tag{C5}$$

The full integrand in (C1b) has dominant low-temperature poles at

$$z=E_0 \text{ (double pole) and } z=E_0-\varepsilon_1+\varepsilon_2 . \tag{C6}$$

Thus

$$G_B(i\omega_n)\to Z^2(E_0)\Sigma_0^{1/N}(E_0)\left[\frac{-\beta}{i\omega_n-T_A}-\frac{1}{(i\omega_n-T_A)^2}\right]+\frac{1}{i\omega_n-T_A}\frac{\partial}{\partial z}\left[\Sigma_0^{(1/N)}(z)\frac{(z-E_0)^2}{[z-\Sigma_0^{(1)}(z)]^2}\right]_{E_0}$$
$$+\frac{(NV^2)^2}{N}Z(E_0)\sum_{kk'}\frac{(1-f_k)f_{k'}}{(\varepsilon_{k'}-T_A)^2}\frac{1}{i\omega_n-\varepsilon_k+\varepsilon_{k'}-T_A}\frac{1}{[E_0-\varepsilon_k+\varepsilon_{k'}-\Sigma_0^{(1)}(E_0-\varepsilon_k+\varepsilon_{k'})]^2} . \tag{C7}$$

The complete expression for $G_f(i\omega_n)$ at zero temperature follows by combining terms:

$$G_f^{(1)}(i\omega_n)+G_f^{(1/N)}(i\omega_n)=Q(i\omega_n)+B_1(i\omega_n)+B_2(i\omega_n) \tag{C8a}$$

with

$$Q(i\omega_n)=\frac{1}{i\omega_n-T_A}\left[Z(E_0)+\frac{\partial}{\partial z}\left[\Sigma_0^{(1/N)}(z)\frac{(z-E_0)^2}{[z-\Sigma_0^{(1)}(z)]^2}\right]_{E_0}\right],$$
$$B_1(i\omega_n)=\frac{1}{(i\omega_n-T_A)^2}Z(E_0)\left[V^2\sum_k\frac{1-f_k}{i\omega_n+E_0-\varepsilon_k-\Sigma_0^{(1)}(i\omega_n+E_0-\varepsilon_k)}-Z(E_0)\Sigma_0^{(1/N)}(E_0)\right], \tag{C8b}$$
$$B_2(i\omega_n)=-V^2Z(E_0)\sum_k\frac{f_k}{(\varepsilon_k-T_A)^2}\left[\frac{1}{-i\omega_n+E_0+\varepsilon_k-\Sigma_0^{(1)}(-i\omega_n+E_0+\varepsilon_k)}\right.$$
$$\left.-NV^2\sum_{k'}\frac{1-f_{k'}}{i\omega_n+\varepsilon_k-\varepsilon_{k'}-T_A}\frac{1}{[E_0+\varepsilon_k-\varepsilon_{k'}-\Sigma_0^{(1)}(E_0+\varepsilon_k-\varepsilon_{k'})]^2}\right] .$$

Note that the contribution from Eq. (C2) is canceled by a contribution from the double pole in Eq. (C7). The last expression is discussed in detail in Sec. II.D.

Although Eq. (C8) is quite complicated, its imaginary part (the spectral density ρ_f) assumes a simple form for a flat density of band states. Note first that $Q(\omega)$ is real for $\omega\neq T_A$. In addition,

$$\mathrm{Im}B_1(\omega+i0^+)=\frac{1}{N}Z(E_0)\frac{N\Gamma}{\pi}\frac{1}{(\omega-T_A)^2}\mathrm{Im}\int_0^D\frac{d\varepsilon}{\omega+E_0-\varepsilon-\Sigma_0^{(1)}(\omega+E_0-\varepsilon)+i0^+}$$
$$=-\frac{\pi}{N}Z^2(E_0)\frac{N\Gamma}{\pi}\frac{1}{(\omega-T_A)^2}\theta(\omega)-\pi S(\omega)\theta(\omega-T_A) ,$$
$$S(\omega)=\frac{1}{N}Z(E_0)\left[\frac{N\Gamma}{\pi}\right]^2\frac{1}{(\omega-T_A)^2}\int_0^{\omega-T_A}\frac{d\varepsilon}{[\omega+E_0-\varepsilon-\mathrm{Re}\Sigma_0^{(1)}(\omega+E_0-\varepsilon)]^2+(N\Gamma)^2} \tag{C9}$$
$$=\frac{1}{N}Z(E_0)\left[\frac{N\Gamma}{\pi}\right]^2\frac{1}{(\omega-T_A)^2}\int_{T_A}^{\omega}d\varepsilon\frac{1}{[\varepsilon-(N\Gamma/\pi)\ln(\varepsilon/T_A-1)]^2+(N\Gamma)^2} .$$

Finally, note that

$$\mathrm{Im}B_2(\omega+i0^+)=-\frac{1}{N}Z(E_0)\frac{N\Gamma}{\pi}\mathrm{Im}\int_{-D}^D\frac{d\varepsilon}{(\varepsilon-T_A)^2}\frac{1}{-\omega+E_0+\varepsilon-\Sigma_0^{(1)}(-\omega+E_0+\varepsilon)-i0^+}$$
$$+\frac{1}{N}Z(E_0)\left[\frac{N\Gamma}{\pi}\right]^2\mathrm{Im}\int_{-D}^0\frac{d\varepsilon}{(\varepsilon-T_A)^2}\int_0^D\frac{d\varepsilon'}{[E_0+\varepsilon-\varepsilon'-\Sigma_0^{(1)}(E_0+\varepsilon-\varepsilon')]^2}\frac{1}{\omega+i0^++\varepsilon-\varepsilon'-T_A}$$
$$=-\frac{\pi}{N}Z^2(E_0)\frac{N\Gamma}{\pi}\frac{1}{(\omega-T_A)^2}\theta(-\omega)-\pi R(\omega)\theta(-\omega-T_A)-\pi T(\omega)\theta(\omega-T_A) ,$$
$$R(\omega)=\frac{1}{N}Z(E_0)\left[\frac{N\Gamma}{\pi}\right]^2\int_{T_A}^{-\omega}\frac{d\varepsilon}{(\omega+\varepsilon-T_A)^2}\frac{1}{[\varepsilon-(N\Gamma/\pi)\ln(\varepsilon/T_A-1)]^2+(N\Gamma)^2} , \tag{C10}$$
$$T(\omega)=\frac{1}{N}Z(E_0)\left[\frac{N\Gamma}{\pi}\right]^2\left[\frac{1}{T_A}-\frac{1}{\omega}\right]\frac{1}{[\omega-T_A+(N\Gamma/\pi)\ln(\omega/T_A)]^2} .$$

It follows that throughout the intervals $(-D,T_A)$ and (T_A,D)

$$\rho_f(\omega)=-\frac{1}{\pi}\mathrm{Im}G_f(\omega+i0^+)=\frac{1}{N}Z^2(E_0)\frac{N\Gamma}{\pi}\frac{1}{(\omega-T_A)^2}+R(\omega)\theta(-\omega-T_A)+[S(\omega)+T(\omega)]\theta(\omega-T_A)\,. \tag{C11}$$

This relatively simple result is discussed at length in Sec. II.D.

APPENDIX D: OPERATOR AVERAGES IN THE AUXILIARY BOSON REPRESENTATION OF THE INFINITE-U ANDERSON MODEL

In this appendix we discuss the evaluation of operator averages and correlation functions for the infinite-U Anderson model within the auxiliary boson approach introduced in Sec. III.A. Recall that, within this approach, the partition function may be written

$$Z=\mathrm{Tr}_1 e^{-\beta H}\,, \tag{D1a}$$

with H the pseudo-Hamiltonian of Eq. (3.3), defined on a mixed Hilbert space of Fermi and Bose states. The trace is restricted to the subspace of states with $Q=1$, where

$$Q=b^\dagger b+\sum_m f_m^\dagger f_m\,. \tag{D1b}$$

The only operators $\hat{O}$ defined on the full Hilbert space which correspond to physical operators in the infinite-U Anderson model are those which commute with Q:

$$[\hat{O},Q]=0\,. \tag{D2}$$

Such operators have a simple restriction to the $Q=1$ subspace and do not connect physical and unphysical states. Operator averages take the form

$$\langle\hat{O}(\tau)\rangle_1\equiv\frac{1}{Z}\mathrm{Tr}_1 e^{-\beta H}(e^{\tau H}\hat{O}e^{-\tau H})\,. \tag{D3}$$

We mention two equivalent techniques for evaluating the operator trace in this expression.

Technique 1. The trace may be extended to the full Hilbert space by inserting the operator delta function

$$\int_{-\pi T}^{\pi T}\frac{\beta d\lambda}{2\pi}e^{-i\beta\lambda(Q-1)}\,.$$

Since $\hat{O}$ commutes with Q,

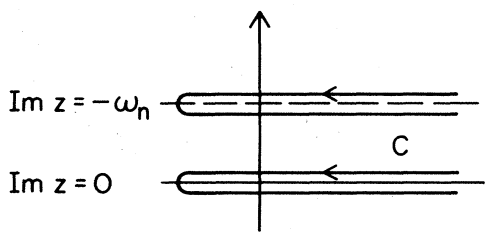

FIG. 33. Contour of integration C for Eq. (B4). The contour encircles all singularities of the integrand in a counterclockwise fashion.

$$O(\tau)=e^{\tau H}\hat{O}e^{-\tau H}$$
$$=\exp[\tau(H+i\lambda Q)]\hat{O}\exp[-\tau(H+i\lambda Q)]\,, \tag{D4}$$

for arbitrary λ. This relation holds for the operators $\hat{O}$ and H acting on the full Hilbert space (states of arbitrary Q) and for the restriction of these operators to the $Q=1$ subspace. Hence

$$\langle\hat{O}(\tau)\rangle_1=\frac{1}{Z}\mathrm{Tr}\left[e^{-\beta H}e^{\tau H}\hat{O}e^{-\tau H}\int_{-\pi T}^{\pi T}\frac{\beta d\lambda}{2\pi}e^{-i\beta\lambda(Q-1)}\right]$$
$$=\frac{1}{Z}\int_{-\pi T}^{\pi T}\frac{\beta d\lambda}{2\pi}e^{i\beta\lambda}\mathrm{Tr}e^{-\beta H(\lambda)}e^{\tau H(\lambda)}\hat{O}e^{-\tau H(\lambda)}\,, \tag{D5}$$

with

$$H(\lambda)\equiv H+i\lambda Q\,.$$

In the last expression, the time development of $\hat{O}$ is governed by the same operator $H(\lambda)$ that appears in the statistical weighting factor; thus standard Feynman techniques may be used to evaluate the trace.

A linked cluster expansion for the trace may be obtained if $\hat{O}$ annihilates states with $Q=0$. This is the case for all operators of interest. The trace is then $O(e^{-i\beta\lambda})$, since the first nonzero contribution arises from the $Q=1$ subspace. Note next that

$$Z^\lambda\equiv\mathrm{Tr}e^{-\beta H(\lambda)}=Z_{\mathrm{band}}+O(e^{-i\beta\lambda})\,, \tag{D6a}$$

with Z_{band} the partition function of the conduction-electron system. It follows that

$$\frac{Z_{\mathrm{band}}}{Z^\lambda}=1+O(e^{-i\beta\lambda})\,. \tag{D6b}$$

If this expression is placed inside the integral in Eq. (D5), the correction of $O(e^{-i\beta\lambda})$ is projected away. Thus

$$\langle\hat{O}(\tau)\rangle_1=\frac{1}{Z/Z_{\mathrm{band}}}\int_{-\pi T}^{\pi T}\frac{\beta d\lambda}{2\pi}e^{i\beta\lambda}\frac{1}{Z^\lambda}\mathrm{Tr}e^{-\beta H(\lambda)}$$
$$\times e^{\tau H(\lambda)}\hat{O}e^{-\tau H(\lambda)}\,. \tag{D7}$$

The quantity inside the integral now obeys a linked cluster theorem. Note, however, that the factor of Z/Z_{band} must still be evaluated independently.

Technique 2. The restricted trace may equally well be evaluated by introducing

$$H(\mu)\equiv H+\mu Q\,, \tag{D8}$$

with μ real. Again it may be assumed that $\hat{O}$ annihilates states with $Q=0$. It is easy to show, by the same arguments applied above, that

$$\langle \hat{O}(\tau)\rangle_1 = \frac{1}{Z}\lim_{\mu\to 0} e^{\beta\mu}\mathrm{Tr}\, e^{-\beta H(\mu)} e^{\tau H(\mu)}\hat{O} e^{-\tau H(\mu)}$$
$$= \frac{1}{Z/Z_{\text{band}}}\lim_{\mu\to\infty} e^{\beta\mu}\frac{1}{Z^{\mu}}\mathrm{Tr}\, e^{-\beta H(\mu)} e^{\tau H(\mu)}\hat{O} e^{-\tau H(\mu)} \tag{D9}$$

with

$$Z^{\mu}\equiv \mathrm{Tr}\, e^{-\beta H(\mu)} .$$

In analogy with Eq. (D7), the quantity inside the limit obeys a linked cluster theorem.

When the expressions in (D7) and (D9) are evaluated by perturbation theory, intermediate states (which arise from inserting the identity $\sum_N |N\rangle\langle N| = 1$ between consecutive operators) are automatically restricted to the $Q=1$ subspace. This is because $\hat{O}$ and all parts of the Hamiltonian commute with Q.

Operator product averages (including time-dependent correlation functions) may be evaluated using the same techniques. The only physical operator products are those in which every factor commutes with Q; in particular, if an operator has no matrix elements diagonal in Q, all products containing that operator vanish within the $Q=1$ subspace. This has important consequences for correlation functions. If, for some operator $\hat{A}$,

$$\langle \hat{A}\rangle_1 = 0 , \tag{D10}$$

then the correlation function $\langle \hat{A}(\tau)A^{\dagger}\rangle_1$ also vanishes, even if $[\hat{A}(\tau)\hat{A}^{\dagger}, Q]=0$. This follows since the correlation function may be rewritten as

$$\sum_{N_1 N_2} \langle N_1|\hat{A}(\tau)|N_2\rangle\langle N_2|\hat{A}^{\dagger}|N_1\rangle , \tag{D11}$$

with both $|N_1\rangle$ and $|N_2\rangle$ in the $Q=1$ subspace. For example, the correlation functions $\langle b(\tau)b^{\dagger}\rangle_1$ and $\langle f_m(\tau)f_m^{\dagger}\rangle_1$ vanish identically. The operators b and f_m are off-diagonal in Q. On the other hand, operators such as $b^{\dagger}f_m$ and $f_m^{\dagger}f_m$, which commute with Q, fall into the class discussed previously. The correlation functions $\langle f_m^{\dagger}(\tau)b(\tau)b^{\dagger}f_m\rangle_1$ and $\langle f_m^{\dagger}(\tau)f_m(\tau)f_m^{\dagger}f_m\rangle_1$ are physical (and nonzero).

The reader may observe an apparent paradox in these statements: surely a quantity like $\langle b^{\dagger}b\rangle_1$ may be viewed alternately as (a) the mean value of a physical operator or (b) the equal-time correlation function of two unphysical operators. Do not the two treatments above give contradictory results? In fact, there is no contradiction. The operator $b^{\dagger}b$ may be defined by its matrix elements (without reference to its composite character); a second operator may be defined by the product of the matrices representing $b^{\dagger}$ and b. When the full Hilbert space (states with arbitrary Q) is considered, the operators defined in this way coincide, since their matrix elements are identical. If only the $Q=1$ subspace is considered, the $b^{\dagger}b$ submatrix is nonzero, while the $b^{\dagger}$ and b submatrices vanish identically: the operators do not coincide within the restricted space.

Note that correlation functions for operators that satisfy (D10) are not given correctly by applying (D7) or (D9). There are two reasons for this failure: (a) since $[\hat{A},Q]\neq 0$,

$$\hat{A}(\tau) = e^{\tau H}\hat{A}e^{-\tau H} \neq e^{\tau H(\lambda)}\hat{A}e^{-\tau H(\lambda)} . \tag{D12}$$

For example,

$$b(\tau) = e^{i\lambda\tau}e^{\tau H(\lambda)}be^{-\tau H(\lambda)} . \tag{D13}$$

(b) Even if the correct expression for $\hat{A}(\tau)$ is employed, spurious contributions to $\langle \hat{A}(\tau)\hat{A}^{\dagger}\rangle_1$ may be obtained in perturbation theory if the constraint is not explicitly imposed in intermediate states. This follows again since $\hat{A}$ and Q do not commute.

APPENDIX E: VARIATIONAL DETERMINATION OF THE GROUND-STATE ENERGY OF THE INFINITE-U ANDERSON MODEL TO $O(1/N)$

In this appendix we derive an expression for the ground-state energy of the infinite-U Anderson model [see Eq. (4.1)] to terms of $O(1/N)$ using the variational technique of Sec. IV. The variational state in this case takes the form

$$|\varphi_0^{(1/N)}\rangle = A\left\{|\Omega\rangle + \frac{1}{\sqrt{N}}\sum_{k_1 m}^{\text{occ}}\left[\alpha_1|\varepsilon_f\varepsilon_{k_1}m\rangle + \sum_{k_2}^{\text{unocc}}\left[\beta_{12}|E_{k_2}\varepsilon_{k_1}m\rangle + \frac{1}{\sqrt{N}}\sum_{k_3 m'}^{\text{occ}}\gamma_{123}|(\varepsilon_f\varepsilon_{k_3}m)(E_{k_2}\varepsilon_{k_1}m')\rangle\right]\right]\right\}$$

with

$$|\varepsilon_f\varepsilon_{k_1}m\rangle = f_m^{\dagger}c_{k_1 m}|\Omega\rangle ,$$
$$|E_{k_2}\varepsilon_{k_1}m\rangle = c_{k_2 m}^{\dagger}c_{k_1 m}|\Omega\rangle , \tag{E1}$$
$$|(\varepsilon_f\varepsilon_{k_3}m)(E_{k_2}\varepsilon_{k_1}m')\rangle = f_m^{\dagger}c_{k_3 m}c_{k_2 m'}^{\dagger}c_{k_1 m'}|\Omega\rangle ,$$

where

$$\alpha_1\equiv\alpha_{k_1}$$

and so on. To prevent overcompleteness in the third class of states we restrict $\varepsilon_{k_3}<\varepsilon_{k_1}$ for $m=m'$. The variational equations follow from minimizing

$$\langle\varphi_0^{(1/N)}|H|\varphi_0^{(1/N)}\rangle - E_G(\langle\varphi_0^{(1/N)}|\varphi_0^{(1/N)}\rangle - 1) \tag{E2}$$

and take the form

$$\partial/\partial A^2:\ E_G=\frac{\langle\varphi_0^{(1/N)}|H|\varphi_0^{(1/N)}\rangle}{\langle\varphi_0^{(1/N)}|\varphi_0^{(1/N)}\rangle}\equiv E_0+\Delta E_0\ ,$$

$$\partial/\partial\alpha_1:\ (\varepsilon_f-\varepsilon_{k_1}-E_G)\alpha_1+\sqrt{N}V+V\sum_{k_2}^{\text{unocc}}\beta_{12}=0\ ,$$

$$\partial/\partial\beta_{12}:\ (E_{k_2}-\varepsilon_{k_1}-E_G)\beta_{12}+V\alpha_1+\sqrt{N}V\sum_{k_3}^{\text{occ}}\gamma_{123}=0\ , \tag{E3}$$

$$\partial/\partial\gamma_{123}:\ (\varepsilon_f-\varepsilon_{k_3}+E_{k_2}-\varepsilon_{k_1}-E_G)\gamma_{123}+\sqrt{N}V[\beta_{12}+(1/N)\beta_{32}]=0\ .$$

For convenience we have set $E_G=E_0+\Delta E_0$, with E_0 the ground-state energy to $O(1)$ and ΔE_0 the $O(1/N)$ correction.

To the required order, the β_{32} term in the fourth equation may be ignored; this equation then yields

$$\gamma_{123}=\beta_{12}\frac{\sqrt{N}V}{E_G+\varepsilon_{k_1}-E_{k_2}+\varepsilon_{k_3}-\varepsilon_f}\ . \tag{E4}$$

This simplification in solving for γ_{123} is essential. Otherwise, the next higher equation in the chain is an integral equation. [Integral equations are guaranteed to arise whenever states containing multiple band holes or electrons appear in the variational ground state; to obtain accuracy of $O(1/N^2)$ or higher, these equations must be solved by iteration to the required order in $1/N$.] Continuing backward up the chain of equations, one finds

$$\beta_{12}=\alpha_1\frac{V}{E_G+\varepsilon_{k_1}-E_{k_2}-\Sigma_0^{(1)}(E_G+\varepsilon_{k_1}-E_{k_2})} \tag{E5a}$$

with

$$\Sigma_0^{(1)}(z)=NV^2\sum_k^{\text{occ}}\frac{1}{z-\varepsilon_f+\varepsilon_k}\ , \tag{E5b}$$

as in Sec. II. Finally,

$$\alpha_1=\frac{\sqrt{N}V}{E_G-\varepsilon_f+\varepsilon_{k_1}-\tilde{\Sigma}(E_G+\varepsilon_{k_1})}\ ,$$

$$\tilde{\Sigma}(z)=V^2\sum_k^{\text{unocc}}\frac{1}{z-E_k-\Sigma_0^{(1)}(z-E_k)}\ . \tag{E6}$$

Substituting these results into the first equation in (E1) gives

$$\begin{aligned}E_0+\Delta E_0&=NV^2\sum_k^{\text{occ}}\frac{1}{E_0+\Delta E_0-\varepsilon_f+\varepsilon_k-\tilde{\Sigma}(E_0+\Delta E_0+\varepsilon_k)}\\&=\Sigma_0^{(1)}(E_0+\Delta E_0)+NV^4\sum_{k_1}^{\text{occ}}\frac{1}{(E_0+\Delta E_0-\varepsilon_f+\varepsilon_{k_1})^2}\\&\quad\times\sum_{k_2}^{\text{unocc}}\frac{1}{E_0+\Delta E_0+\varepsilon_{k_1}-E_{k_2}-\Sigma_0^{(1)}(E_0+\Delta E_0+\varepsilon_{k_1}-E_{k_2})}+O(1/N^2)\ .\end{aligned} \tag{E7}$$

In the last step the denominator containing $\tilde{\Sigma}$ has been expanded to $O(1/N)$. To solve for ΔE_0, it is necessary to expand $\Sigma_0^{(1)}(E_0+\Delta E_0)$ to $O(1/N)$:

$$\Sigma_0^{(1)}(E_0+\Delta E_0)=\Sigma_0^{(1)}(E_0)+\frac{\partial\Sigma_0^{(1)}}{\partial E_0}\Delta E_0\ . \tag{E8}$$

Since, from the $O(1)$ solution [Eq. (4.13)],

$$E_0=\Sigma_0^{(1)}(E_0)\ ,$$

it follows that

$$\Delta E_0=\frac{(NV^2)^2}{N}Z(E_0)\sum_{k_1}^{\text{occ}}\sum_{k_2}^{\text{unocc}}\frac{1}{(\varepsilon_{k_1}-T_A)^2}\frac{1}{E_0+\varepsilon_{k_1}-E_{k_2}-\Sigma_0^{(1)}(E_0+\varepsilon_{k_1}-E_{k_2})}\ ,$$

$$Z(E_0)=\left[1-\frac{\partial\Sigma_0^{(1)}}{\partial E_0}\right]^{-1}\ . \tag{E9}$$

This is precisely the result found by the diagrammatic approach in the zero-temperature limit [cf. Eq. (2.43)].

APPENDIX F: VARIATIONAL EQUATIONS FOR THE GROUND-STATE ENERGY AND WAVE FUNCTION OF THE FINITE-U ANDERSON MODEL TO $O(1)$

Sections II–IV treat exclusively the infinite-U limit of the Anderson model. In physical systems, U is finite, and multiply occupied impurity configurations may conceivably be of importance. The finite-U Anderson model is much more difficult to treat by a $1/N$ expansion than the infinite-U model. In general, analytical results cannot be obtained even in the zero-temperature limit. Algebraic equations for the infinite-U model are replaced by integral equations at $O(1)$. The most extensive studies of finite-U systems have been carried out by Gunnarsson and Schönhammer within the variational approach (1985). In this appendix we merely point out the difficulties of the finite-U model by rederiving the equations for the ground-state energy and wave function to $O(1)$.

From Sec. I.B, the finite-U Hamiltonian for a rare-earth impurity takes the form

$$H=H_{\rm band}+H_f+H_{\rm mix},\quad H_{\rm band}=\sum_{km}\varepsilon_k n_{km}\ ,$$

$$H_f=\varepsilon_f\sum_m n_m+U\sum_{m>m'} n_m n_{m'}\ , \tag{F1}$$

$$H_{\rm mix}=V\sum_{km}(c_{km}^\dagger f_m+{\rm H.c.})\ .$$

As in Sec. IV.A, let $|\Omega\rangle$ denote the noninteracting Fermi sea, and define

$$|\varepsilon_f\varepsilon_k m\rangle=f_m^\dagger c_{km}|\Omega\rangle\ . \tag{F2}$$

These are the only states that enter the $O(1)$ ground-state calculation of Sec. IV for the infinite-U limit. In the case of finite U, one additional set of states must be considered at $O(1)$. This is

$$|(\varepsilon_f\varepsilon_k m)(\varepsilon_f\varepsilon_{k'}m')\rangle=f_m^\dagger c_{km}f_{m'}^\dagger c_{k'm'}|\Omega\rangle\ . \tag{F3}$$

To avoid an overcomplete basis we require $\varepsilon_k<\varepsilon_{k'}$ for $m=m'$. The variational ground-state wave function takes the form

$$|\phi_0^{(1)}\rangle=A\left[|\Omega\rangle+\frac{1}{\sqrt{N}}\sum_{km}^{\rm occ}\left[\alpha_k|\varepsilon_f\varepsilon_k m\rangle+\frac{1}{\sqrt{N}}\sum_{k'm'}^{\rm occ}\beta_{kk'}|(\varepsilon_f\varepsilon_k m)(\varepsilon_f\varepsilon_{k'}m')\rangle\right]\right]\ . \tag{F4}$$

The required off-diagonal matrix elements of the Hamiltonian are

$$\begin{aligned}&\langle\varepsilon_f\varepsilon_k m|H_{\rm mix}|\Omega\rangle=V\ ,\\&\langle(\varepsilon_f\varepsilon_k m)(\varepsilon_f\varepsilon_{k'}m')|H_{\rm mix}|\varepsilon_f\varepsilon_{k''}m''\rangle\\&\qquad=V(\delta_{kk''}\delta_{mm''}+\delta_{k'k''}\delta_{m'm''})\ .\end{aligned} \tag{F5}$$

The variational equations are in this case

$$\begin{aligned}&\partial/\partial A^2:\ E_0=\frac{\langle\varphi_0^{(1)}|H|\varphi_0^{(1)}\rangle}{\langle\varphi_0^{(1)}|\varphi_0^{(1)}\rangle}\ ,\\&\partial/\partial\alpha_k:\ (\varepsilon_f-\varepsilon_k-E_0)\alpha_k+\sqrt{N}V+\sqrt{N}V\sum_{k'}\beta_{kk'}=0\ ,\\&\partial/\partial\beta_{kk'}:\ (2\varepsilon_f+U-\varepsilon_k-\varepsilon_{k'}-E_0)\beta_{kk'}\\&\qquad+\sqrt{N}V(\alpha_k+\alpha_{k'})=0\ .\end{aligned} \tag{F6}$$

A complicating feature is the presence of two different coefficients α_k and $\alpha_{k'}$ in the third equation: each two-hole state couples at the same order to two one-hole states. This complication does not arise at $O(1)$ or $O(1/N)$ in the infinite-U treatment. Substituting for $\beta_{kk'}$ in the second equation gives

$$(E_0+\varepsilon_k-\varepsilon_f)\alpha_k-NV^2\sum_{k'}^{\rm occ}\frac{\alpha_k+\alpha_{k'}}{E_0-(2\varepsilon_f+U)+\varepsilon_k+\varepsilon_{k'}}=\sqrt{N}V\ ,$$

i.e.,

$$[E_0+\varepsilon_k-\varepsilon_f-\Sigma_0^{(1)}(E_0-\varepsilon_f-U+\varepsilon_k)]\alpha_k-NV^2\sum_{k'}^{\rm occ}\frac{\alpha_{k'}}{E_0-(2\varepsilon_f+U)+\varepsilon_k+\varepsilon_{k'}}=\sqrt{N}V\ , \tag{F7a}$$

with

$$\Sigma_0^{(1)}(z)=NV^2\sum_k^{\rm occ}\frac{1}{z+\varepsilon_k-\varepsilon_f}\ . \tag{F7b}$$

This is an integral equation for the coefficient α_k. (For $U\to\infty$, the two expressions containing U vanish, and α_k is determined by an algebraic equation.) Substituting the expressions for the coefficients α_k and $\beta_{kk'}$ in the first of Eqs. (F6) gives

$$E_0=\sqrt{N}V\sum_k\alpha_k,\quad \alpha_k=\alpha_k(E_0)\ . \tag{F8}$$

For $U\to\infty$, Eq. (F8) becomes a simple transcendental equation for the ground-state energy E_0. The equation for finite U is considerably more complex; E_0 again satisfies a transcendental equation,

$$E_0=F(E_0)\ . \tag{F9}$$

In this case, however, the function F can only be determined by solving an integral equation.

Gunnarsson and Schönhammer (1986) have shown that the function F may be determined analytically in the limit $U\gg D$; they have obtained closed-form results for the static susceptibility and the f^0 and f^2 occupancies in this limit. Results obtained in this way should be viewed as the lowest-order terms in a joint expansion in $1/N$ and D/U. For a discussion of these results and extensive numerical results for the finite-U f spectral density, the reader should consult the original treatment by Gunnarsson and Schönhammer (1985) and the review article by the same authors (1986).

APPENDIX G: THERMODYNAMICALLY SELF-CONSISTENT APPROXIMATIONS FOR THE INFINITE-U ANDERSON MODEL

1. Hierarchy of self-consistent solutions

An important criterion for approximate solutions of many-body models is that they be internally consistent. A self-consistency criterion for solutions of the interacting electron gas (Φ-derivability) was established long ago by

Baym (1962). One of the properties of a Φ-derivable approximation is the consistency of alternate representations of the partition function. For example, one possible representation is obtained by integrating the particle number with respect to the chemical potential; an alternate representation is obtained by performing a coupling-constant integration of $\mathrm{Tr}\hat{\Sigma}\hat{G}$, where $\hat{\Sigma}$ and $\hat{G}$ are the self-energy and propagator matrices. These two representations are equivalent if the exact self-energy and propagator are employed; if arbitrary approximations are introduced, the representations may differ.

The analogs of these representations for the infinite-U Anderson model are the following:

$$Z_f \equiv Z/Z_{\text{band}} = \int_\Gamma \frac{dz}{2\pi i} e^{-\beta z} \mathrm{Tr}_f \frac{1}{z - H_f - \hat{\Sigma}_f(z)} \tag{G1a}$$

and

$$Z_f = 1 + N e^{-\beta\varepsilon_f} - \beta \int_0^1 \frac{dg}{g} \int_\Gamma \frac{dz}{2\pi i} e^{-\beta z} \mathrm{Tr}_f \frac{\hat{\Sigma}_f(z,g)}{z - H_f - \hat{\Sigma}_f(z,g)} , \tag{G1b}$$

with $\hat{\Sigma}_f$ as in Eq. (2.15). As in the electron-gas problem, these representations may differ if arbitrary approximations are introduced for the self-energy matrix $\hat{\Sigma}_f$. It is easy to state one criterion that guarantees that the representations are the same: the self-energies Σ_0 and Σ_m (the matrix elements of $\hat{\Sigma}_f$) must be such that the approximation includes only complete *families* of diagrams (Grewe, 1983), i.e., sets of diagrams related by a cyclic permutation of vertices.

It may require some work to determine whether a specific choice of self-energies sums complete families. Kuramoto (1983) has derived an infinite hierarchy of approximations that satisfy this criterion and has explicitly constructed for them a generating function Φ (analogous to the generating function in the electron-gas problem). The generating function, once constructed, may be used to show that all approximate representations of the partition function derived by integrating thermodynamic derivatives (for example, temperature or field derivatives) are equivalent. We sketch Kuramoto's approach below.

The hierarchy of consistent approximations may be generated from *skeleton diagrams*. A self-energy is said to be *reducible* if it may be generated from a lower-order diagram by adding a self-energy insertion on an occupied or empty f line; skeleton diagrams are those which may not be reduced in this way. A consistent approximation may be obtained by writing down *all* skeleton diagrams up to a specified order in the hybridization V, then dressing the internal lines in these diagrams with all allowed self-energy insertions. (It may be seen that diagrams produced in this way constitute complete families by writing down an arbitrary diagram, then rotating the vertices once. The important point is that the number of crossing band lines is conserved by such rotations.) The lowest-order skeleton diagram approximation is just the self-consistent expansion of Sec. V. Since all the diagrams included in this approximation may be drawn with non-crossing conduction lines, this has been termed the "non-crossing approximation," or NCA.

Derivation of Φ. Consider representation (G1b). The nth-order skeleton diagram contribution to the self-energy matrix with bare internal lines takes the form

$$g^n \hat{\Sigma}_f^{(n)}(\hat{G}_f^0(z),z) \tag{G2}$$

with

$$\langle 0 | \hat{G}_f^0(z) | 0 \rangle = \frac{1}{z} , \qquad \langle m | \hat{G}_f^0(z) | m \rangle = \frac{1}{z - \varepsilon_f} . \tag{G3}$$

Thus a dressed skeleton diagram contribution to $\hat{\Sigma}_f$ becomes

$$g^n \hat{\Sigma}_f^{(n)}(\hat{G}_f(z,g),z) ,$$

with

$$\langle 0 | \hat{G}_f(z,g) | 0 \rangle = \frac{1}{z - \Sigma_0(z,g)} , \qquad \langle m | \hat{G}_f(z,g) | m \rangle = \frac{1}{z - \varepsilon_f - \Sigma_m(z,g)} . \tag{G4}$$

Σ_0 and Σ_m are the full self-energies in the approximation considered. Summing on the skeleton diagrams included in an Lth-order approximation gives

$$\hat{\Sigma}_f(z,g) = \sum_{n=2}^{L} g^n \hat{\Sigma}_f^{(n)}(\hat{G}_f,z) . \tag{G5}$$

The expression

$$\int_0^1 \frac{dg}{g} g^n \mathrm{Tr}_f \hat{\Sigma}_f^{(n)}(\hat{G}_f,z)\hat{G}_f(z,g) \tag{G6a}$$

may be integrated by parts to give

$$\frac{1}{n}\mathrm{Tr}_f \hat{\Sigma}_f^{(n)}(\hat{G}_f,z)\hat{G}_f - \frac{1}{n}\int_0^1 dg\, g^n \mathrm{Tr}_f \frac{\partial}{\partial g}[\hat{\Sigma}_f^{(n)}(\hat{G}_f(z,g),z)\hat{G}_f] . \tag{G6b}$$

The matrix $\hat{\Sigma}_f^{(n)}\hat{G}_f$ is dependent on the coupling constant through its explicit dependence on $\hat{G}_f$ and through the implicit dependence on $\hat{\Sigma}_f^{(n)}$ on $\hat{G}_f$. The self-energy $\hat{\Sigma}_f^{(n)}$ contains the dressed propagator exactly $n-1$ times. Since the skeleton approximation includes complete families of diagrams, the factors of $\partial\hat{G}_f/\partial g$ from each differentiation may be brought to the end of the trace (using cyclic invariance). Thus

$$\mathrm{Tr}_f \frac{\partial}{\partial g}(\hat{\Sigma}_f^{(n)}\hat{G}_f) = n\,\mathrm{Tr}_f\left[\hat{\Sigma}_f^{(n)}\frac{\partial\hat{G}_f}{\partial g}\right] . \tag{G7}$$

Note finally that

$$\hat{\Sigma}_f = z - H_f - \hat{G}_f^{-1} , \tag{G8a}$$

so

$$\int_0^1 dg\,\mathrm{Tr}_f\left[\hat{\Sigma}_f\frac{\partial}{\partial g}\hat{G}_f\right]=(z-H_f)[\hat{G}_f(z)-(z-H_f)^{-1}]-\ln(z-H_f)\hat{G}_f(z)=\hat{\Sigma}_f(z)\hat{G}_f(z)-\ln(z-H_f)\hat{G}_f(z)\ . \tag{G8b}$$

Thus the representation in (G1b) is equivalent to

$$Z_f=1+Ne^{-\beta\varepsilon_f}-\beta\Phi\{\hat{G}_f\}+\beta\int_\Gamma\frac{dz}{2\pi i}e^{-\beta z}\mathrm{Tr}_f[\hat{\Sigma}_f(z)\hat{G}_f(z)-\ln(z-H_f)\hat{G}_f(z)]\ , \tag{G9a}$$

with

$$\Phi=\sum_{n=2}^{L}\frac{1}{n}\int_\Gamma\frac{dz}{2\pi i}e^{-\beta z}\mathrm{Tr}_f\hat{\Sigma}_f^{(n)}(\hat{G}_f,z)\hat{G}_f(z)\ . \tag{G9b}$$

It is now easy to show that Φ is indeed a generating function, i.e., that the self-energy matrix may be generated as the functional derivative of Φ with respect to the propagator matrix. To carry out the functional differentiation, suppose $\hat{G}_f$ depends on some (artificial) parameter α. Then

$$\frac{\partial\Phi}{\partial\alpha}\equiv\int_\Gamma dz\,\mathrm{Tr}_f\frac{\delta\Phi}{\delta\hat{G}_f}(z)\frac{\partial\hat{G}_f}{\partial\alpha}=\sum_{n=2}^{L}\frac{1}{n}\int_\Gamma\frac{dz}{2\pi i}e^{-\beta z}\frac{\partial}{\partial\alpha}\mathrm{Tr}_f\hat{\Sigma}_f^{(n)}\hat{G}_f=\sum_{n=2}^{L}\frac{1}{n}\int_\Gamma\frac{dz}{2\pi i}e^{-\beta z}n\,\mathrm{Tr}_f\hat{\Sigma}_f^{(n)}\frac{\partial\hat{G}_f}{\partial\alpha}\ , \tag{G10}$$

since the approximation contains only complete diagrammatic families. Thus

$$\frac{\delta\Phi}{\delta\hat{G}_f}(z)=\frac{e^{-\beta z}}{2\pi i}\hat{\Sigma}_f(z)\ . \tag{G11}$$

This is the analog Baym's generating-function relation for the electron gas.

2. Use of the generating function

To illustrate how the generating function Φ may be employed to prove two representations of Z_f equivalent, we rederive Eq. (G1a) from (G1b). First, the mean occupancies

$$n_0\equiv Z^{-1}\mathrm{Tr}e^{-\beta H}|0\rangle\langle 0|\quad\text{and}\quad n_m\equiv Z^{-1}\mathrm{Tr}e^{-\beta H}|m\rangle\langle m|$$

may be derived directly from (G1b) by attaching a chemical potential to the empty and occupied f states:

$$H_f=\varepsilon_f|m\rangle\langle m|\to\sum_m(\varepsilon_f-\mu_m)|m\rangle\langle m|-\mu_0|0\rangle\langle 0|\ . \tag{G12}$$

For example, the empty-state occupancy is just

$$n_0=\frac{\partial}{\partial(\beta\mu_0)}\ln Z_f|_{\mu_0=0}$$

$$=\frac{1}{Z_f(\mu_0)}\frac{\partial}{\partial(\beta\mu_0)}\left[e^{\beta\mu_0}-\beta\Phi(\mu_0)+\beta\int_\Gamma\frac{dz}{2\pi i}e^{-\beta z}\mathrm{Tr}_f[\hat{\Sigma}_f(\mu_0)\hat{G}_f(\mu_0)-\ln[z-H_f(\mu_0)]\hat{G}_f(\mu_0)]\right]\Bigg|_{\mu_0=0}\ , \tag{G13}$$

where

$$\langle 0|\hat{G}_f(\mu_0)|0\rangle=\frac{1}{z+\mu_0-\Sigma_0(z+\mu_0)},\quad\langle m|\hat{G}_f(\mu_0)|m\rangle=\frac{1}{z-\varepsilon_f-\Sigma_m(z)}\ . \tag{G14}$$

Using again the fact that complete diagrammatic families are present,

$$\frac{\partial}{\partial(\beta\mu_0)}\mathrm{Tr}_f\hat{\Sigma}_f^{(n)}\hat{G}_f=n\,\mathrm{Tr}_f\hat{\Sigma}_f^{(n)}\frac{\partial\hat{G}_f}{\partial(\beta\mu_0)} \tag{G15a}$$

and

$$\frac{\partial(-\beta\Phi)}{\partial(\beta\mu_0)}=-\int_\Gamma\frac{dz}{2\pi i}e^{-\beta z}\mathrm{Tr}_f\hat{\Sigma}_f\frac{\partial}{\partial(\beta\mu_0)}\hat{G}_f\ . \tag{G15b}$$

Also note that

$$\frac{\partial}{\partial(\beta\mu_0)}\mathrm{Tr}_f[\hat{\Sigma}_f\hat{G}_f-\ln(z-H_f)\hat{G}_f]=-\frac{1}{\beta(z+\mu_0)}+\frac{\partial\Sigma_0}{\partial(\beta\mu_0)}G_0+\Sigma_0\frac{\partial G_0}{\partial(\beta\mu_0)}+G_0\left[\frac{1}{\beta}-\frac{\partial\Sigma_0}{\partial(\beta\mu_0)}\right]\ . \tag{G15c}$$

Combining terms gives finally

$$n_0=Z_f^{-1}(\mu_0)\int_\Gamma \frac{dz}{2\pi i}\frac{e^{-\beta z}}{z+\mu_0-\Sigma_0(z+\mu_0)}\bigg|_{\mu_0=0}=Z_f^{-1}\int_\Gamma \frac{dz}{2\pi i}\frac{1}{z-\Sigma_0(z)}\ . \tag{G16}$$

The equation

$$\frac{\partial}{\partial(\beta\mu_0)}\ln Z_f(\mu_0)=Z_f^{-1}(\mu_0)e^{\beta\mu_0}\int_\Gamma \frac{dz}{2\pi i}\frac{e^{-\beta z}}{z-\Sigma_0(z)} \tag{G17}$$

may now be integrated with respect to $\beta\mu_0$ to recover the empty-state contribution to the partition function; the value of the μ_m derivative is also required to determine Z_f fully. Thus

$$Z_f=\int_\Gamma \frac{dz}{2\pi i}\frac{e^{-\beta z}}{z-\Sigma_0(z)}+A(T)\ . \tag{G18}$$

The undetermined function $A(T)$ is the part of the partition function independent of μ_0, i.e., the occupied-state contribution.

As a second illustration of the power of the generating function we demonstrate that the expression for the static susceptibility derived in Eq. (5.8) using the magnetization correlation function is the same as the expression that follows from differentiating the partition function with respect to the field. The static magnetization is just

$$M(h)=\frac{\partial \ln Z_f(h)}{\partial(\beta h)}=\frac{1}{Z_f(h)}\frac{\partial}{\partial(\beta h)}Z_f(h)\ ,$$

where

$$Z_f(h)=1+\sum_m e^{-\beta(\varepsilon_f-mg\mu_B h)}-\beta\Phi+\beta\int_\Gamma \frac{dz}{2\pi i}e^{-\beta z}\mathrm{Tr}_f[\hat{\Sigma}_f\hat{G}_f-\ln(z-H_f(h))\hat{G}_f]\ . \tag{G19}$$

Note first that

$$\frac{\partial}{\partial(\beta h)}(-\beta\Phi)=-\int_\Gamma \frac{dz}{2\pi i}e^{-\beta z}\mathrm{Tr}_f\hat{\Sigma}_f\frac{\partial}{\partial h}\hat{G}_f\ , \tag{G20}$$

by the same arguments used in deducing Eq. (G15). In addition,

$$\frac{\partial}{\partial(\beta h)}\beta\int_\Gamma \frac{dz}{2\pi i}e^{-\beta z}\mathrm{Tr}_f[\hat{\Sigma}_f\hat{G}_f-\ln(z-H_f(h))\hat{G}_f]=-g\mu_B\sum_m m e^{-\beta(\varepsilon_f-mg\mu_B h)}$$
$$+\int_\Gamma \frac{dz}{2\pi i}e^{-\beta z}\left[\mathrm{Tr}_f\left[\Sigma_f\frac{\partial}{\partial h}\hat{G}_f\right]+g\mu_B\sum_m mG_m(z)\right]\ . \tag{G21}$$

Thus

$$M(h)=\frac{1}{Z_f(h)}g\mu_B\sum_m m\int_\Gamma \frac{dz}{2\pi i}e^{-\beta z}G_m(z)$$

and (G22)

$$\chi(0)=-\frac{\partial^2 F}{\partial h^2}\bigg|_{h=0}$$
$$=\frac{1}{Z_f}g\mu_B\sum_m m\int_\Gamma \frac{dz}{2\pi i}e^{-\beta z}\frac{\partial}{\partial h}G_m(z)\bigg|_{h=0}\ .$$

This equation states that within any self-consistent approximation (and within the NCA, in particular), the static susceptibility is simply obtained by writing down all diagrams for G_m, then breaking a single line by differentiating with respect to h. The NCA expression obtained in this way is exactly that in Eq. (5.8).

The sense in which the skeleton diagram summations discussed above are self-consistent deserves some additional comment. By integrating various *static* thermodynamic derivatives, it is possible to produce a number of equivalent representations of the exact partition function. Φ-derivability ensures that these representations remain equivalent when approximate self-energies are introduced. Kuramoto (1983) has considered a generalization of the infinite-U Anderson model, which includes the interaction of the f level with *time-dependent,* Gaussian-distributed auxiliary fields. If the auxiliary fields are treated perturbatively in parallel with the hybridization, a generalized skeleton diagram expansion may be written down, and a generating function Φ constructed as before (the number of distinct interaction vertices is simply increased). Imaginary-time (or frequency) f-level correlation functions may be generated by differentiating the logarithm of the generalized partition function with respect to a set of auxiliary fields, then setting all auxiliary field interactions to zero. This procedure is a techni-

cally elegant means to generate time-dependent correlation functions. However, the generalized function Φ contains artificial interactions and has no implications for the self-consistency of dynamic and static properties beyond the implications of the function constructed in Eq. (G9b) without time-dependent field vertices.

In particular, a number of exact theorems relate static and dynamic properties of the infinite-U Anderson model. The criterion of Φ-derivability does not ensure that a specified approximation satisfies these rules. For example, one such sum rule states that

$$\int_{-\infty}^{\infty} d\varepsilon f(\varepsilon)\rho_f(\varepsilon)=\frac{1}{N}n_f \ , \tag{G23}$$

with ρ_f the f Green's function and n_f the f valence. The NCA *does* in fact satisfy this relation, but the proof does not follow from Φ-derivability (see Appendix H). Furthermore, thermodynamically consistent approximations need *not* satisfy Fermi-liquid relations for the Anderson model, such as the Friedel-Langreth (Friedel, 1952; Langreth, 1966) and Shiba (1975) relations of Sec. V.B.

We reserve the name "sum rule" for global (i.e., integrated) frequency relations, based on the properties of equal-time correlation functions, and the name "Fermi-liquid relation" for identities connecting thermodynamic derivatives or zero-frequency correlation functions and thermodynamic derivatives. As shown in Appendix H, the lowest-order self-consistent approximation, the NCA, satisfies all pertinent sum rules. Nevertheless, it violates a number of Fermi-liquid relations (see Sec. V.B).

APPENDIX H: SUM RULES FOR THE INFINITE-U ANDERSON MODEL

In this appendix we derive several exact sum rules for the infinite-U Anderson model and demonstrate that these rules are satisfied within the self-consistent approximation (the noncrossing approximation) of Sec. V.

1. Sum rules from analyticity

Recall from Eq. (2.18) that the Anderson model partition function may be written

$$\begin{aligned} Z/Z_{\rm band} &= \int_\Gamma \frac{dz}{2\pi i} e^{-\beta z}\mathrm{Tr}_f \frac{1}{z-H_f-\hat{\Sigma}_f(z)} \\ &= \int_\Gamma \frac{dz}{2\pi i}\frac{e^{-\beta z}}{z-\Sigma_0(z)} \\ &\quad + N\int_\Gamma \frac{dz}{2\pi i}\frac{e^{-\beta z}}{z-\varepsilon_f-\Sigma_m(z)} \ , \end{aligned} \tag{H1}$$

where the contour Γ encircles the real axis in a counterclockwise fashion. The "propagators" $(z-\Sigma_0)^{-1}$ and $(z-\varepsilon_f-\Sigma_m)^{-1}$ are analytic in the upper and lower half-planes and decay at infinity as $1/z$, independent of the detailed form of Σ_0 and Σ_m. Distorting the contour Γ into a circle at infinity gives immediately

$$\int_\Gamma \frac{dz}{2\pi i}\frac{1}{z-\Sigma_0(z)}=\int_{-\infty}^{\infty} d\varepsilon\rho_0(\varepsilon)=1$$

with

$$\rho_0(\varepsilon)=-\frac{1}{\pi}\mathrm{Im}\frac{1}{\varepsilon+i0^+-\Sigma_0(\varepsilon+i0^+)} \ ; \tag{H2a}$$

and

$$\int_\Gamma \frac{dz}{2\pi i}\frac{1}{z-\varepsilon_f-\Sigma_m(z)}=\int_{-\infty}^{\infty} d\varepsilon\rho_m(\varepsilon)=1$$

with

$$\rho_m(\varepsilon)=-\frac{1}{\pi}\mathrm{Im}\frac{1}{\varepsilon+i0^+-\varepsilon_f-\Sigma_m(\varepsilon+i0^+)} \ . \tag{H2b}$$

2. Sum rules from equal-time correlation functions

$G_f(\tau)$: Recall that the correlation function

$$G_f(\tau)\equiv-\langle T_\tau F_m(\tau)F_m^\dagger(0)\rangle, \quad F_m=|0\rangle\langle m| \ , \tag{H3a}$$

has the frequency decomposition

$$\begin{aligned} G_f(\tau) &= \frac{1}{\beta}\sum_n e^{-i\omega_n\tau}\int_\Gamma \frac{dz}{2\pi i}\frac{G_f(z)}{i\omega_n-z} \\ &= \int_{-\infty}^{\infty} d\varepsilon\rho_f(\varepsilon)\frac{1}{\beta}\sum_n \frac{e^{-i\omega_n\tau}}{i\omega_n-\varepsilon} \ , \\ \rho_f(\varepsilon) &= -\frac{1}{\pi}G_f(\varepsilon+i0^+) \ . \end{aligned} \tag{H3b}$$

From the definition,

$$\begin{aligned} G_f(\tau\to 0^+) &= -\langle F_m F_m^\dagger\rangle \\ &= -\langle(|0\rangle\langle m|\cdot|m\rangle\langle 0|)\rangle \\ &= -[1-n_f(T)] \ ; \end{aligned} \tag{H4}$$

likewise,

$$G_f(\tau\to 0^-)=\langle F_m^\dagger F_m\rangle=\frac{1}{N}n_f(T) \ . \tag{H5}$$

Since

$$\sum_n \frac{e^{-i\omega_n 0^\pm}}{i\omega_n-\varepsilon}=\frac{\mp 1}{e^{\mp\beta\varepsilon}+1} \ , \tag{H6}$$

it follows that

$$\int_{-\infty}^{\infty} d\varepsilon\rho_f(\varepsilon)[1-f(\varepsilon)]=1-n_f(T) \ , \tag{H7a}$$

$$\int_{-\infty}^{\infty} d\varepsilon\rho_f(\varepsilon)f(\varepsilon)=\frac{1}{N}n_f(T) \ , \tag{H7b}$$

and

$$\int_{-\infty}^{\infty} d\varepsilon\rho_f(\varepsilon)=1-\left[1-\frac{1}{N}\right]n_f(T) \ . \tag{H7c}$$

$\hat{\Sigma}_f(\tau)$: Recall from Eq. (2.16) the expression for the z-dependent f self-energy matrix:

$$\langle N_f \mid \hat{\Sigma}_f(z) \mid N_f \rangle = \sum_{N_{\rm band}} \frac{e^{-\beta E_N^{\rm band}}}{Z_{\rm band}} \langle N_f N_{\rm band} \mid \hat{\Sigma}(z+E_N^{\rm band}) \mid N_f N_{\rm band} \rangle ,$$

where

$$\langle N \mid \hat{\Sigma}(z) \mid N \rangle = \langle N \mid H_{\rm mix}[1-(z-H_0)^{-1}Q_N H_{\rm mix}]^{-1} \mid N \rangle , \tag{H8}$$

$Q_N = 1-P_N$, $P_N = \mid N \rangle\langle N \mid$.

It is easy to check (Kojima *et al.*, 1984) that $\langle N \mid \hat{\Sigma}(z) \mid N \rangle$ is the Laplace transform of the quantity

$$\langle N \mid \hat{\Sigma}(\tau) \mid N \rangle = \langle N \mid H_{\rm mix} e^{-\tau Q_N H} Q_N H_{\rm mix} \mid N \rangle ,$$

i.e.,

$$\langle N \mid \hat{\Sigma}(z) \mid N \rangle = -\int_0^\infty d\tau e^{\tau z} \langle N \mid \hat{\Sigma}(\tau) \mid N \rangle , \tag{H9}$$

for $\mathrm{Re}\, z < \mathscr{E}_0$, the ground-state energy of H.

Proof. Note that

$$\langle N \mid \hat{\Sigma}(\tau) \mid N \rangle = \int_\Gamma \frac{dz'}{2\pi i} e^{-\tau z'} \left\langle N \left| H_{\rm mix} \frac{1}{z'-Q_N H} Q_N H_{\rm mix} \right| N \right\rangle , \tag{H10}$$

where Γ encircles the singularities of $(z'-Q_N H)^{-1}$ in a counterclockwise fashion. Now, performing the τ integration in Eq. (H9) gives

$$\begin{aligned} -\int_0^\infty d\tau e^{\tau z} \langle N \mid \hat{\Sigma}(\tau) \mid N \rangle &= \int_\Gamma \frac{dz'}{2\pi i} \frac{1}{z-z'} \left\langle N \left| H_{\rm mix} \frac{1}{z'-Q_N H} Q_N H_{\rm mix} \right| N \right\rangle \\ &= \left\langle N \left| H_{\rm mix} \frac{1}{z-Q_N H} Q_N H_{\rm mix} \right| N \right\rangle \\ &= \langle N \mid H_{\rm mix}[1-(z-H_0)^{-1}Q_N H_{\rm mix}]^{-1}(z-H_0)^{-1}Q_N H_{\rm mix} \mid N \rangle = \langle N \mid \hat{\Sigma}(z) \mid N \rangle . \end{aligned} \tag{H11}$$

It follows that the matrix $\hat{\Sigma}(\tau)$ is the inverse Laplace transform of $\hat{\Sigma}(z)$, i.e.,

$$\hat{\Sigma}(\tau) = -\int_{a-i\infty}^{a+i\infty} \frac{dz}{2\pi i} e^{iz\tau} \hat{\Sigma}(z) , \tag{H12}$$

with a less than the ground-state energy.

The matrix $\hat{\Sigma}(\tau)$ has a trivial $\tau \to 0$ limit:

$$\langle N \mid \hat{\Sigma}(\tau \to 0) \mid N \rangle = \langle N \mid H_{\rm mix}^2 \mid N \rangle . \tag{H13}$$

Distorting the contour in Eq. (H12) to encircle the singularities of $(z-H)^{-1}$ in a counterclockwise fashion gives immediately

$$\int_\Gamma \frac{dz}{2\pi i} \langle N \mid \hat{\Sigma}(z) \mid N \rangle = \langle N \mid H_{\rm mix}^2 \mid N \rangle . \tag{H14}$$

Thus, from Eq. (H8),

$$\begin{aligned} \int_\Gamma \frac{dz}{2\pi i} \hat{\Sigma}_f(z) &= \sum_{N_{\rm band}} \frac{e^{-\beta E_N^{\rm band}}}{Z_{\rm band}} \langle N_{\rm band} \mid H_{\rm mix}^2 \mid N_{\rm band} \rangle \\ &= NV^2 \sum_k f_k \mid 0 \rangle\langle 0 \mid + V^2 \sum_{km} (1-f_k) \mid m \rangle\langle m \mid , \end{aligned}$$

i.e.,

$$-\frac{1}{\pi} \int_{-\infty}^{\infty} d\omega\, \mathrm{Im}\Sigma_0(\omega+i0^+) = NV^2 \sum_k f_k \tag{H15a}$$

and

$$-\frac{1}{\pi} \int_{-\infty}^{\infty} d\omega\, \mathrm{Im}\Sigma_m(\omega+i0^+) = V^2 \sum_k (1-f_k) . \tag{H15b}$$

3. Sum rules within the noncrossing approximation

The sum rules (H2a) and (H2b) are trivially satisfied within the noncrossing approximation. The sum rules (H7a)–(H7c) and (H15a) and (H15b) are also satisfied.

Proof. The NCA expression for the f spectral density is

$$\begin{aligned} \rho_f^{\rm NCA}(\omega) &= \frac{1}{Z^{\rm NCA}}(1+e^{-\beta\omega}) \times \int_{-\infty}^{\infty} d\varepsilon\, e^{-\beta\varepsilon} \rho_0^{\rm NCA}(\varepsilon) \rho_m^{\rm NCA}(\omega+\varepsilon) , \\ Z^{\rm NCA} &= \int_{-\infty}^{\infty} d\varepsilon [\rho_0^{\rm NCA}(\varepsilon) + N\rho_m^{\rm NCA}(\varepsilon)] . \end{aligned} \tag{H16}$$

Thus

$$\begin{aligned} \int_{-\infty}^{\infty} d\omega\, \rho_f^{\rm NCA}(\omega)[1-f(\omega)] &= \frac{1}{Z^{\rm NCA}} \int_{-\infty}^{\infty} d\omega \int_{-\infty}^{\infty} d\varepsilon\, e^{-\beta\varepsilon} \rho_0^{\rm NCA}(\varepsilon) \rho_m^{\rm NCA}(\omega+\varepsilon) \\ &= \frac{1}{Z^{\rm NCA}} \int_{-\infty}^{\infty} d\varepsilon\, e^{-\beta\varepsilon} \rho_0^{\rm NCA}(\varepsilon) = 1-n_f(T) , \end{aligned} \tag{H17}$$

by Eq. (H2b). Sum rules (H7b) and (H7c) follow in similar fashion.

The sum rules for the NCA self-energies (H15a) and (H15b) are also easy to verify. Substituting the explicit form for the empty-state self-energy from Eq. (5.2) gives

$$\begin{aligned} \int_\Gamma \frac{dz}{2\pi i} \Sigma_0^{\rm NCA}(z) &= \int_\Gamma \frac{dz}{2\pi i} NV^2 \sum_k f_k G_m^{\rm NCA}(z+\varepsilon_k) \\ &= NV^2 \sum_k f_k , \end{aligned} \tag{H18a}$$

by Eq. (H2b). Likewise,

$$\int_\Gamma \frac{dz}{2\pi i}\Sigma_m^{\rm NCA}(z)=V^2\sum_k(1-f_k)\ . \tag{H18b}$$

APPENDIX I: ANALYSIS OF TOY MODELS AT ZERO AND FINITE TEMPERATURES

In this appendix the large-N expansion for two trivial ionic models is investigated using functional integral techniques. The models are formally the Coqblin-Schrieffer and infinite-U Anderson models in the absence of conduction-band mixing. This analysis illustrates several features of the interacting models (Sec. VI.B) in a simpler context. Exact results may be obtained using a saddle-point approximation at zero temperature; the saddle-point approximation deteriorates at finite temperature, giving in some cases a continuous phase transition analogous to that found in treatments of the full models. For the toy models the violation of occupancy constraints at finite temperature may be calculated explicitly.

The ionic models are

$$\begin{aligned}&\text{(i)}\ \ H=\varepsilon_f\sum\hat N_m,\ \ \sum_m\hat N_m=1\\ &\text{(ii)}\ \ H=\varepsilon_f\sum_m\hat N_m+\varepsilon_0\hat N_0,\ \ \hat N_0+\sum_m\hat N_m=1,\ \ \varepsilon_0=0\ .\end{aligned} \tag{I1}$$

$\hat N_0$ and $\hat N_m$ are number operators for the nondegenerate state $|0\rangle$ and the N-fold degenerate states $|m\rangle$; the statistics of these states need not be specified, since the constraints strictly prevent multiple occupancy. Model (i) is just the Coqblin-Schrieffer model with $J=0$; similarly, model (ii) is the infinite-U Anderson model with $V=0$. In the treatments below we consider a generalized version of these models, with occupancy constraints

$$\begin{aligned}&\text{(i)}\ \ \sum_m\hat N_m=qN\ ,\\ &\text{(ii)}\ \ \hat N_0+\sum_m\hat N_m=qN\ ,\end{aligned} \tag{I2}$$

with q rational and qN integral. For example, for $q=\frac{1}{6}$, the allowed values of N are integral multiples of 6. The large-N limit is in this case a thermodynamic limit (the fractional occupancy q is an intensive quantity). Large-N perturbation theory takes the form of a loop expansion. Even in the "physical limit" $q=1/N$, such an expansion is expected to retain some validity. The finite-temperature behavior of the toy-model loop expansions indicates the way in which similar expansions for the full alloy models break down with increasing T. Note that the statistics of the levels $|0\rangle$ and $|m\rangle$ become important when multiple occupancy is allowed.

1. Toy model (i)

We consider first the constrained Hamiltonian

$$H=\varepsilon_f\sum_m\hat N_m,\ \ \sum_m\hat N_m\equiv\hat Q=qN\ , \tag{I3}$$

with $|m\rangle$ a set of N degenerate levels obeying Fermi statistics. This system has partition function

$$Z=P(q,N)e^{-\beta\varepsilon_f(qN)} \tag{I4a}$$

and entropy

$$S=\ln P(q,N)\ ,$$

with

$$P(q,N)=\frac{N!}{(qN)![(1-q)N]!}\ . \tag{I4b}$$

Note that for $qN=1$, $P(q,N)=N$.

Alternatively, the partition function may be reexpressed exactly as a Fermi functional integral:

$$Z=\int_{-\pi T}^{\pi t}\frac{\beta d\lambda}{2\pi}{\rm Tr}e^{-\beta H(\lambda)}$$

with

$$H(\lambda)=\varepsilon_f\hat Q+i\lambda(\hat Q-qN)\ , \tag{I5a}$$

i.e.,

$$\begin{aligned}&Z=\int_{-\pi T}^{\pi T}\frac{\beta d\lambda}{2\pi}e^{i\beta\lambda(qN)}\int_f e^{-S}\ ,\\ &S=\sum_m\bar f_m(\tau)\left[\frac{\partial}{\partial\tau}+\varepsilon_f+i\lambda\right]f_m(\tau)\ .\end{aligned} \tag{I5b}$$

Here $f_m(\tau)$ and $\bar f_m(\tau)$ are sets of anticommuting (Grassmann) variables. Transforming to a frequency-space representation and dividing through by the partition function Z_0 for a set of N zero-energy fermions gives

$$\frac{Z}{Z_0}=\int_{-\pi T}^{\pi T}\frac{\beta d\lambda}{2\pi}e^{i\beta\lambda(qN)}\times\exp\left[N\sum_n e^{i\omega_n 0^+}\ln\left[\frac{i\omega_n-\varepsilon_f-i\lambda}{i\omega_n}\right]\right]\ . \tag{I6}$$

The frequency sum and constraint integral may be evaluated exactly, reproducing Eq. (I4). Alternatively, the constraint integral may be evaluated by a saddle-point approximation. To accomplish this it is necessary to shift the integration path into the complex plane. The shift

$$\lambda\to\lambda+i\varepsilon_{\rm MF} \tag{I7}$$

does not alter the value of the integral. This is simplest to see in the representation of Eq. (I5a), where λ multiplies $\hat Q-qN$. Thus separating (I6) into mean-field and fluctuation contributions gives

$$\begin{aligned}&Z=Z_{\rm MF}Z_{\rm fluct},\ \ Z_{\rm MF}=e^{-\beta F_{\rm MF}}\ ,\\ &F_{\rm MF}=\varepsilon_{\rm MF}(qN)-NT\ln(1+e^{\beta(\varepsilon_{\rm MF}-\varepsilon_f)})\ ,\\ &Z_{\rm fluct}=\int_{-\pi T}^{\pi T}\frac{\beta d\lambda}{2\pi}e^{-\beta F_{\rm fluct}}\ ,\\ &F_{\rm fluct}=-i\lambda(qN)-NT\sum_n\ln\left[1-\frac{i\lambda}{i\omega_n+\varepsilon_{\rm MF}-\varepsilon_f}\right]\ .\end{aligned} \tag{I8}$$

The mean-field, or saddle-point, condition is

$$\frac{\partial F_{\rm MF}}{\partial \varepsilon_{\rm MF}}=0\ ,$$

i.e.,

$$f(\varepsilon_f-\varepsilon_{\rm MF})=\frac{1}{e^{\beta(\varepsilon_f-\varepsilon_{\rm MF})}+1}=q\ . \tag{I9}$$

Thus

$$\begin{aligned}&\varepsilon_{\rm MF}=\varepsilon_f-T\ln(q^{-1}-1)\ ,\\ &Z_{\rm MF}=\frac{e^{-\beta\varepsilon_f(qN)}}{q^{qN}(1-q)^{(1-q)N}}\ .\end{aligned} \tag{I10}$$

This is precisely the approximation for Z that follows from the asymptotic expansion of the combinatoric factor $P(q,N)$ [Eq. (I4)] to leading order using Stirling's formula,

$$\ln N!\approx N(\ln N-1)\ . \tag{I11}$$

For the thermodynamic-limit model with fixed q, the mean-field approximation is the leading term in a $1/N$ expansion of the partition function. We shall comment on the validity of the expansion for the model with $qN=1$ after examining $1/N$ corrections.

Corrections to $Z_{\rm MF}$ may be computed to any order by performing Gaussian integrations. Note first that

$$\begin{aligned}&T\sum_n \ln\left[1-\frac{i\lambda}{i\omega_n+\varepsilon_{\rm MF}-\varepsilon_f}\right]\\ &\quad=T\sum_n\sum_{m=1}^{\infty}\frac{(-i\lambda)^m(-)^{m-1}}{m}\left[\frac{1}{i\omega_n+\varepsilon_{\rm MF}-\varepsilon_f}\right]^m\\ &\quad=-\sum_{m=1}^{\infty}\frac{(i\lambda)^m}{m!}\left[\frac{d^{m-1}}{dz^{m-1}}\frac{1}{e^{\beta z}+1}\right]\Bigg|_{z=\varepsilon_f-\varepsilon_{\rm MF}}\ .\end{aligned} \tag{I12}$$

The linear term in $F_{\rm fluct}$ is just

$$-i\lambda N\left[q-\frac{1}{e^{\beta(\varepsilon_f-\varepsilon_{\rm MF})}+1}\right]=0\ , \tag{I13}$$

by the saddle-point condition (I9). The Gaussian correction to Z is

$$\begin{aligned}&\int_{-\pi T}^{\pi T}\frac{\beta\,d\lambda}{2\pi}\exp\left[-\beta N(-\lambda^2/2)\frac{-\beta e^{\beta(\varepsilon_f-\varepsilon_{\rm MF})}}{(e^{\beta(\varepsilon_f-\varepsilon_{\rm MF})}+1)^2}\right]\\ &\quad=\int_{-\pi T}^{\pi T}\frac{\beta\,d\lambda}{2\pi}\exp[-N\beta^2q(1-q)\lambda^2/2]\ .\end{aligned} \tag{I14}$$

Neglecting corrections exponentially small in N, the limits of integration may be extended to $\pm\infty$. The result for Z to Gaussian order is then

$$Z\approx\frac{Z_{\rm MF}}{[2\pi Nq(1-q)]^{1/2}}\ . \tag{I15}$$

Note also that at Gaussian order the mean-square fluctuation in λ is just

$$\langle\lambda^2\rangle=\frac{T^2}{Nq(1-q)}=O(1/N)\ . \tag{I16}$$

To extend the expansion of Z to higher orders in $1/N$, non-Gaussian contributions to $Z_{\rm fluct}$ must be expanded in powers of λ, then integrated term by term. For example, terms contributing to the relative $1/N$ correction are

$$\begin{aligned}&\exp\left[-\beta N\sum_{m=3}^{\infty}\frac{(i\lambda)^m}{m!}\left[\frac{d^{m-1}}{dz^{m-1}}\frac{1}{e^{\beta z}+1}\right]\right]\Bigg|_{z=\varepsilon_f-\varepsilon_{\rm MF}}\approx 1+O(\lambda^3)-\frac{N^2}{72}(\beta\lambda)^6[q(1-q)]^2(2q-1)^2\\ &\qquad+\frac{N}{24}(\beta\lambda)^4q(1-q)(6q^2-6q+1)\ .\end{aligned} \tag{I17}$$

The λ^6 term arises from the expansion of the cubic term in the exponent. After performing the Gaussian integrations associated with the two correction terms, one obtains for Z to $O(1/N)$

$$Z\approx\frac{e^{-\beta\varepsilon_f(qN)}}{q^{qN}(1-q)^{(1-q)N}}\frac{1}{[2\pi Nq(1-q)]^{1/2}}\left[1-\frac{1}{12N}\frac{q^2-q+1}{q(1-q)}+O\left[\frac{1}{N^2}\right]\right]\ . \tag{I18}$$

This $1/N$ expansion could also be generated to arbitrary order by applying Stirling's formula directly to each factorial in $P(q,N)$ [Eq. (I4)], then collecting terms. In this context, note that the combination of factorials in $P(q,N)$ has a simple expression in terms of known functions (Gradshteyn and Ryzhik, 1980):

$$\begin{aligned}\frac{N!}{(qN)![(1-q)N]!}&=\frac{1}{N+1}\frac{\Gamma(N+2)}{\Gamma(qN+1)\Gamma((1-q)N+1)}\\ &=\frac{1}{N+1}\frac{1}{B(qN+1,(1-q)N+1)}\ ,\end{aligned} \tag{I19}$$

with B the beta function. In this case, the proof that the expansion generated for the partition function is asymptotic to the exact result relies on properties of simple analytic functions. For more complicated partition functions, such a complete proof cannot be furnished.

The expansion has a number of interesting properties. First of all, the free energy per level is

$$\frac{1}{N}F=-\frac{1}{N}T\ln Z$$
$$=q\varepsilon_f+T[q\ln q+(1-q)\ln(1-q)]+O\left[\frac{1}{N}\ln N\right]. \tag{I20}$$

For $T\to O$, this reproduces the exact ground-state energy $E_0/N=q\varepsilon_f$, for *all* q. It is clear in hindsight that the mean-field calculation should be sufficient to compute the ground-state energy, since

$$\left[\frac{1}{N}E_0\right]_{\rm MF}=\frac{1}{N}\varepsilon_f\langle\hat{Q}\rangle_{\rm MF}$$
and
$$\langle\hat{Q}\rangle_{\rm MF}=qN\ ; \tag{I21}$$

in this case, the constraint need only be satisfied on average to obtain the exact value of E_0/N.

The mean-field treatment does not produce an exact result for the entropy, which counts the number of available states. Since the system has $P(q,N)$ degenerate configurations,

$$\left[\frac{1}{N}S(T)\right]_{\rm exact}=\frac{1}{N}\ln P(q,N)\ . \tag{I22}$$

On the other hand, the mean-field entropy is

$$\left[\frac{1}{N}S(T)\right]_{\rm MF}=-[q\ln q+(1-q)\ln(1-q)]\ . \tag{I23}$$

This is the entropy of a system of independent fermion states, each with probability q for occupancy; these states may suggestively be viewed as noninteracting quasiparticles. The fact that the probability for occupancy is less than 1, even for $\varepsilon_f<0$, reflects the occupancy constraint at mean-field level.

Expansions based on this limit are certainly sensible when the mean occupancy $\langle\hat{Q}\rangle$ is large. How good are such expansions in the case of initial interest, $\hat{Q}=1$, i.e., $qN=1$? (The same question arises for the full Coqblin-Schrieffer and infinite-U Anderson models.) In the present case, $N=q^{-1}$ corresponds to a point far outside the range of validity of the asymptotic expansion: the Stirling series representing $\ln(qN)!$ breaks down for $N\sim q^{-1}$. The same numerical breakdown is expected for any partition function in which a unit-occupancy constraint is treated as a constraint extensive in N. The breakdown need *not* be uniform in temperature (this is the key to the success of saddle-point expansions for the Coqblin-Schrieffer and Anderson models in the Fermi-liquid regimes). For the simple system considered above, the exact ground-state energy emerges from a mean-field calculation. Furthermore, for $N=q^{-1}$, the fluctuation in the "constraint field" λ [Eq. (I16)] is

$$\langle\lambda^2\rangle=\frac{T^2}{1-q}\ . \tag{I24}$$

This fluctuation is large at high temperatures (even for $q\to 0$, but vanishes at zero temperature.

The violation of the unit occupancy constraint may be quantified for this simple model. The mean-square fluctuation $\langle(\hat{Q}-qN)^2\rangle$ measures the degree of contamination from ghost states in the functional integral. To evaluate this quantity at Gaussian order, a dimensionless "source" j may be introduced,

$$\lambda\to\lambda+j/\beta\ , \tag{I25}$$

in Eq. (I5). It is easy to check that

$$\langle\hat{Q}-qN\rangle=i\frac{\partial}{\partial j}\ln Z(j)\bigg|_{j=0}\ ,$$
$$\langle(\hat{Q}-qN)^2\rangle-\langle\hat{Q}-qN\rangle^2=-\frac{\partial^2}{\partial_j^2}\ln Z(j)\bigg|_{j=0}\ . \tag{I26}$$

If no approximations are made, these expressions vanish identically, since the integrand in Eq. (I5) is periodic in λ. At Gaussian order,

$$Z_{\rm fluct}(j)=\int_{-\pi T}^{\pi T}\frac{\beta\,d\lambda}{2\pi}\exp[-Nq(1-q)\beta^2(\lambda+j)^2/2]$$
$$=\int_{-\pi+j}^{\pi+j}\frac{dx}{2\pi}e^{-Ax^2}$$

with

$$A\equiv Nq(1-q)/2\ . \tag{I27}$$

Thus

$$\frac{\partial}{\partial j}Z_{\rm fluct}=\frac{1}{2\pi}(e^{-A(\pi+j)^2}-e^{-A(-\pi+j)^2})$$

and

$$-\frac{\partial^2}{\partial j^2}Z_{\rm fluct}=\frac{1}{2\pi}[2A(\pi+j)e^{-A(\pi+j)^2}$$
$$+2A(\pi-j)e^{-A(\pi-j)^2}]\ . \tag{I28}$$

It follows that

$$\langle\hat{Q}-qN\rangle=0 \tag{I29}$$

(the constraint is satisfied on average, as remarked earlier) and

$$\langle(\hat{Q}-qN)^2\rangle=\frac{2Ae^{-A\pi^2}}{Z_{\rm fluct}(j=0)}$$
$$=\frac{4\pi Ae^{-A\pi^2}}{(\pi/A)^{1/2}\mathrm{erf}(\pi\sqrt{A})}\ . \tag{I30}$$

TABLE XII. Gaussian fluctuations in the constrained level occupancy. In a functional integral treatment based on the saddle-point approximation, the level occupancy Q in toy model (i) is not exactly constrained. The magnitude of the temperature-independent fluctuation in the occupancy is tabulated below for various values of the relative filling parameter q.

q^{-1}	$\langle(\hat{Q}-1)^2\rangle$	$\langle(\hat{Q}-1)^2\rangle^{1/2}$
2	0.077	0.28
4	0.040	0.20
6	0.031	0.18
∞	0.018	0.13

This term is exponentially small in qN for $qN\to\infty$ and may be neglected in constructing an asymptotic expansion in $1/N$ for fixed q (the thermodynamic-limit model). The occupancy constraint is enforced up to exponentially small, or subdominant, terms. We have retained these terms to examine the physically interesting case $N=q^{-1}$. In this case,

$$A=\tfrac{1}{2}(1-q)\ . \tag{I31}$$

The magnitude of the unphysical fluctuations for various choices of q is recorded in Table XII.

Note that the fluctuations are temperature independent in this toy model. The root-mean-square fluctuation is large for all values of $q^{-1}=N$, indicating the presence of an admixture of ghost states in thermal averages. One might hope that the fluctuations could be reduced by extending the bounds of the constraint integral; e.g., the constraint could be enforced using the operator delta function

$$\int_{-\pi MT}^{\pi MT}\frac{\beta d\lambda}{2\pi M}\exp[-i\beta\lambda(\hat{Q}-qN)]\ , \tag{I32}$$

for arbitrarily large M. Note, however, that *before* approximations are made, the λ integrand is periodic with period $2\pi T$. The integral in this case has M saddle points (at $\lambda=2\pi nT+i\varepsilon_{MF}$, n an integer). The integral over each interval of length $2\pi T$ is identical with the constraint integral considered previously, and the computed fluctuations in $\hat{Q}-1$ do not depend on M.

Thus, for the interesting case $qN=1$, the occupancy constraint is only approximately enforced. This conclusion holds not just in the present treatment, but in all treatments of an occupancy constraint by perturbation theory (in particular, for the infinite-U Anderson and Coqblin-Schrieffer models). Previous treatments which have concluded that the constraint may be enforced exactly, order by order, omit "subdominant" terms, which are in general quite large when $qN=1$. (Despite this fact, saddle-point expansions for the magnetic alloy models are well controlled at zero temperature and in the Fermi-liquid regime. In this limit, the constraint need not be enforced exactly to obtain exact answers.)

2. Toy model (ii)

In the last section we have attempted to illustrate some possible pitfalls of large-N expansions about the thermodynamic limit: extrapolations beyond the range of validity of the expansion may lead to unreliable conclusions. In this section we should like to pursue this point with a more extreme example, viz., a possible generalization of toy model (ii) in Eq. (I1). We consider the case in which level $|0\rangle$ lies lowest, i.e., $\varepsilon_f>0$.

In this case, the N levels $|m\rangle$ with energy ε_f and the nondegenerate level $|0\rangle$ with energy 0 may be chosen to have any combination of Fermi and Bose statistics. The occupancy constraint ensures that only $N+1$ different configurations of the system are realizable and that the partition function is

$$Z=1+Ne^{-\beta\varepsilon_f}\ , \tag{I33}$$

independent of the underlying level statistics. If, however, the constraint is rewritten

$$\sum_m \hat{N}_m+\hat{N}_0=qN\ , \tag{I34}$$

each choice of statistics corresponds to a distinct system. If various approximations are made before attempting to recover the limit $N=q^{-1}$, a number of quite different results may be obtained. If, for example, $\varepsilon_f>0$ and

$$\begin{aligned}&\hat{N}_m\to f_m^\dagger f_m,\ \text{fermions}\ ,\\ &\hat{N}_0\to b^\dagger b,\ \text{boson}\ ,\end{aligned} \tag{I35}$$

the presence of a low-lying Bose level allows the phenomenon of condensation, or macroscopic occupancy, at saddle-point level. For $N=q^{-1}$, the appearance of Bose condensation is completely unphysical: no level in the system may have occupancy larger than 1. The appearance of a condensate at low temperatures is in this case an artifact of the approximate solution, unrelated to the simple physics of the system with unit occupancy.

Bose condensation is prevented *a priori* (for any qN) if one chooses

$$\begin{aligned}&\hat{N}_m\to f_m^\dagger f_m,\ \text{fermions}\ ,\\ &N_0\to f_0^\dagger f_0,\ \text{fermion}\ ,\end{aligned} \tag{I36}$$

or

$$\begin{aligned}&\hat{N}_m\to b_m^\dagger b_m,\ \text{bosons}\ ,\\ &\hat{N}_0\to f_0^\dagger f_0,\ \text{fermion}\ .\end{aligned} \tag{I37}$$

In both cases, since the lower level has Fermi character, it can be at most singly occupied and plays no part in the physics of the system in the thermodynamic limit $N\to\infty$. This means that these cases are equivalent at saddle-point level to the Fermi and Bose representations of the system in Eq. (I3).

For toy model (ii) with $\varepsilon_f>0$, a particular representation is required to obtain sensible results for the ground-

state energy and level occupancies at mean-field level. The exact results for the unit-occupancy system are

$$\left[\frac{1}{N}E_0\right]_{\text{exact}}=0,\quad \frac{1}{N}\langle\hat{N}_0\rangle\Big|_{\text{exact}}=1/N\ . \tag{I38}$$

If the nondegenerate level is assumed to have Fermi character, its contribution to properties vanishes in the thermodynamic limit $N\to\infty$ and

$$\left[\frac{1}{N}E_0\right]_{\text{MF}}=q\varepsilon_f,\quad \frac{1}{N}\langle\hat{N}_0\rangle\Big|_{\text{MF}}=0\ . \tag{I39}$$

These expressions are qualitatively incorrect when extrapolated to $N=q^{-1}$. On the other hand, if the nondegenerate level has Bose character,

$$\left[\frac{1}{N}E_0\right]_{\text{MF}}=0,\quad \frac{1}{N}\langle\hat{N}_0\rangle\Big|_{\text{MF}}=q\ , \tag{I40}$$

by virtue of condensate formation; these expressions are *exact* when extrapolated to $N=q^{-1}$. This is not especially deep. It is clear that a single Bose level can have macroscopic effects, while a single Fermi level cannot. If a nondegenerate level dominates a system's behavior in some regime, that level must be represented by a boson if its influence is to be felt at all at saddle-point level in an expansion about the thermodynamic limit.

This does not mean that more general features of condensate formation are relevant to the system with unit-occupancy constraint. To clarify this statement we discuss at greater length the representation that exhibits Bose condensation. (An analogous treatment may be applied to the Coqblin-Schrieffer and infinite-U Anderson models—see Secs. VI.A and VI.B.) The partition function for the mixed Fermi-Bose system may be represented exactly by the functional integral

$$Z=\int_{-\pi T}^{\pi T}\frac{\beta d\lambda}{2\pi}e^{i\beta\lambda(qN)}(1+e^{-\beta(\varepsilon_f+i\lambda)})^N \times\int_\xi\exp\left[-\beta\sum_m|\xi_m|^2(-i\nu_m+i\lambda)\right]. \tag{I41}$$

At high temperature (where there is no condensate), the saddle-point solution is completely analogous to that for toy model (i). Shifting λ into the complex plane as in Eq. (I7) gives

$$\begin{aligned}&Z=Z_{\text{MF}}Z_{\text{fluct}},\quad Z_{\text{MF}}=e^{-\beta F_{\text{MF}}},\\&F_{\text{MF}}=\varepsilon_{\text{MF}}(qN)-NT\ln(1+e^{\beta(\varepsilon_{\text{MF}}-\varepsilon_f)})\ \ (\text{high } T),\\&Z_{\text{fluct}}=\int_{-\pi T}^{\pi T}\frac{\beta d\lambda}{2\pi}\int_\xi e^{-\beta F_{\text{fluct}}},\\&F_{\text{fluct}}=-i\lambda(qN)-NT\sum_n\ln\left[1-\frac{i\lambda}{i\omega_n+\varepsilon_{\text{MF}}-\varepsilon_f}\right]\\&\qquad+\sum_m|\xi_m|^2(-i\nu_m-\varepsilon_{\text{MF}}+i\lambda)\ \ (\text{high } T).\end{aligned} \tag{I42}$$

Since the saddle-point free energy is the same as that for toy model (i) [cf. Eq. (I8)], the saddle-point condition is again

$$f(\varepsilon_f-\varepsilon_{\text{MF}})=q \tag{I43a}$$

and

$$Z_{\text{MF}}=\frac{e^{-\beta\varepsilon_f(qN)}}{q^{qN}(1-q)^{(1-q)N}}\ , \tag{I43b}$$

as before.

The fluctuations in λ and ξ_m are independent at Gaussian order. This implies immediately that the violation of the occupancy constraint at high temperature is the same as that for toy model (i) [cf. Eq. (I30)]. For $N=q^{-1}$, the constraint is violated by large amounts for all values of q: the physical model lies far outside the range of validity of the expansion. Nevertheless, a number of interesting results may be obtained by pursuing the expansion further. The expression for Z_{fluct} at Gaussian order (neglecting terms exponentially small in qN) is

$$Z_{\text{fluct}}=\frac{1}{[2\pi Nq(1-q)]^{1/2}}\frac{1}{1-e^{\beta\varepsilon_{\text{MF}}}}\ . \tag{I44}$$

The Gaussian correction diverges at low temperature; specifically,

$$\frac{1}{1-e^{\beta\varepsilon_{\text{MF}}}}\to\infty \tag{I45a}$$

(indicating an instability of the system at this order) when

$$\varepsilon_{\text{MF}}\to 0\ . \tag{I45b}$$

This instability occurs where

$$f(\varepsilon_f)=q\ ,$$

i.e., at

$$T_c=\frac{\varepsilon_f}{\ln(q^{-1}-1)}\ . \tag{I46}$$

Below this temperature, the saddle-point solution described above is unstable with respect to Gaussian fluctuations, and the zero-frequency component of the Bose field ξ_0 takes on a nonzero expectation value.

The general saddle-point equations are derived by minimizing

$$F_{\text{MF}}=\varepsilon_{\text{MF}}(qN)-NT\ln(1+e^{\beta(\varepsilon_{\text{MF}}-\varepsilon_f)})-\langle\xi_0\rangle^2\varepsilon_{\text{MF}}\ . \tag{I47}$$

The saddle-point equations are

$$\begin{aligned}&\frac{\partial}{\partial\varepsilon_{\text{MF}}}:\ \langle\xi_0\rangle^2=N[q-f(\varepsilon_f-\varepsilon_{\text{MF}})]\ ,\\&\frac{\partial}{\partial\langle\xi_0\rangle}:\ \langle\xi_0\rangle\varepsilon_{\text{MF}}=0\ .\end{aligned} \tag{I48}$$

Above T_c,

$$\langle\xi_0\rangle=0$$

and

$$\varepsilon_{\rm MF}=\varepsilon_f - T\ln(q^{-1}-1)\ . \tag{I49a}$$

Below T_c,

$$\varepsilon_{\rm MF}=0$$

and

$$\langle\xi_0\rangle^2=\langle\hat{N}_0\rangle_{\rm MF}=N[q-f(\varepsilon_f)]=O(N)\ . \tag{I49b}$$

The partition function takes the form

$$Z_{\rm MF}=\frac{e^{-\beta\varepsilon_f(qN)}}{q^{qN}(1-q)^{(1-q)N}},\quad T>T_c$$

$$=(1+e^{-\beta\varepsilon_f})^N,\quad T<T_c\ . \tag{I50}$$

The saddle-point solution exhibits a continuous phase transition at T_c (see Fig. 34) with order parameter $\langle\hat{N}_0\rangle/N$. This phase transition is a real feature of the system in the thermodynamic limit $N\to\infty$, q fixed. In this limit, fluctuations in intensive variables, such as $\langle\hat{N}_0\rangle/N$, vanish, and the mean-field theory presented above becomes exact. The system exhibits macroscopic condensation into the Bose level. This is analogous to condensation in an ideal Bose gas. At zero temperature a macroscopic number of particles ($qN\to\infty$) occupy a microscopic quantum state. Outside the thermodynamic limit (qN large, but finite), no phase transition occurs. In the system's ground state, the Bose level is occupied by qN particles, but the previous transition is rounded by "finite-size" effects. As N decreases, such effects become increasingly important; in the extreme limit $qN=1$, Bose statistics have no manifestation and the crossover from high to low temperatures is completely smooth.

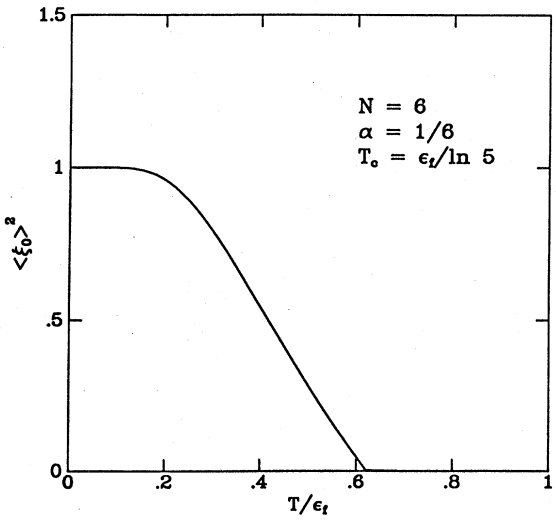

FIG. 34. Order parameter of the mean-field solution of toy model (ii) [Eq. (I1)]. Results are shown for the case $qN=1$, $N=6$. The order parameter, or Bose level occupancy, vanishes above the transition temperature $T_c=\varepsilon_f/\ln 5$. For $T\to 0$, the order parameter saturates to unity, indicating complete occupancy of the Bose level.

It is instructive to compute the specific heat in mean-field theory for comparison with the exact result for $qN=1$. Above the transition, the entropy is constant and the specific heat vanishes; below T_c,

$$\left[\frac{1}{N}S\right]_{\rm MF}=\ln(1+e^{-\beta\varepsilon_f})+\frac{\varepsilon_f}{T}\frac{1}{e^{\beta\varepsilon_f}+1} \tag{I51}$$

and

$$\left[\frac{1}{N}C\right]_{\rm MF}=\left[\frac{\varepsilon_f}{T}\right]^2\frac{e^{\beta\varepsilon_f}}{(e^{\beta\varepsilon_f}+1)^2}\ . \tag{I52}$$

Specifically, for $T\to T_c^-$,

$$\left[\frac{1}{N}S^-\right]_{\rm MF}=-[q\ln q+(1-q)\ln(1-q)]$$

and

$$\left[\frac{1}{N}C^-\right]_{\rm MF}=q(1-q)\ln^2(q^{-1}-1)\ . \tag{I53}$$

The mean-field specific heat is compared with the exact result for $N=q^{-1}=6$ in Fig. 35. Note that as the temperature is raised to T_c, the mean-field entropy achieves its high-temperature limit, corresponding to a system of N independent fermion levels, each with probability q for occupancy [compare the discussion following Eq. (I23)]. At this order the Bose level does not contribute to the high-temperature properties of the system. It is a single

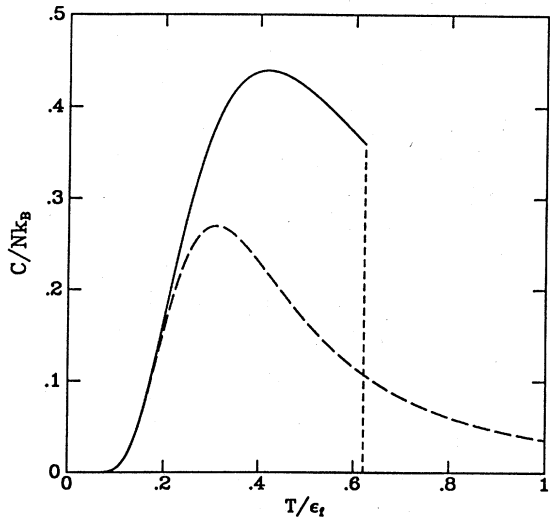

FIG. 35. Mean-field and exact specific heat for toy model (ii) [Eq. (I1)]. Results are shown for $qN=1$, $N=6$. The mean-field solution is indicated by the solid line, and the exact solution by the dashed line. The mean-field specific heat vanishes above the transition temperature $T_c=\varepsilon_f/\ln 5$, but agrees with the exact specific heat to exponential accuracy for $T\to 0$. The peak in the mean-field solution occurs at $T/\varepsilon_f=0.42$, and the peak in the exact solution at $T/\varepsilon_f=0.31$. The values of the entropy S/k_B at T_c are 2.703 (mean-field) and 1.666 (exact). The exact high-temperature limit for S/k_B is $\ln 7=1.946$.

level with microscopic occupancy in a macroscopic sea of fermions. For $T\to 0$, the mean-field specific heat approaches the exact result

$$\left[\frac{1}{N}C\right]_{\text{exact}}=\left[\frac{\varepsilon_f}{T}\right]^2\frac{e^{-\beta\varepsilon_f}}{(1+Ne^{-\beta\varepsilon_f})^2},\quad N=q^{-1}, \tag{I54}$$

with exponential accuracy. The approximate result deteriorates rapidly with increasing T, exhibiting a sharp discontinuity at T_c.

This toy model exhibits the same qualitative features found in saddle-point solutions for the full magnetic alloy models. The sharp phase transition at T_c results from the approximate treatment of the level-occupancy constraint: at finite temperature, the constraint integrations should be performed nonperturbatively, rather than in saddle-point approximation. Nevertheless, exact results may be obtained within a saddle-point expansion for $T\to 0$. For the alloy models, the validity of a saddle-point expansion within the Fermi-liquid regime justifies the elegant transformation to quasiparticle modes discussed in Sec. VI.C.

APPENDIX J: DERIVATION OF THE $O(1/N)$ FREE ENERGY FOR THE INFINITE-U ANDERSON MODEL BY THE SADDLE-POINT APPROACH

In this appendix we examine a functional integral approach, first proposed by Read (1985), for calculating $1/N$ corrections to the ground-state energy of the infinite-U Anderson model. This approach is an extension of the saddle-point analysis in Sec. VI.B. As in the previous treatment, a partition function depending on the static variables λ and ξ_0 [cf. Eq. (6.22)] is approximated by its saddle-point value; in this case, the static free energy is augmented by corrections from Gaussian fluctuations in the finite-frequency variables. This treatment of fluctuations is somewhat different from that in Appendix I. In that section a saddle-point approximation (involving only static variables) was introduced at mean-field level, but static and finite-frequency variables were considered on the same footing in the fluctuation free energy. In the analysis that follows, static variables are singled out for a saddle-point approximation at each order.

This approach reproduces the results for the ground-state energy and Fermi-liquid thermodynamics found in Secs. II–V. As in Sec. VI.B, the level-occupancy constraint may be treated perturbatively at low temperature. The saddle-point approximation is equivalent to locating the lowest singularity in the empty-state propagator $1/[\omega-\Sigma_0(\omega)]$ (cf. Sec. II). This singularity determines all zero-temperature properties. The saddle-point approximation deteriorates at finite temperature, however. In this case, the approach does not reproduce the results of other $1/N$ techniques and introduces errors associated with the violation of the occupancy constraint.

Since the saddle-point value of λ [cf. Eq. (6.102)] is actually imaginary (as in the mean-field treatment of Sec. VI.B), it is simplest to shift λ into the complex plane from the start by letting

$$\bar{\lambda}=\lambda+i\lambda_0\,. \tag{J1}$$

At lowest order, λ_0 is just $\varepsilon_{\text{MF}}=E_0$, the ground-state energy of Sec. VI.C.

The partition function may be conveniently divided into static and dynamic contributions. Without approximation,

$$Z=\int_{-\pi T}^{\pi T}\frac{\beta d\lambda}{2\pi}\int d\bar{\xi}_0 d\xi_0 e^{-\beta F_{\text{stat}}(\xi_0,\bar{\lambda})}\int_{\xi_m}e^{-\beta F_{\text{dyn}}(\xi,\bar{\lambda})}, \tag{J2}$$

where

$$\begin{aligned}
&F_{\text{stat}}(\xi_0,\bar{\lambda})=i\bar{\lambda}(|\xi_0|^2-1)-NT\ln(1+e^{-\beta(\varepsilon_f+i\bar{\lambda})})-NT\,\mathrm{Tr}\ln(1-V^2|\xi_0|^2G^{\lambda}G)\,,\\
&F_{\text{dyn}}(\xi,\bar{\lambda})=\sum_{m\neq 0}|\xi_m|^2(-i\nu_m+i\bar{\lambda})-NT\,\mathrm{Tr}\ln[1-V^2(1-V^2|\xi_0|^2G^{\lambda}G)^{-1}(G^{\lambda}XGX^{\dagger}-|\xi_0|^2G^{\lambda}G)]\,,\\
&\int_{\xi_m}=\int\prod_{m\neq 0}d\bar{\xi}_m d\xi_m,\quad (G^{\lambda})_{nn'}=\frac{\delta_{nn'}}{i\omega_n-i\bar{\lambda}-\varepsilon_f},\quad G_{nn'}=\delta_{nn'}\sum_k\frac{1}{i\omega_n-\varepsilon_k},\quad X_{nn'}=\xi_{n-n'}\,.
\end{aligned} \tag{J3}$$

Note that the variables $\bar{\lambda}$ and ξ_0 appear in both the static and dynamic free energies, but that F_{stat} is purely static. In a mean-field treatment, the minimum of the static free energy F_{stat} is located: static and dynamic fluctuations are ignored. As shown in Sec. VI.B, a mean-field approximation is essentially equivalent to an $O(1)$ calculation. The mean-field approximation may be extended by computing Gaussian fluctuations in the finite-frequency variables. Since F_{dyn} depends on $\bar{\lambda}$ and ξ_0, these fluctuations generate a correction ΔF_{stat} to the static free energy. A new saddle point may be determined for the static integrals with free energy $F_{\text{eff}}=F_{\text{stat}}+\Delta F_{\text{stat}}$. The integral over the static variable ξ_0 should *not* be included in the Gaussian corrections; it would not make sense to integrate over ξ_0, then subsequently minimize a function of this variable.

At this point it is possible to see why the saddle-point approximation is successful at zero temperature. The effective free energy F_{eff} may be used to compute the static Bose propagator, as well as thermodynamic properties. Before the integral over λ is evaluated the static propagator has the general form

$$D^{\lambda}(0)=\frac{1}{Z}\int d\bar{\xi}_0 d\xi_0|\xi_0|^2e^{-\beta F_{\text{eff}}(\xi_0,\bar{\lambda})}\,. \tag{J4}$$

The effective free energy may be expanded as

$$F_{\rm eff}=A+B\,|\xi_0|^2+C\,|\xi_0|^4+O(|\xi_0|^6)\,, \tag{J5}$$

where the coefficients A, B, and C depend on $\bar{\lambda}$ and the temperature. In evaluating the static propagator to a specified order in $1/N$, $F_{\rm eff}$ must be truncated. In an $O(1/N)$ calculation, terms of $O(|\xi_0|^6)$ may be dropped. B^{-1} is then the static Bose proapgator, including all self-energy corrections to $O(1/N)$ *except* those with a static internal line. These last corrections can only be obtained by considering the quartic term. If the quartic coefficient C vanishes (the case for a flat density of conduction states—see below), B^{-1} is precisely the static Bose propagator to $O(1/N)$. If, however, C is nonzero, then B omits a static contribution to the Bose self-energy at $O(1/N)$. This may be computed in the standard way by expanding the quartic portion of $\exp(-\beta F_{\rm eff})$ in a power series. When C vanishes, the prescription of setting

$$\partial F_{\rm eff}/\partial|\xi_0|^2=0 \Longleftrightarrow B=0 \tag{J6}$$

amounts to locating the lowest singularity of the Bose propagator to $O(1/N)$. This singularity completely determines thermodynamic properties in the limit $T\to 0$. Remarkably, the additional terms that appear in $F_{\rm eff}$ for nonzero C *cancel* in results for the ground-state energy, and the prescription succeeds even in this case. Such a cancellation is essential at higher orders in the expansion, since the coefficients of $|\xi_0|^{2n}$ with n odd are nonzero even for a flat density of states.

We work out below the $1/N$ saddle-point approximation for a general density of band states. The resulting expression for the free energy is just that derived in Eq. (2.44). Hence all previous results for zero-temperature thermodynamic properties may be reproduced within the saddle-point formalism. The first derivations of the Sommerfeld ratio to $O(1/N)$ were performed using saddle-point techniques (Read and Newns, 1983; Read, 1985).

The dynamic free energy may be expanded to $O(1/N)$ as

$$\begin{aligned}F_{\rm dyn}&\approx\sum_{m\neq 0}|\xi_m|^2(-i\nu_m+i\bar{\lambda})+NV^2\frac{1}{\beta}{\rm Tr}(G^\lambda XGX^\dagger-|\xi_0|^2G^\lambda G)\\&\quad+\frac{(NV^2)^2}{N}|\xi_0|^2\frac{1}{\beta}{\rm Tr}(G^\lambda G)(G^\lambda XGX^\dagger-|\xi_0|^2G^\lambda G)+O(1/N^2)\\&=\sum_{m\neq 0}|\xi_m|^2[(-i\nu_m+i\bar{\lambda})+\Pi_1(i\nu_m)+\Pi_2(i\nu_m)]\,,\end{aligned} \tag{J7}$$

where

$$\begin{aligned}\Pi_1(i\nu_m)&=NV^2\frac{1}{\beta}\sum_{kn}\frac{1}{i\omega_n-i\bar{\lambda}-\varepsilon_f}\frac{1}{i(\omega_n-\nu_m)-\varepsilon_k}=NV^2\sum_k\frac{f(\varepsilon_k)-f(i\bar{\lambda}+\varepsilon_f)}{i\nu_m+\varepsilon_k-i\bar{\lambda}-\varepsilon_f}\,,\\\Pi_2(i\nu_m)&=|\xi_0|^2\frac{(NV^2)^2}{N}\frac{1}{\beta}\sum_{kk'n}\frac{1}{i\omega_n-\varepsilon_k}\frac{1}{(i\omega_n-i\bar{\lambda}-\varepsilon_f)^2}\frac{1}{i(\omega_n-\nu_m)-\varepsilon_{k'}}\,.\end{aligned} \tag{J8a}$$

Note that for $T\to 0$ and $\varepsilon_f-\lambda_0>0$,

$$\Pi_1(z)=\Sigma_0^{(1)}(z-i\bar{\lambda})\,, \tag{J8b}$$

with $\Sigma_0^{(1)}$ the ubiquitous self-energy first introduced in Eq. (2.15).

If the static component *were* included in the dynamic free energy, the Gaussian integral over $\{\xi_m\}$ would give

$$\begin{aligned}e^{-\beta\Delta F_{\rm stat}}&=\frac{1}{1-e^{-i\beta\bar{\lambda}}}\exp\left[-\sum_m\ln\left[1-\frac{\Pi_1(\nu_m)}{i\nu_m-i\bar{\lambda}}\right]-\sum_m\ln\left[1-\frac{\Pi_2(i\nu_m)}{i\nu_m-i\bar{\lambda}-\Pi_1(i\nu_m)}\right]\right]\\&=\frac{1}{1-e^{-i\beta\bar{\lambda}}}\exp\left[-\sum_m\ln\left[1-\frac{\Pi_1(i\nu_m)}{i\nu_m-i\bar{\lambda}}\right]+\sum_m\frac{\Pi_2(i\nu_m)}{i\nu_m-i\bar{\lambda}-\Pi_1(i\nu_m)}\right]\,,\end{aligned} \tag{J9}$$

retaining only terms of $O(1)$ and $O(1/N)$ in the exponent. As argued previously, the static Gaussian integral should *not* be included in this calculation. If it is omitted, the result above should be multiplied by

$$\beta[i\bar{\lambda}+\Pi_1(0)+\Pi_2(0)]\,. \tag{J10}$$

Thus, including all terms to $O(1/N)$,

$$e^{-\beta\Delta F_{\rm stat}}=\frac{\beta(i\bar{\lambda})}{1-e^{-i\beta\bar{\lambda}}}\exp\left[-\sum_{m\neq 0}\ln\left[1-\frac{\Pi_1(i\nu_m)}{i\nu_m-i\bar{\lambda}}\right]+\sum_{m\neq 0}\frac{\Pi_2(i\nu_m)}{i\nu_m-i\bar{\lambda}-\Pi_1(i\nu_m)}\right]\,. \tag{J11}$$

In a previous derivation (Read, 1985) of this fluctuation correction, only the term containing Π_2 was included. We show subsequently that the other terms vanish for $T\to 0$ and may be safely omitted in the Fermi-liquid regime; on the other

hand, their contribution at finite temperature is of the same order in $1/N$ as the lowest-order saddle-point solution. Note that if λ_0 is set to zero in Eq. (J1) (i.e., if one dispenses with the saddle-point approximation entirely), these terms are exactly those which arise in the treatment of Sec. III.B at $O(1)$. The inclusion of these terms reveals the close relationship between this approach and that in Sec. III.

The Matsubara frequency sums in Eqs. (J8a) and (J11) must now be performed. Note first that

$$-\frac{1}{\beta}\sum_{m\neq 0}\frac{\Pi_2(i\nu_m)}{i\nu_m-i\bar{\lambda}-\Pi_1(i\nu_m)}=-\frac{(NV^2)^2}{N}|\xi_0|^2\frac{1}{\beta}\sum_{kk'n}\frac{1}{i\omega_n-\varepsilon_k}\frac{1}{(i\omega_n-i\bar{\lambda}-\varepsilon_f)^2}S(i\omega_n)\,,$$
$$S(i\omega_n)=\frac{1}{\beta}\sum_{m\neq 0}\frac{1}{i(\omega_n-\nu_m)-\varepsilon_{k'}}\frac{1}{i\nu_m-i\bar{\lambda}-\Pi_1(i\nu_m)}\,. \tag{J12}$$

The sum S may be reduced to a contour integral along three cuts (see Fig. 36). For $\bar{\lambda}$ imaginary (the case at the saddle point) two of the cuts coalesce. We temporarily consider the more general case $\bar{\lambda}=\lambda+i\lambda_0$; in this case,

$$S(i\omega_n)=S_1(i\omega_n)+S_2(i\omega_n)$$
$$-\frac{1-f(\varepsilon_{k'})}{i\omega_n-\varepsilon_{k'}-i\bar{\lambda}-\Pi_1(i\omega_n-\varepsilon_{k'})}\,, \tag{J13}$$
$$S_i(i\omega_n)=\int_{\Gamma_i}\frac{dz}{2\pi i}\frac{b(z)}{z-i\bar{\lambda}-\Pi_1(z)}\frac{1}{i\omega_n-z-\varepsilon_{k'}}\,,$$

with b the Bose function and Γ_i the contours in Fig. 36.

The evaluation of S_1 and S_2 may be simplified, since Π_2 [Eq. (J8a)] is explicitly of order $1/N$: the $O(1)$ saddle-point value $E_0=\varepsilon_f-T_A$ may be substituted in all energy denominators. The only contribution to S_1 arises from the pole of the Bose function:

$$S_1(i\omega_n)=-\frac{1}{\beta}\frac{1}{-i\bar{\lambda}-\Pi_1(0)}\frac{1}{i\omega_n-\varepsilon_{k'}}\,; \tag{J14}$$

this accounts for the $m=0$ term omitted from S. When $T\to 0$ and λ_0 takes on its $O(1)$ value E_0, S_2 reduces to a pole contribution from $z=i\lambda$:

$$S_2(i\omega_n)=-Z(E_0)\frac{b(i\lambda)}{i\omega_n-i\lambda-\varepsilon_{k'}}\,, \tag{J15a}$$

with

$$Z(E_0)=\left[1-\frac{\partial\Sigma_0^{(1)}}{\partial E_0}\right]^{-1}\,. \tag{J15b}$$

For the case of interest (ξ_0 and $\bar{\lambda}$ at their saddle-point values), $\lambda=0$ and the contours Γ_1 and Γ_2 coalesce. For $\lambda_0=E_0$, Eqs. (J14) and (J15) may be expanded in λ as

$$-\frac{1}{\beta}\frac{1}{-i\bar{\lambda}-\Pi_1(0)}\frac{1}{i\omega_n-\varepsilon_{k'}}$$
$$=\left[Z(E_0)\frac{T}{i\lambda}+O(\lambda,T)\right]\frac{1}{i\omega_n-\varepsilon_{k'}} \tag{J16a}$$

and

$$-Z(E_0)\frac{b(i\lambda)}{i\omega_n-i\lambda-\varepsilon_{k'}}=\left[-Z(E_0)\frac{T}{i\lambda}+\frac{1}{2}Z(E_0)+O(\lambda,T)\right]\frac{1}{i\omega_n-\varepsilon_{k'}}\,. \tag{J16b}$$

When these contributions are combined, the singular terms cancel, and the only term that remains in the zero-temperature limit is

$$\tfrac{1}{2}Z(E_0)\frac{1}{i\omega_n-\varepsilon_{k'}}\,. \tag{J17}$$

Thus, substituting in Eq. (J12), the contribution to $\Delta F_{\rm stat}$ from S_1 and S_2 is

$$\frac{1}{N}|\xi_0|^2 W(T_A)$$

with

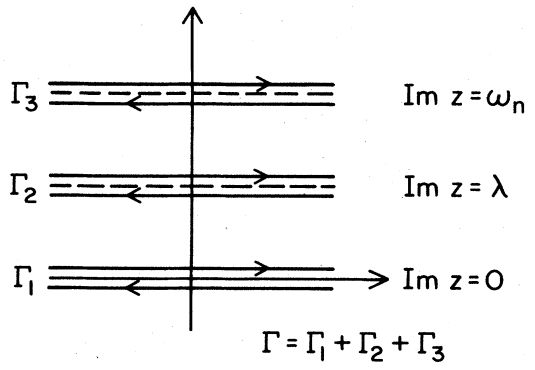

FIG. 36. Contour of integration for performing the Bose frequency sum in Eq. (J12). The cuts along $\mathrm{Im}z=\lambda$ and $\mathrm{Im}z=0$ coalesce for $\bar{\lambda}$ imaginary ($\lambda=0$).

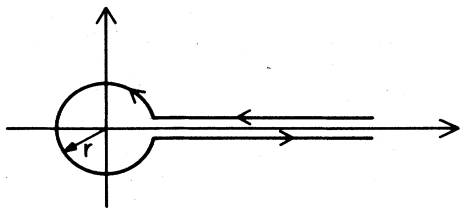

FIG. 37. Contour of integration for performing the Bose frequency sum in Eq. (J21) in the limit $T\to 0$.

$$W(T_A)=-\tfrac{1}{2}(NV^2)^2 Z(E_0) \times\frac{1}{\beta}\sum_{kk'n}\frac{1}{i\omega_n-\varepsilon_k}\frac{1}{i\omega_n-\varepsilon_{k'}}\frac{1}{(i\omega_n-T_A)^2}\,. \tag{J18}$$

This term vanishes at zero temperature for a flat density of states [the form assumed in the initial derivation (Read, 1985)]; it is nonzero (but of order D^{-1}, with D a typical band energy) in the more general case.

For $\bar{\lambda}=E_0$, the contribution to $\Delta F_{\rm stat}$ from the last term in Eq. (J13) is

$$|\xi_0|^2\frac{(NV^2)^2}{N}\frac{1}{\beta}\sum_{kk'n}\frac{1-f(\varepsilon_{k'})}{i\omega_n-\varepsilon_k}\frac{1}{(i\omega_n-T_A)^2}\frac{1}{i\omega_n-\varepsilon_{k'}+E_0-\Sigma_0^{(1)}(i\omega_n-\varepsilon_{k'}+E_0)} \rightarrow |\xi_0|^2\frac{(NV^2)^2}{N}\sum_{kk'}\frac{f(\varepsilon_k)[1-f(\varepsilon k')]}{(\varepsilon_k-T_A)^2}\frac{1}{\varepsilon_k-\varepsilon_{k'}+E_0-\Sigma_0^{(1)}(\varepsilon_k-\varepsilon_{k'}+E_0)}\,, \tag{J19}$$

for $T\rightarrow 0$. [In the last step, contributions proportional to $f(T_A)$ and $f(\varepsilon_{k'})$ have been dropped.]

The remaining contributions to $\Delta F_{\rm stat}$ in Eq. (J11) are

$$-T\ln\beta(i\bar{\lambda})+T\ln(1-e^{-i\beta\bar{\lambda}}) +T\sum_{m\neq 0}\ln\left[1-\frac{\Pi_1(i\nu_m)}{i\nu_m-i\bar{\lambda}}\right]. \tag{J20}$$

[Note that the $O(1)$ saddle-point value for $\bar{\lambda}$ should not be used in evaluating these contributions, since they are themselves $O(1)$.] The first two terms vanish in the zero-temperature limit. The sum

$$T\sum_{m\neq 0}\ln\left[1-\frac{\Pi_1(i\nu_m)}{i\nu_m-i\bar{\lambda}}\right] \tag{J21}$$

may be performed exactly for $T\rightarrow 0$; for $i\lambda=0$, it may be rewritten as the contour integral

$$-\int_\Gamma\frac{dz}{2\pi i}b(z)\ln\left[1-\frac{\Sigma_0^{(1)}(z+\lambda_0)}{z+\lambda_0}\right]\equiv I_1+I_2\,. \tag{J22}$$

The contour Γ is illustrated in Fig. 37; the contributions I_1 and I_2 arise from the small circle of radius r and the cut along the real axis. To integrate over the small circle, note that

$$\ln\left[1-\frac{\Sigma_0^{(1)}(z+\lambda_0)}{z+\lambda_0}\right]=\ln\left[\frac{zZ^{-1}(\lambda_0)}{\lambda_0}\right]+O(z)\,. \tag{J23}$$

Parametrizing the circle as $re^{i\theta}$, $0\leq\theta\leq 2\pi$ gives

$$I_1=-\frac{1}{2\pi i}\int_0^{2\pi}(ire^{i\theta}d\theta)\frac{T}{re^{i\theta}}[1+O(r)]\left[\ln\left[\frac{rZ^{-1}(\lambda_0)}{|\lambda_0|}\right]+i(\theta-\pi)+O(r)\right] =-T\ln\left[\frac{rZ^{-1}(\lambda_0)}{|\lambda_0|}\right]+O(r\ln r)\,. \tag{J24}$$

Since $\Sigma_0^{(1)}(z+\lambda_0)$ is real valued for $0\leq z\leq\varepsilon_f-\lambda_0$, the contribution from the branch cut is just

$$I_2=\int_r^{\varepsilon_f-\lambda_0}\frac{dx}{2\pi i}b(x)(-2\pi i)+(\text{exponentially small corrections})=-T\ln(1-e^{-\beta x})\Big|_r^{\varepsilon_f-\lambda_0}\rightarrow T\ln\beta r\,. \tag{J25}$$

Setting $T\rightarrow 0$ gives

$$I_1+I_2=T\ln[\beta|\lambda_0|Z(\lambda_0)]\,. \tag{J26}$$

This term also vanishes in the zero-temperature limit.

All the contributions to $\Delta F_{\rm stat}$ at $O(1/N)$ have now been found. An additional term of $O(1/N)$ arises in general from $F_{\rm stat}$ [Eq. (J3)]. Setting $i\bar{\lambda}=-\lambda_0$ and retaining terms to $O(1/N)$ gives

$$-NT\,\mathrm{Tr}\ln(1-V^2|\xi_0|^2G^\lambda G)=|\xi_0|^2\Sigma_0^{(1)}(\lambda_0)+\tfrac{1}{2}\frac{(NV^2)^2}{N}|\xi_0|^4\frac{1}{\beta}\sum_{kk'n}\frac{1}{i\omega_n-\varepsilon_k}\frac{1}{i\omega_n-\varepsilon_{k'}}\frac{1}{(i\omega_n+\lambda_0-\varepsilon_f)^2}+O(1/N^2)$$

$$=|\xi_0|^2\Sigma_0^{(1)}(\lambda_0)-\frac{1}{N}|\xi_0|^4Z^{-1}(E_0)W(T_A)\,. \tag{J27}$$

[The $O(1)$ value $\varepsilon_f-\lambda_0=T_A$ has been substituted in the second term.] The second term vanishes at zero temperature for a flat density of states.

The complete form for $F_{\rm eff}$ at zero temperature and to $O(1/N)$ is, finally,

$$F_{\rm eff}=\lambda_0(1-|\xi_0|^2)+|\xi_0|^2\Sigma_0^{(1)}(\lambda_0)+|\xi_0|^2\frac{(NV^2)}{N}\sum_{kk'}\frac{f(\varepsilon_k)[1-f(\varepsilon_{k'})]}{(\varepsilon_k-T_A)^2}\frac{1}{\varepsilon_k-\varepsilon_{k'}+E_0-\Sigma_0^{(1)}(\varepsilon_k-\varepsilon_{k'}+E_0)}$$
$$+\frac{1}{N}|\xi_0|^2[1-|\xi_0|^2Z^{-1}(E_0)]W(T_A)\,. \tag{J28}$$

As stated previously, the last two terms vanish identically for a flat density of states [the case treated by Read (1985)]. More generally, these terms account for static contributions to the Bose propagator. Similar terms arise in higher order as well, if the static component is selected for special treatment.

A saddle-point approximation may now be introduced to calculate the ground-state energy; the terms proportional to W disappear from final results. The saddle-point equation associated with $|\xi_0|^2$ takes the form

$$\lambda_0-\Sigma_0^{(1)}(\lambda_0)-\frac{(NV^2)^2}{N}\sum_{kk'}\frac{f(\varepsilon_k)[1-f(\varepsilon_{k'})]}{(\varepsilon_k-T_A)^2}\frac{1}{\varepsilon_k-\varepsilon_{k'}+E_0-\Sigma_0^{(1)}(\varepsilon_k-\varepsilon_{k'}+E_0)}-\frac{1}{N}W(T_A)[1-2|\xi_0|^2Z^{-1}(E_0)]=0\,. \tag{J29}$$

Writing

$$\lambda_0=E_0+\frac{1}{N}\Delta\lambda_0,\quad |\xi_0|^2=Z(E_0)+O(1/N)\,, \tag{J30}$$

and expanding to $O(1/N)$ gives

$$\frac{1}{N}\Delta\lambda_0 Z^{-1}(E_0)-\frac{(NV^2)^2}{N}\sum_{kk'}\frac{f(\varepsilon_k)[1-f(\varepsilon_{k'})]}{(\varepsilon_k-T_A)^2}\frac{1}{\varepsilon_k-\varepsilon_{k'}+E_0-\Sigma_0^{(1)}(\varepsilon_k-\varepsilon_{k'}+E_0)}+\frac{1}{N}W(T_A)=0\,,$$

i.e.,

$$\frac{1}{N}\Delta\lambda_0=\frac{(NV^2)^2}{N}Z(E_0)\sum_{kk'}f(\varepsilon_k)[1-f(\varepsilon_{k'})]\frac{1}{(\varepsilon_k-T_A)^2}\frac{1}{[\varepsilon_k-\varepsilon_{k'}+E_0-\Sigma_0^{(1)}(\varepsilon_k-\varepsilon_{k'}+E_0)]}-\frac{1}{N}Z(E_0)W(T_A)\,. \tag{J31}$$

Substituting this result in Eq. (J28) for $F_{\rm eff}$ and applying the saddle-point condition (J29) gives for the ground-state energy

$$F(T=0)=E_0+\frac{1}{N}\Delta\lambda_0+\frac{1}{N}|\xi_0|^2W(T_A)+O(1/N^2)$$
$$=E_0+\frac{(NV^2)^2}{N}Z(E_0)\sum_{kk'}f(\varepsilon_k)[1-f(\varepsilon_{k'})]\frac{1}{(\varepsilon_k-T_A)^2}\frac{1}{[\varepsilon_k-\varepsilon_{k'}+E_0-\Sigma_0^{(1)}(\varepsilon_k-\varepsilon_{k'}+E_0)]}+O(1/N^2)\,. \tag{J32}$$

This is precisely the result derived in Secs. II–V. Note the remarkable cancellation of terms proportional to W, which have no analog in the other approaches. Similar terms may be expected in higher orders of the expansion as well. This is clear from Eq. (J27) which includes static corrections proportional to $|\xi_0|^{2(n+1)}$ at $O(1/N^n)$.

Corrections to zero-temperature thermodynamic properties at $O(1/N)$ may be derived from the free energy in Eq. (J32) in the same way that $O(1)$ properties were derived in Sec. VI.C. The results found in previous sections may be reproduced in this way.

In conclusion we emphasize that the approach discussed above, which singles out the static variables ξ_0 and λ for saddle-point approximation, is a reliable means to generate a $1/N$ expansion within the Fermi-liquid regime ($T\to 0$), but *not* at higher temperatures. At zero temperature the occupancy constraint is effectively enforced exactly, and the approach yields the same results found by other techniques; in this case, minimizing $F_{\rm eff}$ is equivalent to locating the lowest singularity in the empty-state (or Bose) propagator. At finite temperature, the occupancy constraint is not enforced, and the approximation deteriorates with increasing T.

REFERENCES

Abe, R., 1972, Prog. Theor. Phys. **48**, 1414.

Abrikosov, A. A., 1965, Physics **2**, 5.

Abrikosov, A. A., 1969, Usp. Fiz. Nauk **97**, 403 [Sov. Phys. Usp. **12**, 168 (1969)].

Anderson, P. W., 1961, Phys. Rev. **124**, 41.

Anderson, P. W., 1967, Phys. Rev. Lett. **18**, 1049.

Anderson, P. W., 1981, in *Valence Fluctuation in Solids,* edited by L. M. Falicov, W. Hanke, and M. B. Maple (North-Holland, Amsterdam), p. 451.

Anderson, P. W., G. Yuval, and D. R. Hamann, 1970, Phys. Rev. B **1**, 4464.

Andrei, N., K. Furuya, and J. H. Lowenstein, 1983, Rev. Mod. Phys. **55**, 331.

Andrei, N., and J. H. Lowenstein, 1981, Phys. Rev. Lett. **46**, 356.

Ashcroft, N. W., and N. D. Mermin, 1976, *Solid State Physics*

(Saunders College, Philadelphia).
Auerbach, A., and K. Levin, 1986a, Phys. Rev. Lett. **57**, 877.
Auerbach, A., and K. Levin, 1986b, Phys. Rev. B **34**, 3524.
Barnes, S. E., 1976, J. Phys. F **6**, 1375.
Baym, G., 1962, Phys. Rev. **127**, 1391.
Bickers, N. E., 1986, Ph.D. thesis (Cornell University).
Bickers, N. E., 1987, unpublished.
Bickers, N. E., D. L. Cox, and J. W. Wilkins, 1985, Phys. Rev. Lett. **54**, 230.
Bickers, N. E., D. L. Cox, and J. W. Wilkins, 1987, Phys. Rev. B **36**, 2036.
Bickers, N. E., and G. E. Zwicknagl, 1987, Phys. Rev. B **36**, 6746.
Brandt, U., H. Keiter, and F.-S. Liu, 1985, Z. Phys. B **58**, 267.
Bringer, A., and H. Lustfeld, 1977, Z. Phys. B **28**, 213.
Chakravarty, S., 1982, Bull. Am. Phys. Soc. **27**, 305.
Coleman, P., 1983, Phys. Rev. B **28**, 5255.
Coleman, P., 1984, Phys. Rev. B **29**, 3035.
Coleman, P., 1985a, J. Magn. Magn. Mater. **47**, 323.
Coleman, P., 1985b, in *Theory of Heavy Fermions and Valence Fluctuations,* edited by T. Kasuya and T. Saso (Springer, New York), p. 163.
Coleman, P., 1987, Phys. Rev. B **35**, 5072.
Coleman, P., and N. Andrei, 1986, J. Phys. C **19**, 3211.
Coqblin, B., and J. R. Schrieffer, 1969, Phys. Rev. **185**, 847.
Cox, D. L., 1985, Ph.D. thesis (Cornell University).
Cox, D. L., 1987a, unpublished.
Cox, D. L., 1987b, Phys. Rev. B **35**, 4561.
Cox, D. L., 1987c, Phys. Rev. B **35**, 6504.
Cox, D. L., N. E. Bickers, and J. W. Wilkins, 1985, J. Appl. Phys. **57**, 3166.
Daybell, M. D., 1973, in *Magnetism,* edited by H. Suhl (Academic, New York), Vol. V, p. 121.
de Châtel, P. F., 1982, Solid State Commun. **41**, 853.
Ernst, H. J., H. Grühl, T. Krug, and K. Winzer, 1984, in *Proceedings of the 17th International Conference on Low Temperature Physics,* edited by U. Eckern *et al.* (North-Holland, Amsterdam), p. 137.
Felsch, W., 1978, Z. Phys. B **29**, 211.
Fischer, K., 1970 in *Springer Tracts in Modern Physics,* edited by G. Höhler (Springer, New York), Vol. 54, p. 1.
Friedel, J., 1952, Philos. Mag. **43**, 153.
Galera, R. M., D. Givord, J. Pierre, A. P. Murani, C. Vettier, and K. R. A. Ziebeck, 1985, J. Magn. Magn. Mater. **47**, 139.
Goldstone, J., 1961, Nuovo Cimento **19**, 154.
Gradshteyn, I. S., and I. M. Ryzhik, 1980, *Table of Integrals, Series and Products* (Academic, New York), 8.384.1.
Grewe, N., 1982, Z. Phys. B **52**, 193.
Grewe, N., 1983, Z. Phys. B **53**, 271.
Grewe, N., 1984, Solid State Commun. **50**, 19.
Grewe, N., and H. Keiter, 1981, Phys. Rev. B **24**, 4420.
Grüner, G., and A. Zawadowski, 1974, Rep. Prog. Phys. **37**, 1497.
Grüner, G., and A. Zawadowski, 1978, in *Progress in Low-Temperature Physics,* edited by D. F. Brewer (North-Holland, Amsterdam), Vol. VIIB.
Gubernatis, J. E., J. E. Hirsch, and D. J. Scalapino, 1987, Phys. Rev. B **35**, 8478.
Gunnarsson, O., and K. Schönhammer, 1983a, Phys. Rev. Lett. **50**, 604.
Gunnarsson, O., and K. Schönhammer, 1983b, Phys. Rev. B **28**, 4315.
Gunnarsson, O., and K. Schönhammer, 1985, Phys. Rev. B **31**, 4815.
Gunnarsson, O., and K. Schönhammer, 1986, in *Handbook on the Physics and Chemistry of Rare Earths,* edited by K. A. Gschneidner, Jr. and L. Eyring (North-Holland, Amsterdam), in press.
Hewson, A. C., and J. W. Rasul, 1983, J. Phys. C **16**, 6799.
Hirsch, J. E., and R. M. Fye, 1986, Phys. Rev. Lett. **56**, 2521.
Hirst, L. L., 1978, Adv. Phys. **27**, 231.
Holland-Moritz, E., D. Wohlleben, and M. Loewenhaupt, 1982, Phys. Rev. B **25**, 7482.
Houghton, A., N. Read, and H. Won, 1987, Phys. Rev. B **35**, 5123.
Inagaki, S., 1979, Prog. Theor. Phys. **62**, 1441.
Keiter, H., and G. Czycholl, 1983, J. Magn. Magn. Mater. **31**, 477.
Keiter, H., and J. C. Kimball, 1971, Int. J. Magn. **1**, 233.
Keiter, H., and G. Morandi, 1984, Phys. Rep. **109**, 227.
Kojima, H., Y. Kuramoto, and M. Tachiki, 1984, Z. Phys. B **54**, 293.
Kondo, J., 1964, Prog. Theor. Phys. **32**, 37.
Kondo, J., 1969, in *Solid State Physics,* edited by H. Ehrenreich, F. Seitz, and D. Turnbull (Academic, New York), Vol. 23, p. 183.
Kotliar, G., and A. E. Ruckenstein, 1986, Phys. Rev. Lett. **57**, 1362.
Krishna-murthy, H. R., 1984, private communication.
Krishna-murthy, H. R., J. W. Wilkins, and K. G. Wilson, 1980a, Phys. Rev. B **21**, 1003.
Krishna-murthy, H. R., J. W. Wilkins, and K. G. Wilson, 1980b, Phys. Rev. B **21**, 1044.
Kuramoto, Y., 1983, Z. Phys. B **53**, 37.
Kuramoto, Y., and H. Kojima, 1984, Z. Phys. B **57**, 95.
Kuramoto, Y., and E. Müller-Hartmann, 1985, J. Magn. Magn. Mater. **52**, 122.
Langreth, D. C., 1966, Phys. Rev. **150**, 516.
Lavagna, M., A. J. Millis, and P. A. Lee, 1987, Phys. Rev. Lett. **58**, 266.
Lawrence, J. M., P. S. Riseborough, and R. D. Parks, 1981, Rep. Prog. Phys. **44**, 1.
Lee, P. A., T. M. Rice, J. W. Serene, L. J. Sham, and J. W. Wilkins, 1986, Comments Condensed Matter Phys. **12**, 99.
Lee, T. K., 1985, J. Phys. C **18**, L31.
Ma, M., and E. Fradkin, 1983, Phys. Rev. B **28**, 2990.
Ma, S., 1973, Phys. Rev. A **7**, 2172.
Maekawa, S., S. Kashiba, S. Takahashi, and M. Tachiki, 1985a, in *Theory of Heavy Fermions and Valence Fluctuations,* edited by T. Kasuya and T. Saso (Springer, New York), p. 90.
Maekawa, S., S. Takahashi, S. Kashiba and M. Tachiki, 1985b, J. Phys. Soc. Jpn. **54**, 1955.
Mermin, N. D., and H. Wagner, 1966, Phys. Rev. Lett. **17**, 1133.
Migdal, A. A., 1983, Phys. Rep. **102**, 199.
Millis, A. J., and P. A. Lee, 1987, Phys. Rev. B. **35**, 3394.
Müller-Hartmann, E., 1984, Z. Phys. B **57**, 281.
Newns, D. M., and A. C. Hewson, 1980, J. Phys. F **10**, 2429.
Newns, D. M., and N. Read, 1987, Adv. Phys., in press.
Nozières, P., 1974, J. Low Temp. Phys. **17**, 31.
Nozières, P., 1975, in *Proceedings of the 14th International Conference on Low-Temperature Physics,* edited by M. Krusius and V. Vuorio (North-Holland, Amsterdam), Vol. V, p. 339.
Nozières, P., and C. T. de Dominicis, 1969, Phys. Rev. **178**, 1097.
Nunes, A. C., J. W. Rasul, and G. A. Gehring, 1986, J. Phys. C **19**, 1017.
Ogievetskii, E., A. M. Tsvelick, and P. B. Wiegmann, 1983, J.

Phys. C **16**, L797.
Onuki, Y., Y. Furukawa, and T. Komatsubara, 1983, J. Phys. Soc. Jpn. **53**, 2197.
Oppermann, R., and F. J. Wegner, 1979, Z. Phys. B **34**, 327.
Popov, V. N., 1983, *Functional Integrals in Quantum Field Theory and Statistical Physics* (Reidel, Boston).
Ramakrishnan, T. V., 1981, in *Valence Fluctuations in Solids,* edited by L. M. Falicov, W. Hanke, and M. B. Maple (North-Holland, Amsterdam), p. 13.
Ramakrishnan, T. V., and K. Sur, 1982, Phys. Rev. B **26**, 1798.
Rasul, J. W., and A. C. Hewson, 1984a, J. Phys. C **17**, 2555.
Rasul, J. W., and A. C. Hewson, 1984b, J. Phys. C **17**, 3332.
Rasul, J. W., and A. C. Hewson, 1984c, Solid State Commun. **52**, 217.
Rasul, J. W., N. Read, and A. C. Hewson, 1983, J. Phys. C **16**, L1079.
Read, N., 1984, Solid State Commun. **52**, 993.
Read, N., 1985, J. Phys. C **18**, 2651.
Read, N., K. Dharamvir, J. W. Rasul, and D. M. Newns, 1986, J. Phys. C **19**, 1597.
Read, N., and D. M. Newns, 1983a, J. Phys. C **16**, 3273.
Read, N., and D. M. Newns, 1983b, J. Phys. C **16**, L1055.
Read, N., D. M. Newns, and S. Doniach, 1984, Phys. Rev. B **30**, 3841.
Rizzuto, C., 1974, Rep. Prog. Phys. **37**, 147.
Schlottmann, P., 1982, Z. Phys. B **49**, 109.
Schlottmann, P., 1983, Z. Phys. B **51**, 49.
Schotte, K. D., and U. Schotte, 1975, Phys. Lett. A **55**, 38.
Schrieffer, J. R., and P. A. Wolff, 1966, Phys. Rev. **149**, 491.
Shiba, H., 1975, Prog. Theor. Phys. **54**, 967.
Suhl, H., 1973, Ed., *Magnetism: Magnetic Properties of Metallic Alloys* (Academic, New York), Vol. V.
Takano, F., and T. Ogawa, 1966, Prog. Theor. Phys. **35**, 343.
't Hooft, G., and M. Veltman, 1974, "Diagrammar," reprinted in *Particle Interactions at Very High Energies,* Vol. 2 (Plenum, New York), p. 177.
Tsvelick, A. M., and P. B. Wiegman, 1983, Adv. Phys. **32**, 453.
Varma, C. M., 1976, Rev. Mod. Phys. **48**, 219.
Varma, C. M., and Y. Yafet, 1976, Phys. Rev. B **13**, 2950.
Wilkins, J. W., 1982, in *Proceedings of the International Conference on Valence Instabilities (Zurich),* edited by P. Wachter and H. Boppart (North-Holland, Amsterdam), p. 1.
Wilson, K. G., 1975, Rev. Mod. Phys. **47**, 773.
Winzer, K., 1975, Solid State Commun. **16**, 521.
Withoff, D., and E. Fradkin, 1986, Phys. Rev. B **34**, 8172.
Yaffe, L. G., 1982, Rev. Mod. Phys. **54**, 407.
Yamada, K., 1975, Prog. Theor. Phys. **53**, 970.
Yamada, K., and K. Yosida, 1982, Prog. Theor. Phys. **68**, 1504.
Yoshimori, A., 1976, Prog. Theor. Phys. **55**, 67.
Yoshimori, A., and A. Sakurai, 1970, Prog. Theor. Phys. Suppl. **46**, 162.
Yosida, K., and K. Yamada, 1975, Prog. Theor. Phys. **53**, 1286.
Yosida, K., and A. Yoshimori, 1973, in *Magnetism,* edited by H. Suhl (Academic, New York), Vol. V, p. 253.
Zhang, F. C., and T. K. Lee, 1983, Phys. Rev. B **28**, 33.
Zhang, F. C., and T. K. Lee, 1984, Phys. Rev. B **30**, 1556.